CONTROLLED-POROSITY OSMOTIC PUMP TABLETS: INFLUENCES OF MEMBRANE AND FORMULATION VARIABLES ON DRUG RELEASE IN *IN VITRO* AND *IN VIVO*

SIRACHA TUNTIKULWATTANA

A THESIS SUBMITTED IN PARTIAL FULFILLMENT
OF THE REQUIREMENTS FOR
THE DEGREE OF DOCTOR OF PHILOSOPHY
(PHARMACEUTICS)
FACULTY OF GRADUATE STUDIES
MAHIDOL UNIVERSITY
2007

Thesis
Entitled

CONTROLLED-POROSITY OSMOTIC PUMP TABLETS: INFLUENCES OF MEMBRANE AND FORMULATION VARIABLES ON DRUG RELEASE IN *IN VITRO* AND *IN VIVO*

…………………………..
Ms. Siracha Tuntikulwattana
Candidate

…………………………..
Assoc. Prof. Nuttanan Sinchaipanid, Ph.D.
Major-Advisor

…………………………..
Prof. Ampol Mitrevej, Ph.D.
Co-Advisor

…………………………..
Dr. Desmond B. Williams, Ph.D.
Co-Advisor

…………………………..
Assist. Prof. Teerakiat Kerdcharoen, Ph.D.
Co-Advisor

…………………………..
Prof. Banchong Mahaisavariya, M.D.
Dean
Faculty of Graduate Studies

…………………………..
Prof. Ampol Mitrevej, Ph.D.
Chair
Doctor of Philosophy Programme
in Pharmaceutics
Faculty of Pharmacy

Thesis
Entitled

CONTROLLED-POROSITY OSMOTIC PUMP TABLETS: INFLUENCES OF MEMBRANE AND FORMULATION VARIABLES ON DRUG RELEASE IN *IN VITRO* AND *IN VIVO*

was submitted to the Faculty of Graduate Studies, Mahidol University
for the degree of Doctor of Philosophy (Pharmaceutics)
on
November 20, 2007

…………………………..
Ms. Siracha Tuntikulwattana
Candidate

…………………………..
Assoc. Prof. Nuwat Visavarungroj, Ph.D.
Chair

…………………………..
Dr. Desmond B. Williams, Ph.D.
Member

…………………………..
Assoc. Prof. Nuttanan Sinchaipanid, Ph.D.
Member

…………………………..
Assist. Prof. Teerakiat Kerdcharoen, Ph.D.
Member

…………………………..
Prof. Ampol Mitrevej, Ph.D.
Member

…………………………..
Prof. Banchong Mahaisavariya, M.D.
Dean
Faculty of Graduate Studies
Mahidol University

…………………………..
Prof. Ampol Mitrevej, Ph.D.
Dean
Faculty of Pharmacy
Mahidol University

ACKNOWLEDGEMENTS

CONTROLLED-POROSITY OSMOTIC PUMP TABLETS: INFLUENCES OF MEMBRANE AND FORMULATION VARIABLES ON DRUG RELEASE IN *IN VITRO* AND *IN VIVO*

SIRACHA TUNTIKULWATTANA 4336417 PYPT/D

Ph.D. (PHARMACEUTICS)

THESIS ADVISORS: NUTTANAN SINCHAIPANID, Ph.D., AMPOL MITREVEJ, Ph.D., DESMOND B. WILLIAMS, Ph.D., TEERAKIAT KERDCHAROEN, Ph.D.

ABSTRACT

The aims of this study were to prepare alternative hydrogels of chitosan-polyacrylic acid:hydroxypropyl methylcellulose (CS-PAA:HPMC) and to use them as osmogents for the development of propranolol controlled-porosity osmotic pump tablets (CPOP). A response surface methodology was employed in order to determine the optimum membrane compositions on the *in vitro* release conforming to the criteria of USP 28. The micro/nanoporous CPOPs fabricated with cellulose acetate (CA) coating containing PVP K30 or PVP K90 as pore formers released the drug up to 70% by a zero-order kinetic over a prolonged period of time regardless of environmental conditions. The drug release was dependent on the molecular weight of PVP, PVP content and membrane weight increase. Only PVP K30 provided the desired release profile for both 12 and 24 h. The alternative hydrogels of CS-PAA:HPMC were prepared in order to be used as osmogents. The molecular weight of CS and the ratios of CS-PAA and HPMC influenced the swelling behaviors of the hydrogels. The CS-PAA:HPMC at the proportion of 1-1:1 was selected for the development of CPOPs with the CA coating containing 60% PVP K30 as a pore former and 10% PEG 400 as a plasticizer. The *in vitro* drug releases achieved the zero-order kinetics and the *in vivo* absorption profiles of the drug were prolonged. The pharmacokinetics of propranolol CPOPs were evaluated in pigs using a 3-way crossover study design in order to explore the relationship between *in vitro* dissolution and *in vivo* absorption. The results of the present study have demonstrated that the bilayered CPOP containing 20 mg of CS-PAA:HPMC at 8% coating level provided the *in vitro* releases more than 10% and 37% at 1 h and 3 h, respectively, and revealed comparable *in vivo* availability of propranolol in pigs, comparing with commercial immediate-release tablets. In conclusion, CPOPs with ternary mixtures of CS-PAA:HPMC as osmogents are feasible for controlling the drug release both *in vitro* and *in vivo* conditions. The results could provide useful information for the development of CPOPs for industrial purposes in particular.

KEY WORDS: CONTROLLED-POROSITY OSMOTIC PUMP / PVP / CHITOSAN / POLYACRYLIC ACID / PIG

246 P.

ยาเม็ดออสโมติคปั๊มชนิดควบคุมรูพรุน: อิทธิพลของตัวแปรเมมเบรนและสูตรตำรับต่อการ
ปลดปล่อยยาในหลอดทดลองและสัตว์ทดลอง
(CONTROLLED-POROSITY OSMOTIC PUMP TABLETS: INFLUENCES OF MEMBRANE
AND FORMULATION VARIABLES ON DRUG RELEASE IN *IN VITRO* AND *IN VIVO*)

สิรชา ตันติกุลวัฒนา 4336417 PYPT/D

ปร.ด. (เภสัชการ)

คณะกรรมการควบคุมวิทยานิพนธ์: ฉัฐนันท์ สินชัยพานิช,   Ph.D.,   อำพล ไมตรีเวช, Ph.D.,
DESMOND B. WILLIAMS, Ph.D., ธีรเกียรติ์ เกิดเจริญ, Ph.D.

บทคัดย่อ

        การศึกษานี้มีวัตถุประสงค์เพื่อเตรียมไฮโดรเจลไคโตแซน-กรดโพลิอะไครลิคและไฮโดรซีโปรพิลเมทิล
เซลลูโลส (CS-PAA:HPMC) และใช้ไฮโดรเจลที่เตรียมได้เป็นสารโพลิเมอร์ก่อแรงดันในการพัฒนายาเม็ดออสโม
ติคปั๊มชนิดควบคุมรูพรุนควบคุมการปลดปล่อยยาโปรปรานอลอล ยาเม็ดออสโมติคปั๊มเคลือบด้วยเมมเบรน
เซลลูโลสอะซิเตทซึ่งประกอบด้วยพีวีพีเค 30   และพีวีพีเค 90   เป็นสารก่อรู การทดลองใช้ response surface
methodology   เพื่อหาส่วนประกอบของเมมเบรนที่เหมาะสมต่อการปลดปล่อยยาตามข้อกำหนดทางเภสัชกรรม
การปลดปล่อยยาจนถึงปริมาณร้อยละ 70 เป็นไปตามจลนศาสตร์อันดับศูนย์โดยไม่ขึ้นกับสภาวะแวดล้อม ปัจจัยที่
มีผลต่อการปลดปล่อยยาได้แก่ น้ำหนักโมเลกุลและปริมาณของพีวีพี และปริมาณในการเคลือบเมมเบรน พบว่า ยา
เม็ดที่เมมเบรนประกอบด้วยพีวีพีเค 30 เท่านั้นที่สามารถควบคุมการปลดปล่อยยาตามข้อกำหนดในระยะเวลา 12
และ 24 ชั่วโมง จากการศึกษาการพองตัวของไฮโดรเจล พบว่า ปัจจัยที่มีผลต่อการพองตัวได้แก่ น้ำหนักโมเลกุล
ของไคโตแซน อัตราส่วนของไคโตแซนและกรดโพลิอะไครลิค และอัตราส่วนของไฮโดรซีโปรพิลเมทิล
เซลลูโลส เมื่อนำยาเม็ดออสโมติคปั๊มชนิดควบคุมรูพรุนที่พัฒนาขึ้นไปทำการศึกษาการปลดปล่อยยาใน
สัตว์ทดลอง โดยใช้ 3-way crossover study design เพื่อศึกษาความสัมพันธ์ของการปลดปล่อยยาในหลอดทดลอง
และการดูดซึมในสัตว์ทดลอง พบว่า ยาเม็ดออสโมติคปั๊มในรูปแบบยาเม็ดสองชั้นที่ประกอบด้วยไฮโดรเจล CS-
PAA:HPMC ในอัตราส่วน 1-1:1 ปริมาณ 20 มก. เคลือบด้วยเมมเบรนเซลลูโลสอะซิเตทที่ประกอบด้วย พีวีพีเค 30
ปริมาณร้อยละ 60   เป็นสารก่อรูและพีอีจี 400   ปริมาณร้อยละ 10 เป็นพลาสติไซเซอร์ เคลือบด้วยปริมาณน้ำหนัก
ของเมมเบรนเพิ่มขึ้น ร้อยละ 8 มีค่าชีวประสิทธิผลสัมพัทธ์เทียบเท่ากับยาเม็ดโปรปรานอลอลชนิดปลดปล่อยทันที
ที่มีขายในท้องตลาด ผลการศึกษาแสดงในเห็นว่าไฮโดรเจล CS-PAA:HPMC มีคุณสมบัติเหมาะสมในการนำมาใช้
เป็นสารโพลิเมอร์ก่อแรงดันในยาเม็ดออสโมติคปั๊มชนิดควบคุมรูพรุนเพื่อควบคุมการปลดปล่อยตัวยาทั้งในหลอด
ทดลองและสัตว์ทดลอง

246 หน้า

CONTENTS

CONTENTS (cont.)

LIST OF TABLES

LIST OF TABLES (cont.)

LIST OF TABLES (cont.)

LIST OF TABLES (cont.)

LIST OF FIGURES

LIST OF FIGURES (cont.)

LIST OF FIGURES (cont.)

LIST OF FIGURES (cont.)

LIST OF FIGURES (cont.)

LIST OF FIGURES (cont.)

LIST OF ABBREVIATIONS

%	percent
°C	degree Celsius
AFM	atomic force microscopy
ANOVA	analysis of variance
AUC	area under the plasma concentration–time curve
AUMC	area of the first moment of the plasma concentration–time curve
BCS	Biopharmaceutics Classification System
BE	bioequivalence
CA	cellulose acetate
cm	centimeter
C_{max}	maximum observed plasma drug concentration
CPOP	controlled-porosity osmotic pump
CS	chitosan
EOP	elementary osmotic pump
EOPT	effervescent osmotic pump tablet
et al.	et alii, and others
f_1	difference factor
f_2	similarity factor
F	relative bioavailability
F_a	fraction drug absorbed
g	gram
GI	gastrointestinal
h	hour
H-CS	high molecular weight chitosan
HPLC	high performance liquid chromatography
HPMC	hydroxypropyl methylcellulose
i.e.	id est, that is

LIST OF ABBREVIATIONS (cont.)

IR	immediate release
IS	internal standard
IVIVC	*in vitro–in vivo* correlation
L	liter
L-CS	low molecular weight chitosan
LLOQ	lower limit of quantification
k_e	elimination rate constant
µg	microgram
µL	microliter
µm	micrometer
M-CS	medium molecular weight chitosan
mg	milligram
min	minute
mL	milliliter
mm	millimeter
MRT	mean residence time
N	Newton
ng	nanogram
nm	nanometer
no.	number
OCDDS	osmotically controlled drug delivery systems
p	p-value
PAA	polyacrylic acid
pH	the negative logarithm of the hydrogen ion concentration
pKa	the negative logarithm of the dissociation constant
PPOP	push-pull osmotic pump
QC	quality control
R	reference formulation
r^2	coefficient of determination

LIST OF ABBREVIATIONS (cont.)

rpm	revolutions per minute
RSD	relative standard deviation
s	second
SD	standard deviation
SEM	scanning electron microscopy
SEM	standard error of mean
SOTS	sandwiched osmotic tablet system
T	test formulation
$t_{1/2}$	half-life
T_{max}	time to maximum observed plasma drug concentration
US FDA	the United State Food and Drug Administration
USP	the United State Pharmacopeia

PUBLICATIONS AND PRESENTATIONS

PUBLICATIONS

Tuntikulwattana S, Mitrevej A, Kerdcharoen T, Williams DB, Sinchaipanid N. Development and optimization of micro/nanoporous osmotic pump tablets for propranolol hydrochloride. In preparation.

Tuntikulwattana S, Ketjinda W, Mitrevej A, Sinchaipanid N. Evaluation of ternary mixtures of chitosan-polyacrylic acid:HPMC as osmogents for development of osmotic pump tablets. In preparation.

Tuntikulwattana S, Rees M, Kuchel TR, Mitrevej A, Sinchaipanid N, Williams DB. *In vivo* evaluation of osmotic pump formulations used ternary mixtures of chitosan-polyacrylic acid:HPMC as osmogents. In preparation.

PRESENTATIONS

Tuntikulwattana S, Mitrevej A, Sinchaipanid N. Evaluation of the swelling characteristics of the ternary mixtures of chitosan, polyacrylic acid and hydroxypropyl methylcellulose hydrogel. Poster presentation at RGJ-Ph.D. Congress V, April 24-26, 2004, Jomtien Palm Beach Resort, Pattaya, Thailand.

Tuntikulwattana S, Mitrevej A, Kerdcharoen T, Williams DB, Sinchaipanid N. Influence of hydrogel on drug release from microporous osmotic pump tablets. Poster presentation at the Fourth Indochina Conference on Pharmaceutical Sciences, November 10–13, 2005, HoChiMinh City, Vietnam.

Tuntikulwattana S, Mitrevej A, Williams DB, Sinchaipanid N. Evaluation of PVP K30 and K90 as pore formers in propranolol microporous osmotic pump tablet. Poster presentation at the Fifth World Meeting on Pharmaceutics, Biopharmaceutics and Pharmaceutical Technology of International Association for Pharmaceutical Technology, March 27–30, 2006, Geneva, Switzerland.

PUBLICATIONS AND PRESENTATIONS (cont.)

Tuntikulwattana S, Mitrevej A, Sinchaipanid N, Williams DB. Development of propranolol controlled-porosity osmotic pump tablets used novel *in-house* ternary mixtures as polymeric osmogents. Poster presentation at the Annual Conference of the Australasian Pharmaceutical Science Association, December 3–5, 2006, Adelaide, Australia.

Tuntikulwattana S, Rees M, Kuchel TR, Mitrevej A, Sinchaipanid N, Williams DB. *In vivo* evaluation of osmotic pump formulations used ternary mixtures of chitosan-polyacrylic acid:HPMC as osmogents. Oral presentation at the Fifth Indochina Conference on Pharmaceutical Sciences, November 21–24, 2007, Bangkok, Thailand.

CHAPTER I
INTRODUCTION

Osmotically controlled drug delivery systems offer several advantages over conventional dosage forms including pH and gastric motility independence and predictable/programmable drug release (1, 2). Consequently, it is possible to achieve and sustain a drug plasma concentration within the therapeutic window of drug, thus reducing undesired side effects and the frequency of administration, and increasing patient compliances considerably. According to these benefits, the osmotic pump tablet is the system of choice for delivery an anti-hypertensive drug, of which the constant plasma profile is important and desirable. Controlled-porosity osmotic pump (CPOP) is one type of osmotic tablets in which the delivery orifices are formed by incorporation of a leachable component into the coating solution (3-6). After coming in contact with water, this soluble additive dissolves, resulting in an *in situ* formation of a microporous semipermeable membrane. The method to create the delivery orifice is relatively simple with the elimination of the common laser drilling technique.

The mechanism of drug release from this system was found to be primarily osmotic with simple diffusion playing a minor role (4, 5). The release rate, ideally a zero-order kinetic, is dependent on formulation variables, i.e., solubility of the drug in the tablet core and osmotic pressure gradient across the membrane; and membrane variables, i.e., coating thickness and level of leachable component in the coating (6-11). Water soluble additives that can be used for the formation of the orifices in the membrane consist of sorbitol, urea, lactose, diols and polyols, as well as other water-soluble polymeric materials, such as povidone (PVP K30) (3, 6, 12-20). Erodible materials such as poly(glycolic), poly(lactic) acid or their combinations can also be used for this purpose (18).

For controlling the drug release from the osmotic pump systems, it is of great magnitude to optimize the osmotic pressure gradient between inside the compartment and the external environment. If a drug does not posses sufficient osmotic pressure, an

osmogent should be added in the formulation. Generally, compounds that can be used as osmotic agents are water-soluble salts, e.g., potassium chloride (4) and sodium chloride (21); carbohydrates, e.g., cyclodextrin derivatives (17); water-soluble amino acids and organic polymeric osmogents (9). The swellable hydrophilic polymers commonly used as polymeric osmogents are polyethylene oxide (22), hydroxypropyl methylcellulose (HPMC), and polyacrylic acid (PAA) (9).

The present study was aimed to develop the CPOP tablets using alternative hydrogels of chitosan (CS)-PAA:HPMC as an osmogent. Propranolol, a β-adrenergic blocker, was used as a water-soluble model drug. An optimization technique based on a response surface methodology was employed in order to determine the influences of the membrane variables, i.e., type (PVP K30 and PVP K90) and amount of pore forming agent, and coating level, on the *in vitro* drug release in order to specify an optimal membrane composition that achieves the desired drug release profiles. The swelling characteristics of the alternative hydrogels were determined. The effects of molecular weight of CS, ratio of the CS:PAA, and proportion of HPMC in CS-PAA:HPMC hydrogels on the swelling properties of the hydrogels were also investigated. Subsequently, the formulation variables, i.e., amount of osmogent and tablet characteristics, were evaluated. Furthermore, the pharmacokinetics of propranolol CPOP systems were evaluated in pigs in order to explore the relationship between *in vitro* dissolution and *in vivo* absorption. Consequently, the result could provide useful information of the formulation that exhibited a satisfactory drug release for the development of controlled-porosity osmotic pump tablets for industrial purposes in particular.

The objectives of this study were:

1. To develop the controlled-porosity osmotic pump tablets using alternative hydrogels of chitosan-polyacrylic acid:hydroxyprolyl methylcellulose (CS-PAA:HPMC) as osmotic agents,

2. To investigate the influences of membrane variables on the characteristics of propranolol hydrochloride controlled-porosity osmotic pump tablets,

3. To determine the swelling properties of the ternary mixtures of chitosan, polyacrylic acid and HPMC,

4. To evaluate the use of selected ternary mixtures of chitosan-polyacrylic acid: HPMC as osmotic agents for the development of controlled-porosity osmotic pump tablets,

5. To access the *in vivo* performance of the developed controlled-porosity osmotic pump tablets containing propranolol hydrochloride.

CHAPTER II
LITERATURE REVIEW

1. Osmotically Controlled Drug Delivery Systems

Osmotically controlled drug delivery systems (OCDDS) utilize osmosis, the natural movement of water through a membrane, to control the systemic delivery of drug within the body (1). As one type of controlled release systems, OCDDS provide a uniform amount of drug at the absorption site and thus, after absorption, allow maintenance of plasma concentration within a therapeutic range, which minimizes side effects and also reduces the frequency of administration and increases patient compliances. Additionally, drug release from these systems is independent of pH of the gastrointestinal (GI) tract and other physiological factors, for examples, gastric motility and presence or absence of food in the GI tract. The release characteristics can be predicted/programmed from knowledge about the properties of the drug and the dosage form (2, 7-9).

Historical background

An implantable osmotic injector was first introduced for fluid-delivery of drug to the gut of sheep and cattle at a constant rate for weeks in pharmacological research in 1955 by Rose and Nelson, two Australian physiologists (23). Their pump consisted of three chambers (Figure 1a): a drug chamber, a salt chamber containing excess solid salt, and a water chamber. The salt and water chambers are separated by a rigid semipermeable membrane. The difference in osmotic pressure across the membrane moves water from the water chamber into the salt chamber. This water flow allows the increase in volume of the salt chamber, resulting distension of the latex diaphragm separated the salt and drug chamber, thereby pumping drug out of the device.

(a)

Salt chamber

Drug chamber

Water chamber

Regid
semipermeable
membrane

Elastic diaphragm

(1)   (2)

(3)   (4)

(b)

Dispensing head
with orifice

Regid
housing
member

Active agent
formulation

Movable
separator

$MgSO_4$

Semipermeable
membrane

Porous membrane
support

Saturated solution of
$MgSO_4$ containing
excess solid $MgSO_4$

(c)

Coating containing solid
osmotic compound

Means for releasing
agent from chamber

Wall of flexible
collapsible material

Wall of semipermeable
membrane

(d)

Saturated
agent solution

Delivery
orifice

Water

Semi-permeable
membrane

Core
containing agent

Figure 1.   Cross-sectional diagram of different osmotic pumps: (a) Rose-Nelson
pump;   (b) Higuchi-Leeper   pump;   (c) Higuchi-Theeuwes   pump;
(d) Elementary osmotic pump; (e) Push-pull osmotic pump; (f) Controlled-
porosity osmotic pump; (g) OROS-CT pump; (h) Liquid OROS system;
(i) Sandwiched osmotic tablet.

(e)

Semipermeable membrane

Osmotic drug core

Delivery orifice

Polymeric push compartment

Expanded push compartment

Before operation

During operation

(f)

Rigid semipermeable membrane

Microporous membrane

Osmotic drug core

Before operation

During operation

(g)

Orifice

Semipermeable membrane

Osmotic drug compartment

Osmotic push compartment

Enteric impermeable membrane

(h)

Delivery orifice

Rate-controlling membrane

Soft gelatin

Osmotic layer

Liquid drug formulation

Inner layer

Before operation

During operation

(i)

Semipermeable CA membrane with plasticizer

Orifice

Drug layer

Push layer

Orifice

Drug release

Water imbibing

Water imbibing

Water imbibing

Expanded push layer

Drug release

Before operation

During operation

Figure 1.   Cross-sectional diagram of different osmotic pumps: (a) Rose-Nelson pump;   (b) Higuchi-Leeper   pump;   (c) Higuchi-Theeuwes   pump; (d) Elementary osmotic pump; (e) Push-pull osmotic pump; (f) Controlled-porosity osmotic pump; (g) OROS-CT pump; (h) Liquid OROS system; (i) Sandwiched osmotic tablet. (cont.)

In the early 1970s, a series of simplifications of the Rose-Nelson pumps were initially described by the Alza Corporation (24-26). An example of one of these pumps is the Higuchi-Leeper pump (24) with no water chamber as shown in Figure 1b. The device, containing a rigid housing and the semipermeable membrane which is supported on a perforated frame, is activated by water imbibed from the surrounding environment. This makes the pump can be prepared loaded with drug and then stored for a long period prior to use.

Higuchi and Theeuwes (26) further modified and developed an osmotic based system as shown schematically in Figure 1c. In this system also, imbibition of the water from the surrounding environment activates the device. The desired agent is loaded to the device immediately prior to use. When the device is contacted to an aqueous environment, release of drug follows a time course set by the salt used in the salt coating layer and the permeability of the outer membrane casing. These forms are sold under the trade name Alzet$^{®}$ (Alza Corp., CA) and are frequently used as implantable controlled-release delivery systems in experimental studies with animals.

In 1975, Theeuwes (1, 27) pioneered the solid tablet osmotic dosage form. This system is known as the elementary osmotic pump (EOP) which is simplified and developed from the Rose-Nelson pump. The device is formed by compressing a drug having a suitable osmotic pressure into a tablet. The tablet is then coated with a semipermeable membrane, usually cellulose acetate, and a small hole is drilled through the membrane coating (Figure 1d). After that seminal invention, Alza Corp. made osmotic delivery (the Oros$^{®}$ system) in various configurations of which have been marketed since 1983. Currently, more than 10 products using Oros technology are marketed for the treatment of various conditions as described in Table 1 (2).

Table 1. Commercial products based on osmotic systems (adapted from reference
          no. 2)

Alpress® LP (prazosin), once daily extended-release tablet sold in France for the treat-
    ment of hypertension (Novartis Pharmaceuticals Corporation, East Hanover, NJ)

Cardura XL® (doxazosin mesylate), for the treatment of hypertension (Pfizer Inc, New
    York)

Concerta™ (methylphenidate HCl), once-daily extended-release tablet for the treat-
    ment of attension deficit hyperactivity disorder (ADHD) (Alza Pharmaceuticals,
    Mountain View, CA)

Covera-HS® (verapamil), a controlled onset extended release (COER-24™) system
    for the management of hypertension and angina (GD Searle & Co, Chicago, IL)

Diutropan XL® (oxybutynin chloride), extended-release tablet for the once-daily treat-
    ment of overactive bladder with symptoms of urge urinary incontinence,
    urgency, and frequency (Alza Pharmaceuticals, Mountain View, CA)

DynaCirc CR® (isradipine), once-daily extended-release tablet for the treatment of hy-
    pertension (Novartis Pharmaceuticals Corporation, East Hanover, NJ)

Glucotrol XL® (glipizide), extended-release tablet used as an adjunct to diet for the
    control of hyperglycemia in patients with non-insulin-dependent diabetes (Pfizer
    Inc, New York)

Procardia XL® (nifedipine), extended-release tablet for the treatment of angina and
    hypertension (Pfizer Inc, New York); Adalat CR® (Bayer, Berlin, Germany)

Sudafed® 24 Hour (pseudoephedrine HCl), for the temporary relief of nasal
    congestion due to the common cold, hay fever, and other respiratory allergies,
    and nasal congestion associated with sinusitis (Warner-Lambert Consumer
    Healthcare, Morris Plains, NJ)

Volmax® (albuterol sulfate), extended-release tablet for relief of bronchospasm in
    patients with reversible obstructive airway disease (Muro Pharmaceutical Inc.,
    Tewksbury, MA)

Tegretol® XL (carbamazepine), extended-release tablets for use as an anticonvulsant
    drug (Novartis Pharmaceuticals Corporation, East Hanover, NJ)

Theory of operation

The basic osmotically controlled tablet, as shown in Figure 1d, consists of an osmotic drug-containing core surrounded by a semipermeable membrane with an orifice for drug release. In the aqueous environment of the GI tract, water is drawn by osmosis across the semipermeable membrane into the system core at a rate controlled by the composition and thickness of the membrane. The imbibition of water leads the development of hydrostatic pressure inside the tablet. Drug in solution or suspension is released through the orifice at the same rate that water is imbibed into the system, reducing the pressure. The release process continues at a constant rate until the entire solid substance inside the tablet has been dissolved, and only a solution-filled coating membrane is left. This residual continues to be delivered at declining rate until the osmotic pressure inside and outside the tablet are equal.

The general expression for the solute delivery rate *dM/dt* from osmotic system can be described by the following equation (1):

$$\frac{dM}{dt} = \frac{AL_p\,(\sigma\Delta\pi - \Delta\rho)C}{h} \qquad\qquad [1]$$

where A and h are the membrane area and membrane thickness, respectively; L_p is the mechanical permeability; σ is the reflection coefficient; $\Delta\pi$ and $\Delta\rho$ are the osmotic and hydrostatic pressure differences, respectively, between the inside and outside of the system; and C is the concentration (or solubility, when excess solid is present inside the core) of compound in the dispensed fluid. As the size of the delivery orifice increases, hydrostatic pressure inside the system is minimized ($\Delta\pi > \Delta\rho$). Also, when the osmotic pressure of the formulation is large compared to the osmotic pressure of the environment, π can be substituted for $\Delta\pi$. Equation 1 then reduces to a much simpler expression in which constant K replaces the product $L_p\sigma$. After simplification, the following equation is obtained:

$$\frac{dM}{dt} = \frac{AK\pi.C}{h} \qquad\qquad [2]$$

The release rate defined by Equation 2 remains zero order as long as the terms in the equation remain constant. The first three terms on the right-hand side of Equation 2 can be maintained constant through proper selection and optimization of the semipermeable membrane. Therefore, a constant release of drug from the device is

maintained as long as excess solid substance is present inside the device to maintain both π and C in Equation 2 at constant levels.

Types of osmotic controlled systems

Elementary osmotic pump

The elementary osmotic pump (EOP) was first described by Theeuwes in 1975 (1). It consists of a drug-containing core (with or without an osmogent) coated with a semipermeable membrane made of water-permeable cellulose polymers having an orifice for drug release (see Figure 1d). Water is drawn into the system by osmosis, driving drug in the core which is then released through the orifice. A lag time of 30–60 min is observed in most of the cases as the system hydrates before zero-order delivery from the system starts, about 60–80% of drug is released at a constant rate from EOP (28).   The release rate determined by the fluid permeability of the membrane and osmotic pressure of core formulation declines when solid drug in the core decreased; therefore, a drug with high solubility cannot maintain prolonged zero-order release.   A drug with poor solubility, however, lacks the ability to create sufficient osmotic pressure, resulting moderate soluble drugs as the most appropriate for the EOP system (2).

Push-pull osmotic pump

The push-pull osmotic pump (PPOP) uses a multi-compartment core to deliver drugs of a wide range of solubility. The basic PPOP resembles a simple tablet in shape and has two layers as viewed in Figure 1e. Drug along with osmogents is present in the upper layer whereas lower layer or push layer consists of polymeric osmotic agents. To promote the transport of drug, the push layer swells and expands to gently push the drug suspension or solution out through the orifice (29). A number of modifications are available for this type of system such as delayed push-pull system (as used in Covera HS, extended release formulation for verapamil), multi-layer push-pull system (for pulsatile or delayed drug delivery), and push-stick system (for delivery of insoluble drugs requiring high loading, with an optional delayed, patterned, or pulsatile release profile) (9). Adjustments to composition and thickness of the system's semipermeable membrane are made to achieve a precise delivery rate that is independent of GI pH and external agitation.

Controlled-porosity osmotic pump

The controlled-porosity osmotic pump (CPOP) contains water-soluble additives in the coating membrane, which dissolve after coming in contact with water, resulting in an *in situ* formation of a microporous membrane (Figure 1f). The resulting membrane is substantially permeable to both water and dissolved solutes and the mechanism of drug release from these systems was found to be primarily osmotic, with simple diffusion playing a minor role (3-5, 18).

Other types

The OROS-CT used for colon-targeted drug delivery comprises of a single osmotic unit or as many as five to six push-pull osmotic units filled in a hard gelatin capsule as illustrated in Figure 1g (30). When the system enters into a small intestine, the enteric coating dissolves and water is imbibed into the core, causing the push compartment to swell. Figure 1h shows the cross-sectional diagram for L-OROS Softcap delivery system before and during operation (9). These systems are designed to deliver liquid-form drugs in extended-release manner with high bioavailability including lipophilic self-emulsifying formulatuion.

The sandwiched osmotic tablet system (SOTS), a tablet core consisting of a middle push layer and two attached drug layers, is coated with a semipermeable membrane (31). As shown in Figure 1i, both the drug layers are connected to the outside environment via two delivery orifices, one on each side. After coming in contact with the aqueous environment, the middle push layer containing swelling agents swells and pushes the drug layer released from the delivery orifices. The advantage with this type of system is that the drug is released from the two orifices situated on two opposite sides of the tablet and thus can be advantageous in case of drugs which are prone to cause local irritation of gastric mucosa.

Use of asymmetric membrane in osmotic drug delivery that consist of very thin, dense skin structure supported by a thicker, porous sub-structural layer is also described in the literature (32-34). These membranes have high flux characteristics and thus, higher release rates for poorly water-soluble drug can be obtained. Moreover, the permeability of the membranes to water can be easily adjusted by controlling the membrane structure and porosity. The asymmetric membranes can be applied to tablets, capsules, or multi-particulate formulations.

Formulations aspects

Various factors that affect the drug release from OCDDS which should be considered in the formulation development are as follows.

a. Drug solubility

The kinetics of osmotic drug release is directly related to the solubility of the drug within the core as expressed in Equation 2. Assuming a tablet core of pure drug, the fraction of core release with zero-order kinetics is given by the following equation (3, 6):

$$F(z) = 1 - \frac{S}{\rho} \qquad [3]$$

where F(z) is the fraction released by a zero-order kinetic, S is the drug solubility (g/mL), and ρ is the density (g/mL) of the core tablet. Drugs with a solubility of ≤ 0.05 g/mL would be released with $\geq 95\%$ zero-order kinetics with respect to Equation 3. However, the zero-order release rate would be slow according to Equation 2, due to the small osmotic pressure gradient. Conversely, highly water-soluble drugs would demonstrate a high release rate that would be zero-order for a small percentage of the initial drug load. Thus, the intrinsic water solubility of many drugs might preclude them from incorporation into an osmotic pump. Though, it is possible to modulate the solubility of drugs within the core, and thus, extend this technology for delivery of drugs that might otherwise have been poor candidates for osmotic delivery. Some of the approaches that have been used to deliver drugs having extremes of solubility are:

[1] Use of cyclodextrin derivatives

Incorporation of the cyclodextrin–drug complex has also been used as an approach for delivery of poorly water-soluble drugs from the osmotic systems. A CPOP has been developed for testosterone (solubility = 0.039 mg/mL at 37 °C), of which formed complexation with sulfobutyl ether-β-cyclodextrin sodium salt, $(SBE)_{7m}$-β-CD, the solubility was improved to 76.5 mg/mL (13). In a comparative study with hydroxypropyl-β-cyclodextrin (HP-β-CD) and a sugar mixture, it was found that testosterone release from the device in the presence of $(SBE)_{7m}$-β-CD was mainly due to osmotic pumping while for HP-β-CD, the major contribution was due to diffusion. In case of the sugar mixture, the drug was poorly released due to the

absence of solubilizer. Similar results were obtained with prednisolone (14), and chlorpromazine (15, 16). It was reported that several $(SBE)_{7m}$-β-CD salt forms could serve both as a solubilizer and osmotic agent (35). In addition, conventional β-CD was also used as a solubilizer in the development of EOP for glipizide (36).

[2] Resin modulation approach

Release of a highly water-soluble drug, diltiazem hydrochloride from a CPOP was modulated effectively using positively charged anion-exchange resin, poly (4-vinyl pyridine) (3). Pentaerythritol was used as osmotic agent and citric and adipic acids were added to maintain a low core pH to ensure that both the drug and resin carry a positive charge. The solubility of diltiazem hydrochloride was reduced for an extended period and pH-independent zero-order release was obtained without chemical modification of the drug.

[3] Co-compression of drug with excipients

Incorporation of excipients that modulate the solubility of drug within the core can be one approach to control the release of drugs from the osmotic systems. McClelland and co-workers (3, 6) reported CPOP of a highly water-soluble drug, diltiazem hydrochloride (solubility more than 590 mg/mL at 37 °C). The majority of the drug fraction was release predominantly at a first-order rather than the desired zero-order rate, because of very high water-solubility. As a result of incorporation of sodium chloride (1 M) into the core tablet formulation, the solubility of diltiazem hydrochloride was reduced to 155 mg/mL. The modification resulted in more than 75% of the drug to be released by zero-order kinetics over a 14–16-h period.

In another study, doxazosin, which has pH-dependent solubility, was improved its solubility by organic acids (succinic and adipic acid) within the tablet cores coated with asymmetric membranes. The solubility of doxazosin was increased in the presence of organic acids and pH-independent release patterns were obtained (32).

As a similar approach, tromethamine was added in the core of OCDDS of glipizide, as a solubility modifier, to increase the microenvironmental pH of the core above the pKa of the drug (19). Glipizide is a weakly acidic drug that is practically insoluble in water and buffer media of acidic pH. Inclusion of tromethamine as alkalinizing agent in the developed formulations was clearly evident that the

concentration of tromethamine had a direct effect on glipizide release. Tromethamine increased the solubility of glipizide and hence, its release from the developed systems.

[4] Use of effervescent mixtures

A controlled release effervescent osmotic pump tablet (EOPT) of Traditional Chinese Medicine Compound Recipe (TCMCR), named Fuzilizhong prescription which includes acidic drugs consisted of many known and unknown effective components, was prepared with sodium chloride, sodium hydrogen carbonate and hydroxypropyl methylcellulose (HPMC) as osmotic agents (37). The accumulative water-insoluble drug release was improved up to 96% at 14 h, since the osmotic pressure in EOPT with sodium chloride and sodium hydrogen carbonate increased greatly, which was induced mostly by carbon dioxide gas generating from the reaction of sodium hydrogen carbonate and the acidic drugs in TCMCR after the fluid being imbibed into the compartment through the semipermeable membrane.

[5] Use of encapsulated excipients

Use of encapsulated excipients can be another approach to deliver poorly water-soluble drug from osmotic dosage forms. A capsule device coated with asymmetric membranes for the delivery of glipizide incorporated with encapsulated excipients (pH-controlling excipients) was described by Thombre et al. (38). The solubility modifier (meglumine) in the form of mini-tablets was coated with a rate controlling membrane to prolong its availability within the core. Thus, the solubility of glipizide was improved leading to its prolonged release from the device.

b. Osmotic pressure

For zero-order release, the π term in Equation 2 must keep a constant value. The simplest and most predictable way to achieve a constant osmotic pressure is to maintain a saturated solution of osmotic agent in the compartment (28). In case of a drug does not possess sufficient osmotic pressure, an additional osmotic agent should be added to the core formulation. Some of the compounds that can be used as osmogents are listed in Table 2 (9). The osmotic pressure of the commonly used solutes in controlled-release formulations is particularly high, as described in Table 3 (39). In addition to these, potassium bicarbonate (40), cyclodextrin derivatives (17) have also been used as osmotic agents.

Polymeric osmogents are mainly use in the fabrication of PPOPs and other modified devices for controlled release of drugs with poor water solubility. These are swellable and hydrophilic polymers that interact with the aqueous fluids and swell or expand to an equilibrium state. These polymers have a capacity to retain a significant portion of the imbibed water within the polymer structure (41).

c. Size of delivery orifice

Osmotic delivery systems have at least one delivery orifice in the membrane for drug release. The size of delivery orifice must be optimized in order to control the drug release from osmotic systems. If the size of delivery orifice is too large, solute diffusion from orifice may take place. In contrast, size of delivery orifice should not also be too small otherwise; zero-order delivery will be affected because of development of hydrostatic pressure inside the system, resulting in unpredictable drug delivery. Mathematical calculations that can be used to calculate the optimum size of the delivery orifice was reported in the literature (1), indicating that drug release from osmotic systems is not affected by the size of the delivery orifice within certain limits.

In a study by Theeuwes (1), a complete membrane controlled release of potassium chloride was obtained with orifice diameter in the range of 0.075–0.274 mm. At orifice size of 0.368 mm and above, control was lost because of significant contribution from diffusion. However, no systematic trends were observed within the orifice diameter between 0.075 and 0.274 mm.

Liu et al. (42) studied nifedipine release from osmotic pumps as a function of orifice diameter and no significant differences were found in the release profiles for orifice diameter ranging from 0.25 to 1.41 mm. However, the release was somewhat rapid with an orifice diameter of 2.0 mm probably because of significant diffusion. On the other hand, a longer lag time and uncontrollable/unpredictable and lower release rate were observed in the systems without any orifice.

Delivery orifices in the OCDDS can be created with use of a mechanical drill (43), but for commercial production scale, tablets need to be produced using a continuous process. Some of the reported processes to created delivery orifices in the OCDDS are as follows.

Table 2.   Compounds that can be used as osmogents

Category	Examples
Water-soluble salts of inorganic acids	magnesium chloride or sulfate lithium, sodium, or potassium chloride lithium, sodium, or potassium sulfate sodium or potassium hydrogen phosphate etc.
Water-soluble salts of organic acids	sodium or potassium acetate, magnesium succinate, sodium benzoate, sodium citrate, sodium ascorbate, etc.
Carbohydrates	arabinose, ribose, xylose, glucose, fructose, galactose, mannose, sucrose, maltose, lactose, raffinose, etc.
Water-soluble amino acids	glycine, leucine, alanine, methionine, etc.
Organic polymeric osmogents	sodium carboxy methylcellulose, HPMC, hydroxyethyl methylcellulose, cross-linked PVP, polyethylene oxide, carbopols, poly-acrylamides, etc.

Table 3. Osmotic pressure of saturated solutions of common pharmaceutical solutes (adapted from ref. no. 39)

Compound or mixture	Osmotic pressure (atm)
Lactose-fructose	500
Dextrose-fructose	450
Sucrose-fructose	430
Mannitol-fructose	415
Sodium chloride	356
Fructose	355
Lactose-sucrose	250
Potassium chloride	245
Lactose-dextrose	225
Mannitol-dextrose	225
Dextrose-sucrose	190
Manitol-sucrose	170
Dextrose	82
Potassium sulfate	39
Mannitol	38
Sodium phosphate tribasic 12.H_2O	36
Sodium phosphate dibasic 7.H_2O	31
Sodium phosphate dibasic 12.H_2O	31
Sodium phosphate dibasic anhydrous	29
Sodium phosphate monobasic H_2O	28

[1] Laser drilling

Laser drilling is one of the most commonly used techniques to create delivery orifice in OCDDS. Figure 2a shows the top view of the portion of the apparatus used to drill hole in the osmotic tablets (44). In simple words, the tablets in which holes are to be formed are charged in the hopper. The tablets drop by gravity into the slots of the rotating feed wheel and are carried at a predetermined velocity to the passageway forming station. At the passageway forming station, each tablet is tracked by an optical tracking system. If the speed of the moving tablets increases, the hole may become elliptical because of movement of tablets during the laser firing time. To avoid this problem, tracking velocity is synchronized with the velocity at which the tablets are moving. As shown in Figure 2b, the tracking is carried out by the rotational oscillation of the mount and tracking mirror of the optical tracking system. During tracking, laser beam is fired in a pulse mode fashion and the beam is transmitted by the optical tracking mechanism onto the surface of the moving tablets and moves with the moving tablets as the mirror oscillates clockwise. The walls of the tablet adsorb the energy of the beam and gets heated ultimately causing piercing of the wall and, thus forming passageway. After completion, the tracking mirror oscillates counterclockwise back to its starting position to track the next tablet. It is possible to control the size of the orifice by varying the laser power, firing duration (pulse time), thickness of the wall, and the dimensions of the beam at the wall.

Sinchaipanid et al. (11) designed salbutamol EOP tablets and evaluated the fundamental variables affecting their release characteristics. A carbon dioxide laser beam was developed in order to deliver a power of 100 mJ and successfully used to make an opening of about 0.4 mm through the film. The intensity of the laser beam was high and instant enough to cut through the film without damaging the tablet surface. Drug release from the system was found to follow zero order kinetics.
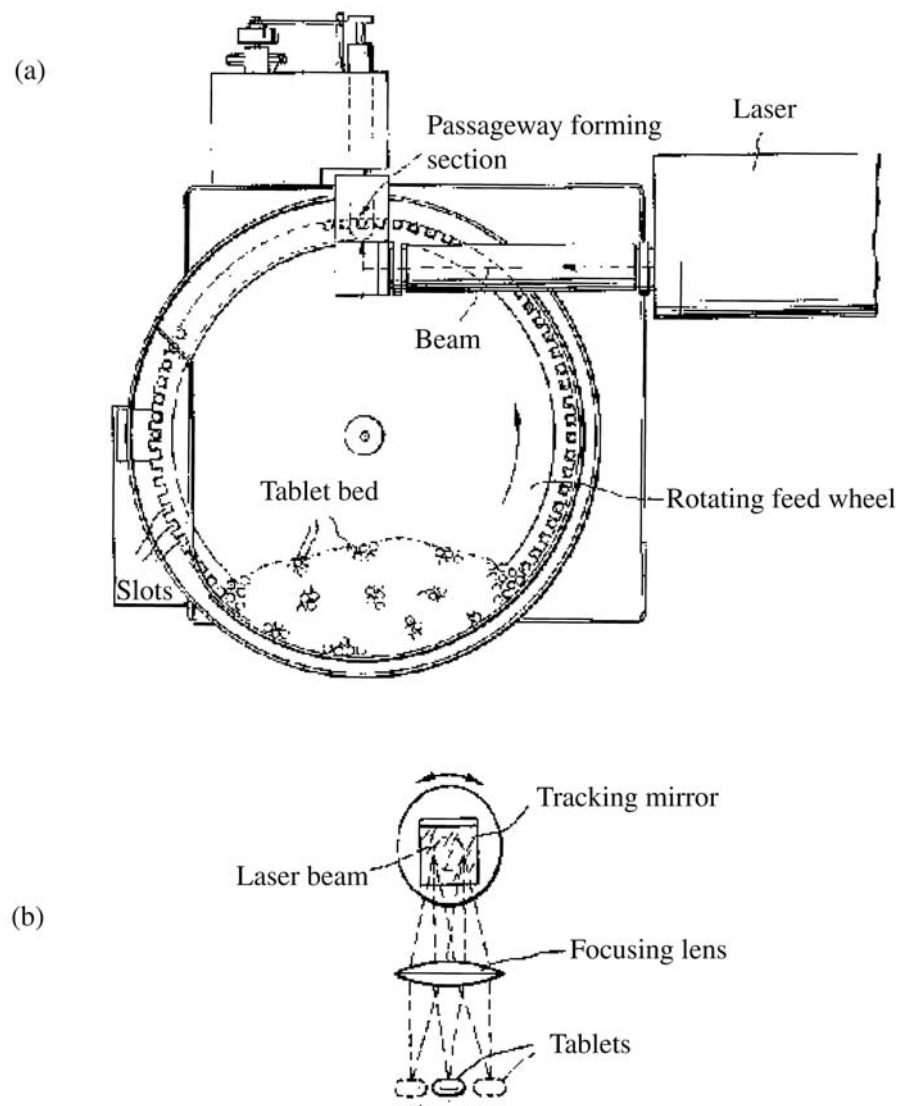
Figure 2. Top view of the laser hole-drilling system for osmotic dosage forms (a); and the pill tracking means (b) (44)

[2] Indentation that is not covered during the coating process

Coating the indented core tablet compressed by the punch with a needle is one approach to create the orifice in OCDDS. Liu et al. (21) prepared the osmotic formulation by coating the indented core tablet, using atenolol as a model drug; then optimized. The optimal osmotic tablet was found to be able to deliver atenolol at an approximately constant rate up to 24 h, independent of both release media and agitation rate. Indentation size of core tablet in the range of 1.00–1.14 mm hardly affected drug release. This method that is simply by coating the indented core tablet with the elimination of laser drilling may be promising in the field of the preparation of OCDDS.

[3] Use of pore forming agent

CPOPs are extension of EOPs and are essentially similar, except that there is no need to create a delivery orifice. Drug release from these types of system takes place through controlled porosity pores formed *in situ*. Incorporation of leachable substances in the coating membrane is the most widely reported method for the formation of pores in CPOP (3-5, 45). These water-soluble additives dissolve on coming into contact with water, leaving behind pores in the membrane through which drug release takes place. Drug release from these types of system is independent of pH and has been shown to follow zero-order kinetics (4, 5). Water soluble additives that can be used for this purpose consist of amino acid, sorbitol, mannitol, organic aliphatic and aromatic acid, including diols and polyols, as well as other water-soluble polymeric materials (46). Erodible material such as poly(glycolic), poly(lactic) acid or their combinations can also be used for this purpose (18).

These erodible or leachable materials produce one or more passageways with different geometrical shapes. The pores may also be formed in the membrane prior to the operation of the system by gas formation within curing polymer solutions, resulting in voids and pores in the final form of the membrane. The pores may also be formed in the membrane by the volatilization of components in the polymer solution leading to evolution of gases prior to application or during application of the solution to the core tablets resulting in the creation of the polymer foams serving as the porous membrane for drug release (46).

Zentner and co-workers (4, 5) determined drug release from CPOP as a function of water-soluble additive (sorbitol) in the coating membrane and reported that the release rate increased as the sorbitol content in the membrane increased from 10% to 50% w/w of cellulose acetate (CA).

In a similar study by Appel and Zentner (12) potassium chloride release from CPOP was found to increase with increasing pore-former (urea) concentration in the membrane. There was also a critical point (50% urea) above which there was a near-linear dependence of release rate on urea content. In device with less than 50% urea, swelling of the devices was observed; whereas devices with more than 50% urea retained their characteristic tablet shape. It was suggested that at lower urea concentration, the pores were not continuous and at higher concentrations greater fraction of the pores were continuous.

Okimoto et al. (16) defined the membrane controlling factors responsible for chlorpromazine release from a CPOP. The dosage form was spray coated with CA solutions varying the amount and size of micronized lactose (pore former). It was reported that the release rate of the drug increased with increasing amount of micronized lactose and decreasing lactose particle size in the membrane. The membrane surface area of the CPOPs were also measured by the gas absorption method and found that the membrane surface area of the CPOPs following release of membrane components had a linear relationship to the drug release rates from the CPOPs.

Kelbert et al. (47) prepared propranolol tablets coated with CA latex plasticized with either triethyl citrate (TEC) or triacetin (TA). Membrane permeability to the drug was increased by the addition of HPMC or sucrose. In case of TA plasticized films (at 150% w/w level), tablets with 15% w/w of HPMC had a tendency to swell and the film to rupture, showing insufficient porosity and/or film strength. Sucrose containing films showed a decrease in lag time with an increase in sucrose content. However, higher levels of sucrose (20% w/w and higher) caused rupturing of CA films. In case of TEC plasticized films (at 120% w/w level), higher levels of sucrose (50% w/w and higher) caused rupturing of CA films in the dissolution medium. It was concluded that the film plasticized with TEC and containing 40% sucrose and 10% PEG 8000 were found to provide the best release characteristics in

terms of small lag time and extended drug release profile for over 12 h. When sucrose was added to TA and TEC plasticized films, a macroporous membrane was created during exposure to the dissolution medium because of release of sucrose from the film. The mechanism of drug release was mainly a combination of molecular diffusion and osmosis.

In another study, the effect of level of pore former (PVP) in the membrane of OCDDS of glipizide was studied (19). Glipizide release was directly related to the initial level of PVP in the membrane. However, Burst strength decreased with an increase in the level of pore former. Results of SEM studies showed the formation of pores in the membrane from where the drug release occurred. The numbers of pores were directly proportional to the initial level of pore former in the membrane.

d. Semipermeable membrane type and characteristics

The choice of a rate-controlling membrane is an important aspect in the formulation development of OCDDS. From Equation 2, the importance of rate-controlling membrane in the drug release can be easily recognized. Drug release from OCDDS is independent of the pH and agitational intensity of the GI tract to a large extent. This is because of selectively water permeable membrane and effective isolation of dissolution process from the gut environment (1). To ensure that the coating is able to withstand the pressure within the device, the thickness of the semipermeable membrane is usually kept between 200 and 300 μm (7). However, this may be problematic in cases where the drug is having low osmotic pressure because of incomplete/slow drug release may take place. Selecting membranes that have high water permeabilities can be a solution to this problem. One approach is by using composite wall (48). The tablet cores are coated with a membrane that has a passageway through the wall for releasing the agent. The wall is formed from a multiplicity of materials comprising a material permeable to an external fluid and substantially impermeable to agent (like CA) and at least one additional material selected from a group of materials that imparts stability to the wall and enhances the permeability of the wall to fluids (like HPMC and hydroxylbutyl methylcellulose).

Some of the membrane variables that are important in the design of OCDDS are as follows.

[1] Type and nature of polymer

Since the membrane in OCDDS is semipermeable in nature, any polymer that is permeable to water but impermeable to solute can be used. Some of the polymers that can be selected for the above purpose include cellulose esters such as cellulose acetate, cellulose diacetate, cellulose triacetate, cellulose propionate, cellulose acetate butyrate, etc. (49); cellulose ethers like ethyl cellulose (12); and eudragits (50, 51).

Cellulose acetate (CA) has been widely used to form rate-controlling membranes for OCDDS. CA films are insoluble, yet semipermeable to allow water to pass through the tablet coating. The water permeability of CA membranes is relatively high and can be easily adjusted by varying the degree of acetylation. As the acetyl content in the CA increases, the CA film permeability decreases, and solvent resistance increases. The permeabilities of these films can be further increased by the addition of hydrophilic flux enhancers. Incorporation of plasticizer in CA coating formulations generally lowers the glass transition temperature, increases the polymer-chain mobility, enhances the flexibility, and affects the permeability of the film (52).

[2] Membrane thickness

Thickness of the membrane has a profound effect on the drug release from OCDDS. It can be seen from Equation 2 that the release rate from OCDDS is inversely proportional to membrane thickness. Monolithic osmotic pump tablets of nifedipine coated with CA membrane were found to release the drug mainly through the mechanism of osmotic pumping (42). On studying the release as a function of coating thickness, it was found that as the coating thickness increased from 85 to 340 μm, the drug release decreased in an inversely proportional manner. An increased resistance of the membrane to water diffusion resulted in this effect.

On the other hand, thickness of asymmetric membrane was found to have insignificant effect on drug release. Herbig et al. (32) reported that release rates were unaffected by the overall membrane thickness in the range of 95–150 μm. One possible reason for this may be the unique structure of the asymmetric membrane coatings in which the porous substrate consists of open pores, void volume between 60–90%. Since most of resistance to the transport is the skin structure rather than the porous substrate of the asymmetric membranes, the thickness of the porous substrate had only a slight effect on the release kinetics.

[3] Type and amount of plasticizer

Plasticizer can change viscoelastic behavior of polymers significantly. Particularly, plasticizers can turn a hard and brittle polymer into a softer, more pliable material, and possibly make it more resistant to mechanical stress. These changes also affect the permeability of polymer films (12, 16, 53).

2. Chitosan-Polyacrylic Acid Interpolymer Complexes

Chitosan

Chitosan (CS), a polycationic biopolymer obtained by alkaline deacetylation of chitin, is non-toxic, biocompatible, and biodegradable (54). Chitosan molecule is a copolymer of D-glucosamine and N-acetyl-D-glucosamine (Figure 3). The structure of chitosan is very similar to that of cellulose; it consists of β-(1,4)-linked D-glucosamine residue with the 2-hydroxyl group being substituted by an amino or acetylated amino group (55). The term chitosan refers to a group of polymers, which differ in their degree of N-deacetylation (40–98%) and molecular weight (50 000–2 000 000 Da). These two characteristics are very important to the physico-chemical properties of the chitosans and hence, they have a major effect on the biological properties (56).

Chitin is found in the exoskeleton of crustacea, insects, and some fungi. Chitosan has a rigid crystalline structure through inter- and intra-molecular hydrogen bonding. The main commercial sources of chitin are the shell wastes of shrimp, lobster, krill and crab (54, 55). In terms of availability, chitin is next to cellulose, available to the extent of over 10 gigatons annually (57).

Chitosan is a weak base with a pKa value of the D-glucosamine residue of about 6.2–7.0, therefore, insoluble at neutral and alkaline pH values. However, it does make salts with inorganic and organic acid such as hydrochloric acid, acetic acid, glutamic acid, and lactic acid. In acidic media, the amine groups of the polymer are protonated resulting in a soluble, positively charged polysaccharide that has a high charge density (one charge for each D-glucosamine unit). Chitosan can form gels by interacting with different types of divalent and polyvalent anions (58, 59).

(A)
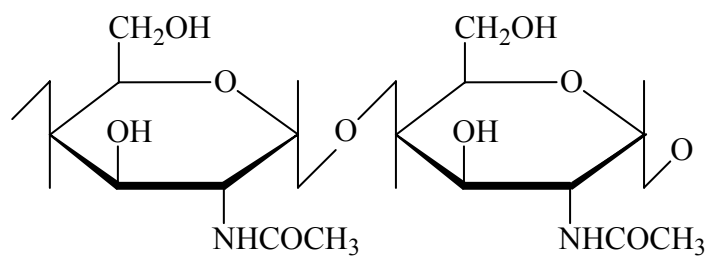
(B)
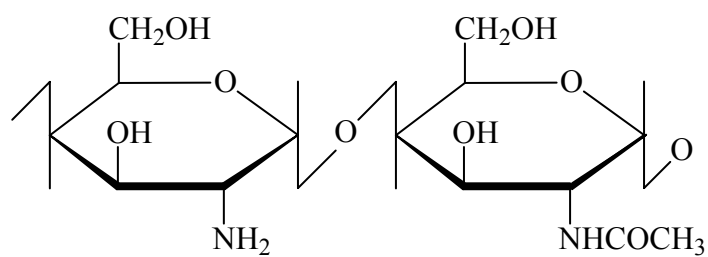
Figure 3.   Structures of chitin (A) and chitosan (B)

Chitosan exhibits a variety of physicochemical and biological properties resulting in numerous applications in fields such as waste water treatment, agriculture, fabric and textiles, cosmetics, nutritional enhancement and food processing. In addition to its lack of toxicity and allergenicity, its biocompatibility, biodegradability and bioactivity make it a very attractive substance for diverse applications as a biomaterial in the pharmaceutical and medical fields (58-66).

In the pharmaceutical industry, chitosan has been investigated as an excipient, to be used in direct tablet compression, as a tablet disintegrant, for the production of controlled release solid dosage forms or for the improvement of drug dissolution. Chitosan has, compared to traditional excipients, been shown to have superior characteristics and especially flexibility in its use. Furthermore, chitosan has been used for production of controlled release implant systems for delivery of hormones over extended periods of time. Lately, the transmucosal absorption promoting characteristics of chitosan has been exploited especially for nasal and oral delivery of polar drugs to include peptides and proteins and for vaccine delivery. These properties, together with the very safe toxicity profile, make chitosan a promising excipient for the pharmaceutical industry for present and future applications (67).

Interpolymer complexes of chitosan-polyacrylic acid

Polymer complexes are formed by the association of two or more complement-tary polymers, and may arise from electrostatic forces, hydrophobic interactions, hydrogen bonding, van der Waals forces, or combination of these interactions. The formation of complexes may strongly affect the polymer solubility, rheology, conductivity, and turbidity of polymer solutions. Similarly, the mechanical properties, permeability, and electrical conductivity of the polymeric systems may be greatly affected by complexation (68).

Particularly, polyelectrolyte complexes are formed by the reaction of a polyelectrolyte with an oppositely charged polyelectrolyte in an aqueous solution. Electrostatic interactions are considerably stronger than most secondary binding interactions. Thus, electrostatic polyelectrolyte complexes exhibit unique physical and chemical properties with reasonable biocompatibility. Therefore, great attention has been focused on their application in biotechnology, pharmaceutics and medicine (69).

When chitosan (CS), a cationic polymer, interacted with an anionic polymer such as polyacrylic acid (PAA) (Figure 4), an expandable hydrogel can be produced (68). The electrostatic attraction between protonated amino groups on chitosan and carboxylate groups on PAA generated hydrogels with non-covalent complexation have been reported (58, 61-65, 69-74).

Freeze-dried interpolymer complexes based on CS-PAA were developed for amoxicillin delivery in an acidic environment (61, 62). The electrostatic polymer/polymer interactions generate polyionic complexes with different porous structures when indicated by scanning electron microscopy. In gastric simulated fluid (SGF), these kinds of interactions caused a greater swelling extent and a slower eroding rate of these interpolymer complexes, compared to freeze-dried hydrogel without PAA. The presence of higher CS content in the complexes generated a higher repulsion between the polymeric chains, therefore, a further increase in its maximum swelling ratio and a more sustained erosion profile were obtained in the SGF.

CS-PAA polyionic complexes have been prepared for prolonged gastric antibiotic delivery (63). Different polyioinic complexes of amoxicillin, CS and PAA were prepared and employing a non-invasive method; the gastric residence time of the formulations was evaluated by mean of ^{13}C-octanoic acid breath test. All the complexes showed extensive swelling, and diffusion of the antibiotic was controlled by the degree of polymer-drug interaction.

CS-PAA complex nanoparticles have been prepared by template polymerization (64). It was found that the prepared nanoparticles carried a positive charge and showed the size in the range from 50 to 400 nm. The remarkable advantage of this system is that it is solely made of hydrophilic polymers: CS and PAA, which are non-toxic and biodegradable. These nanoparticles are stable under acidic and neutral conditions ranging from pH 4 to pH 8; and appropriate as carriers for the delivery of drugs in the gastric cavity.

$$\left[\!\!-CH_2\!\!-\!\!\underset{\underset{\displaystyle COOH}{|}}{CH}\!\!-\right]_n$$
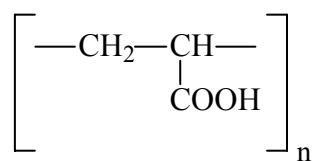
Figure 4.   Structure of polyacrylic acid

Rossi et al. (65) investigated the buccal delivery of acyclovir from films based on CS and PAA. The addition of PAA to CS produced a decrease in film hydration. Films based on CS-PAA weight ratio close to interaction product stoichiometry were characterized by higher rigidity and better wash away properties with respect to the other films and the commercial cream formulation. All the films examined promoted the permeation of acyclovir across epithelium when compared with acyclovir suspension and the commercial cream.

Ahn and co-workers (72, 73) studied a mucoadhesive polymer composed of CS and PAA by template polymerization. FTIR results indicated that polymer complex was formed between PAA and CS through hydrogen bonding.   Triamcinolone acetonide (TA) was loaded into the CS-PAA polymer complex film. Release behavior of TA from the mucoadhesive film was dependent on time, pH, loading content of drug, and CS-PAA ratio.

3. Optimization Techniques in Pharmaceutical Formulation and Processing

A computer optimization technique based on a response surface methodology (RSM) utilizing polynomial equations has been widely used for the optimization of formulations with various kinds of drug in the development of controlled-release formulation design (75-80). The RSM is a useful approach to minimize the number of experiment trials, especially for an unknown system with single or multiple responses in multi-variable systems; approximate the true system behavior as a function of the formulation and process variables; and determine the apparent optimum conditions (81, 82).

The most common experimental design used in RSM is the central composite design (CCD), which has equal predictability in all directions from the center (83). CCD is popular because of its high efficiency with respect to the number of run required (84). In addition, CCD is optimized designs for fitting quadratic model. The number of experimental points in the CCD is sufficient to test statistical validity of the fitted model and lack-of-fit of the model. The central point in CCD is replicated several times to estimate the error due to experimental or random variability (81).

Sastry and co-workers (76) used RSM in order to optimize atenolol gastrointestinal therapeutic systems. Preliminary studies on the screening of formulation variables using a Plackett-Burman design revealed that orifice size, coating level and the amount of Carbopol 934P, a viscolyzing agent, had pronounced effects on the *in vitro* release kinetics of atenolol (85). Therefore, for formulation optimization, a three-factor, three-level CCD was employed with independent variables of orifice size, coating level and the amount of Carbopol 934P. The optimization model predicted more than 90% drug release at the optimum formulation variables. Preparation and testing of the optimized formulation showed a good correlation between predicted and observed data.

Huang et al. (77) developed and optimized the propranolol once-daily extended release formulation containing HPMC, microcrystalline cellulose (MCC) and lactose by RSM. The constrained mixture experimental design was used to prepare systematic model formulations, which were composed of three formulation variables: the content of HPMC, MCC and lactose. The drug release percent at 1.5, 4, 8, 14 and 24 h were the target responses and were restricted to 15–30, 35–55, 55–75, 75–90 and 90–110%, respectively. The results showed that the optimized formulation provided a dissolution pattern equivalent to the predicted curve, which indicated that the optimal formulation could be obtained using RSM.

In another study, meloxicam sodium gel formulations were optimized using the RSM (79). A uniform design was applied to prepare model formulations systematically that were composed of four independent variables: the content of ethanol, propylene glycol, menthol, and azone. The penetration rate (flux) of meloxicam sodium gel through rat skin was chosen as the response which had to be higher than 400 μg/h.cm^2 the required flux of meloxicam gel to maintain a therapeutic concentration. The result showed optimal formulation could be obtained from this RSM. Menthol had the greatest potential influence on the penetration absorption of meloxicam sodium, followed by azone, ehanol and propylene glycol, respectively.

Recently, the RSM and multiple response optimization utilizing the polynomial equation were used to search for the optimal coating formulation in the development of oral controlled-release formulation for tamsulosin hydrochloride using a combination of two cellulose ester derivatives, HPMC and hydroxypropyl

methylcellulose phthalate (HPMCP), with Surelease® as a coating material (80). A three-factor, three-level CCD was used to prepare systematic model formulations, which were composed of three formulation variables, the content of HPMC and HPMCP, and the coating level as independent variables. The optimal coating formulation was achieved with 10% HPMC and 20% HPMCP at a coating level of 25%, and the observed responses coincided well with the predicted values from the RSM optimization technique.

4. *In Vitro–In Vivo* Correlation

A key goal in pharmaceutical development of dosage forms is a good understanding of the *in vitro* and *in vivo* performance of the dosage forms. One of the challenges of biopharmaceutics research is correlating *in vitro* drug release information of various drug formulations to the *in vivo* drug profiles, commonly known as an *in vitro/in vivo* correlation (IVIVC) (86). Such a tool shortens the drug development period, economizes the resources and leads to improved product quality. Increased activity in developing IVIVCs indicates the value of IVIVCs to the pharmaceutical industry (87).

IVIVC can be used in the development of new pharmaceuticals to reduce the number of human studies during the formulation development as the main objective of an IVIVC is to serve as a surrogate for *in vivo* bioavailability and to support biowaivers (88, 89). It supports and/or validates the use of dissolution methods and specification settings. This is because the IVIVC includes *in vivo* relevance to *in vitro* dissolution specifications (87). It can also assist in quality control for certain scale-up and post-approval changes (SUPAC) (90). With the proliferation of modified-release products, it becomes necessary to examine the concept of IVIVC in greater depth. Investigations of IVIVC are increasingly becoming an integral part of extended release drug development (91-94). There must be some *in vitro* means of assuring that each batch of the same product will perform identically *in vivo* (87-90).

Four categories of IVIVCs have been described in the FDA guidance (86):

Level A: A level A correlation represents a point-to-point relationship between *in vitro* dissolution and the *in vivo* input rate (e.g. the *iv vivo* dissolution of the drug from the dosage form). Generally these correlations are linear, however, non-linear

correlation are also aceeptable. A level A correlation is considered most informative and very useful from a regulatory viewpoint.

Level B: A level B correlation uses the principles of statistical moment analysis. The mean *in vitro* dissolution time is compared either to the mean residence time or to the mean *in vivo* dissolution time. Although this type of correlation uses all of the *in vitro* and *in vivo* data, it is not considered a point-to-point correlation. Further, since it does not uniquely reflect the actual *in vivo* plasma level curve, this is not very useful from the regulatory point of view.

Level C: A level C correlation establishes a single point relationship between a dissolution parameter (e.g. $t_{50\%}$ or percent dissolved in 4 h) and a pharmacokinetic parameter (e.g. AUC or C_{max}). A level C correlation does not reflect the complete shape of the plasma concentration time curve, therefore is not the most useful correlation from a regulatory point of view. However, this type of correlation can be useful in early formulation development.

Multiple level C: A multiple level C correlation relates one or several pharmacokinetic parameters of interest to the amount of drug dissolved at several time points of the dissolution profile. Multiple level C correlation can be as useful as level A IVIVC from a regulatory point of view. However, if one can develop a multiple level C correlation, it is likely that a level A correlation can be developed as well.

IVIVCs are generally seen when the *in vitro* dissolution is the rate-limiting step in the absorption and appearance of the drug in *in vivo* circulation. Therefore, if the drug is highly permeable and *in vitro* dissolution is the rate-limiting step, it is very highly likely that a successful IVIVC can be developed (89).

General principles in the development of a correlation (86, 95)

Generally, IVIVC should be developed using two or more formulations with different release rates (only one release rate is sufficient if dissolution is condition-independent). Data obtained from human studies are required for regulatory consideration of the correlation. When two or more drug product formulations with different release rates are developed, their *in vitro* dissolution profiles should be generated using an appropriate dissolution methodology. The dissolution method used should be the same for all the formulations. A bioavailability study should be

conducted to determine the *in vivo* plasma concentration time profiles for each of the formulations. Preferably, this study should be of a crossover study design in adequate number of subjects. However, in certain cases, data from across studies can be used in the development of an IVIVC, if a common reference is included in these studies. One method to develop a level A correlation is to estimate the *in vivo* absorption or dissolution time course using an appropriate deconvolution technique for each formulation and subject (using Wagner–Nelson method, numerical deconvolution, etc.). The *in vivo* absorption profile is plotted against the *in vitro* dissolution profile to obtain a correlation. One could use alternative approaches other than that mentioned above to develop correlations. Also, if there is no one to one relationship, then dissolution conditions may be altered (prior to evaluation of predictability), or time scaling approaches used to develop the correlation. However, the time scaling factor should be the same for all the formulations. Different time scales for each of the formulations indicates absence of an IVIVC.

It is necessary to emphasize that the relationship between *in vitro* dissolution and *in vivo* dissolution, or absorption, should be the same for all the formulations studied. If one out of the three formulations (only if this is the slowest or the fastest release rate formulation) shows a different relationship, then, such a formulation may be dropped from the IVIVC development.

5. Animal Models

In product development, several trial formulations may be manufactured and evaluated the impact of any formulation changes on *in vivo* performance. Apart from evaluating the trial formulations in humans, which has significant economics and ethical implications, alternative methods have generally shown a limit potential for bioavailability assessment. The lack of a reliable model has hindered product development in the past. Alternative methods for assessing bioavailability therefore need to be examined (96).

Therefore, there is a need for a suitable screening model that will evaluate the bioavailability of potential dosage formulations intended for use in humans. This tool should be sensitive, rapid, reproducible, have economic benefits and most importantly to have shown a correlation with *in vivo* bioavailability in humans. This model should

be able to be used for discriminating unsuitable dosage forms and enable selection of those products which are most likely to perform satisfactorily in humans.

The data obtained from *in vitro* dissolution tests which measure the rate and extent of dissolution of the drug in a defined medium can be correlated with parameters for *in vivo* drug absorption. There are three main uses for in vitro dissolutions; (i) to assist in the selection of candidate formulations in the pharmaceutical development process; (ii) as a quality control procedure in pharmaceutical production; and (iii) as an in vivo surrogate under strictly defined conditions or for carefully selected products (86, 95).

For the prediction and correlation of human bioavailability data, the use of animal models as alternatives to humans has been suggested by the US FDA (97). Major benefits for using the accurate animal models as surrogates for human bioavailability studies are; (i) intact-physiological model: has advantages over in vitro or in situ models as all aspects of GI physiology and anatomy are present, enabling a more accurate assessment of bioavailability; (ii) economic: the use of an animal model during product development is considerably cheaper than the evaluation of each formulation change in humans. The model could be used to screen new drug formulations and modifications to existing formulations and enable formulation scientists to rapidly identify compounds/formulations/dosing strategies that will encounter/overcome limitations to absorption. Ultimately this will increase product development and turnover rate; (iii) risk: there may be ethical issues for the evaluation in healthy human volunteers especially potentially toxic drugs. However, due to the limited number of studies performed, no single animal has been recommended to date.

A number of anatomical and physiological conditions that may influence drug absorption are needed to be considered when choosing an appropriate animal model (96). The anatomy and general dimension of the various compartments within the GI tract needs to be proportional to that in humans. For the evaluation of intact solid oral dosage forms, the animal must be physically large enough for it to be administered the drug product without trauma to the mucosa. It is also desirable that the GI physiology resemble that in humans. The GI mucosa is important as well as absorption windows, and the presence and distribution of various drug metabolizing enzymes (98).

Gastric emptying and motility patterns need to be controlled by similar mechanisms and approximate the rates seen in humans. The supply of blood and lymph to the gut should be analogous, as both the rate and extent of absorption can be dependent upon these factors. The gastric and pancreatic secretions should exhibit close similarity as they establish the pH profile along the GI tract and provide the majority of digestive enzymes which may influence drug dissolution and absorption. Bile which is the main source of surfactant in the GI tract should have a composition resembling that in humans and be secreted by similar mechanisms and rates. It has been suggested that the transit time of solid dosage forms in dogs is rapid in comparison to man and that the dog might not be a good model to evaluate oral sustained release preparation (96). Examples of a poor predictability of the availability of sustained release formulation and short transit times in dogs were reported in the literature (99, 100).

The blood volume of the animal is needed to be large enough to enable removal of sufficient blood samples to adequately describe the concentration versus time profile of the drug. This may be an important especially if cross-over studies are planned. Further, the animal must be able to cope with the human equivalent dose without any abnormal physiological response, such as altered motility, delayed gastric emptying, or toxic effects of the drug itself, which may influence the drug absorption characteristics. Finally the animal chosen must be relatively inexpensive and be readily available. The temperament of the animal should allow easy handling by humans.

The pig is considered to be the most suitable non-primate animal model since it resembles the human situation better than any other non-primate animal species with regard to eating behavior, anatomy and physiology of the GI tract (98, 101). Their gastric emptying is somewhat slower than that found in man, but that small intestinal transit and total transit seem to be similar to those found in man (102). Moreover, the pig, being a large animal, enables a human dosage form to be orally administered, and can also provide a large number of blood samples with little change in haematocrit or haemodynamics, which is especially important in multiple cross-over bioavailability studies. Unfortunately, studies with repeated blood sampling require surgical implantation of deep vein catheters as there are no readily available surface blood

vessels (103). As a result, the pig can be considered to be a suitable model for the evaluation of the performance of oral pharmaceutical products.

Oral bioavailability of a miconazole/cyclodextrins/tartaric acid inclusion complex was determined in pigs (104). Preliminary *in vitro* dissolution data showed that the inclusion complex exhibits a faster and higher dissolution rate than either physical mixture of those compounds or miconazole alone. Similar results were obtained from *in vivo* evaluation in pigs. Following the inclusion complex oral administration, mean under the plasma concentration–time curve (AUC) for micronazole was significantly higher than those after oral administration of the physical mixture and drug alone.

The pharmacokinetics of theophylline in pigs was investigated following the oral and intravascular (IV) administration of single doses of theophylline free base (105). The mean half-life of theophylline following IV administration was 11 h, and the apparent specific volume of distribution was 0.61 L/kg. Following oral administration, theophylline in solution was absorbed quite rapidly with a bioavailability of 79%. The similarity of the pharmacokinetics of theophylline in pigs and humans suggests that pigs may provide a useful model for the study of bioequivalence of theophylline dosage forms intended for human use.

Larsen et al. (106) studied multiple oral administration of a ketoprofen-dextran ester prodrug in pig. The prodrug was given to three pigs at interval of 12 h and in seven doses. Frequent blood sampling was carried out at the first, third and seventh intervals. The obtained cumulated *in vivo* dissolution/release profiles revealed similar release rates for the three pigs and similar extents of release. Following administration of the dextran prodrug the AUC and the release profiles are uniform, with small inter-individual variations. This study shows that multiple dosing in pigs seems to result in reproducible plasma concentration–time courses.

Kostewicz et al. (103) assessed the ability of the pig to discriminate the *in vivo* release characteristics of two sustained release nifedipine formulations, which had previously been evaluated in human, under both fasting and fed conditions. Unlike that observed in the pig in this study, the presence of food caused significant alterations in the release characteristics of the experiment nifedipine formulations in humans. It is highly likely that the food effect observed in humans may be due to

altered dissolution of this product as a result of pH changes with food ingestion. Likewise, the food effect may also be a result of food dependent changes in stomach emptying rate. The authors were unclear as to why food dependant changes were not observed in the pig. Possibly, the critical gut physiological parameters of the pig during both the fed and fasting conditions are similar to the fed condition in humans. This may be related to a slightly elevated fasted gastric pH compared to man or in complete gastric emptying in the pig even after a 24-h fast. The results showed that the pig appeared to give similar results to that observed in human-fed study and suggested that the pig may be a useful model for the fed state.

From the limited number of studies published in the open literature to date, results have indicated that further studies using the pig as a preclinical surrogate model for bioavailability evaluation is justified.

6. Model Drug – Propranolol Hydrochloride

Propranolol, a beta-adrenergic blocker, is a suitable candidate for the preparation of an osmotically-controlled release dosage form due to it is one of the most wildly prescribed in the long-term treatment of hypertension, angina pectoris and many other cardiovascular disorders, including migraine. It is classified into the Class I according to Biopharamceutics Classification System (BCS) with the high solubility and high permeability property (107). Propranolol is lipophilic, with log P 3.56 (108), and is almost completely absorbed after oral administration. However, its systemic bioavailability is restricted, approximately 33%, as a result of significant hepatic first-pass metabolism. Its elimination half-life is also relatively short, about 4–6 h (109, 110). Propranolol is bound to lipoproteins independently of drug concentration and also to α_1 acid glycoprotein and this protein is responsible for 75% of binding of propranolol in plasma at therapeutic drug concentration (111). A linear relationship of the area under the plasma concentration–time curve (AUC) with dose is exhibited over the range of 40 to 160 mg propranolol (111). The predetermined controlled-release dosage form would result in a better patient compliance.

Propranolol possesses one chiral center and the *S*-isomer is 100–130 times as active as its *R*-isomer (112). Propranolol hydrochloride has molecular weight of 295.8

(113) and its chemical structure is schematic in Figure 5. It is a highly soluble drug (solubility > 50 mg/mL) with the pKa of 9.5 (113).

Controlled release propranolol formulations have been developed in various types of drug delivery systems. The matrix-based tablets have been investigated in both the formulation design and the scientific basis for regulatory policy developed on the scale-up and post approval changes for modified release dosage forms (SUPAC-MR) (77, 114-117). The product originally launched on the market is Inderal LA[®] (AstraZeneca, USA) in the form of coated pellets filling in hard-gelatin capsules. Formulation development in other dosage forms such as a matrix tablet containing HPMC, microcrystalline cellulose and lactose (77); HPMC and Carbopol[®] (116) and dextran (117), and a matrix-in-cylinder system consisting of a hot-melt extruded ethylcellulose pipe surrounding a drug containing HPMC-Gelucire[®] 44/14 core (114) were described. The drug releases from hydrophilic matrix tablets were influenced by environment conditions. On the other hand, propranolol release from the matrix-in-cylinder system was only slightly affected by the composition of the dissolution medium. Moreover, the elementary osmotic pump (EOP) system, which its drug release is independent of environment conditions, was developed (118). However, the preparation of other types of OCDDS including controlled porosity osmotic pump tablets (CPOPs), which the method to create the delivery orifice is relatively simple with the elimination of the common laser drilling technique, has not been reported.
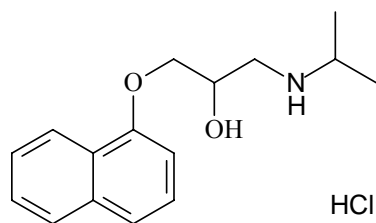
Figure 5.   Structure of propranolol hydrochloride

CHAPTER III
MATERIALS AND METHODS

MATERIALS

Chemicals

1. Propranolol (Lot number 961206, Sinochem, Shanghai, China)

2. Fructose (Lot number TK4B1704J, Rama Production, Bangkok, Thailand)

3. Lactose (Lot number EN/20200 A6644, Lactose New Zealand, Taranaki, New Zealand)

4. Pregelatinized starch (Starch$^®$ 1500, Lot number 908030, Colorcon, West Point, USA)

5. PVP K30 (Lot number 03200076145, International Specialty Products, Wayne, USA)

6. PVP K90 (Lot number 49-3213, BASF, Ludwigshafen, Germany)

7. Magnesium stearate (Lot number 90055/00218, Unimer, Switzerland)

8. Talcum (Lot number 21013-040816, Liaoning Metals and Minerals, Liaoning, China)

9. Colloidal silicon dioxide (Aerosil$^®$ 200, Lot number 0060446, Degussa, Brussels, Belgium)

10. Cellulose acetate (Lot number 13713LB, Aldrich Chemical, St.Louis, USA)

11. Sodium hydroxide (Lot number 802239, Ajax Chemicals, Auburn, Australia)

12. Chitosan-low molecular weight (MW 150 kDa, Lot number 22741, Fluka Chemie AG, Buchs, Switzerland)

13. Chitosan-medium molecular weight (MW 400 kDa, Lot number 22742, Fluka Chemie AG, Buchs, Switzerland)

14. Chitosan-high molecular weight (MW 600 kDa, Lot number 22743, Fluka Chemie AG, Buchs, Switzerland)

15. Polyacylic acid (Carbopol$^{\circledR}$ 934P, Lot number CC57JBB895, Noveon, Cleveland, USA)

16. Hydroxypropyl methylcellulose (Type 2910, Grade 615, Lot number 910441, Shin-Etsu Chemical, Tokyo, Japan)

17. Citric acid (Lot number 2C261012G, Carlo Erba Reagent, Milan, Italy)

18. Disodium hydrogen phosphate (Lot number 3E613010N, Carlo Erba Reagent, Milan, Italy)

19. Sodium chloride (Lot number 3C303063F, Carlo Erba Reagent, Milan, Italy)

20. Methanol (ChromAR, Lot number B35H06, Mallinckrodt Baker, Phillipsburg, USA)

21. Acetonitrile (HPLC grade, Lot number C38805, Mallinckrodt Baker, Phillipsburg, USA)

22. Ethanol 95% (Lot number 8006-05, J.T. Baker, Malaysia)

23. Acetone (Union Chemical, Thailand)

24. Isopropanol (Lot number 01050150, LabScan Asia, Bangkok, Thailand)

25. Hydrochloric acid (Lot number 01040121, LabScan Asia, Bangkok, Thailand)

26. Acetic acid (Lot number 01100156, LabScan Asia, Bangkok, Thailand; Lot number AH510214, Ajax, Seven Hill, Australia)

27. Triethylamine (Lot number 84289, Prolabo, Paris, France)

28. n-Heptane (BDH HPS for HPLC, Lot number I262783546, VWR International, Poole, UK)

29. Dichloromethane (BDH HiPerSolv for HPLC, Lot number K34681276519, VWR International, Poole, UK)

30. Toluene (BDH AnalR, Lot number K34593050526, VWR International, Poole, UK)

31. Dichlorodimethylsilane (99%, Lot number 03129DC, Sigma-Aldrich, St.Louis, USA)

Commercially available propranolol immediate release product

1. Deralin 40® (Lot number 6B329, Alphapharm, Carole Park, Australia)

EQUIPMENT

1. Dissolution test apparatus (SR8-plus Q-pak™, Hanson Research, Chatsworth, CA, USA)

2. UV/VIS spectrophotometer (DU-650, Beckman Instruments, Fullerton, CA, USA)

3. Peristaltic pump 6 channels (Gilson® Miniplus 3, Gilson, Villiers Le Bel, France)

4. Single punch tablet machine (Model Exacta 1, Fette, Hamburg, Germany)

5. Analytical balance (Model A 200S, Sartorius, Goettingen, Germany)

6. Electronic precision balance (Model 1581 MP 8-1, Sartorius, Goettingen, Germany)

7. Electronic tablet hardness, diameter, thickness tester (Model PTB 311 D-6452, Pharma Test, Hainburg, Germany)

8. Roche type friabilator (Model PTFR-A, Pharma Test, Hainburg, Germany)

9. Disintegration test apparatus (QC-21, Hanson Research, Chatsworth, CA, USA)

10. Tumbling mixer (Rotomixer®, Forster Equipment, Leicester, England)

11. Perforated pan coater (Thai Coater®, Model 15"(L), Pharmaceuticals and Medical Supply LP, Bangkok, Thailand)

12. Sonicator (Model 2510E-MT, Branson Ultrasonics, Danbury, CT, USA)

13. Magnetic stirrer (Pyro-Mac Stir Model L344, Labinco BV, Breda,   The Netherlands)

14. Texture analyzer (TA-XT plus, Stable Micro Systems, Surrey, UK)

15. Differential scanning calorimeter (Model DSC 7, Perkin-Elmer, Norwalk, USA)

16. Fourier transform infrared spectrophotometer (Magna-IR 550, Nicolet Instrument, Wisconsin, USA)

17. Scanning electron microscope (Model S-2360N, Hitachi, Tokyo, Japan)

18. Atomic force microscope (SPA 400, SII Nanotechnology, Chiba, Japan)

19. High performance liquid chromatography

  - High pressure pump (Model LC-10AS, Shimadzu, Kyoto, Japan)

  - Fluorescence detector (Model RF-10A XL, Shimadzu, Kyoto, Japan)

  - Auto injector (Model SIL-10AD VP, Shimadzu, Kyoto, Japan)

20. Hypersil CN column (250×4.6 mm; 5 µm) fitted with a cyano guard column (10×4.6 mm) (Thermo Fisher Scientific, Waltham, USA)

21. Rotating mixer (Model 7, Analite, Australia)

22. Centrifuge (Model MP4R, International Equipment, Needham, USA)

23. Vortex mixer (Model G560E, Scientific Industrial, Bohemia, USA)

24. Micropipette 5–40 µl, 20–200 µl, and 200–1000 µl (Finnipipette; Lab-systems, Helsinki, Finland)

METHODS

Part I: Influences of Membrane Variables on Characteristics of Propranolol Hydrochloride Controlled-Porosity Osmotic Pump Tablets

1. Preparation of propranolol core tablets

Each tablet comprised propranolol, as an active ingredient, and excipients, including, osmogents, a binder and lubricants. The osmogent system consisted of fructose and lactose at the ratio of 1:1 and the lubricant system consisted of magnesium stearate, talcum and colloidal silica. The tablet composition is summarized in Table 4. The tablets were prepared by a wet granulation process using an ethanolic solution of PVP K30 as a binder. The granules were compressed to 9 mm concave tablets using a single punch press. The tablet weight was set to be 300 mg and the acceptable tablet hardness was more than 80 N. The compressed tablets were stored in well-closed containers prior to coating.

2. Preparation of propranolol osmotic pump tablets

2.1. Preliminary study

The effects of type and amount of PVP, a pore-forming agent of the cellulose acetate membrane, on the drug release from osmotic tablets were investigated in a preliminary study. The result was intended to be use in the optimization step of the coating composition by experimental design. Core tablets were coated with 3% w/v cellulose acetate in acetone:isopropyl alcohol (3:1) solution. The effects of the amount of PVP were studied at three different concentrations, i.e., 12.5%, 25% and 50% by weight with respect to cellulose acetate. The effects of the type of PVP were evaluated at two molecular weights, i.e., 50 000 (PVP K30) and 1 000 000 (PVP K90). The coating level was set at 3% weight gain. Seven formulations were prepared as described in Table 5. All coatings were performed in a perforated pan coater.

Table 4. Core tablet composition

Components	Amount (mg)
Propranolol hydrochloride	80
Fructose:lactose (1:1)	208
PVP K30	3
Talcum	2.25
Colloidal silica	0.75
Magnesium stearate	6

Table 5. Coating composition of the formulations in preliminary study

Formulations	Composition		
	CA (% w/w)	PVP K30 (% w/w of CA content)	PVP K90 (% w/w of CA content)
P-0	3	-	-
P-K30-12.5	3	12.5	-
P-K30-25	3	25	-
P-K30-50	3	50	-
P-K90-12.5	3	-	12.5
P-K90-25	3	-	25
P-K90-50	3	-	50

Coating conditions were as follows:

inlet air temperature	55 ºC
outlet air temperature	35 ºC
atomization air pressure	1 kgf/cm^2
spray rate	15 mL/min
pan speed	5–7 rpm
drying temperature	35 ºC
drying time	15 min.

Propranolol core tablets were placed in the coating pan. Two kilograms filler tablets were added in order to achieve the appropriate batch size. Initially, the pan was rotated at low speed (1–2 rpm) and heated air was passed through the tablet bed. Coating process started once the outlet air temperature reached 35 °C and was maintained above this temperature by keeping the inlet air temperature in the range of 55–60 °C. The revolution per minute of the pan, the rate of spraying of coating solution and the atomization pressure was kept as listed above. Coating was continued until the desired weight gain was obtained. Finally, coated tablets were dried at 35 °C for 12 h before analysis.

2.2. Experimental design

A central composite design was applied to this study in order to verify the effects of independent variables on response variables as response surface curves. Two factors of interest, i.e., PVP content and membrane weight gain, at 2 levels were observed for each PVP type. The independent variables (factors) and their experimental domain are shown in Table 6. Eleven experiments of each type of PVP, i.e., PVP K30 and K90, are given in Table 7, including 4 factorial design runs, 4 axial runs and 3 center runs. The dependent variables (responses) were drug release at the predetermined time intervals and their limits based on the criteria of *Propranolol Hydrochloride Extended-Release Capsules* (USP 28) (119) are listed in Table 8. The values of the response obtained allow the calculation of mathematical estimation models for each response, which were subsequently used to characterize the nature of the response surface. All statistical analyses were carried out using a statistical software; MINITAB®.

Table 6.   Factors and experimental domains in central composite design

Factors	Experimental domains				
	(-1.414) -level	(-1) -level	(0) -level	(+1) -level	(+1.414) -level
X_1 = PVP content (%)	7.33	12.5	25	37.5	42.68
X_2 = membrane weight gain (%)	1.59	2	3	4	4.41

Table 7.   Experimental designs

Formulations	Coded variables		Uncoded variables	
	X_1	X_2	PVP content (%)	Membrane thickness (%)
K30/90-1	-1	-1	12.5	2
K30/90-2	+1	-1	37.5	2
K30/90-3	-1	+1	12.5	4
K30/90-4	+1	+1	37.5	4
K30/90-5	-1.414	0	7.33	3
K30/90-6	+1.414	0	42.68	3
K30/90-7	0	-1.414	25	1.59
K30/90-8	0	+1.414	25	4.41
K30/90-9	0	0	25	3
K30/90-10	0	0	25	3
K30/90-11	0	0	25	3

Run 1 – 4 = 2^2 factorial design;
Run 5 – 8 = axial points of central composite design;
Run 9 – 11 = center points of central composite design.

Table 8.   Responses and their constraints in response surface methodology

| Response | Constraints | | | | Criteria of USP 28[a] (%) |
	Low	Target	High	Goal	
For 24 h-CPOP					
$Y_{1.5}$ drug release (%) at 1.5 h	0	15	30	Target	< 30
Y_4 drug release (%) at 4 h	35	45	60	Target	35–60
Y_8 drug release (%) at 8 h	55	70	80	Target	55–80
Y_{14} drug release (%) at 14 h	70	90	95	Target	70–95
Y_{24} drug release (%) at 24 h	81	110	110	Maximize	81–110
For 12 h-CPOP					
Y_1 drug release (%) at 1 h	0	10	20	Target	< 20
Y_3 drug release (%) at 3 h	20	30	45	Target	20–45
Y_6 drug release (%) at 6 h	45	60	80	Target	45–80
Y_{12} drug release (%) at 12 h	80	100	100	Maximize	> 80

[a] Based on the criteria of *Propranolol Hydrochloride Extended-Release Capsules*, USP 28 (119)

2.2.1. Effects of PVP content and membrane thickness on drug release

To determine the effects of the PVP content and the membrane thickness on drug release, core tablets were coated with 3% w/v cellulose acetate in acetone:isopropyl alcohol (3:1) solution containing PVP as pore formers at the contents of 7.33% to 42.68% by weight based on cellulose acetate to obtain 1.59% to 4.41% additional weight, respectively, as described in Table 7. The range of each independent variable was predetermined in the preliminary experiments. All coatings were performed in the same manner as described above.

2.2.2. Effects of PVP molecular weight on drug release

The core tablets were coated with a mixture of coating solution containing two molecular weights of PVP, i.e., 50 000 (PVP K30) or 1 000 000 (PVP K90), as pore former at the conditions as shown in Table 7 in order to evaluate the effect of the molecular weight of PVP on drug release.

3. Evaluation of propranolol core tablets

Propranolol core tablets were examined for their physical properties, i.e., average weight, hardness and friability. The hardness and friability of core tablets were considered critical parameters since the core tablets had to withstand the tumbling motion of tablet beds in the pan coater. Disintegration time, drug dissolution and content were determined to ascertain that they have appropriate properties for the further study.

3.1. Weight variation

Weight variation was determined by weighing 20 tablets individually. The average weight and their standard deviation were calculated.

3.2. Thickness, diameter and hardness

Ten tablets were randomly sampled and individually measured their thickness, diameter and hardness using a multipurpose measuring device. Their means and standard deviations were reported.

3.3. Friability

Approximately 6.5 g of tablets were accurately weighed and then loaded into a Roche type friabilator. The drum was rotated at 25 rpm for 4 min. Loss of weight with respect to the initial value was calculated as percent friability.

3.4. Disintegration test

The determination was based on USP 28 method for uncoated tablets using disintegration apparatus USP type. Six tablets from each preparation were tested for their disintegration time using water as a disintegration medium at the temperature of 37 ± 2 °C. Means and standard deviations of six tablets were calculated.

3.5. Content uniformity

Content uniformity was determined with ten tablets individually. Each tablet was powdered and transferred into a 100-mL volumetric flask, added with 70 mL of methanol and sonicated for 30 min. Then, the volume was adjusted with methanol to 100 mL. A portion of the solution was filtered through a filter paper and diluted with methanol to obtain a solution containing about 40 μg of propranolol hydrochloride per mL. The absorbance of propranolol in the solution was measured with a 1-cm cell at the wavelength of 288 nm by a UV/VIS spectrophotometer using methanol as a blank. The absorbance was compared with the standard curve of propranolol hydrochloride in methanol and percent drug content was calculated.

4. *In vitro* dissolution of propranolol core tablets

4.1. Calibration curve of propranolol HCl in pH 1.2 medium

An accurate weight of 200 mg of propranolol HCl was transferred to a volumetric flask and dissolved in pH 1.2 buffer to achieve the concentration of 2 mg/mL. Appropriate dilutions with pH 1.2 buffer were made to obtain a series of standard solutions between 40 ang 120 μg/mL. An absorbance of each standard solution was determined by a UV spectrophotometer at the maximum absorption wavelength of 318 nm. The pH 1.2 buffer was used as a blank.

4.2. Dissolution of propranolol core tablets

The dissolution test was performed by a USP apparatus 1 (basket type) connecting with a UV/visible spectrophotometer equipped with six 1-cm flow cells and a six-channel peristaltic pump at a temperature of 37 ± 0.5 °C. The procedure

employed for the drug release was modified from USP 28, *Propranolol Hydrochloride Extended-Release Capsules*. A 900 mL of pH 1.2 buffer was used as a dissolution medium. The basket rotation speed was set at 50 rpm. The drug release was determined at 318 nm every 5 min for 1 h. The percentage of drug release was calculated according to the standard curve of propranolol HCl in pH 1.2 buffer.

5. Evaluation of propranolol osmotic pump tablets

Weight variation, thickness, diameter and hardness of propranolol osmotic pump tablets were examined with the method described in the sections 3.1 and 3.2.

6. *In vitro* drug release studies of osmotic pump tablets

6.1. Calibration curve of propranolol HCl

6.1.1. In pH 1.2 medium

The standard curve of propranolol HCl in pH 1.2 buffer was prepared as described in the section 4.1.

6.1.2. In pH 6.8 medium

The standard curve of propranolol HCl in pH 6.8 buffer was prepared as described in the section 4.1 excepted that pH 6.8 buffer was used instead of pH 1.2 buffer.

6.1.3. In pH 7.5 medium

The standard curve of propranolol HCl in pH 7.5 buffer was prepared as described in the section 4.1 excepted that pH 7.5 buffer was used instead of pH 1.2 buffer.

6.2. Determination of drug release from propranolol osmotic pump tablets

The dissolution test was performed as described in the section 4.2. The procedure and criterion employed for the drug release was based on USP 28, according to *Propranolol Hydrochloride Extended-Release Capsules* as described in Tables 9 and 10. The experiment was conducted in two stages, initially pH 1.2 buffer was used as a dissolution medium, then the medium was changed to either pH 6.8 or pH 7.5 medium based on the criterion applied. The dissolution profiles were constructed by plotting the average percent release of propranolol HCl against time. Six tablets of each formulation were determined. The mean and SD of percent drug dissolved were calculated.

Table 9. Dissolution procedures for propranolol osmotically-controlled release tablets (119)

	24 h-CPOP	**12 h-CPOP**
Drug Release (USP 28)	*Test 1*	*Test 2*
Basket rotation speed	100 rpm	50 rpm
Wavelength	318 nm	318 nm
First stage		
time	1.5 h	1 h
medium	900 mL; pH 1.2 buffer	900 mL; pH 1.2 buffer
Second stage		
time	22.5 h	11 h
medium	900 mL; pH 6.8 buffer	900 mL; pH 7.5 buffer

Table 10. Acceptance criteria of drug dissolved for propranolol osmotically-controlled release tablets (119)

	Time (h)	Drug dissolved (%)
For 24-h CPOP	1.5	not more than 30%
	4	between 35% and 60%
	8	between 55% and 80%
	14	between 70% and 95%
	24	between 81% and 110%
For 12-h CPOP	1	not more than 20%
	3	between 20% and 45%
	6	between 45% and 80%
	12	not less than 80%

Release profiles of various formulations were compared using model independent method, which is the calculation of 'similarity factor' f_2 that is more sensitive for dissolution profile dissimilarity than the 'difference factor' f_1 (120). After introduction of this factor by Moore and Flanner (121), it has been adopted by the Center for Drug Evaluation and Research (US FDA) and by Human Medicines Evaluation Unit of the European Agency for the Evaluation of Medicinal Products (EMEA) as a criterion for the assessment of the similarity between two dissolution profiles. It is included in various guidance documents (86, 95). The equation for calculating f_2 is as follows:

$$f_2 = 50 \cdot \log\left\{\left[1 + \frac{1}{n}\sum_{t=1}^{n}(R_t - T_t)^2\right]^{-0.5} \times 100\right\} \qquad [4]$$

where R_t and T_t are percent drug dissolved at time t from the reference and test products, respectively. The two release profiles were considered to be similar, if f_2 value was more than 50 (between 50 and 100). For the calculation of f_2 values, only one data point was taken into consideration after 85% drug released (122).

6.3. Effect of pH of dissolution media on drug release

Drug releases of the optimized formulations of CPOPs with either PVP K30 or K90 containing membrane in different pH media, i.e., pH 6.8, pH 7.5 and two-stage media with pH 1.2/pH 6.8, were compared using dissolution apparatus at 50 rpm for 24 h, as described in Table 9; *Drug Release Test 1*.

6.4. Effect of agitation intensity on drug release

To evaluated the effect of agitation intensity, drug release studies of the optimized formulations were performed at different rotational speeds, i.e., 50, 100 and 150 rpm, using dissolution apparatus in two-stage dissolution media accordingly *Drug Release Test 1* for 24 h.

6.5. Effect of osmolarity of dissolution media on drug release

To study the influence of osmolarity on drug release, drug release studies of the optimized formulation of each PVP type were performed additionally in the media of different osmotic pressure, i.e., 0, 0.5, 1 and 2 osm. Sodium chloride (osmotically effective solute) was added in the dissolution medium in order to increase the osmotic pressure of the medium (123). The dissolution was carried out in 900 mL of phosphate buffer pH 6.8 at a basket rotation speed of 100 rpm at 37 ± 0.5 °C for 24 h.

6.6. Kinetic analysis

In order to characterize the release kinetic of the drug from the optimized CPOP, the experimental data were fitted to the zero-order, first-order and Higuchi equations as shown in Table 11.

7. Characterization of tablet membrane

7.1. Surface morphology

In order to evaluate the surface morphology of osmotic pump tablets, the surfaces of the tablets both before and after the dissolution test was studied by scanning electron microscopy (SEM) and atomic force microscopy (AFM). Formulations K30/K90-1 to K30/K90-9 of each PVP type were determined. Surface pore diameters were measured by visual inspection of SEM pictures and of line profiles of AFM pictures which were generated by a nanoscope's image processing program. All line profiles created along selected lines in the images were helpful for the analysis of surface pore characteristics and of single pores. Each membrane was measured for 50 pores (124). The smallest and largest diameters and the mean values, including their relative standard deviations of all 50 pores were determined.

7.2. Membrane porosity

To determine the porosity of semipermeable membrane, the weight of the membrane after dissolving a core part were determined. Fifty core tablets were weighed before and after coating with various formulations, at different PVP content (7.33, 25, 42.68%), in order to indicate a weight of solely membrane. Then, they were subjected to the dissolution test in water which was changed periodically until the core tablet dissolved completely. In case that the core part was remained, the membrane was then cut in order to make complete dissolution of the core. All 50 membranes of tablets were pooled and dried at 50 ºC for 24 h before accurately weighing the residual weight. Mean of membrane porosity and their relative standard deviations were calculated from 3 determinations.

Table 11. Mathematical models used to describe drug dissolution curves

Models	Equations
Zero order	$Q_t = Q_0 + K_0 t$
First order	$\ln Q_t = \ln Q_0 + K_1 t$
Higuchi	$Q_t = K_H \sqrt{t}$

8. Optimization of the formulation

In this study, the optimization of the PVP concentration and the membrane thickness to achieve the appropriate drug release was assessed by the response surface curves. The contour plots of each response variable were superimposed and the optimized condition was presented as a non-shaded area. All requirements regarding USP 28 criteria were also taken into account.

Part II: Swelling Properties of Ternary Mixtures of Chitosan, Polyacrylic Acid and Hydroxypropyl Methylcellulose

In this present study, the alternative hydrogel of chitosan (CS)-polyacrylic acid (PAA):hydroxypropyl methylcellulose (HPMC) ternary mixtures was introduced as a polymeric osmotic agent. Hence, in this part, the objectives were to prepare the different mixtures of CS-PAA:HPMC hydrogel by varying their ratios; and to evaluate their swelling behavior, which was the important factor in controlling drug release. Then, the selected polymer proportion was incorporated into propranolol osmotically controlled-release formulations and drug release based on the compendial criteria (119) were determined in the following part.

9. Preparation of interpolymer complexes of CS and PAA
Effects of molecular weight of CS and ratio of CS:PAA

To determine an appropriate molecular weight of CS and optimum ratio of CS:PAA for CS-PAA interpolymer complexes, the studies were conducted with three molecular weights of CS, i.e., low (150 000; L-CS), medium (400 000; M-CS) and high (600 000; H-CS), and with three ratios of polymer blends, i.e., CS:PAA; 1:2, 1:1, and 2:1. The polymer blends were prepared by dissolving CS and PAA in 1 M acetic acid (3.3% w/v) and neutralized with 3 M sodium hydroxide to reach a pH of 5.0. The mixtures were kept at room temperature overnight and then washed with distilled water. The wet mass was dried at 50 °C for 24 h and pulverized to fine powder.

10. Preparation of ternary mixture of CS-PAA:HPMC hydrogel composition
Effects of proportion of ternary hydrogel composition

The optimum ratio of CS:PAA complex was chosen in order to study the effect of HPMC incorporated on the swelling properties of the complex. The ternary mixture of CS-PAA:HPMC hydrogel were prepared by varying the proportions of complex:HPMC compositions, i.e., 1:0, 0.75:0.25, 0.5:0.5, 0.25:0.75, and 1:0. The ternary mixture was prepared by mixing CS:PAA hydrogel and HPMC solution in

water (5% w/v) homogeneously. The blends were dried at 50 °C for 24 h and pulverized to fine powder.

11. Fourier transform infrared (FTIR) spectrophotometry studies

The powdered hydrogels were examined by FTIR spectrophotometer to identify whether the new functional group introduced into the polymer. The KBr method was used. Each sample was mixed with KBr powder in the weight ratio of 1:100 using mortar and pestle. The mixture was filled in the die and compressed at 5 kN for 1 min. The compressed disc was placed in the sample holder and scanned from 4000 to 400 cm^{-1}.

12. Evaluation of swelling characteristics

The powdered CS-PAA and CS-PAA:HPMC hydrogels were studied. A 500 mg of hydrogels was directly compressed to flat-faced tablet of 13-mm diameter × 3-mm thickness by hydraulic press at the pressure of 296 MPa for 1 min. The hydrogel tablets were further evaluated on swelling characteristics.

12.1. Swelling force

A comparison of swelling performance of CS with different blend ratios was carried out using a self-built swelling device where the sample disc was placed inside a cylinder on a 20-mesh sieve, as illustrated in Figure 6. The sample, flat-faced tablet, was placed on the 20-mesh sieve. A punch was placed on the top of the sample and contacted to a probe connecting with a texture analyzer-load cell. The swelling medium (distilled water) at room temperature was added up to the level of the sieve. Upon the medium flew through the sieve, the swelling sample started to swell. The punch was kept in a fixed position during the test and the exerted swelling force was recorded as a function of time. The pre-test speed, the test speed and the post-test speed of the punch were set up at 0.5, 0.5 and 10 mm/s, respectively, with an acquisition rate of 0.1 point. The trigger force was 5 g and the distance was 0.1 mm. The swelling forces were investigated for 6 h. Three repetitions were obtained for each formulation.

12.2. Swelling ratio

The swelling study was examined using a dissolution testing apparatus 2. The pre-weighted tablets were immersed in 500 mL distilled water at $37 \pm 0.5\,°C$. The paddle rotation speed was set at 25 rpm. At every 15-min interval, the samples were removed from swelling medium and blotted on a piece of filter paper to remove excess surface water prior to weighing. The swelling ratio (S_W) was determined according to the following expression:

$$S_W = W_S / W_D \qquad\qquad [5]$$

where W_S is the weight of swollen tablet and W_D is the initial weight of tablet (61). The data represents mean $\pm$ SD from three determinations of each formulation. The studies were carried out for 6 h.
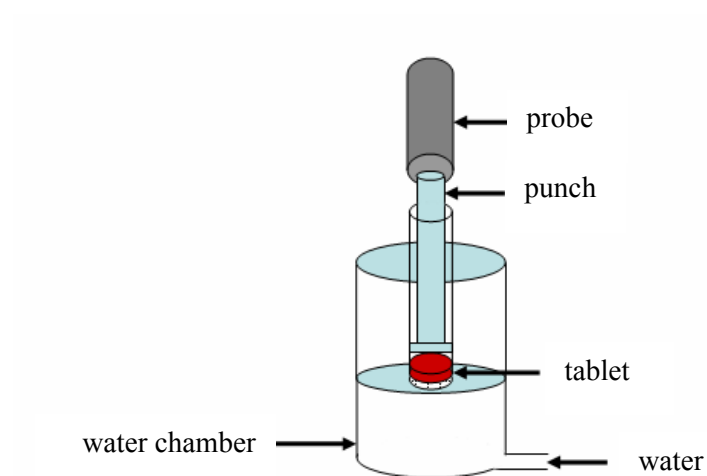
Figure 6.   Swelling-device for the measurement of the swelling force developed by
the swelling sample

Part III: **Use of Ternary Mixtures of CS-PAA:HPMC as Osmotic Agent for the Development of Controlled-Porosity Osmotic Pump Tablets**

The aims of this part were to evaluate the application of ternary mixtures of CS-PAA:HPMC as an osmogent in the osmotic pump formulations *in vitro* and *in vivo*. The selected ternary mixtures of hydrogel were used as polymeric osmotic agent to prepare two types of propranolol controlled-porosity osmotic pumps, i.e., monolithic and bilayered tablets (22, 125). Drug release based on criteria of USP 28 was determined.

13. Preparation of propranolol core tablets containing CS-PAA:HPMC

13.1. Monolithic tablets

Compositions of each formulation are listed in Table 12. Each tablet comprised 80 mg propranolol as an active ingredient, 10–30 mg polymeric hydrogels/ternary mixtures of CS-PAA:HPMC as an osmogent, 80 mg lactose and 132.5–102.5 mg starch as fillers, 2% PVP K30 in ethanol as a binder, and 0.5% magnesium stearate as a lubricant. Additionally, a core tablet without polymeric agent was formulated for comparison (coded as C-0). The tablets were prepared by a wet granulation process and compressed on a single punch press using 9 mm punch and die tooling to the weight of 300 mg and the hardness of approximately 80 N. The compressed tablets were stored in well-closed containers prior to coating.

13.2. Bilayered tablets

Bilayered tablets were prepared manually by double compression method. A 182 mg-drug layer comprised 80 mg propranolol, 48 mg lactose and 53.1 mg starch as fillers, 2% PVP K30 in ethanol as a binder, and 0.5% magnesium stearate as a lubricant. A 118 mg-osmotic layer comprised 10–30 mg polymeric hydrogel as an osmogent, 32 mg lactose and 85.4–55.4 mg starch as fillers, 2% PVP K30 in ethanol as a binder, and 0.5% magnesium stearate as a lubricant. Both layers were separately prepared by a wet granulation process. Then, the granules were compressed on a single punch press using 9 mm punch and die tooling to the weight of 300 mg and the

hardness of approximately 80 N. The compressed tablets were stored in well-closed containers prior to coating. Three formulations were prepared as described in Table 13.

14. Preparation of propranolol osmotic pump tablet

Core tablets from the sections 13.1 and 13.2 were coated with a mixture of 3% w/v cellulose acetate in acetone:isopropyl alcohol (3:1) coating solution containing PVP K30 (60% w/w with respect to cellulose acetate) as a pore former and PEG 400 (10% w/v) as a plasticizer to obtain 8 to 16% weight gain in order to determine the effect of membrane weight increase on the drug release from CPOPs. All coatings were performed by the perforated pan coater under the conditions as described in the section 2.1.

15. Evaluation of propranolol core tablets

Propranolol core tablets were evaluated for their physical properties to ascertain that they have properties appropriate for further study as previously described in the section 3.

16. Evaluation of propranolol osmotic pump tablets

Weight variation, thickness, diameter and hardness of propranolol-polymer osmotic pump tablets were examined by the method as previously described in the section 3.

17. *In vitro* drug release studies of propranolol-polymer osmotic pump tablets

The dissolution tests were performed as described previously in the section 6. The procedure and criteria employed for the drug release were based on USP 28 according to *Propranolol Hydrochloride Extended-Release Capsules, Test 2* (119) as described in Tables 9 and 10. The dissolution profiles were constructed by plotting the average percent release of propranolol against time. Six tablets of each formulation were determined. The mean and SD of percent drug dissolved were calculated.

Table 12. Core composition of monolithic tablets

Composition (mg)	Formulation		
	MN-10	MN-20	MN-30
Propranolol HCl	80	80	80
Polymeric hydrogel	10	20	30
Lactose	80	80	80
Starch	122.5	112.5	102.5
PVP K30	2%	2%	2%
Mg stearate	0.5%	0.5%	0.5%

Table 13. Core composition of bilayered tablets

Composition (mg)	Formulation		
	BI-10	BI-20	BI-30
Drug layer			
Propranolol HCl	80	80	80
Lactose	48	48	48
Starch	53.1	53.1	53.1
PVP K30	2%	2%	2%
Mg stearate	0.5%	0.5%	0.5%
Polymer layer			
Polymeric hydrogel	10	20	30
Lactose	32	32	32
Starch	75.4	65.4	55.4
PVP K30	2%	2%	2%
Mg stearate	0.5%	0.5%	0.5%

18. *In vivo* evaluation of the developed propranolol osmotic pump tablets

The formulations of propranolol controlled-porosity osmotic pump tablet which provided the optimum drug release via the *in vitro* studies, i.e., bilayered tablet CPOPs containing 20 mg of CS-PAA:HPMC at the coating level of 8 and 12%, were selected for the *in vivo* studies. *In vivo* studies were performed in nine female pigs. The plasma drug concentration was analyzed using a validated HPLC method. The pharmacokinetic parameters were compared with the administrations of commercially available immediate-release propranolol tablets as a reference formulation. Cumulative percent absorbed *in vivo* was compared to *in vitro* release profile. Pharmacokinetic parameters were obtained by a noncompartmental method.

18.1. Animal ethics approval

For study involving pigs, approval was obtained from the Animal Ethics Committee of the Institute of Medical and Veterinary Science (Adelaide, Australia), in accordance with the National guidelines of Australia.

18.2. Animals

Female White X Landrace pigs (weight between 22–35 kg; mean weight 27.6 kg) were employed in this study. They were purchased from Pig and Poultry Production Institute (Roseworthy, Australia). The study was carried out after the approval of the protocols by the Animal Ethics Committee. The pigs were housed individually in pens and maintained on a 12 h light–dark cycle. They were fed with a standard diet of commercially available pellets free from any medication (Powerfinish 800; Ridley Agriproducts, Pakenham, Australia). For a period of at least 1 week prior to the study, pigs were acclimatized to their new environment and to human contact. Water was allowed *ad libitum* at all times; however, food was withheld for 12 h prior to surgery and any treatment.

18.3. Study design and procedures

This study was subjected to a nine-subject randomized three-way crossover design. The sequences of the treatments are shown in Table 14. Nine pigs were received two formulations of self-manufactured, osmotically controlled release tablets, i.e., bilayered tablet CPOPs containing 20 mg of CS-PAA:HPMC with a coating level of 8% and 12%, and a commercial immediate release propranolol tablet. A washout period of 3 days separated each treatment. The dose of propranolol administered to

animals was 80 mg for *in house* CPOP tablets, and 40 mg for a rapid release formulation. It was reported that over the range of 40 to 160 mg there was a linear relationship of AUC with dose (111).

18.4. Surgery

Food, but not water, was withheld for 12 h prior to surgery. The animals were surgically catheterized as previously described (126). Briefly, ketamine (10 mg/kg) was injected intramuscularly for sedation before inducing general anesthesia with isoflurane (5% per min with oxygen at a rate of 4 L/min) via a face mask. When a satisfactory depth of anesthesia was achieved, the sedated pigs were placed in a dorsal position on a surgical table, and an endotracheal tube was inserted. The anesthesia was maintained by an isoflurane:oxygen mixture (2–2.5% per min with oxygen at a rate of 4 L/min); the respiration rate was monitored continuously during surgery. The right thoracic region was shaved and scrubbed clean using antiseptic skin cleanser and povidone-iodine was substantially applied over the area. The adjacent areas were covered with sterile dresses.

The right jugular vein was exposed to the larynx by making a skin incision of 6–8 cm followed by a dissection just lateral to the *M. sternomastoideus*. An approximate 3–4 cm section of vessel was freed from the surrounding tissue. The ligatures were placed on either end of the vessel and the cranial ligature tied off. A small incision was made into the cranial segment of the isolated vessel; a catheter tip was inserted in or just proximal to the right atrium for a length of 15–20 cm. Once in position, the coronary ligature was used to secure the catheter with the vessel and additional anchorage was provided by fastening to the cranial ligature. A trochlar was tunneled subcutaneously to exit the skin at the dorsal surface of the neck. The catheter was then threaded through the trochlar. The 15–20 cm free end of the catheter protruding from the neck was rolled into a loop, sutured into position and fitted with a three-way tap. Povidone-iodine was liberally applied over the suture sites. The anesthesia was discontinued and the animal was allowed to resume consciousness. Ketoprofen (3 mg/kg) was administered intramuscularly for analgesia, and enrofloxacin (5 mg/kg) was injected subcutaneously for prevention of post-operative infection.

Table 14. Assignment schedule for propranolol treatment

Sequence	Treatment period		
	I	II	III
1	A	B	C
2	C	A	B
3	B	C	A
4	A	B	C
5	C	A	B
6	B	C	A
7	A	B	C
8	C	A	B
9	B	C	A

Keys: A = 80 mg propranolol CPOPs at coating level of 8%

B = 80 mg propranolol CPOPs at coating level of 12%

C = 40 mg propranolol immediate release tablets.

18.5. Management of catheter patency

The catheter was flushed once daily with 10 mL of heparinized saline (10 units/mL) and catheter patency was maintained for a period of up to 2 weeks. Any sampling problems or thrombotic obstruction were usually cleansed by infusing 10 mL of heparinized saline into the catheter. In situations where this did not improve sampling, a sterile guide wire was used to alleviate the clot. In most cases, catheter patency was reduced, due to the positioning of the catheter within the vessel. Blood sample collection could be improved by an upward extension of the pig's head. In other cases, patency was improved by surgical repositioning or reinsertion of the catheter. Aseptic technique was always used to minimize catheter-related septicemia.

18.6. Blood sampling

Blood sampling was performed by an extension tube attached to the three-way tap to allow animal movement without affecting sampling. Prior to connecting a syringe to the extension tube, the port on the extension tubing was sprayed with 70% ethanol. Immediately before each sampling time, a 5 mL blood sample was removed from the catheter to eliminate residual blood/saline. Then, a 5 mL blood sample was taken and the initial aliquot was returned. After all, the catheter was flushed with 10 mL of heparinized saline (10 units/mL).

The blood samples were collected into heparinized containers at 0 (just before the propranolol dose) and at 0.5, 1, 1.5, 2, 2.5, 3, 3.5, 4, 4.5, 5, 5.5, 6, 8, 10, 12 and 24 h after the oral administration of two developed CPOPs. For a reference rapid release propranolol tablet, the blood sampling was scheduled at 0, 0.25, 0.5, 0.75, 1, 1.25, 1.5, 1.75, 2, 2.5, 3, 3.5, 4, 5, 6, 8 and 12 h. The plasma was separated by centrifugation at 3,000 rpm for 10 min at room temperature, and then kept frozen at -20 °C until assay.

18.7. HPLC conditions

The HPLC system consisted of a Shimadzu High pressure pump, a Shimadzu Fluorescence detector, a Shimadzu Auto injector and Thermo Hypersil CN 250 × 4.6 mm analytical column connected with a cyano guard column 10 × 4.6 mm. Chromatogram acquisition and evaluation were performed with Class VP v6.12 Chromatography Software (Shimadzu, Kyoto, Japan).

Instrumental Parameters:

Mobile phase	the deaerated mixture of 35:65 (v/v) acetonitrile– acetic acid containing triethylamine solution (0.1 mL of triethylamine in 1% acetic acid in water; pH 3.6)
Injection volume	90 µL
Flow rate	1 mL/min
Excitation wavelength	230 nm
Emission wavelength	340 nm
Temparature	ambient
Run time	26 min

18.8. Assay method

The modification of HPLC method with fluorescence detection (127) was used to analyze pig plasma samples. Briefly, to 250 µL plasma sample, 20 µL benzimidazole (10 µg/mL) solution in ultra-purified water (Milli-Q$^®$) was added as an internal standard (IS). Then, the plasma was extracted with 2 mL of n-heptane:dichloromethane (60:40, v/v) mixture. Extraction was carried out on a rotary mixer for a period of 20 min. Samples were then centrifuged for 10 min at 4,000 rpm to obtain phase separation. The organic upper layer was evaporated to dryness under nitrogen stream; the residue was reconstituted in 150 µL of the mobile phase. A 90 µL aliquot was injected into the HPLC system. The concentration of propranolol in plasma was determined based on the calibration curves constructed by plotting peak height ratio between propranolol and IS against a series of propranolol concentration.

All glassware was thoroughly cleaned and silanized with 5% (w/v) dimethyl-dichlorosilane in toluene, rinsed with toluene, followed by 100% methanol, and allowed to dry prior to use (127).

18.9. Stability of propranolol in plasma

It has been reported that propranolol was stable in plasma sample for at least 9 weeks at -20 °C (128). In this study, propranolol spiked plasma samples were kept at -20 °C for 12 weeks. Plasma propranolol contents at 3 concentrations in the range of expected concentrations, so called quality control (QC) samples (low, medium,

high; 2, 20, 40 ng/mL), were analyzed at 1, 2, 4, 8, and 12 weeks. Stability of propranolol in ultra-purified water stock solution was also determined.

18.10. Validation of analytical methods (129)

18.10.1. Separation and specificity

Separation and specificity of the analytical method were evaluated with regard to interference peaks from endogenous plasma constituents by inspecting the chromatograms and comparing their retention times with those of propranolol and IS. There must be no significant interference for propranolol and IS within the regions of interest for the lots of tested pig plasma.

18.10.2. Calibration of standard curve

Stock solutions of propranolol and IS were prepared at a concentration of 1 mg/mL in ultra-purified water as well as that of the stock solution of the QC samples. Daily working solution of propranolol and IS were then prepared with appropriate dilution of the stock solution to the concentration of 1 μg/mL and 10 μg/mL, respectively. To a 0.25 mL aliquot of propranolol working solution, 4.75 mL of drug free plasma were added to prepare a 50 ng/mL standard. By adding the 50 ng/mL standard to drug free plasma, six to eight different concentrations of calibration curve standards between 1 ng/mL and 50 ng/mL of propranolol in pig plasma were prepared and analyzed. The ratios of peak height of propranolol to IS were plotted as a function of propranolol concentrations; the drug content in unknown samples was determined by interpolation. Calibration curve with the coefficient of determination (r^2) of at least 0.99 was acceptable.

Low, medium, and high QC samples were also prepared in duplicate, with the concentrations of 2, 20 and 40 ng/mL, together with the calibration curve samples on each analysis.

18.10.3. Recovery

Extraction efficiency of an analytical method was evaluated at each QC concentration by comparing the peak height ratio of propranolol to IS in plasma after extraction with those obtained after direct injection of standards containing the same concentration of propranolol and IS in ultra-purified water. Recovery of the analyte need not be 100%, but the extent of recovery of an analyte and of the internal standard should be consistent, precise, and reproducible.

18.10.4. Precision and accuracy

Precision of the analytical method was assessed from the %CV values of analyzed drug concentration in spiked plasma samples. To determine within (intraday) and between-assay (interday) precision, three concentrations of QC levels of drug in plasma were prepared and analyzed. Duplicate determinations per concentration were assayed for 6 days; on day seven, six determinations per concentration were examined. Analyses by means of linear mixed-effects model approach (assay "day" as the random effect) was using R software version 2.5.1 (130, 131). This approach offers the within-subject correlations that often present in repeated measures data and supports the random effect as well as uses maximum likelihood estimation to estimate the parameters (General models estimate their parameters as if they were fixed). Moreover, it was employed to account for the unbalanced number of replicates across assay-days (duplicates for 6 days, and 6 replicates for a seventh assay day).

The accuracy of the assay procedure was calculated as percent accuracy of the mean value of the measured concentration and the true value for each QC concentration. The grand mean accuracy at each concentration examined was taken as the mean accuracy.

$$\%Accuracy = \frac{measured\ concentration}{actual\ concentration} \times 100 \qquad [6]$$

The acceptable precision and accuracy were %CV $\leq$ 15 and %Accuracy = 85–115%.

18.10.5. Lower limit of quantification

The lower limit of quantification (LLOQ) was defined as the lowest standard on the calibration curve at which the precision expressed by relative standard deviation (RSD, %CV) was within 20% and the accuracy expressed by a comparison between the measured and the true concentration was in the range 80–120%.

18.11. Pharmacokinetic parameters determination

Noncompartmental pharmacokinetic method was employed to determine the pharmacokinetic parameters of propranolol (132-134). The measured plasma concentrations were used to calculate the area under the plasma concentration–time curve and area under the first moment curve from time zero to the last concentration

time point, i.e., $AUC_{0\text{-last}}$ and $AUMC_{0\text{-last}}$, respectively. The $AUC_{0\text{-last}}$ and $AUMC_{0\text{-last}}$ were determined by the trapezoidal method, and those of from the last concentration time point to infinity were obtained by extrapolation using the following equation:

$$AUC_{0\text{-}\infty} = AUC_{0\text{-last}} + \frac{C_{last}}{k_e} \qquad [7]$$

$$AUMC_{0\text{-}\infty} = AUMC_{0\text{-last}} + \left(\frac{C_{last}t_{last}}{k_e} + \frac{C_{last}}{k_e^2} \right) \qquad [8]$$

The elimination rate constant k_e was estimated as the slope of the linear regression of the log-transformed plasma concentration values versus time data in the terminal phase. Typically 4 to 5 points, at least 3 points, were used to determine the terminal elimination rate constant. The terminal half-life ($t_{1/2}$) was estimated as $0.693/k_e$. The MRT was calculated as $AUMC_{0\text{-}\infty}/AUC_{0\text{-}\infty}$. The maximum plasma concentration (C_{max}), time to C_{max} (T_{max}), and time to absorb (T_{lag}) were observed directly from experimental data. Relative bioavailability of the test and reference formulations was calculated by comparing the $AUC_{0\text{-}\infty}$ of the respective formulations.

18.12. *In Vitro–In Vivo* Correlation (IVIVC)

The data generated in the pharmacokinetic study were used to develop the IVIVC (Level A). The relationship between percent *in vitro* dissolution represented as fraction drug dissolved (F_d) and the fraction of drug absorbed (F_a) *in vivo* was examined. The Wagner–Nelson method (135) was used to calculate the percentage of the propranolol dose absorbed profiles (77, 136, 137):

$$F_t = C_t + k_e AUC_{0\text{-}t} \qquad [9]$$

where F_t is the amount absorbed at time t, C_t is the concentration of drug in the plasma at time t, and k_e is the elimination rate constant. The elimination rate constant (k_e) was calculated from the mean plasma concentration–time profile after administration of immediate release tablets. The percent absorbed is determined by dividing the amount absorbed at any time by the plateau value, $k_e AUC_{0\text{-}\infty}$ and multiplying this ratio by 100:

$$F_a = \frac{F_t}{k_e AUC_{0\text{-}\infty}} \qquad [10]$$

$$\% \, \text{Dose absorbed} = \left(\frac{C_t + k_e \text{AUC}_{0\text{-}t}}{k_e \text{AUC}_{0\text{-}\infty}} \right) \times 100 \,. \tag{11}$$

Linear regression analysis was applied to the IVIV plots. The values of correlation coefficient (r^2), slope and intercept were calculated.

18.13. Statistical analysis of data

Statistical analysis for the comparison of $\text{AUC}_{0\text{-last}}$, $\text{AUC}_{0\text{-}\infty}$, C_{max}, T_{max}, T_{lag}, and MRT at the probability level of 0.05 was performed by one-way analysis of variance (ANOVA) and Student's *t*-test. All experimental results were expressed as mean ± SD values.

CHAPTER IV
RESULTS AND DISCUSSION

Part I: Influences of Membrane Variables on Characteristics of Propranolol Hydrochloride Controlled-Porosity Osmotic Pump Tablets

1. Propranolol core tablets

Propranolol core tablets were prepared by a wet granulation method. Each tablet comprised propranolol, fructose and lactose as osmogents, PVP K30 in ethanol as a binder, and magnesium stearate, talcum and colloidal silica as a lubricant system. A mixture of fructose:lactose (1:1) was used as an osmotic agent owing to its high osmotic pressure (18, 39) instead of sodium chloride, which is commonly used as an osmogent in osmotic pump systems (43, 51, 140, 141) as they are safe for patients with hypertension whose sodium chloride intake is restricted (138, 139).

The drug and osmogent were accurately weighed, passed through 40 mesh-sized sieves and blended. This mass was granulated using PVP K30 in ethanol (10% w/v) as a binder. Compression was performed by a single punch machine using 9 mm concave punches. Core tablets were examined for their physical properties, i.e., average weight, diameter, thickness, hardness, friability, disintegration time and drug content. The results are presented in Table 15. Tablet hardness and friability of core tablets were two important parameters that gave the appropriate characteristic of the core tablets to be able to withstand the tumbling motion of tablet beds in the pan coater.

Table 15. Physical properties of core tablets

Weight, mg (SD)	Thickness, mm (SD)	Diameter, mm (SD)	Hardness, N (SD)	DT, min (SD)	Content uniformity, % LA (SD)	Friability, (%)
(n=20)	(n=10)	(n=10)	(n=10)	(n=6)	(n=10)	
303 (7)	4.14 (0.08)	8.95 (0.02)	100 (9)	6.3 (0.7)	100.5 (0.3)	0.14

The amounts of propranolol dissolved in various media were quantitatively analyzed using UV spectrophotometry method. The calibration curves were plotted between the concentration of propranolol in the media, i.e., methanol and buffer solutions at pH of 1.2, 6.8 and 7.5, and the UV absorbance, as shown in Figures 7–10, respectively. Disintegration time, drug dissolution and drug content were also determined according to the criteria of USP 28 in order to ascertain that core tablets had appropriate properties for the further study. The average disintegration time was 6.3 ± 0.7 min and the drug dissolved in pH 1.2 buffer at 1 h was $86.3 \pm 2.3\%$, as shown in Figure 11. The uniformity of content was $100.5 \pm 0.3\%$ of the labeled amount. All properties of core tablets met the USP 28 requirements (119).

2. Propranolol osmotic pump tablets

2.1. Preliminary study

In any experiments, several experimental variables or factors may influence the results. In order to determine the experimental variables and interactions which may have significant influence on the result, a screening test is performed. The next step is to optimize the process concerning the effects of these significant variables and their interactions. However, the proper experimental domain has to be firstly clarified with the consideration of the limitation of each variable. In this study, the range of each variable was determined in a preliminary study for the further process optimization (142).

To produce propranolol controlled-porosity osmotic pump tablets (CPOPs), the core tablets were coated with 3% w/v cellulose acetate in acetone:isopropanol (3:1) solution containing PVP as a pore former. In the preliminary study, membrane variables were PVP types (PVP K30 and PVP K90) and contents (12.5, 25, 50% w/w based on cellulose acetate). The coating level was set at 3% membrane weight increase. Both types of PVP were examined for the effect of molecular weight of PVP on the drug release followed the same procedure.
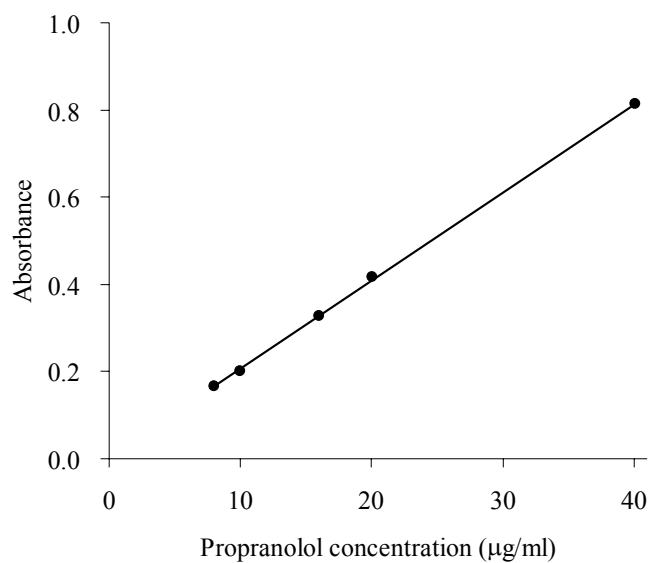
Figure 7.   Calibration curve of propranolol in methanol analyzed by UV spectrophotometry at 288 nm (y = 0.0203x + 0.0032, r^2 = 0.9997)
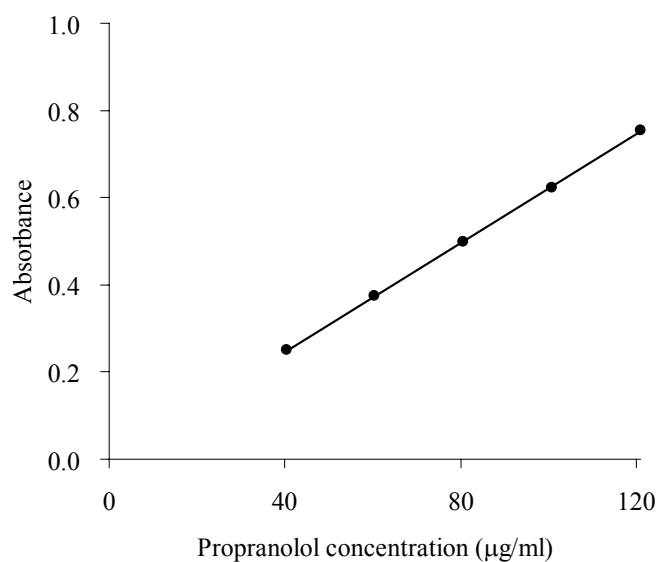
Figure 8.   Calibration curve of propranolol in pH 1.2 buffer analyzed by UV spectrophotometry at 318 nm (y = 0.0062x – 0.0028, r^2 = 0.9998)
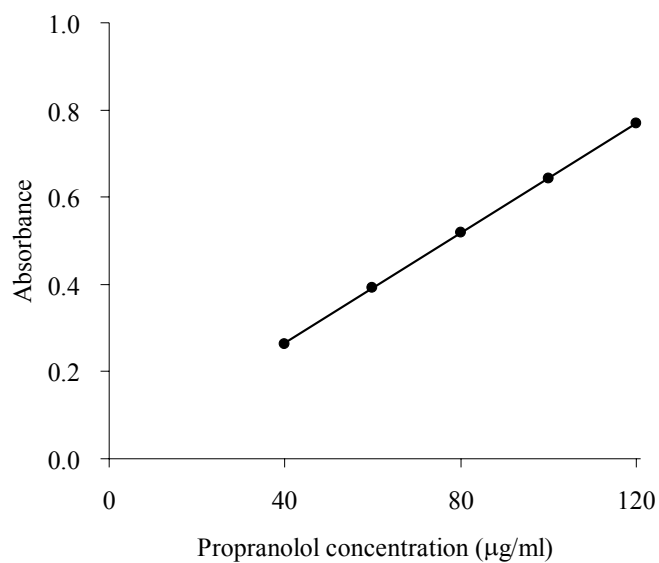
Figure 9.   Calibration curve of propranolol in pH 6.8 buffer analyzed by UV spectrophotometry at 318 nm (y = 0.0063x + 0.0118, r^2 = 0.9999)
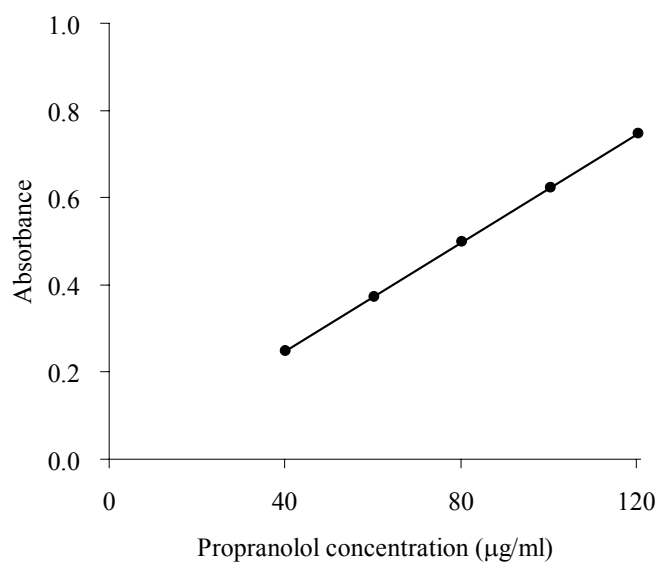
Figure 10. Calibration curve of propranolol in pH 7.5 buffer analyzed by UV spectrophotometry at 318 nm (y = 0.0062x − 0.0005, r^2 = 1)
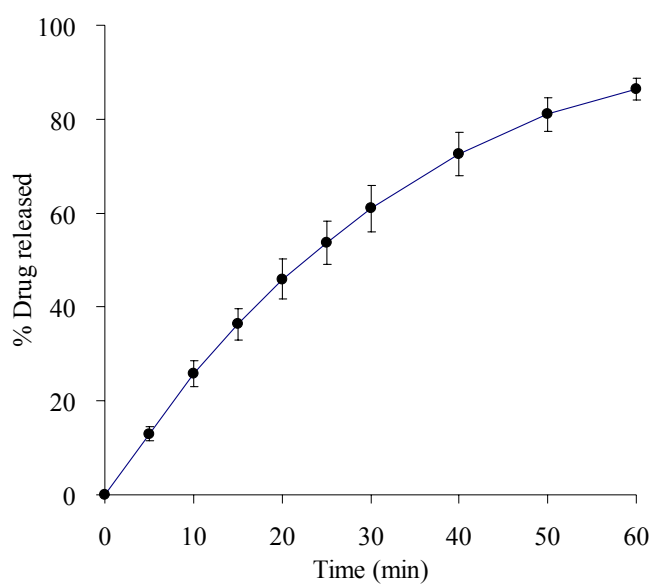
Figure 11. Release profile of propranolol core tablets in pH 1.2 buffer (n=6)

First, seven formulations were prepared in order to define the optimal range of each variable. One formulation did not contain PVP (coded as P-0) and the other each of three contained each type of PVP with various contents, i.e., 12.5, 25 and 50% w/w based on cellulose acetate. All coating formulations were observed as clear solution except the formulation of 50% PVP K90 in which the coating solution became cloudy. As PVPs are soluble in isopropanol but not in acetone which is a solvent for cellulose acetate, the amount of 50% PVP K90 could be above its solubility limit in this solvent mixture (143, 144). Thus only six formulations with clear coating solution were chosen for further studies and the amount of 50% PVP K90 was excluded from the appropriate range of this variable.

Surface morphology of coated tablets showed a smooth and uniform appearance. After coating, the tablets were dried overnight at 35 °C to remove residual solvent. Physical properties of six formulations of CPOPs in the preliminary studies are presented in Table 16. The effects of PVP content on the drug release through the membrane containing PVP K30 and PVP K90 are illustrated in Figures 12 and 13, respectively. The higher level of pore formers in the membrane, the higher drug release was observed. It was found that at PVP contents in the range of 12.5–50%, PVP K90 gave higher drug release than did PVP K30, as illustrated in Figure 14. The effects of PVP K30 level on the drug release from CPOP are in agreement with the earlier report (19). This study revealed that the drug release was dependent on the molecular weight of PVP.

Table 16. Physical properties of CPOPs in preliminary study

Formulations	Weight, mg (SD) (n=20)	Thickness, mm (SD) (n=10)	Diameter, mm (SD) (n=10)	Hardness, N (SD) (n=10)
P-0	314 (3)	4.31 (0.07)	8.99 (0.01)	152 (14)
P-K30-12.5	314 (3)	4.26 (0.04)	8.98 (0.02)	179 (15)
P-K30-25	315 (3)	4.25 (0.04)	9.01 (0.02)	188 (18)
P-K30-50	317 (3)	4.33 (0.07)	9.01 (0.02)	177 (23)
P-K90-12.5	313 (3)	4.28 (0.06)	9.00 (0.02)	157 (8)
P-K90-25	314 (3)	4.25 (0.04)	8.98 (0.02)	194 (16)
P-K90-50	n/a	n/a	n/a	n/a
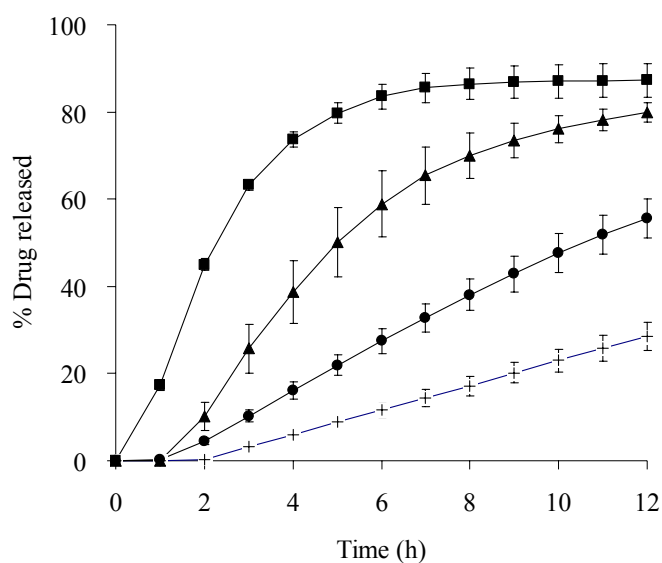
Figure 12. Effect of PVP content on drug release from CPOPs with membrane containing PVP K30 in preliminary study

Keys: +, 0%; ●, 12.5%; ▲, 25%; ■, 50%.
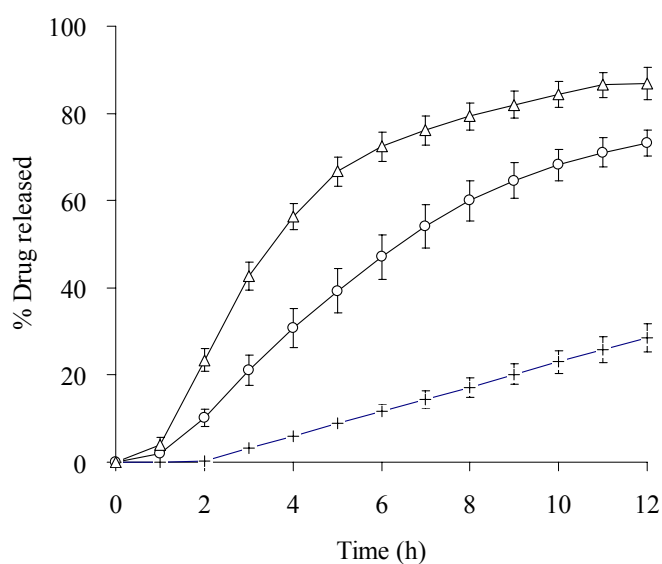
Figure 13. Effect of PVP content on drug release from CPOPs with membrane containing PVP K90 in preliminary study

Keys: +, 0%; ○, 12.5%; Δ , 25%.
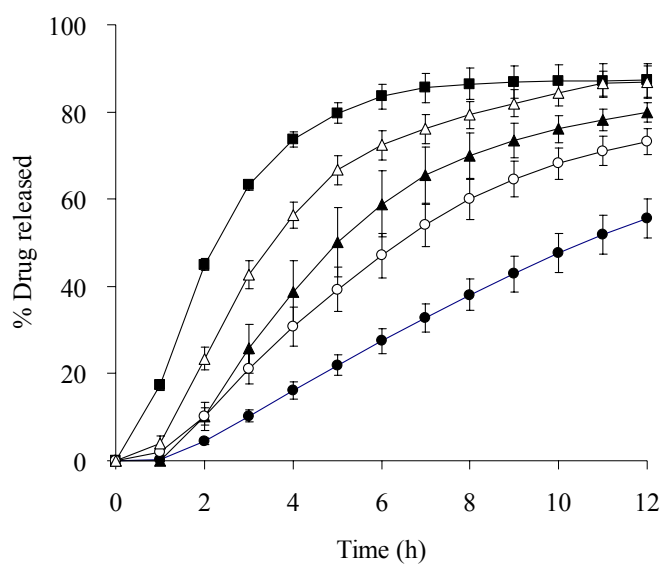
Figure 14. Effect of the molecular weight and content of PVP on drug release from
         CPOPs in preliminary study

         Keys: ○, 12.5%; Δ , 25%; □ , 50%.

                Closed symbol: PVP K30,
                Open symbol: PVP K90.

2.2. Experimental design

In order to achieve the optimal dosage form formulations, statistical optimization designs have been widely used, due to their powerful, efficient and systematic features which can shorten the time required for the development of pharmaceutical dosage forms, improves research and development work, and enhances reliability of performance (75-78, 145). In this study, formulation optimization for the development of once and twice daily dosage forms of propranolol CPOPs were conducted by a central composite design in order to assess the optimal drug release.

The molecular weight of PVP was assigned to a discrete variable. The other two membrane variables, i.e., level of pore forming agent and membrane weight increase, were designated continuous variables. Preliminary study provided the ranges of two independent variables, i.e., PVP content and membrane weight increase. The experimental domain of PVP content at a low level (-1) and a high level (+1) were 12.5 and 37.5%, respectively. While the domain of membrane weight increase at a low level and a high level were 2 and 4%, respectively.

Generally, a k-factor central composite design consists of 2^k-factorial runs, $2k$ axial runs and 3 to 5 center runs which are recommended for providing reasonably stable variance of predicted response in order to estimate the first- and second-order interaction terms of a polynomial. The design meets the requirement that every parameter in the mathematical model can be estimated from a practically small number of experiments (81). The experimental data were fitted to the following second-order polynomial:

$$Y_t = a + bX_1 + cX_2 + dX_1^2 + eX_2^2 + fX_1X_2 \qquad [12]$$

where Y_t are drug releases at various time t as response variables, X_1 and X_2 are PVP content and membrane weight increase, respectively, and a, b, c, d, e and f are the equation constants.

According to the 2-factor 2-level central composite design, experimental space was a symmetric and rotatable circle circumscribed about the factorial square with the equidistant design points from the center and a radius of α, 1.414 [$\alpha = (n_f)^{1/4}$, where n_f is the number of experiments in the factorial design]. The factorial design was performed at the low and high level of the membrane variables in order to evaluate the influence of these variables. The curvature of responses was demonstrated by the

experiments of the axial point where one variable was varied at the distance of ± 1.414 whereas the other variable was kept constant at the center point. Experimental domain for X_1 and X_2 could be ranged between 7.33% to 42.68% and 1.59% to 4.41%, respectively, as listed in Table 6. As a result of 2-factor central composite design, there were 11 experiments (2^2 factorial runs + 4 axial runs + 3 center runs) for each PVP type, as summarized in Table 7.

All experiments were conducted in a random sequence. The effect of a variable was the change in the response after changing the variable from the low level to the high level. The responses were percent drug release at various times.

3. *In vitro* drug release studies of osmotic pump tablets

After evaluation of physical properties of the coated tablets as expressed in Table 17, CPOPs were further investigated their release performances. The criteria employed for the drug release in both 24- and 12-h intervals were based on the monograph of *Propranolol Hydrochloride Extended-Release Capsules USP 28*, *Drug release Test 1* and *2*, respectively, as described in Table 10. According to those two criteria, the factor combinations in CPOPs containing PVP K30 and K90 as pore formers yielded different responses as presented in Tables 18–19 and Tables 20–21, respectively.

3.1. Effects of the PVP content on drug release

To study the effects of the level of pore former, core tablets were coated with a coating solution containing various PVP contents, i.e., 7.33%, 25%, and 42.68%. Figure 15 illustrate the dissolution profiles of propranolol CPOPs containing either type of PVP at various membrane weight increases, i.e., 2%, 3%, and 4%. The higher level of pore formers in the membrane, the higher drug release was observed. This finding was consistent with the preliminary results.

At 3% membrane weight increase, three levels of PVP contents were studied as 24- and 12-h release profiles; and the similarity factors (f_2) defined by US FDA (95) of their release profiles were interpreted. The f_2 values were found to be 13.0 and 17.7 (between PVP K30; 7.33 and 25%), 13.8 and 11.6 (between PVP K90; 7.33 and 25%), 10.7 and 15.8 (between PVP K30; 7.33 and 42.68%), 11.5 and 9.49 (between PVP K90; 7.33 and 42.68%), 46.4 and 57.9 (between PVP K30; 25.0 and 42.68%),

and 54.5 and 50.3 (between PVP K90; 25.0 and 42.68%), respectively. It was found that the similarity factors of the profiles between the low level (7.33%) and the center point (25%) indicated much more dissimilarity than those of the profiles between the high level (42.68%) and the center point (25%). It can be concluded that, at the higher level of pore formers where large openings are provided (further discuss later), the PVP content did not substantially affect the drug release than did at the lower level. This finding was confirmed by the coefficients of the equation as listed in Tables 22 and 23, which PVP contents represented positive signs for all responses. Drug release significantly increased with increasing level of PVP in the membrane ($p < 0.05$). Other researchers have also reported similar results regarding the level of pore forming agents (6-10, 19, 20). The effect of PVP K30 level on the drug release from CPOP is in agreement with the literature (19, 20).

3.2. Effects of membrane weight increase on drug release

To study the effects of membrane weight increase, core tablets were coated with cellulose acetate containing PVP semipermeable membrane to obtain different membrane weight increase, i.e., 1.59, 3.00, 4.41%. The decrease in drug release by increasing membrane weight increase was observed as illustrated in Figure 16. For 24- and 12-h profiles, the f_2 values were found to be 43.5 and 34.7   (between PVP K30; 1.59 and 3.00%), 55.3 and 46.0 (between PVP K90; 1.59 and 3.00%), 21.0 and 19.7 (between PVP K30; 1.59 and 4.41%), 46.5 and 19.7 (between PVP K90; 1.59 and 4.41%), 28.7 and 33.6 (between PVP K30; 3.00 and 4.41%), and 66.9 and 76.1 (between PVP K90; 3.00 and 4.41%), respectively. It was found that weight increase of the membrane containing PVP K90 did not much affect the release profile whereas, with the membrane containing PVP K30, different membrane thickness had much influence on the drug release. The reason might be large openings obtained by dissolved PVP K90 that yielded more effects on drug release than the effect of membrane thickness. In addition, the coefficients of the equation indicated negative signs for some responses. It can be concluded that increasing of membrane thickness decreased the drug release and resulted in a delayed profile.

3.3. Effects of the molecular weight of PVP on drug release

To study the effects of PVP molecular weight, formulations with different types of PVP (PVP K30 and PVP K90) at a constant PVP content and membrane

weight gains were prepared. As shown in Figures 15–16, at a given PVP content and membrane gain, PVP K90 gave higher dissolution than did PVP K30. For example, the f_2 values of 24- and 12-h release profiles from CPOP with 25% of PVP concentration and 3% membrane increase were found to be 47.9 and 38.6 (between PVP K30 and PVP K90), respectively. It might be due to larger openings produced on the membrane containing higher molecular weight of PVP K90 (146).

Table 17. Physical properties of CPOPs in response surface methodology

Formulations	Weight, mg (SD) (n=20)	Thickness, mm (SD) (n=10)	Diameter, mm (SD) (n=10)	Hardness, N (SD) (n=10)
K30-1	307 (5)	4.20 (0.05)	9.01 (0.02)	138 (10)
K30-2	309 (5)	4.21 (0.05)	9.01 (0.01)	143 (12)
K30-3	312 (3)	4.23 (0.04)	9.06 (0.01)	163 (17)
K30-4	313 (4)	4.24 (0.04)	9.07 (0.01)	155 (8)
K30-5	310 (4)	4.21 (0.03)	9.03 (0.01)	169 (12)
K30-6	310 (4)	4.23 (0.04)	9.05 (0.01)	156 (12)
K30-7	302 (3)	4.14 (0.04)	8.99 (0.01)	129 (5)
K30-8	315 (4)	4.26 (0.05)	9.07 (0.02)	186 (13)
K30-9	311 (5)	4.22 (0.09)	9.02 (0.02)	152 (30)
K30-10	310 (4)	4.21 (0.04)	9.02 (0.01)	150 (10)
K30-11	309 (3)	4.21 (0.02)	9.01 (0.01)	166 (11)
K90-1	304 (6)	4.16 (0.08)	9.00 (0.02)	128 (9)
K90-2	308 (5)	4.19 (0.06)	9.03 (0.01)	136 (10)
K90-3	315 (8)	4.25 (0.06)	9.06 (0.01)	184 (6)
K90-4	316 (6)	4.25 (0.07)	9.11 (0.01)	204 (11)
K90-5	310 (9)	4.27 (0.10)	9.03 (0.02)	169 (12)
K90-6	312 (6)	4.20 (0.07)	9.08 (0.01)	166 (10)
K90-7	304 (6)	4.17 (0.08)	9.00 (0.01)	135 (9)
K90-8	312 (5)	4.24 (0.06)	9.11 (0.02)	175 (13)
K90-9	312 (9)	4.23 (0.08)	9.05 (0.01)	150 (11)
K90-10	311 (7)	4.21 (0.05)	9.03 (0.01)	160 (9)
K90-11	310 (4)	4.22 (0.02)	9.02 (0.01)	175 (10)

Table 18. Drug release of CPOPs with membrane containing PVP K30 accordingly *Drug Release Test 1* (SD, in parentheses; n=6)

Run	X_1	X_2	Drug released (%) at time t h					
			$Y_{1.5}$	Y_4	Y_8	Y_{14}	Y_{24}	
K30-1	-1	-1	5.95 (0.51)	19.63 (1.42)	43.80 (2.53)	69.81 (2.54)	82.81 (1.97)	
K30-2	+1	-1	32.20 (0.85)	78.43 (1.69)	96.44 (1.72)	98.99 (1.72)	99.56 (1.72)	
K30-3	-1	+1	0.05 (0.02)	9.04 (0.73)	26.16 (1.58)	51.17 (2.58)	70.57 (2.61)	
K30-4	+1	+1	18.52 (0.85)	59.73 (1.69)	81.82 (2.31)	92.48 (2.90)	96.50 (1.77)	
K30-5	-α	0	0.50 (0.15)	5.20 (1.53)	15.51 (1.88)	31.65 (2.52)	54.02 (3.20)	
K30-6	+α	0	31.57 (2.32)	76.36 (1.93)	91.29 (1.12)	96.66 (1.23)	96.78 (1.50)	
K30-7	0	-α	31.07 (0.84)	81.09 (1.87)	92.76 (1.70)	99.21 (1.65)	101.65 (1.64)	
K30-8	0	+α	4.48 (1.09)	21.93 (2.15)	48.78 (2.05)	72.49 (1.93)	82.87 (1.37)	
K30-9	0	0	17.22 (0.96)	53.01 (2.11)	83.12 (2.08)	93.18 (1.87)	100.10 (1.82)	
K30-10	0	0	18.07 (1.63)	54.37 (2.96)	84.51 (2.31)	95.61 (1.99)	101.79 (1.97)	
K30-11	0	0	19.15 (2.87)	55.76 (3.29)	86.77 (3.04)	96.25 (2.36)	100.50 (2.66)	
Criteria of USP 28			≤30	35–60	55–80	70–95	81–110	

Table 19. Drug release of CPOPs with membrane containing PVP K30 accordingly *Drug Release Test 2* (SD, in parentheses; n=6)

Run	X_1	X_2	Drug released (%) at time t h			
			Y_1	Y_3	Y_6	Y_{12}
K30-1	-1	-1	2.43 (0.54)	17.43 (2.13)	38.12 (3.10)	69.94 (2.08)
K30-2	+1	-1	26.81 (5.65)	71.40 (8.74)	84.18 (5.12)	87.86 (2.18)
K30-3	-1	+1	0.00 (0.02)	7.29 (0.78)	18.74 (1.58)	42.86 (3.26)
K30-4	+1	+1	11.24 (1.49)	49.85 (6.38)	73.96 (4.08)	84.41 (4.38)
K30-5	-α	0	0.45 (0.07)	5.87 (0.53)	13.32 (0.96)	29.63 (2.33)
K30-6	+α	0	12.53 (1.41)	49.12 (2.32)	71.29 (2.90)	81.16 (3.28)
K30-7	0	-α	22.46 (2.37)	69.53 (5.50)	84.26 (2.35)	88.37 (1.19)
K30-8	0	+α	1.87 (0.46)	16.92 (1.26)	39.00 (2.90)	68.84 (2.59)
K30-9	0	0	8.17 (0.83)	37.88 (1.66)	67.22 (1.81)	82.66 (2.01)
K30-10	0	0	8.13 (0.53)	39.43 (1.03)	69.06 (2.73)	84.38 (3.14)
K30-11	0	0	7.80 (1.39)	40.14 (2.42)	72.15 (4.78)	86.71 (3.01)
Criteria of USP 28			≤20	20–45	45–80	80–100

Table 20. Drug release of CPOPs with membrane containing PVP K90 accordingly *Drug Release Test 1*

(SD, in parentheses; n=6)

Run	X_1	X_2	Drug released (%) at time t h					
			$Y_{1.5}$	Y_4	Y_8	Y_{14}	Y_{24}	
K90-1	-1	-1	7.52 (0.65)	26.52 (2.65)	55.39 (5.59)	76.04 (2.63)	84.35 (0.79)	
K90-2	+1	-1	45.41 (2.59)	85.82 (2.27)	95.70 (2.25)	97.63 (2.23)	97.72 (2.23)	
K90-3	-1	+1	0.30 (0.29)	10.57 (2.74)	29.12 (5.02)	56.19 (5.93)	70.94 (4.78)	
K90-4	+1	+1	22.42 (1.88)	67.30 (6.06)	87.43 (4.03)	93.92 (2.97)	95.42 (3.31)	
K90-5	-α	0	2.10 (0.05)	9.36 (0.82)	22.21 (1.53)	42.97 (1.78)	63.53 (2.16)	
K90-6	+α	0	42.89 (2.74)	86.65 (2.36)	94.31 (1.60)	95.52 (1.47)	97.08 (1.59)	
K90-7	0	-α	44.56 (2.52)	84.68 (2.36)	92.31 (1.94)	93.60 (2.12)	93.60 (2.12)	
K90-8	0	+α	22.64 (2.53)	69.41 (4.77)	90.08 (1.62)	98.00 (1.90)	99.22 (1.92)	
K90-9	0	0	29.21 (1.00)	73.69 (2.54)	91.72 (1.33)	94.05 (1.18)	95.09 (1.33)	
K90-10	0	0	30.34 (0.88)	74.99 (1.84)	92.18 (2.14)	95.88 (2.13)	96.93 (2.05)	
K90-11	0	0	31.11 (1.43)	75.12 (3.02)	93.64 (2.74)	96.73 (2.40)	97.73 (2.11)	
Criteria of USP 28			≤ 30	35–60	55–80	70–95	81–110	

Table 21. Drug release of CPOPs with membrane containing PVP K90 accordingly *Drug Release Test 2*

(SD, in parentheses; n=6)

Run	X_1	X_2	Drug released (%) at time t h			
			Y_1	Y_3	Y_6	Y_{12}
K90-1	-1	-1	4.98 (0.82)	27.41 (1.85)	50.78 (1.91)	69.07 (1.76)
K90-2	+1	-1	25.01 (1.35)	74.85 (2.97)	87.68 (3.11)	89.36 (3.35)
K90-3	-1	+1	0.07 (0.05)	7.47 (0.70)	19.72 (2.40)	46.62 (3.90)
K90-4	+1	+1	9.73 (1.27)	56.75 (2.24)	79.84 (2.33)	85.90 (2.32)
K90-5	-α	0	0.46 (0.07)	5.77 (0.65)	14.38 (1.25)	32.91 (2.34)
K90-6	+α	0	25.22 (1.20)	76.28 (4.80)	88.52 (1.65)	90.54 (1.85)
K90-7	0	-α	29.00 (3.21)	79.12 (3.35)	88.54 (1.03)	89.37 (1.17)
K90-8	0	+α	10.76 (2.61)	57.49 (3.87)	81.63 (2.94)	90.77 (1.81)
K90-9	0	0	16.88 (2.49)	68.65 (4.35)	88.82 (2.52)	93.08 (3.06)
K90-10	0	0	16.02 (2.18)	66.14 (3.06)	86.15 (2.75)	91.18 (3.07)
K90-11	0	0	12.44 (1.97)	61.58 (3.36)	84.72 (1.94)	91.57 (1.44)
Criteria of USP 28			≤20	20-45	45-80	80-100

Drug Release Test 1   *Drug Release Test 2*
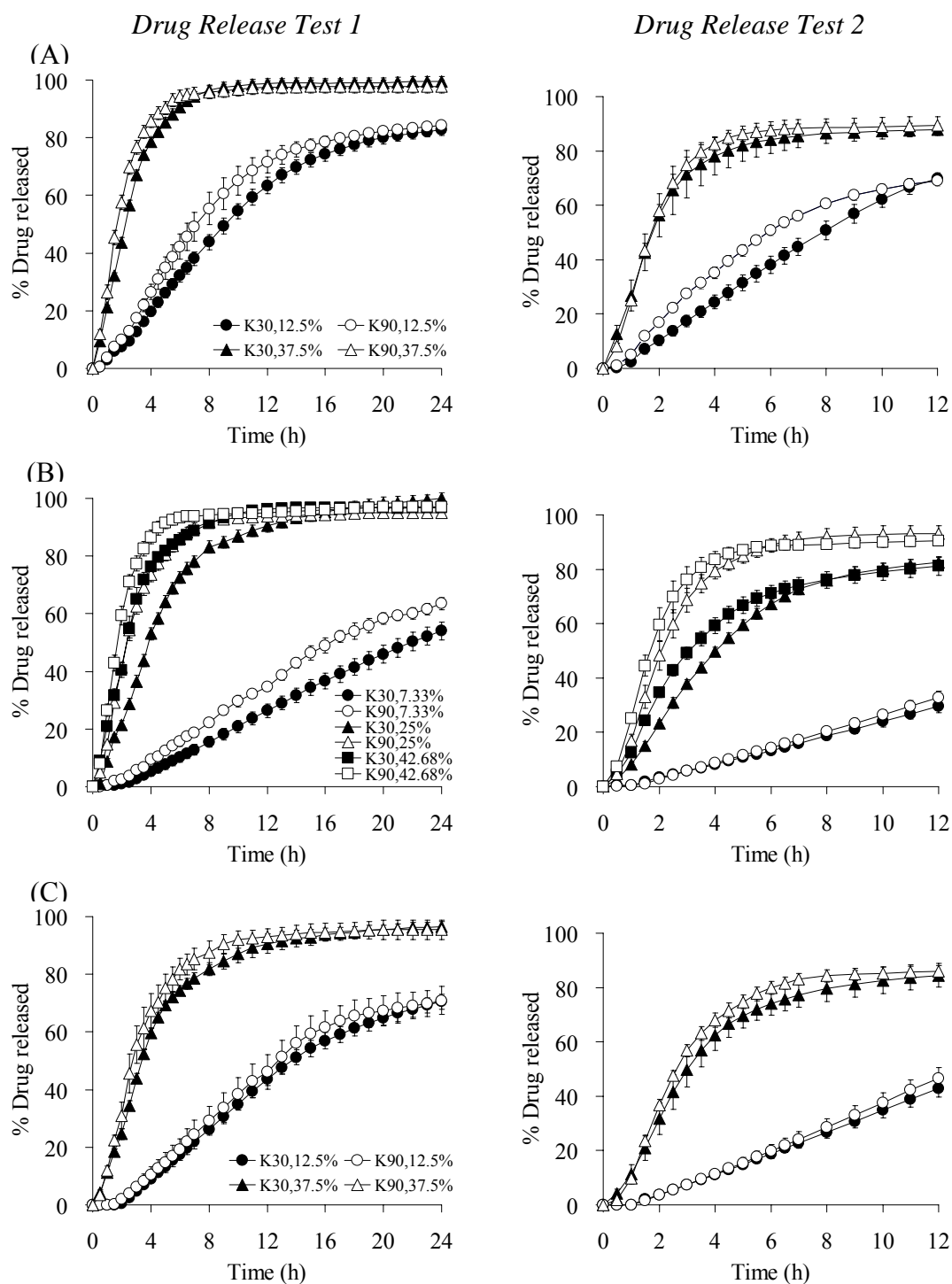
Figure 15. Effect of the molecular weight and content of PVP on drug release of CPOPs at various membrane weight increases (n = 6)

Keys: Membrane weight increase of (A) 2%; (B) 3%, (C) 4%.
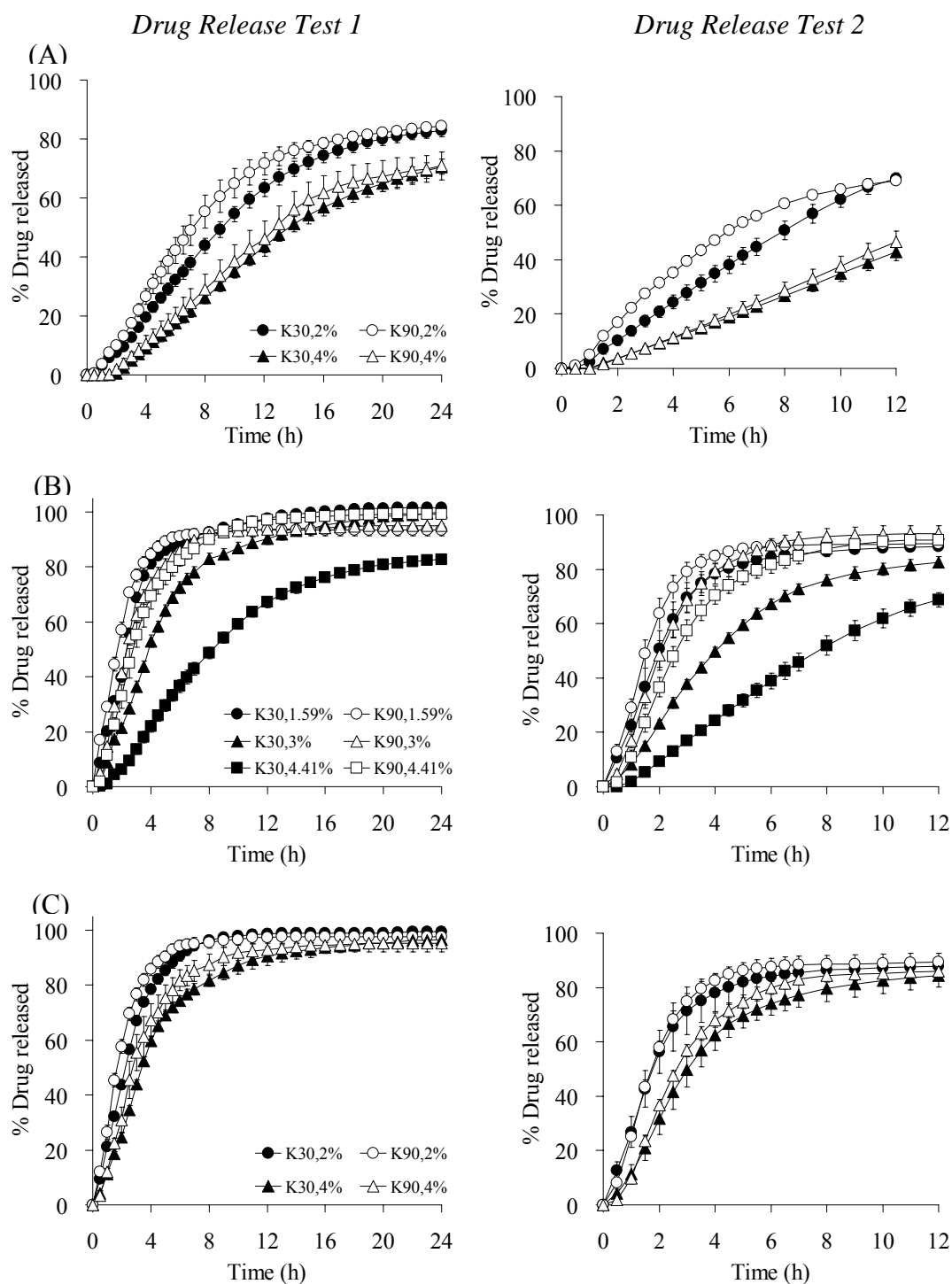
Figure 16. Effect of the molecular weight of PVP and membrane weight increase on
drug release of CPOPs at various PVP concentrations (n = 6)
Keys: PVP concentration of (A) 12.5%; (B) 25%, (C) 37.5%.

4. Response surface methodology

All responses were established according to USP 28 criteria. Response surface plots (3-dimension), showing the effects of the PVP amounts and the increase in membrane weight on the drug release at various times, an example is demonstrated in Figure 17. It was clearly seen that the drug release at any time could be increased by increasing the level of PVP content in semipermeable membrane or decreasing the coating level of the membrane.

Responses of drug release at time t, Y_t, to the membrane variables were analyzed using a statistical software, MINITAB 14, including the analysis of variance (ANOVA) in order to provide the relationship between the variable factors and the responses. Equation 12 as mentioned previously describes the drug release and its coefficients of 24- and 12-h release equations are listed in Tables 22 and 23, respectively. The ANOVA for the model equation fitted to the results, which assesses model relevance, shows significance of the models with a variance ratio of measurements residues compared to the model and the variance of all measured data (F value) with probability $>$ F less than 0.01 which were lower than 0.05, which proved the model relevance (147). The multiple regression coefficient calculated for all responses indicated that more than approximately 90% ($r^2 > 90\%$) of the experimental variance could be explained by the models. The high value of adjusted r^2, more than 80% for all responses, indicated that the model well fitted the observed data (148).

These equations represent the quantitative influence of membrane variables (X_1 and X_2) and their interaction on the response Y_t. Coefficients with more than one factor term and those with higher-order terms correspond to interaction terms and quadratic relationship, respectively. A positive sign denotes a synergistic effect, whereas a negative sign indicates an antagonistic effect (81). The t-test was employed for statistical analysis of the parameter estimates. As seen in Tables 22 and 23, PVP content had a significant positive effect on most responses. On the other hand, membrane weight gain presented an antagonistic influence on the drug release.
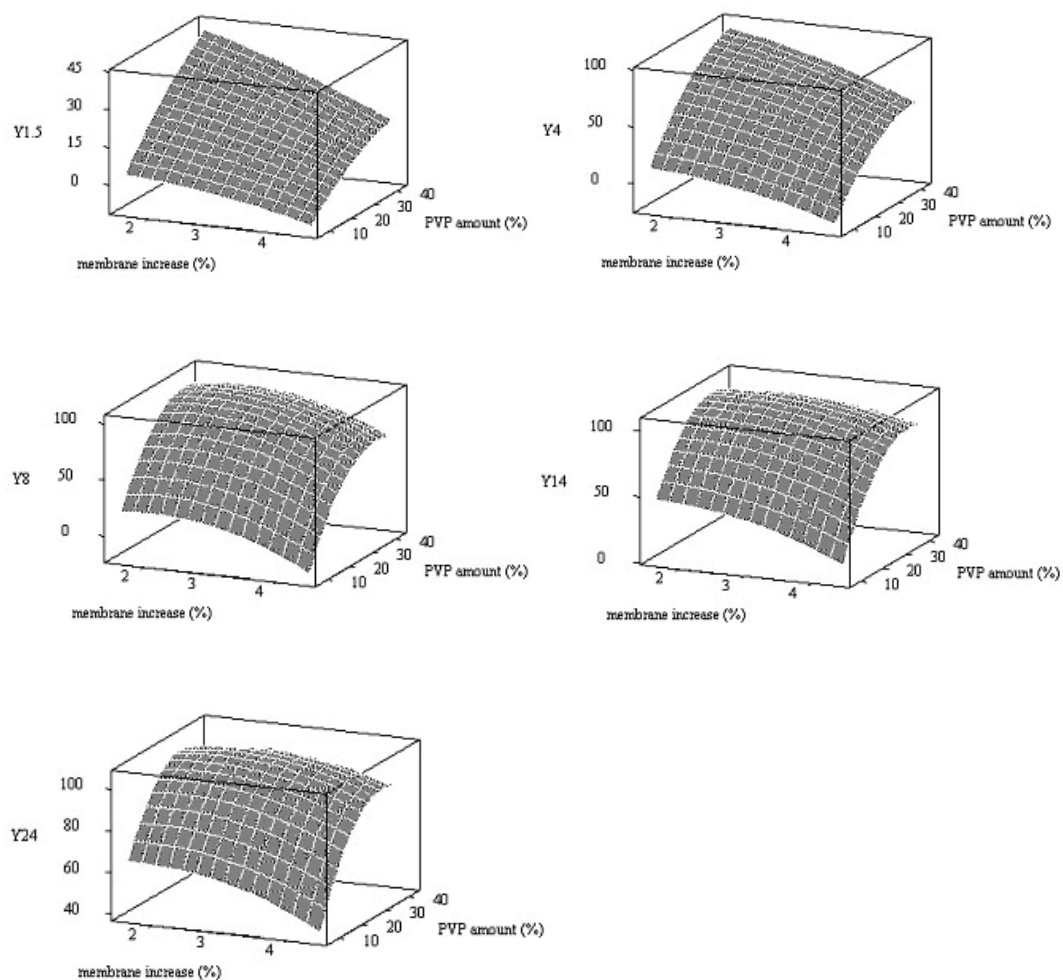
Figure 17. Response surface plots showing the effect of the PVP content and membrane weight gain on the drug release of CPOP with membrane containing PVP K30 at various times according to *Drug Release Test 1*

Table 22. Coefficients of the equations related to the responses and the independent variables, p-values, r^2, and r^2 (adj) of 24 h-CPOPs

Variable	Coefficients	PVP K30					PVP K90				
		$Y_{1.5}$	Y_4	Y_8	Y_{14}	Y_{24}	$Y_{1.5}$	Y_4	Y_8	Y_{14}	Y_{24}
Constant	a	-9.00	-22.5	-55.1	3.36	26.7	-34.4	-75.7	-49.1	19.5	54.6*
PVP concentration	b	1.91*	5.12*	7.00*	5.59*	4.26*	4.23*	8.48*	7.96*	5.12*	2.88*
Membrane increase	c	1.94	5.20	28.8	8.89	10.5	5.36	16.3	13.6	-2.38	-2.59
PVP concentration x PVP concentration	d	-0.0111	-0.0506	-0.101*	-0.0938*	-0.0756*	-0.04	-0.112*	-0.128*	-0.0904*	-0.0559*
Membrane increase x membrane increase	e	-0.867	-2.54	-7.02*	-3.80	-3.39	-0.692	-2.95	-3.48	-0.84	-0.681
PVP concentration x membrane increase	f	-0.156	-0.162	0.0604	0.243	0.184	-0.347	-0.189	0.173	0.256	0.251
p-value of model		0.002	0.003	< 0.001	< 0.001	0.001	0.006	0.005	0.001	0.001	0.003
r^2 (%)		96.1	94.7	98.6	98.0	96.6	93.1	93.8	96.3	97.2	94.8
r^2 (adj)(%)		92.3	89.3	97.2	96.0	93.3	86.3	87.5	92.7	94.4	89.5

*significant terms with p-values less than 0.05

Table 23. Coefficients of the equations related to the responses and the independent variables, p-values, r^2, and r^2 (adj) of 12 h-CPOPs

Variable	Coefficients	PVP K30				PVP K90			
		Y_1	Y_3	Y_6	Y_{12}	Y_1	Y_3	Y_6	Y_{12}
Constant	a	10.9	21.1	-11.4	37.3	-10.8	-62.9	-53.4	17.6
PVP concentration	b	1.50	4.04	5.49*	4.23*	2.38*	7.70*	8.08*	5.28*
Membrane increase	c	-12.9	-21.5	4.59	-7.55	-2.69	11.5	12.5	-3.00
PVP concentration x PVP concentration	d	-0.0037	-0.0355	-0.0841*	-0.0866*	-0.0186	-0.103*	-0.131*	-0.101*
Membrane increase x membrane increase	e	2.26	2.32	-3.48	-1.92	0.621	-2.46	-3.72	-1.67
PVP concentration x membrane increase	f	-0.263	-0.228	0.183	0.473*	-0.258	0.163	0.211	0.397
p-value of model		0.008	0.008	0.001	<0.001	0.022	0.006	0.001	0.002
r^2 (%)		92.2	92.5	96.7	98.2	88.3	93.4	96.2	95.6
r^2 (adj)(%)		84.4	85.0	93.4	96.5	76.6	86.8	92.4	91.3

*significant terms with p-values less than 0.05

4.1. Model adequacy checking

Typically, it is necessary to test the fitted model to guarantee that it presents an adequate approximation to the actual system. Unless the model shows an adequate fit, continuing on examination and optimization of the fitted response surface would provide poor or misleading results. The residual analysis is one technique for determining model adequacy. By constructing a normal probability plot of the residuals from the least squares fit, which is defined by the difference between observed and predicted data of each experimental run, a check of normality assumption can be confirmed. In this study, the normality was satisfied as all residuals plots approximated along a straight line (145), an example as shown in Figure 18. The confidences that the regression equations would predict the observed values well-fitted for most responses were more than 95% for all responses.

4.2. Formulation optimization

One way that we could optimize the formulation for satisfactory drug release profile is to obtain response surfaces for all responses. Then, superimpose the contours for these responses in the PVP amount–membrane increase plane, as illustrated in Figure 19 for CPOPs with PVP K30 and K90. In these figures the contours for percent drug release are demonstrated. The non-shaded area in these figures represents the region containing acceptable drug releases that simultaneously satisfy all requirements of the USP 28 criteria. The results showed that satisfactory 24-h profile or once daily dosing could be accomplished by either PVP K30 or PVP K90-containing membrane. However, acceptable 12 h-drug release profile or twice daily dosage form could be achieved from only specific ranges of PVP K30-containing membrane at the defined membrane thickness.

After generating the polynomial equations relating the dependent and independent variable, the formulation was optimized for the responses $Y_{1.5}$, Y_4, Y_8, Y_{14}, and Y_{24}, and Y_1, Y_3, Y_6, and Y_{12}, in order to develop once and twice daily dosage forms, respectively. Optimization was performed to obtain the level of X_1 and X_2, which targeting or maximizing all of the responses at constrained conditions of $Y_{1.5}$ through Y_{24} and Y_1 through Y_{12} as listed in Table 8.
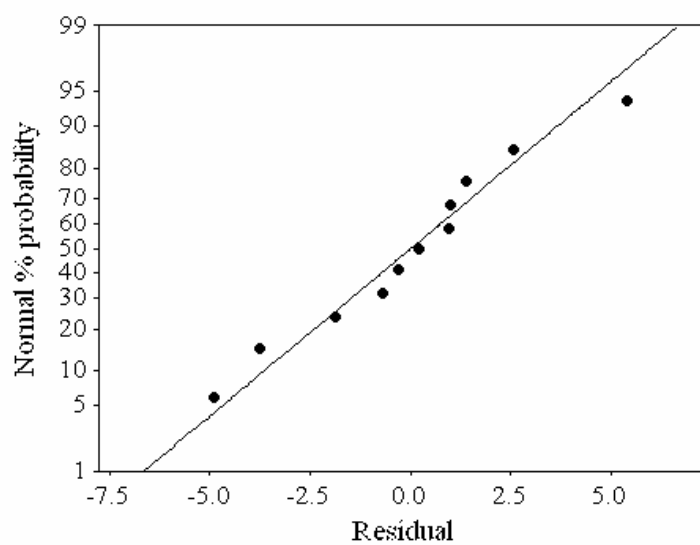
Figure 18. Normal probability plot of residuals for response Y_{24} of CPOP with membrane containing PVP K30 according to *Drug Release Test 1*
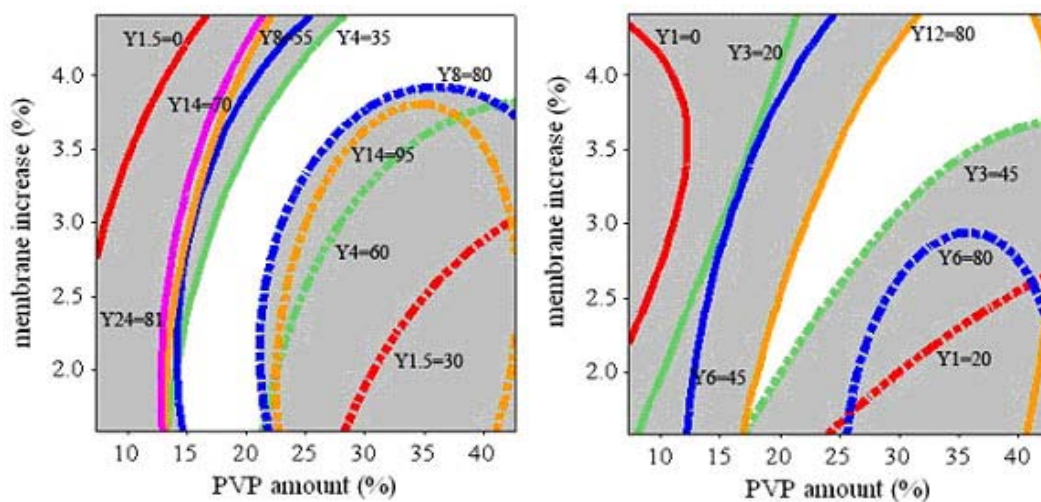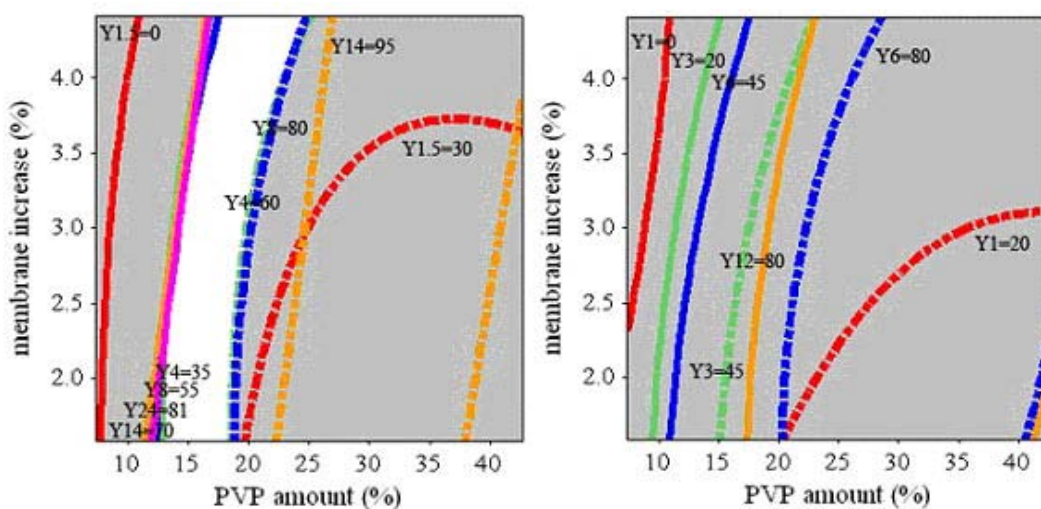
Figure 19. Overlaid contour plots of CPOP with membrane containing (A) PVP K30, and (B) PVP K90.

In this study, the optimized X_1 and X_2 in PVP K30-containing membrane were chosen at 35% and 4.2%, respectively. For PVP K90, X_1 and X_2 were 23% and 4.2%, respectively. The membrane thickness of two formulations was kept constant for comparison between each formula. Propranolol release profiles of the optimized formulations were illustrated in Figures 20–21. An important consideration for the *in vivo* use of this type of delivery system is the mechanical stability and resistance of the film coating to rupture during passage through the GI tract. None of the optimized formulations ruptured during the dissolution studies, as observed visually, and as indicated by the absence of a burst in drug release initially. Empty polymeric shells retained their original shape and floated on the dissolution medium after completion of drug release. Although coatings did not rupture when deformed by hand, they were flexible and fluid was pumped out from the empty shells under hand pressure.

Preparation and testing of the optimized formulation showed a good correlation between predicted and observed values. The observed versus predicted values of $Y_{1.5}$ to Y_{24} and Y_1 to Y_{12} of PVP K30-containing membrane are shown in Figure 22. The observed versus predicted data of $Y_{1.5}$ to Y_{24} of PVP K90-containing membrane are illustrated in Figure 23. These figures prove that the predicted data of all responses from the polynomial equations are in agreement with the observed ones in the range of the operating variables, which were confirmed by the high correlation coefficient value of each figure, i.e., 0.9971, 0.9994 and 0.9655.

Drug Release Test 1   *Drug Release Test 2*
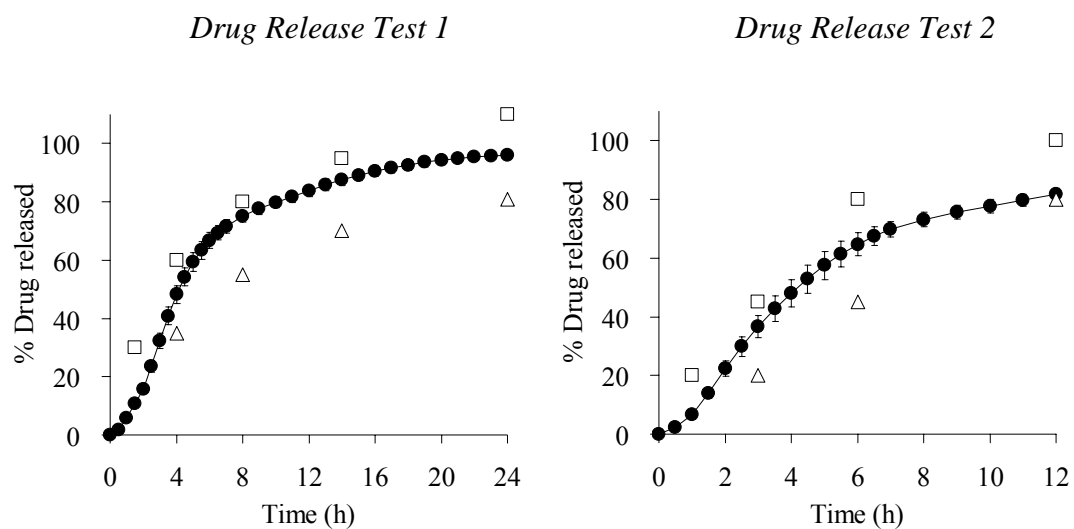
Figure 20. Drug release from CPOP with membrane containing 35% of PVP K30 at 4.2% weight gain (n = 6)

Keys: USP 28 criteria at various times; Δ , lower limit; $\square$, upper limit.
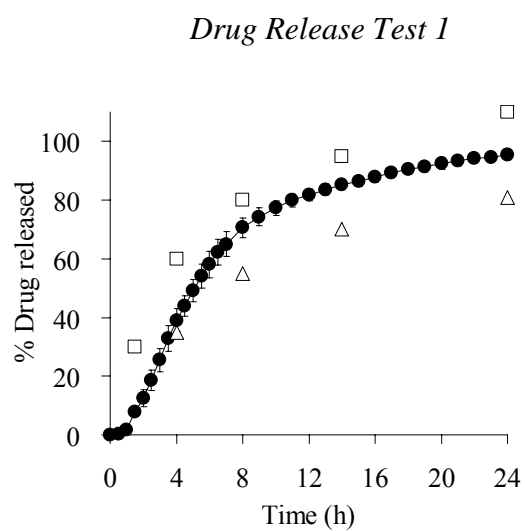
Drug Release Test 1

Figure 21. Drug release from CPOP with membrane containing 23% of PVP K90 at 4.2% weight gain (n = 6)

Keys: USP 28 criteria at various times; Δ , lower limit; $\square$, upper limit.

Drug Release Test 1   *Drug Release Test 2*
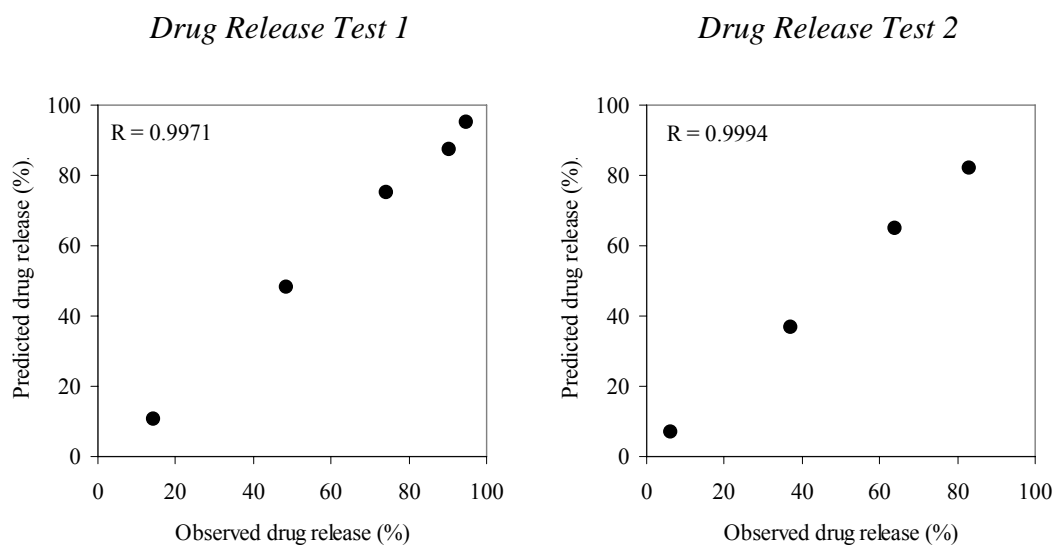
Figure 22. Relationship between the observed drug release and the predicted values of the optimized formulation of CPOP with membrane containing PVP K30 (35% PVP K30, 4.2% weight gain; n = 6)
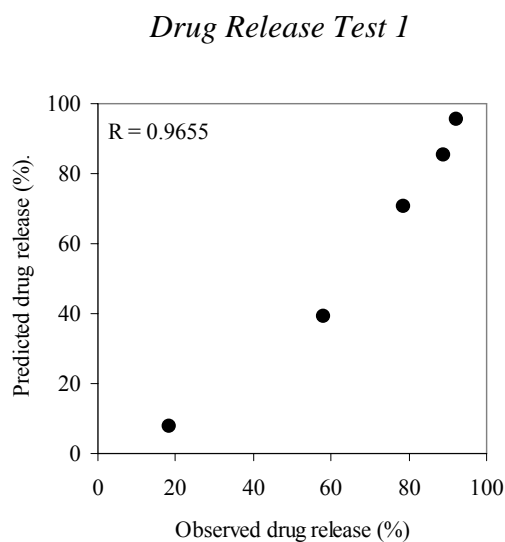
Drug Release Test 1

Figure 23. Relationship between the observed drug release and the predicted values of the optimized formulation of CPOP with membrane containing PVP K90 (23% PVP K90, 4.2% weight gain; n = 6)

4.3. Effects of pH of the dissolution medium

To verify that propranolol release profile from the optimized CPOP is independent of environmental pH, in vitro dissolution tests were also conducted in phosphate buffer media of pH 6.8 and pH 7.5, in addition to those in two-stage medium of pH 1.2/pH 6.8.   The release profiles of the optimized CPOPs with PVP K30 and K90 in different dissolution media are compared in Figures 24 and 25, respectively.   The average percent releases in different media were tested for a similarity using model independent method and the results indicated no dissimilarity ($f_2 > 50$). The f_2 values of CPOPs with PVP K30 and PVP K90 were found to be 98.6 and 70.5 (between pH 6.8 and pH 7.5), 70.2 and 75.1 (between pH 6.8 and pH 1.2/pH 6.8), and 69.2 and 89.0 (between pH 7.5 and pH 1.2/pH 6.8), respectively. Such results suggest that variation of pH does not affect the drug release from the optimized CPOP tablets. This result is in agreement with the earlier reports (45, 149, 150); drug release from the osmotic pump system was independent of the pH of dissolution medium.

4.4. Effect of agitation intensity

To study the effects of hydrodynamics on drug release profiles, dissolution studies were carried out at a relatively high (150 rpm), moderate (100 rpm) and low (50 rpm) revolution speed. Figures 26 and 27 show that there was no dissimilarity in release profiles under different agitation rates ($f_2 > 50$). The f_2 values of CPOPs with PVP K30 and PVP K90 were found to be 73.8 and 83.0 (between 50 and 100 rpm), 75.6 and 95.8 (between 50 and 150 rpm), and 91.7 and 85.0 (between 100 and 150 rpm), respectively. Therefore, it may be expected that the mobility of the GI tract hardly affects the drug release of the CPOP system. This result is similar to reports in the literature (149, 150), no impact of agitation intensity change on the drug release profiles.
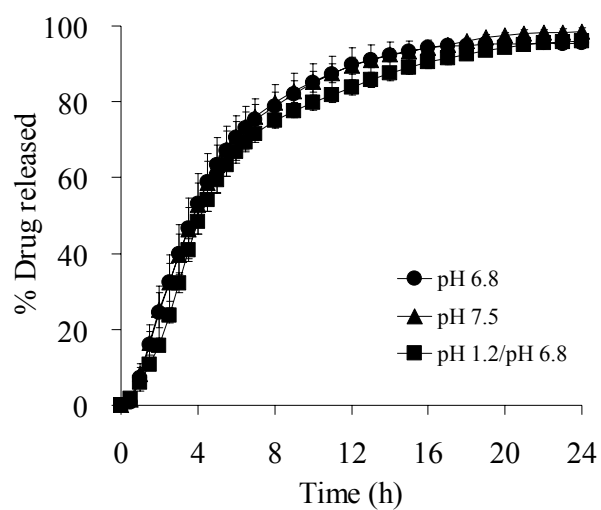
Figure 24. Effect of pH of dissolution medium on release profiles of propranolol from CPOPs with membrane containing 35% PVP K30 at 4.2% weight gain (n = 6)
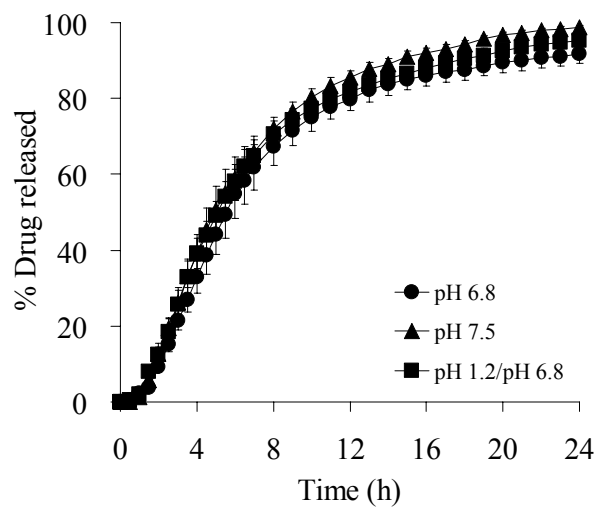
Figure 25. Effect of pH of dissolution medium on release profiles of propranolol from CPOPs with membrane containing 23% PVP K90 at 4.2% weight gain (n = 6)
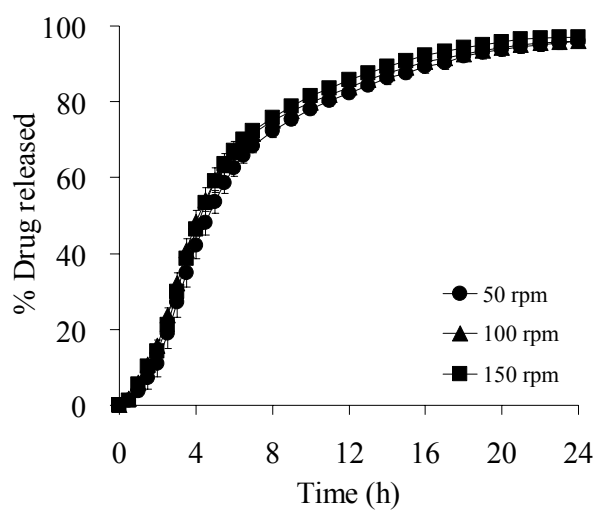
Figure 26. Effect of agitation intensity on release profiles of propranolol from CPOPs
with membrane containing 35% PVP K30 at 4.2% weight gain (n = 6)
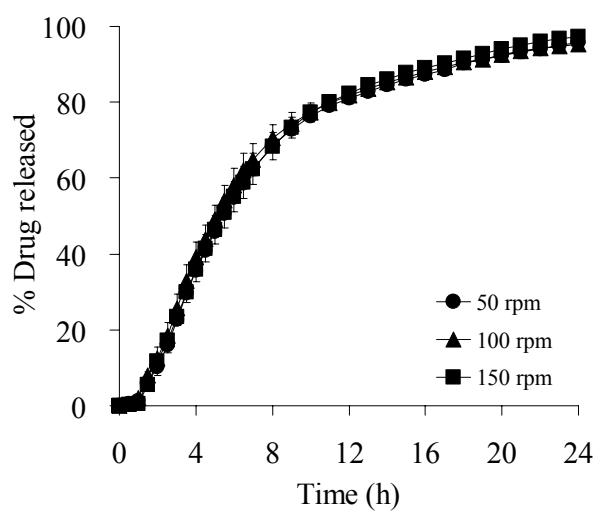
Figure 27. Effect of agitation intensity on release profiles of propranolol from CPOPs
with membrane containing 23% of PVP K90 at 4.2% weight gain (n = 6)

4.5. Effect of osmolarity

To confirm the mechanism of drug release, release studies of the optimized formulation of CPOPs were performed in the dissolution media with different osmolarity. The results show that the drug release is greatly dependent on the osmolarity of the release media. It is clearly evident that there was dissimilarity in release profiles under different osmolarity environment ($f_2 < 50$). The f_2 values of CPOPs with PVP K30 and K90 were found to be 35.5 and 38.3 (between 0 and 0.5 osm), 23.8 and 24.0 (between 0 and 1 osm), 19.6 and 17.6 (between 0 and 2 osm), 30.6 and 30.2 (between 0.5 and 1 osm), 18.4 and 17.8 (between 0.5 and 2 osm), and 28.9 and 35.7 (between 1 and 2 osm), respectively. Propranolol release from both CPOP with PVP K30 and PVP K90 decreased with the increase in the osmolarity of the dissolution media, as shown in Figures 28 and 29, respectively. Similar to reports in the previous publications (149, 150), osmotic contribution played a role in drug release from osmotic pump tablets.

4.6. Kinetics and mechanism of drug release

Dissolution data of the optimized formulations were fitted to various mathematical models (zero-order, first-order and Higuchi) in order to establish the kinetics of drug release. The best goodness-of-fit (r^2), and the smallest value of sum of squared residuals (SSR) and Akaike information criterion (AIC) were indicated the model suitability for a given dissolution data profile (151). Drug release up to 70% from CPOPs used PVP K30 and K90 as pore formers fitted well into zero-order kinetics with r^2 ranging from 0.9670 to 0.9912 (Tables 24 and 25). After that Higuchi's equation could describe the release curves better than the zero-order ones. As similar to the previous reports (4, 5), the microporous membrane was substantially permeable to both water and dissolved solutes. The mechanism of drug release from these systems was found to be primarily osmotic with simple diffusion playing a minor role.
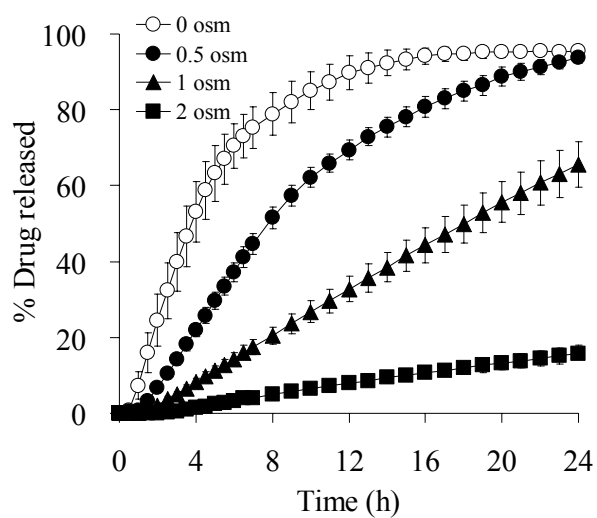
Figure 28. Effect of osmotic pressure on release profiles of propranolol from CPOPs
with membrane containing 35% PVP K30 at 4.2% weight gain (n = 6)
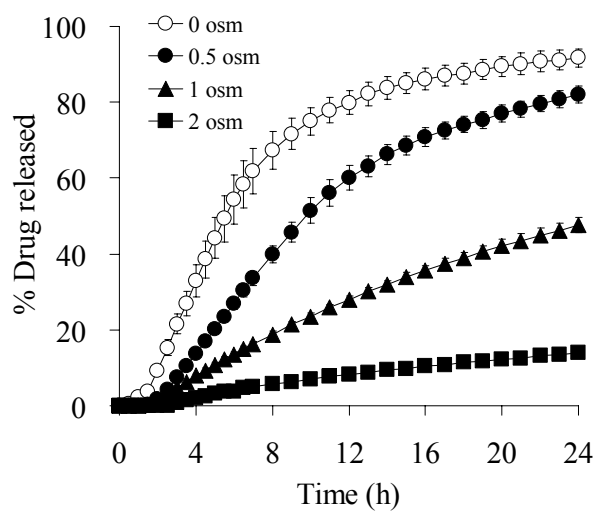
Figure 29. Effect of osmotic pressure on release profiles of propranolol from CPOPs
with membrane containing 23% PVP K90 at 4.2% weight gain (n = 6)

Table 24. Fitting of dissolution data of the optimized formulation of CPOP coated with membrane containing PVP K30 based on mathematical models

Range of drug release (%)	Model	Parameters used to assess the fit of model			
		r^2	k^*	$SSR \times 10^2$	AIC
0–60	Zero-order	0.9854	10.201	0.86	61.5
	First-order	0.8629	0.629	24.68	93.9
	Higuchi	0.8598	30.943	8.27	86.6
0–65	Zero-order	0.9861	9.971	1.00	67.9
	First-order	0.8436	0.570	34.69	105.8
	Higuchi	0.8769	32.113	8.82	94.2
0–70	Zero-order	0.9841	9.662	1.34	76.6
	First-order	0.8239	0.517	45.79	117.6
	Higuchi	0.8918	32.891	9.12	101.4
0–75	Zero-order	0.9674	8.739	3.58	102.1
	First-order	0.7697	0.417	92.93	145.1
	Higuchi	0.9157	33.424	9.25	115.3
0–80	Zero-order	0.9277	7.411	9.87	132.1
	First-order	0.6914	0.316	160.98	172.7
	Higuchi	0.9301	32.592	9.54	129.5
0–85	Zero-order	0.8726	5.761	22.53	170.1
	First-order	0.6030	0.215	199.62	206.0
	Higuchi	0.9354	30.329	11.43	153.9
0–90	Zero-order	0.8372	4.657	35.36	204.1
	First-order	0.5501	0.158	214.90	237.4
	Higuchi	0.9330	28.053	14.54	180.8

r^2, goodness of fit; SSR, sum of squared residuals; AIC, Akaike information criterion; and k^*, release rate constant for respective model (k_0 in mg/h, k_I in h^{-1}, and k_H in $\%/h^{1/2}$ for zero-order, first-order and Higuchi rate equations, respectively)

Table 25. Fitting of dissolution data of the optimized formulation of CPOP coated with membrane containing PVP K90 based on mathematical models

Range of drug release (%)	Model	Parameters used to assess the fit of model			
		r^2	k^*	$SSR \times 10^2$	AIC
0–60	Zero-order	0.9879	8.538	0.80	69.3
	First-order	0.7553	0.675	78.54	124.6
	Higuchi	0.8738	28.716	8.27	100.1
0–65	Zero-order	0.9881	8.374	0.92	75.9
	First-order	0.7389	0.613	96.12	136.4
	Higuchi	0.8873	29.606	8.75	107.6
0–70	Zero-order	0.9850	8.075	1.38	86.8
	First-order	0.7106	0.542	162.45	153.4
	Higuchi	0.9011	30.361	9.10	115.0
0–75	Zero-order	0.9770	7.656	2.47	101.7
	First-order	0.6771	0.473	236.89	169.2
	Higuchi	0.9142	30.781	9.22	122.1
0–80	Zero-order	0.9529	6.717	6.58	131.3
	First-order	0.6145	0.359	326.73	195.1
	Higuchi	0.9338	30.777	9.25	135.8
0–85	Zero-order	0.9122	5.459	16.43	170.9
	First-order	0.5462	0.251	360.96	228.4
	Higuchi	0.9463	29.471	10.05	158.1
0–90	Zero-order	0.8684	4.271	32.51	218.3
	First-order	0.4907	0.172	374.31	271.3
	Higuchi	0.9460	27.099	13.34	193.1

r^2, goodness of fit; SSR, sum of squared residuals; AIC, Akaike information criterion; and k^*, release rate constant for respective model (k_0 in mg/h, k_I in h^{-1}, and k_H in %/h$^{1/2}$ for zero-order, first-order and Higuchi rate equations, respectively)

5. Membrane characteristic study

In membrane sciences, surfaces of microfiltration and ultrafiltration membranes were extensively and profitably investigated by SEM and AFM to understand the characteristics of pore structure for determining their filtration properties (124, 152, 153). Therefore, it was expected that the study of the surface morphology of membrane of osmotic pump tablets could facilitate the identification of the influences of membrane variables on drug release from the tablets. To evaluate the characteristics of pores (pore size and pore size distribution), a high resolution microscope is necessary to observe the small pores in these membranes. For SEM sample preparation, the tablet was attached to the surface of a stub by double-sided adhesive tape. To make the sample conductive, it was coated with gold to a thickness of about 30 nm in a vacuum evaporator. Regarding AFM imaging of the membrane structure, no further preparation was necessary except attaching the membranes to a steel disc sample holder with a double-sided adhesive tape. Additionally, this technique also has advantages over SEM since the resolution is higher (lateral resolution can be as good as 1 nm and height resolution about 1 Å) and no electron beam damage can occur (154, 155).

5.1. Determination of surface pore diameter

Semipermeable membrane without PVP possessed a smooth and nonporous surface as shown in Figure 30. In case of micro/nanoporous membranes containing PVP as pore formers, most surfaces were found to have a network-like fine structure when examined by SEM and AFM as illustrated in Figures 31 and 32. Some might present a network of irregular opening, such as membrane with low level of PVP. Differences in number of pores between those membranes at different PVP contents are clearly visible. The higher level of PVP, the more crowded pores were observed. Surface pore diameters were measured by visual inspection of SEM images and of line profile of AFM images as shown in Figures 31 and 32, respectively. Each membrane was measured for 50 pores (124). The smallest and largest diameters and the mean values, including their relative standard deviations of all 50 pores are listed in Table 26.

(A)   (B)
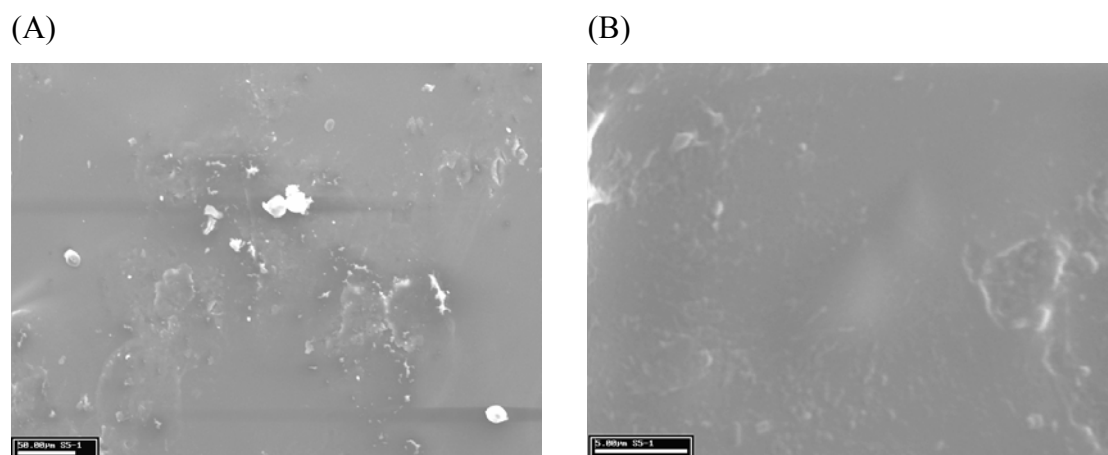
Figure 30. Scanning electron micrographs of CPOP with CA membrane without PVP

Keys: (A) before dissolution; (B) after dissolution

PVP K30   PVP K90

Figure 31. Scanning electron micrographs of various compositions of CPOP membrane with different molecular weights of PVP as pore formers after dissolution study (scale bar = 5 μm)

PVP K30   PVP K90

Figure 31. Scanning electron micrographs of various compositions of CPOP membrane with different molecular weights of PVP as pore formers after dissolution study (scale bar = 5 μm) (cont.)

PVP K30   PVP K90

Figure 31. Scanning electron micrographs of various compositions of CPOP membrane with different molecular weights of PVP as pore formers after dissolution study (scale bar = 5 μm) (cont.)

PVP K30   PVP K90

Figure 32. Atomic force micrographs of various compositions of CPOP membrane
           with different molecular weights of PVP as pore formers after dissolution
           study (with the typical line profile)

PVP K30

PVP K90

Figure 32. Atomic force micrographs of various compositions of CPOP membrane with different molecular weights of PVP as pore formers after dissolution study (with the typical line profile) (cont.)

PVP K30   PVP K90

Figure 32. Atomic force micrographs of various compositions of CPOP membrane
with different molecular weights of PVP as pore formers after dissolution
study (with the typical line profile) (cont.)

PVP K30 PVP K90

Figure 32. Atomic force micrographs of various compositions of CPOP membrane with different molecular weights of PVP as pore formers after dissolution study (with the typical line profile) (cont.)

PVP K30   PVP K90

Figure 32. Atomic force micrographs of various compositions of CPOP membrane with different molecular weights of PVP as pore formers after dissolution study (with the typical line profile) (cont.)

Table 26. Pore characteristics of osmotic pump tablet membranes

Formulation	X_1	X_2	Surface pore diameter (nm ± RSD%)					
			SEM			AFM		
			min	max	mean	min	max	mean
K30-1	12.5	2	108	974	416 ± 59.1	76	400	$194 \pm 43.3^*$
K30-2	37.5	2	153	971	472 ± 50.2	100	497	$222 \pm 33.3^*$
K30-3	12.5	4	72	1048	363 ± 69.1	98	409	208 ± 35.1
K30-4	37.5	4	72	1063	449 ± 61.9	104	448	$225 \pm 41.8^*$
K30-5	7.33	3	81	776	$249 \pm 41.0^*$	100	332	$174 \pm 28.2^*$
K30-6	42.68	3	149	1154	585 ± 54.0	153	562	322 ± 24.8
K30-7	25	1.59	161	1195	482 ± 58.7	167	409	243 ± 23.9
K30-8	25	4.41	80	1125	$374 \pm 71.1^*$	173	606	$254 \pm 29.5^*$
K30-9	25	3	81	896	425 ± 56.9	80	429	$225 \pm 37.3^*$
K90-1	12.5	2	144	1299	507 ± 50.3	120	496	$243 \pm 32.9^*$
K90-2	37.5	2	180	1414	536 ± 55.6	188	605	$360 \pm 28.3^*$
K90-3	12.5	4	144	904	446 ± 38.6	110	482	219 ± 43.8
K90-4	37.5	4	180	1046	535 ± 51.4	172	556	$319 \pm 28.5^*$
K90-5	7.33	3	72	844	$415 \pm 48.4^*$	88	365	$202 \pm 36.1^*$
K90-6	42.68	3	130	1250	602 ± 47.3	200	499	343 ± 25.1
K90-7	25	1.59	144	974	484 ± 54.1	99	551	255 ± 42.4
K90-8	25	4.41	108	1209	$576 \pm 48.8^*$	108	660	$322 \pm 39.8^*$
K90-9	25	3	108	1181	508 ± 60.8	107	553	$286 \pm 31.5^*$

*significant difference with $p < 0.05$ (comparing between different molecular weight of PVP)

The result shows that pores created from PVP ranged from nanometers to micrometers in size. The average pore sizes of membrane containing PVP K30 which measured by SEM and AFM were approximately 400 nm and 200 nm, respectively. Whereas PVP K90 gives larger pore size of around 500 nm and 300 nm measured by SEM and AFM, respectively. It is also indicated that the higher level of PVP content, the significantly larger pore size was created on the micro/nanoporous membrane ($p < 0.05$).

The molecular weight (M_r) of PVP K90 and PVP K30 are 1,000,000 and 50,000, respectively (144). As such the molecular size of PVP K90 is drastically larger than PVP K30. It is expected that when PVP K90 leached from the semipermeable membrane, the larger pore was formed. This finding is in agreement with publications in the area of membrane sciences (146, 156) since PVP has been used as a pore forming agent for ultrafiltration membranes (146, 156-158). It was clearly evident that the addition of PVP changed the membrane porosity, resulting in the increase of permeability without changing the membrane selectivity (156). Gas permeability through the ultrafiltration membranes was observed to be increased remarkably with incremental PVP contents (158) and molecular weight (146). It was also reported that the micropore volume was increased by increasing molecular weight of PVP (146).

The variety in pore diameters was observed within each membrane, indicating broad size distribution of the pores. The deviation was between ± 30–50% from the average values in most cases. Two possible assumptions could be explained as follow. (i) PVP stays in various configuration of its side chain in the membrane. Once it dissolves, various pore sizes are generated in the membrane. The long chain polymers give large openings while the short chain polymers give small openings. (ii) Some of the large entries were not single pores, but were composed of two or more small pores (124). So an overestimation could occur from this cause that multiple pores could not be resolved within one observed large opening.

Considering pore sizes observed by SEM and AFM, the AFM results were approximately 200 nm lower than those estimated with SEM. In AFM, the opening that composed of two or more pores could be identified and excluded. Thus, the overestimation of the pore size could be diminished. Another possibility is that due to

the samples for AFM imaging need not to be dried during the sample preparation, thus the samples were less changed (124, 159). On the other hand, the samples for SEM imaging need to be dried and exposed to vacuum, then treated for increasing conductivity. Thus, the samples were more changed (159), the pore size might be widen. However, the values obtained from both PVP type were correlated in their pattern. Regarding SEM and AFM results, the average surface pore size on membrane with PVP K90 was significantly larger (almost 100 nm) than that with PVP K30 ($p < 0.05$).

At a given PVP content, PVP K90 generally gave higher drug release than did PVP K30 as previously discussed. These surface morphology studies confirmed the *in vitro* release observations that the higher molecular weight of PVP, the larger pore size of the micro/nanoporous was created and the higher drug release was obtained from the CPOP system.

5.2. Membrane porosity

To determine the porosity of membrane, the formulations with various PVP contents (7.33, 25, 42.68%) at 3% membrane weight increase were selected and calculated its porosity of 50 membranes after dissolution study, as listed in Table 27. Despite the fact that its porosity did not equal to the PVP concentration in the membrane, it is clearly presented that the more level of PVP, the more porosity of the membrane was identified. From the visual inspection of the membrane after dissolution, it was observed that the more PVP content in the membrane, the more cloudy and brittle of the membrane was monitored, and much more with PVP K90. It could be due to some amount of PVP did not dissolve and still presented in the membrane that causes the different physical properties of membrane. The deviations of porosity were small, even though their pore size distributions were broad. This result supports the understanding of surface pore size and drug release of the CPOP, the higher level of pore forming PVP, the higher porosity of the membrane was exhibited and the higher drug release was obtained.

Table 27. Porosity of the membrane containing various PVP concentrations
(SD in parentheses, n = 3)

PVP type	PVP Concentration (%)		
	7.33	25	42.68
K30	7.21 (0.26)	21.43 (0.42)	30.57 (0.63)
K90	2.00 (0.05)	18.74 (0.29)	22.19 (0.44)

6. Conclusion

In summary, the micro/nanoporous osmotic pump tablets fabricated with CA coating containing PVP K30 or K90 as pore forming agents released the drug at almost a constant rate over a prolonged period of time regardless of environmental conditions. Drug release up to 70% from CPOPs fitted well into a zero-order kinetic model. The drug release was dependent on the molecular weight and concentration of PVP and the level of coating. The formulation that gave the desired release profile for both once and twice daily dosing interval was only CPOP used PVP K30 as pore formers. In this study, it was found that the optimized formulation was CPOP with CA coating containing 35% of PVP K30 at 4.2% membrane weight increase. For CPOP with CA coating containing PVP K90, the desired release profile for once daily dose was achieved at PVP content of 23% and membrane weight increase of 4.2%. PVP K30 was selected as a pore former for further study.

Part II: Swelling Properties of Ternary Mixtures of Chitosan, Polyacrylic Acid and Hydroxypropyl Methylcellulose

7. CS-PAA interpolymer complex and ternary mixtures of CS-PAA:HPMC

Polymer blends of polyelectrolyte complexes based chitosan (CS) as a polycations polymer and polyacrylic acid (PAA) as a polyanions polymer were prepared at various ratios. The powder of polymers was dispersed in acetic acid and sodium hydroxide was added in order to achieve the pH of 5. The dispersion was in white gel-like precipitates and became more viscous at pH 5. After drying at 50 °C, the golden-yellow membrane was obtained. The color change after drying could be due to the oriented polymer chains of CS and PAA which change a light reflection as reported previously (58). Percent yield of the CS-PAA complex are shown in Figure 33. The preparation of CS-PAA at the ratio of 1:2 provided the highest yield of 92.7%, while at the ratios of 1:1 and 2:1, the yields were 83.7 and 50.3%, respectively.

For preparation of the ternary mixture of CS-PAA:HPMC hydrogel, the other precipitates were not observed after mixing of the polymer solution.

8. FTIR analysis

FTIR is a technique that has been used for examining the interactions of powder blends at the molecular level. If two substances have interaction, the change in their functional groups will depict the change in the FTIR spectra from the individual substances, including additional bands, alterations in wavenumber positions, broaden peak. In this study, the focus of interest is in the range of 1400–1800 cm^{-1} in all spectra, because it is a suitable region to investigate the influence on the vibration modes of carbonyl groups and carboxylate groups of possible hydrogen bonding interactions in the interested CS-PAA complex (71).

Figure 34 shows FTIR spectra of CS, PAA, CS-PAA complex and CS-PAA:HPMC ternary mixtures. Characteristic peaks of amide I and amide II of CS were located at 1654 and 1596 cm^{-1}, respectively (69) whereas absorption band of PAA at around 1714 cm^{-1} referred to C=O stretching vibration of carboxylic groups (160). In the spectrum of CS-PAA complex, two strong peaks at 1560 and 1412 cm^{-1}

presented the asymmetrical and symmetrical stretching of COO$^-$ groups, respectively, while one peak at 1655 cm^{-1} was attributed to the formation of protonated amino groups (NH$_3^+$). These results indicated that the carboxylic groups of PAA were dissociated to COO$^-$ groups which complexed with protonated amino groups of CS through electrostatic interaction and became a polyelectrolyte complex during the formation of CS-PAA hydrogels. Similar electrostatic interaction was observed by Wang et al. (58), de la Torre et al. (62) and Wu et al. (161). However, characteristic peaks of the ternary mixtures of CS-PAA:HPMC showed a similar result with that of the CS-PAA complex. Since no trace of HPMC was observed, it can be suggested that no further interaction between the complex and HPMC polymer.

Figure 35 displays the FTIR spectra of CS:PAA interpolymer complexes at various mass ratios. To indicate the complex formation, three peaks corresponding to the protonated amino groups and the asymmetrical and symmetrical stretching of COO$^-$ groups at around 1655, 1560 and 1412 cm^{-1}, respectively, were observed. Concerning the highest yield of the complex at the 2:1 ratio, the spectrum presented the strongest peak intensity at 1645 cm^{-1} due to the highest amount of protonated amino groups in the complex. In the complexes of 1:2 ratio, a strong band at 1716 cm^{-1} was observed, indicating a high amount of PAA in the complex as reported previously (69). On contrary, the less intense peak was observed from the spectra of the 1:1 and 2:1 ratios complexes. Besides the less amount of PAA, the overlapping of this weak with strong bands of NH$_3^+$ possibly occurred.
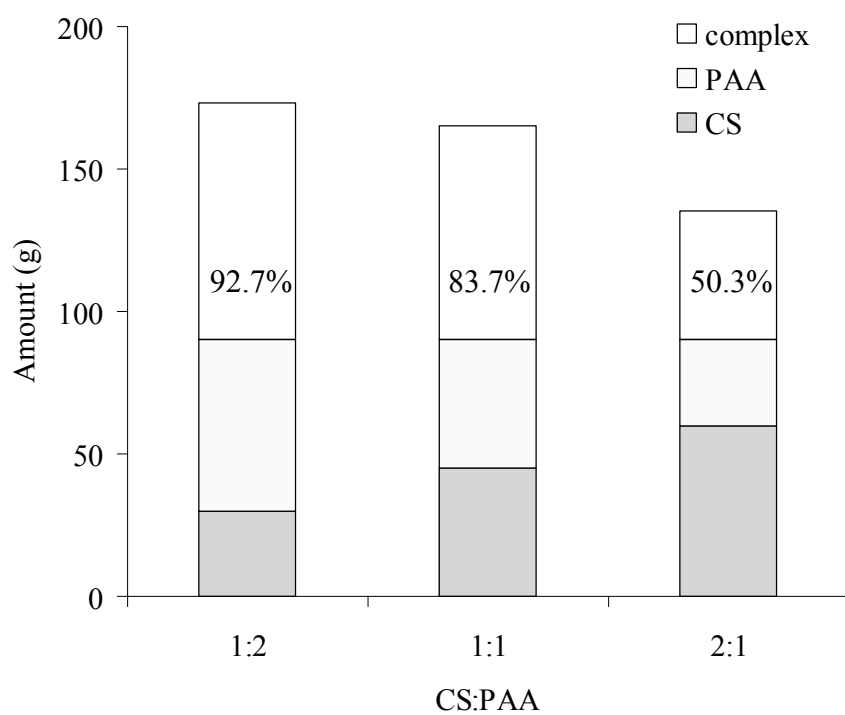
Figure 33. Percent yield of the CS-PAA complex production
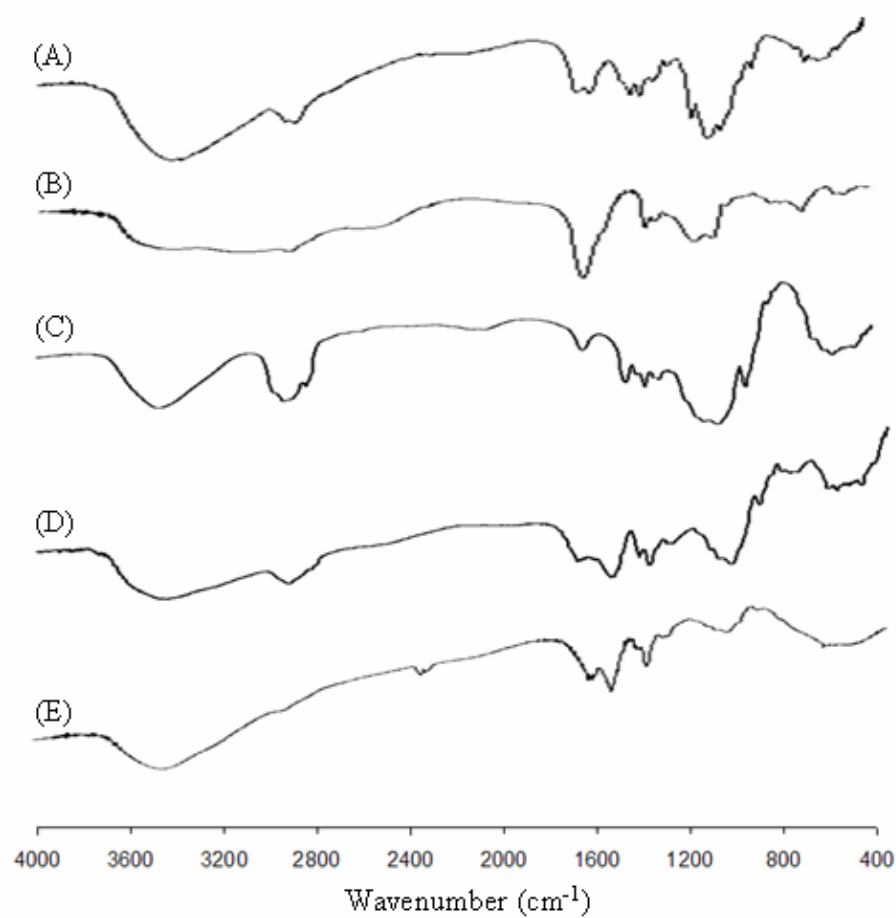
Figure 34. FTIR spectra

Keys: (A) CS; (B) PAA; (C) HPMC; (D) CS-PAA interpolymer complex;
(E) CS-PAA:HPMC ternary mixtures.
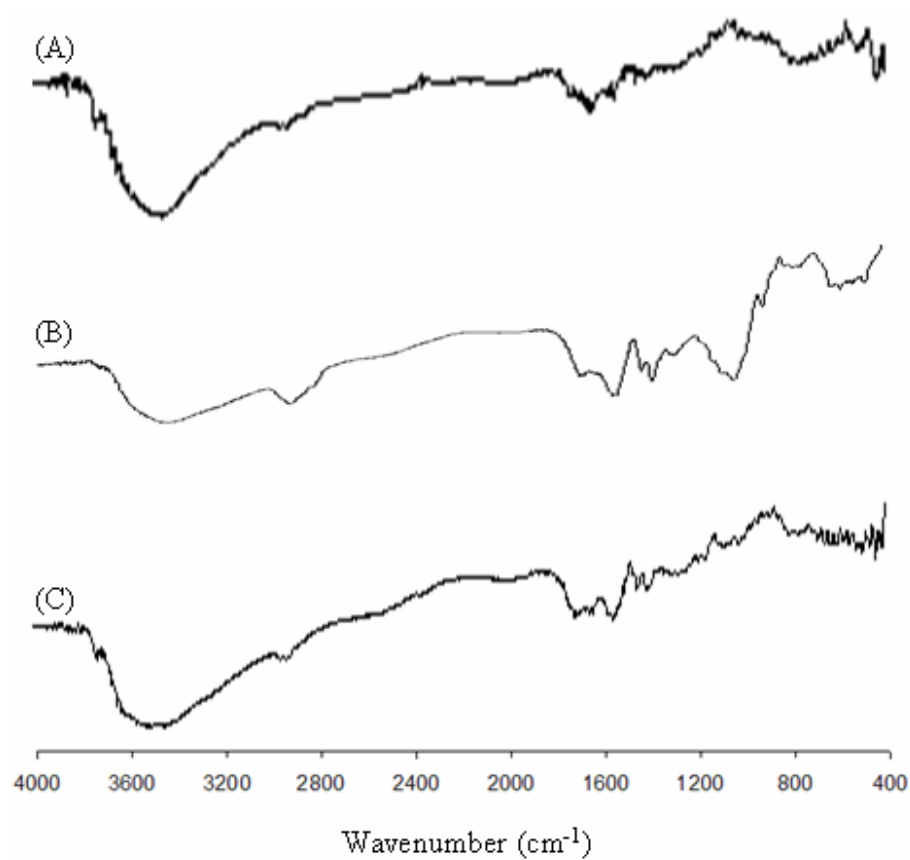
Figure 35. FTIR spectra of CS:PAA interpolymer complex at various mass ratios
Keys: (A) 2:1; (B) 1:1; (C) 1:2.

9. Swelling characteristics of CS-PAA complex and CS-PAA:HPMC mixtures

9.1. Effects of molecular weight of CS

Effects of molecular weight of CS on swelling force are shown in Figure 36. CS:PAA complexes at the ratio of 1:2 with low, medium and high molecular weight of CS, exhibited the maximum swelling force at 8.7, 14.7 and 15.5 N, respectively. Similarly, at the ratio of 1:1 the maximum swelling forces were 7.6, 16.3 and 20.8 N. In the 2:1 complexes, the medium and high molecular weight provided the maximum swelling forces of 29.0 and 27.6 N, respectively, which are obviously higher than the maximum swelling force of 8.0 N of the complex with low molecular weight. It is clearly evident that the high molecular weight of CS, the high swelling force was observed.

Figure 37 shows the effects of molecular weight of CS on swelling ratio. From the evaluation of 1:2 complexes, low to high molecular weight of CS provided similar maximum swelling ratio (from 4.70 to 5.65). Nevertheless, the 1:1 complex presented the increased swelling ratios of 2.01, 6.21 and 8.89 after using CS with low, medium and high molecular weight, respectively. The similar result was observed with the 2:1 complex where the swelling ratios of 2.68, 19.11 and 18.55 were observed by increasing molecular weight of CS.

These results indicated that the swelling force and swelling ratio increased with the increased molecular weight of CS. For further studies, high molecular weight of CS was selected for preparation of CS:PAA interpolymer complex due to its high swelling force and swelling ratio.
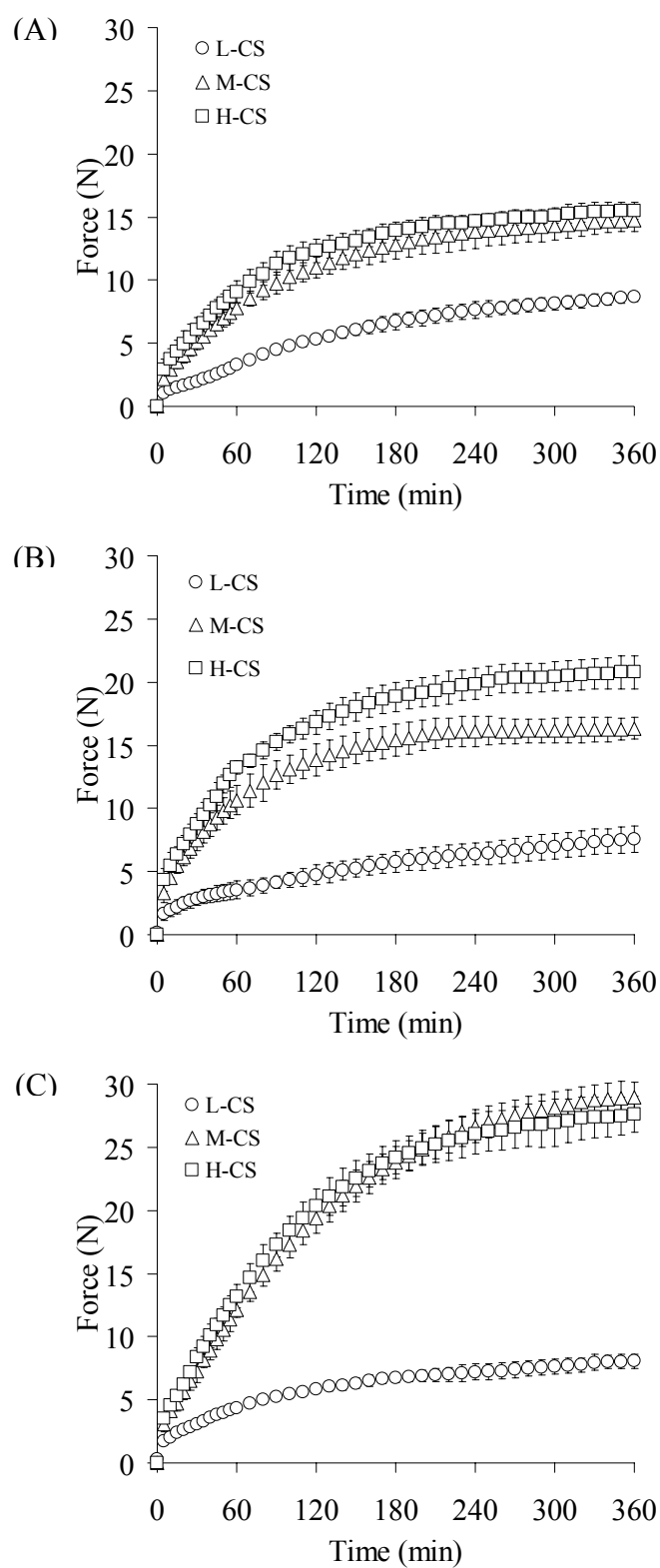
Figure 36. Effect of molecular weight of CS on swelling force of CS-PAA
interpolymer complexes at the CS-PAA ratio of (A) 1:2, (B) 1:1, (C) 2:1.
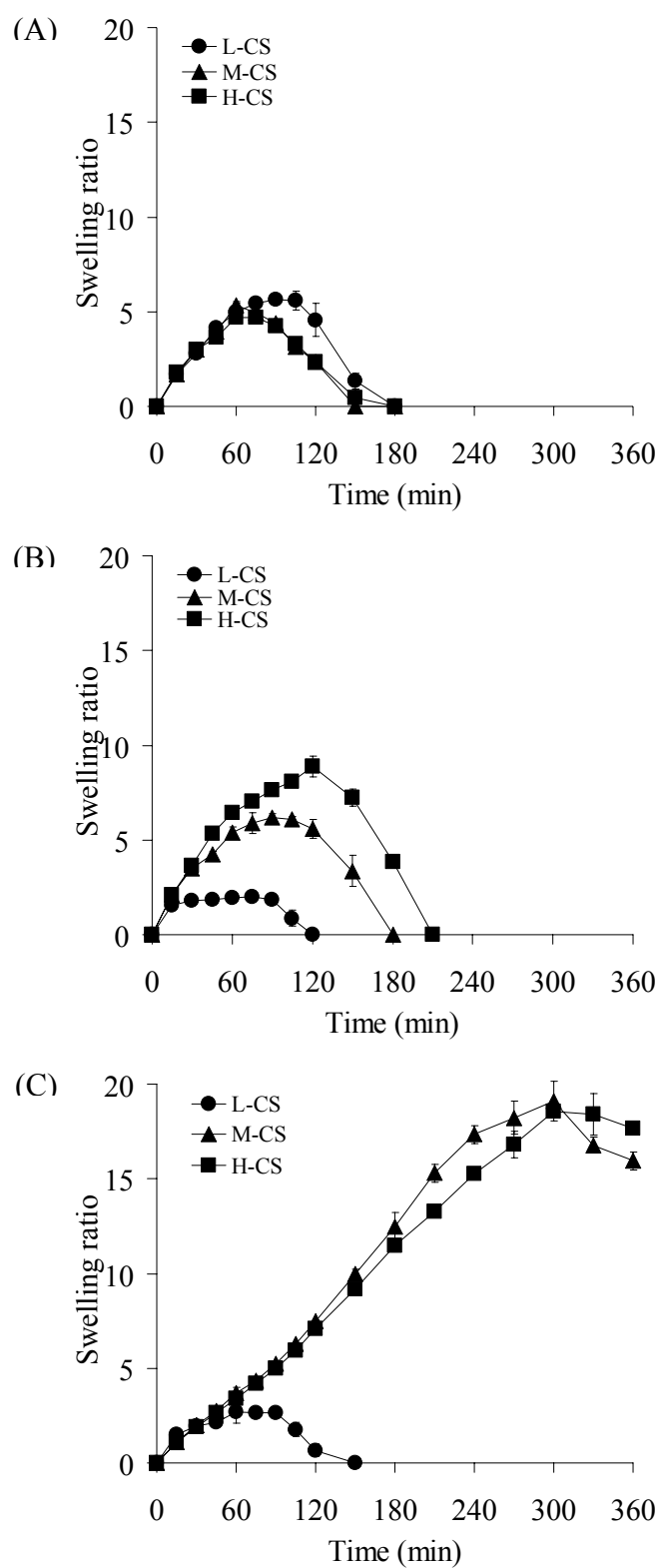
Figure 37. Effect of molecular weight of CS on swelling ratio of CS-PAA interpolymer complexes at the CS-PAA ratio of (A) 1:2, (B) 1:1, (C) 2:1.

9.2. Effects of CS:PAA ratio

Figures 38 and 39 show the effects of the ratio of CS:PAA on the swelling force and swelling ratio of the complexes, respectively. The CS:PAA complexes with high molecular weight of CS at ratio of 1:2, 1:1 and 2:1 exhibited the maximum swelling force at 15.5, 20.8 and 27.6 N, respectively. Similar results were obtained from the complex with medium molecular weight of CS in which the increased swelling forces, i.e., 14.7, 16.3 and 29.0 N, were observed by increasing the CS proportion. The complexes with low molecular weight of CS at 1:2, 1:1 and 2:1 ratios achieved rather low, however, comparable swelling force, i.e., 8.7, 7.6 and 8.0 N, respectively.

Concurrently, the complex that presented the high swelling force would present the high swelling ratio. With high molecular weight of CS, swelling ratio of 1:2, 1:1 and 2:1 complexes were 4.70, 8.89 and 18.55, respectively. Similarity, the complex with medium molecular weight of CS revealed the swelling ratios of 4.96, 6.21 and 19.11, respectively, while the complex with low molecular weight of CS provided the lower swelling ratios of 5.65, 2.01 and 2.68, respectively.

These results show the direct correlation between the increased proportion of CS within the complex and the effect on the maximum swelling force and swelling ratio. For example, with high molecular weight of CS, the complex with the least proportion of CS (CS:PAA; 1:2) displayed the lowest maximum swelling force of 15.5 N and the lowest swelling ratio of 4.70. Increasing CS proportion increased the degree of swelling as shown in the case of the hydrogel containing CS:PAA at 1:1 and 2:1 ratios with the maximum swelling force of 20.8 and 27.6 N, respectively. As similar to swelling force, higher CS content in the polymer blend at 1:1 and 2:1 ratios presented greater maximum swelling ratio of 8.89 and 18.55, respectively.

It is expected that an expansion of polymer chain occurred when ionic groups of CS in the formulation was increased (59). As reported in the literature, the use of pure CS limited the maximum swelling force and swelling ratio; however, these properties were greatly improved by the presence of PAA (62). PAA could help the protonation of the amine groups of CS, causing an electrostatic repulsion among polymeric chains (58, 59, 62). Increasing CS content could increase the expansion of the polymer chains due to ionic repulsion of amino groups. Therefore, the greater

swelling force and swelling ratio were observed. However, PAA could play a role in simultaneous swelling and eroding characteristics. In polyionic complexes with PAA, the erosion rate enlarged as the amount of this polymer increased in the hydrogel (162).

The CS-PAA interpolymer complex at the ratio of 1:2 and 1:1 rapidly hydrated, swelled, and reached the equilibrium within 10–60 min as shown in Figures 37a and 37b. The complex at the ratio of 2:1 gave slower swelling (Figure 37c). In order to control the swelling characteristic, HPMC was added in order to modify the swelling pattern. For further study of ternary mixtures, the ratio of CS:PAA at 1:1 was selected based on the good swelling characteristics and high percent yield of the complex manufacture (83.7%).
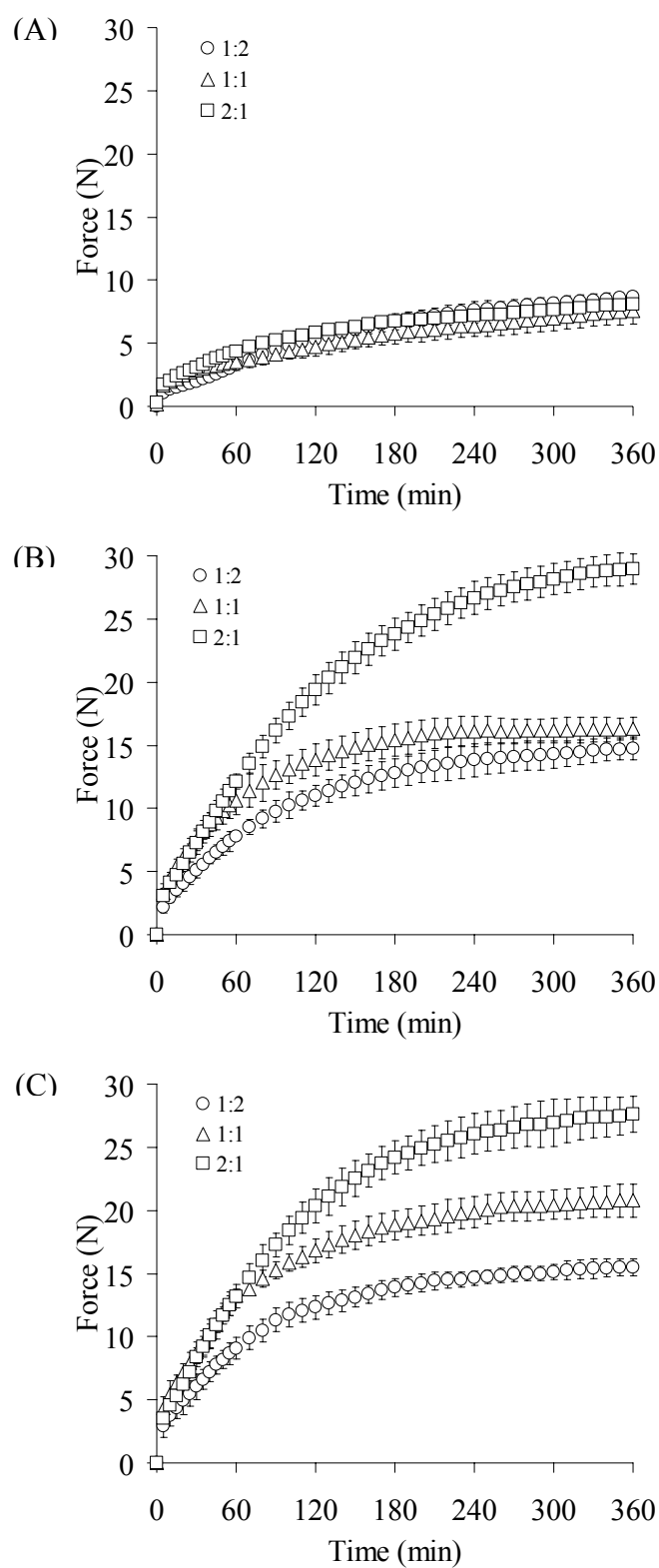
Figure 38. Effect of CS:PAA ratio on swelling force of CS-PAA interpolymer complexes using (A) L-CS, (B) M-CS, (C) H-CS.
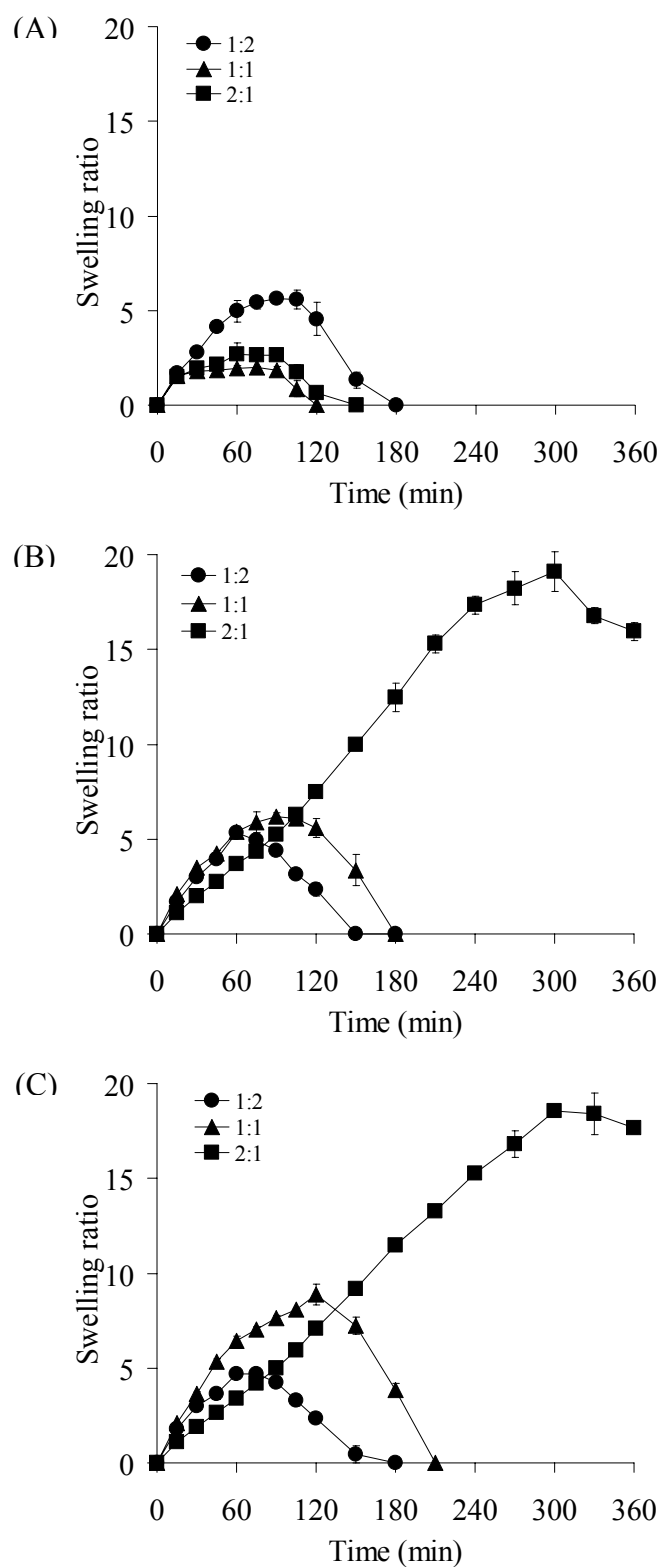
Figure 39. Effect of CS:PAA ratio on swelling ratio of CS-PAA interpolymer complexes using (A) L-CS, (B) M-CS, (C) H-CS.

9.3. Effects of proportion of ternary hydrogel composition

HPMC, a hydrophilic gel-forming polymer, is widely used in oral extended-release drug delivery systems (163). It is frequently added to the core to form polymer matrix. When the polymer contacts to aqueous liquid, it swells and forms a gel layer around the matrix, which may restrict and delay the solvent contact with other molecules and may increase the diffusional path length of solvent (164). It was reported in the literature that when increasing the HPMC loading, the hydration rate is decreased (165). In this present study, HPMC was incorporated into the hydrogels in order to modulate the hydration rate of the CS-PAA interpolymer complex.

The ternary mixture of CS-PAA:HPMC hydrogel were prepared by varying the proportions of the complex and HPMC compositions, i.e., 1:0, 0.75:0.25, 0.5:0.5, 0.25:0.75, and 0:1. It was found that both swelling force and swelling ratio decreased with the increase of HPMC ratio, as shown in Figures 40 and 41. Swelling forces of the complex:HPMC hydrogel at 1:0, 0.75:0.25, 0.5:0.5, 0.25:0.75, and 0:1 ratios were 20.8, 12.0, 12.1, 10.2 and 2.0 N, respectively. The resulting swelling ratios were 8.26, 4.33, 4.53, 3.97 and 0.60, respectively. HPMC might form a gel layer around the tablets; consequently, reduce water uptake into the matrices, resulting in slower swelling rate as shown in Figure 42.   With increasing HPMC proportions, the decreasing order of the swelling rates was observed as 1:0 > 0.75:0.25 > 0.5:0.5 > 0.25:0.75 > 0:1. In addition, the CS-PAA complexes had more swelling property than HPMC as shown in Figures 75 and 76. As the amount of HPMC in ternary mixture increased and the amount of CS-PAA complex decreased, the overall swelling of the mixture would be decreased. For further development of propranolol osmotically-controlled release systems, the proportion of CS-PAA:HPMC at 1:1 was selected.
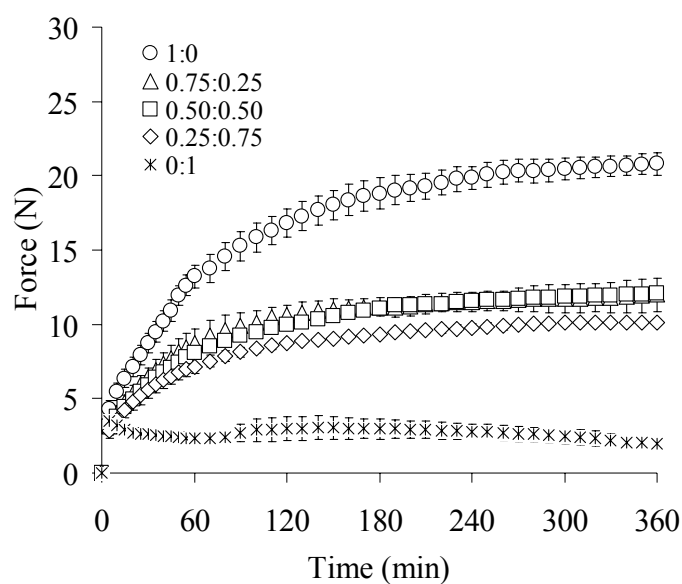
Figure 40. Effect of HPMC proportion on swelling force of CS-PAA:HPMC ternary
mixtures
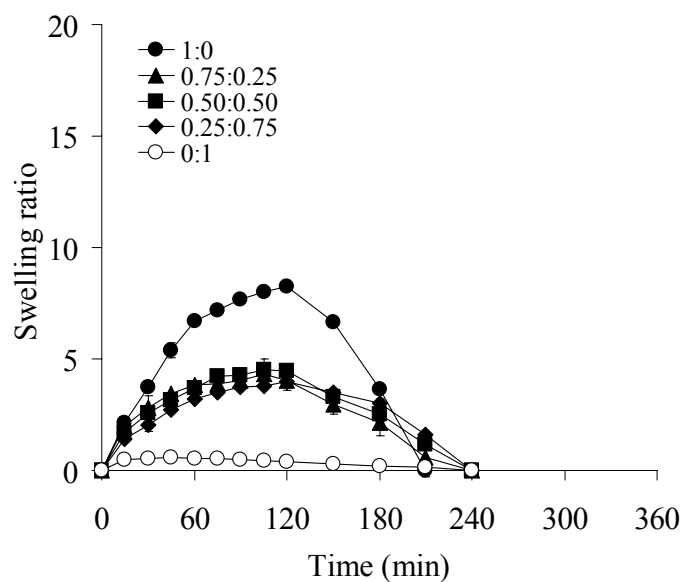
Figure 41. Effect of HPMC proportion on swelling ratio of CS-PAA:HPMC ternary
mixtures
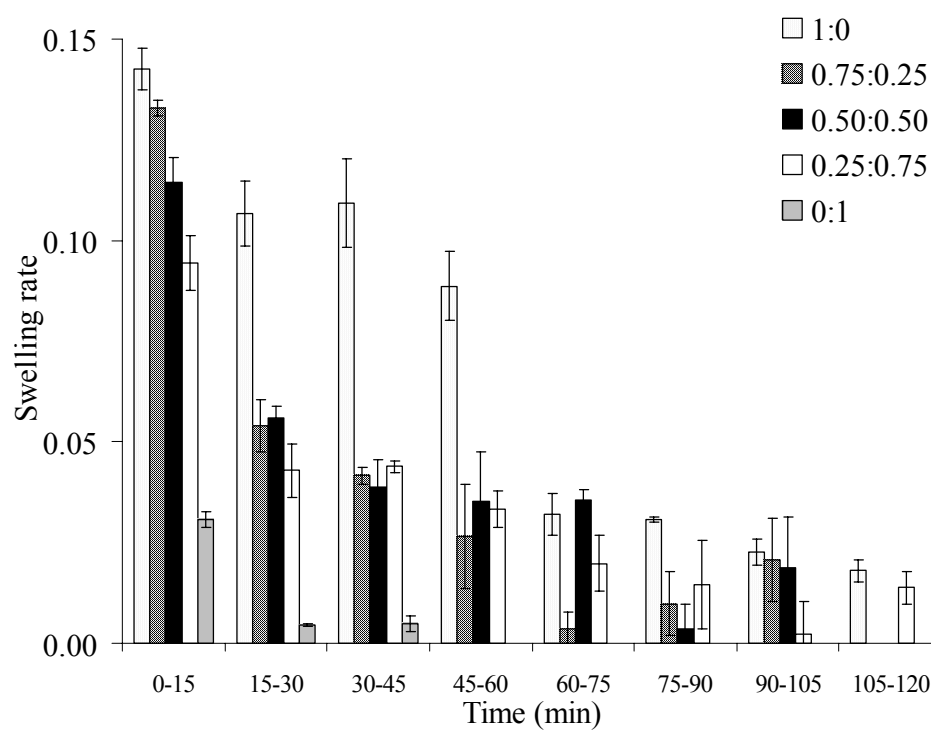
Figure 42. Swelling rate of CS-PAA:HPMC hydrogels at various time intervals

Part III: Use of Ternary Mixtures of CS-PAA:HPMC as Osmotic Agents for the Development of Controlled-Porosity Osmotic Pump Tablets

10. Propranolol CPOP tablets using CS-PAA:HPMC as osmogents

The CPOPs were prepared in two steps, first preparing core tablets and then coating the core tablets. Initially, the core tablets containing various amounts of ternary mixtures of CS-PAA:HPMC, i.e., 10, 20 and 30 mg, were manufactured in monolithic and bilayered tablets. A formulation without polymeric agent was also prepared for a comparison study (coded as C-0). Subsequently, the core tablets were coated with a mixture of coating solution of cellulose acetate containing PEG 400 as a plasticizer and PVP K30 as pore formers. Physical properties of the core and coated tablets are shown in Tables 28 and 29, respectively.

11. *In vitro* drug release studies of propranolol osmotic pump tablets

Figure 43 shows the release profiles of propranolol from monolithic CPOPs containing various amount of CS-PAA:HPMC at 8% coating level. CPOPs with 0–20 mg of CS-PAA:HPMC exhibited no bursting during the dissolution period of 12 h; however, a short lag time was presented at the beginning. Besides, the semipermeable membrane of CPOP containing 30 mg polymer was broken due to the excessive swelling of the core tablets. Increasing polymer amount decreased the release rate and total drug dissolved. The system without polymeric osmogent (coded as C-0) showed the highest drug release of 73.8% at 12 h; however, it was not enough to achieve the criteria of USP 28. The total drug release decreased with the increasing amount of polymer in monolithic systems; drug release at 12 h from CPOPs with 10 and 20 mg polymer were 52.1% and 24.9%, respectively.

The drug release was improved in the case of bilayered CPOPs, as shown in Figure 44. Percent drug releases at 12 h from CPOPs with 10 and 20 mg polymer were 82.1% and 81.9%, respectively. Additionally, CPOPs containing 30 mg polymer exhibited burst release (data is not shown). It was interesting to note that the drug release from bilayered tablets increased with the amount of osmogent. The profiles

show a maximum at 20 mg CS-PAA:HPMC containing. It could be concluded that a CS-PAA:HPMC in the amount of 10–20 mg was sufficient to push the drug out of the tablets in order to accomplish the drug release conforming to the criteria of USP 28.

Two involved contrary mechanisms are hypothesized. Ternary mixtures of polymers swell and expand to push the drug out of the tablets, and, concomitantly, the drug is bound to the polymer network following water uptake. Interactions between propranolol hydrochloride and anionic polymers, such as methacrylic acid copolymers, alginic acid and acrylic-cyclodextrins, were reported previously (166-168). The reason was the presence of preferential hydrogen bonding between the amino group of propranolol hydrochloride and the carboxylic functions of the polymers. In this study, it could be explained that the drug release from the monolithic tablets decreased with the increase of ternary mixtures due to the binding between the amino group of the drug and the COO^- group of the *in house* ternary mixtures of CS-PAA:HPMC. It can be conclude that the bilayer system which polymer can swell and directly push the drug out is more appropriate in order to control the drug release conforming to the USP criteria.

Figure 45 demonstrates the effect of membrane weight gain on the drug release from bilayered CPOPs formulated with 20 mg of CS-PAA:HPMC. The higher membrane weight increase, the longer lag-time was observed. The time for 10% drug released ($T_{10\%}$) from CPOPs with coating levels of 8, 12 and 16% were approximately 1, 1.5 and 2 h, respectively. Drug releases at 4 h from CPOPs at 8%, 12% and 16% coating level were 49.95, 39.40 and 31.05%, respectively. The lower membrane weight gain, the faster drug release was observed. As the amounts of pore formers in all formulations were constant, total drug releases, i.e., 81.93, 83.23 and 80.10%, from 8, 12 and 16% coating level, respectively, were comparable. The release profiles of two formulations of CPOP were compared using a model independent method. The f_2 values between 8–12% and 12–16% coating were found to be 58.2 and 58.9, respectively. It could be concluded that the drug releases from 8% and 12% coating formulations and likewise from the drug release from 12% and 16% coating formulations were comparable. However, the f_2 value between 8 and 16% coating formulations was found to be 44.3, indicating dissimilarity of these profiles. It was shown that the bilayered CPOP tablets with 20 mg of polymeric osmogent at the

coating levels in the range of 8–16% provided acceptable release profiles based on the USP 28 criteria. However, only two formulations at 8 and 12% coating levels were selected for the *in vivo* study as the release profiles at 16% coating level was almost under the limits.

Dissolution data were fitted to various mathematical models (zero-order, first-order and Higuchi) in order to establish the kinetics of drug release (shown in Figures 46–48, respectively). The best goodness-of-fit (r^2), and the smallest values of sum of squared residuals (SSR) and of Akaike information criterion (AIC) indicate the model suitability for a given dissolution data profile (151). Drug release up to 60% from CPOPs containing *in house* CS-PAA:HPMC as osmogents fitted well into the zero-order kinetic (Table 26).

Table 28. Physical properties of core tablets containing various amount of ternary mixtures of CS-PAA:HPMC

	Weight, mg (SD) (n=20)	Thickness, mm (SD) (n=10)	Diameter, mm (SD) (n=10)	Hardness, N (SD) (n=10)	DT, min (SD) (n=6)	Content uniformity, % LA (SD) (n=10)	Friability, (%)
MN-0	304 (1)	4.34 (0.01)	8.99 (0.02)	83 (8)	5.8 (0.5)	100.1 (0.2)	0.13
MN-10	304 (1)	4.35 (0.01)	8.96 (0.02)	85 (8)	6.5 (0.7)	99.9 (0.3)	0.21
MN-20	304 (1)	4.31 (0.01)	8.97 (0.01)	91 (10)	6.9 (0.6)	100.0 (0.1)	0.18
MN-30	304 (1)	4.35 (0.02)	8.96 (0.02)	102 (9)	7.3 (0.9)	100.6 (0.4)	0.15
BI-10	303 (1)	4.34 (0.03)	8.96 (0.01)	86 (7)	6.3 (0.4)	99.8 (0.3)	0.26
BI-20	303 (1)	4.38 (0.02)	8.97 (0.02)	81 (8)	6.1 (0.7)	100.2 (0.1)	0.44
BI-30	302 (1)	4.39 (0.01)	8.95 (0.01)	84 (8)	7.0 (0.7)	100.5 (0.4)	0.31

Table 29. Physical properties of CPOPs containing various amount of ternary mixtures
          of CS-PAA:HPMC at coating level of 8%

Formulations	Weight, mg (SD) (n=20)	Thickness, mm (SD) (n=10)	Diameter, mm (SD) (n=10)	Hardness, N (SD) (n=10)
MN-0	327 (8)	4.68 (0.02)	9.07 (0.01)	> 200
MN-10	328 (7)	4.70 (0.03)	9.06 (0.02)	> 200
MN-20	329 (9)	4.65 (0.02)	9.08 (0.02)	> 200
MN-30	327 (5)	4.67 (0.02)	9.06 (0.02)	> 200
BI-10	326 (6)	4.67 (0.03)	9.05 (0.01)	> 200
BI-20	328 (9)	4.71 (0.03)	9.08 (0.02)	> 200
BI-30	325 (5)	4.72 (0.03)	9.07 (0.02)	> 200
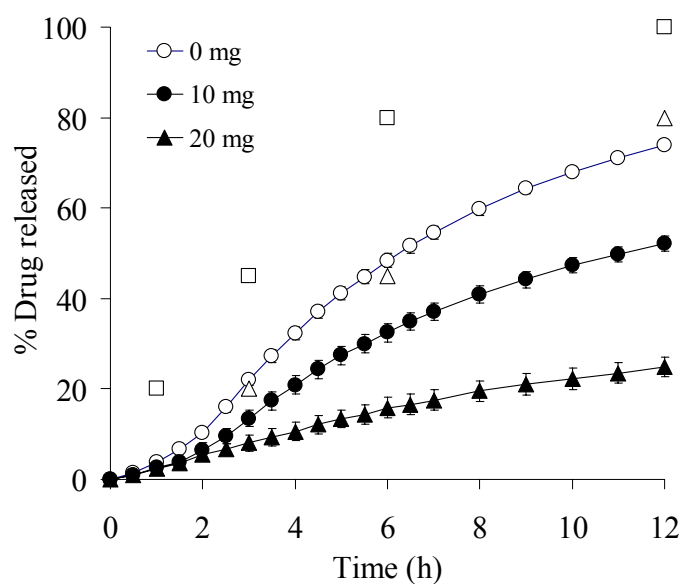
Figure 43. Drug release of monolithic CPOP with various amount of CS-PAA:HPMC
at coating level of 8%

Keys: USP 28 criteria at various times; Δ , lower limits; □ , upper limits
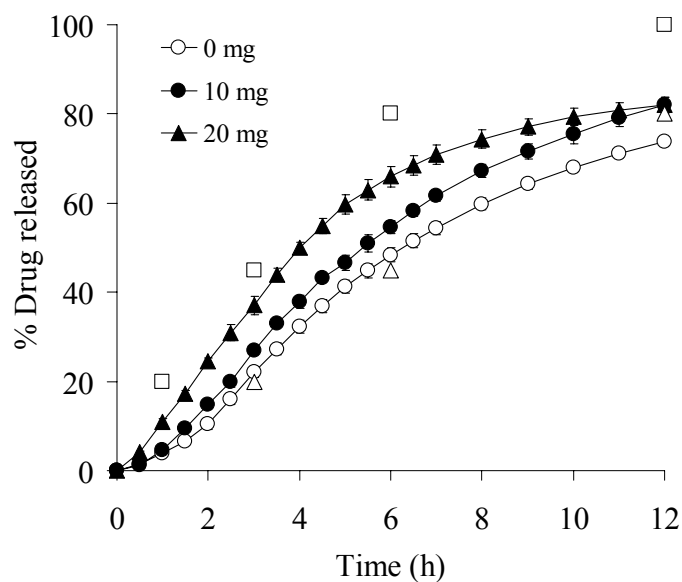
Figure 44. Drug release of bilayered CPOP with various amount of CS-PAA:HPMC
at coating level of 8%

Keys: USP 28 criteria at various times; Δ , lower limits; □ , upper limits
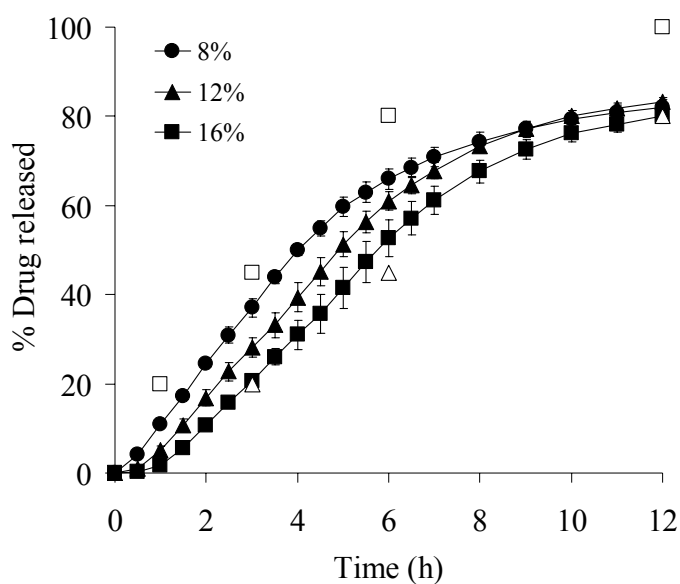
Figure 45. Drug release of bilayered CPOP with 20 mg of CS-PAA:HPMC at various
coating levels

Keys: USP 28 criteria at various times; Δ , lower limits; $\square$, upper limits
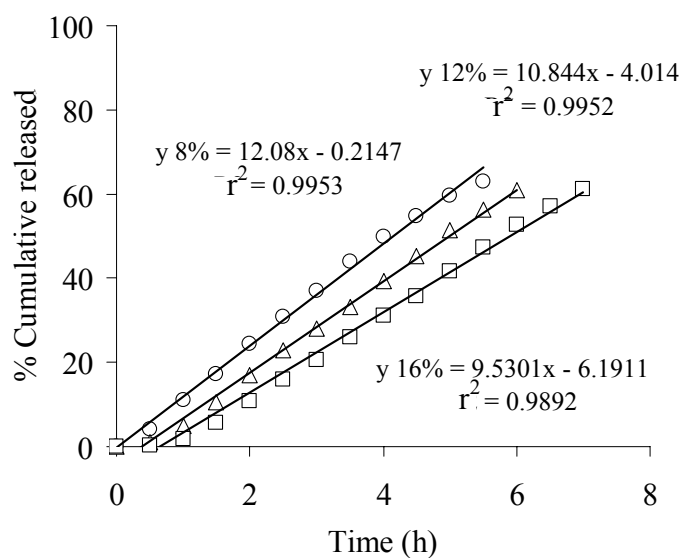
Figure 46. Plots of cumulative propranolol release *vs*. time for the CPOP tablets at
various coating levels
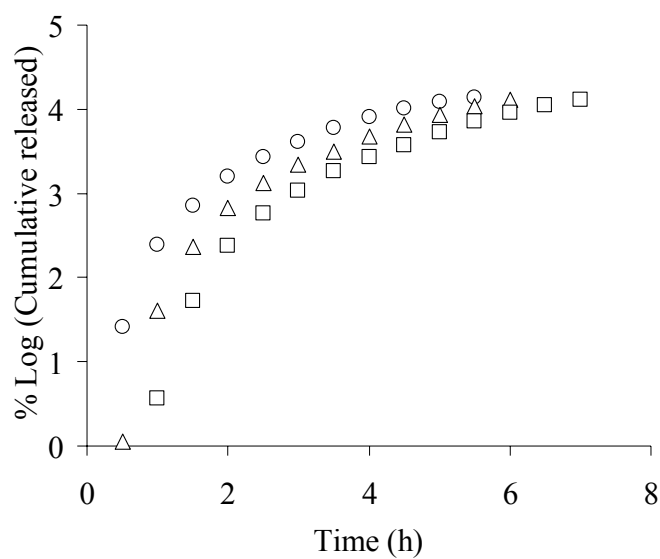
Keys: $\bigcirc$, 8%; Δ , 12%; $\square$, 16%.

Figure 47. Logarithmic plots of cumulative propranolol release *vs.* time for the CPOP

tablets at various coating levels
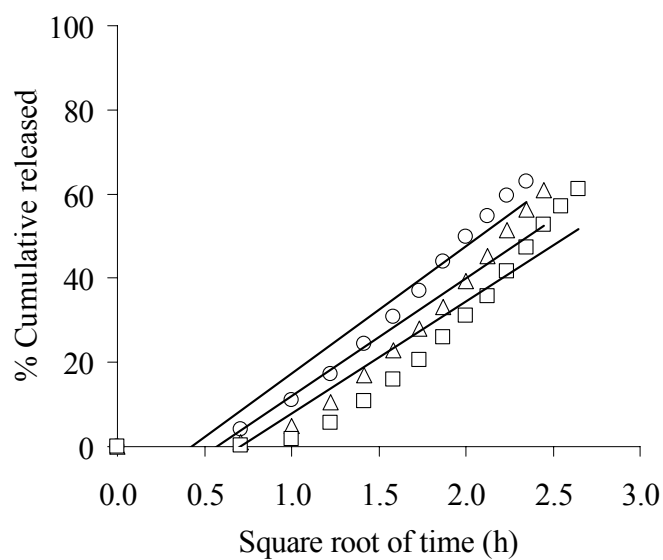
Keys: ○, 8%; Δ , 12%; □ , 16%.

Figure 48. Plots of cumulative propranolol release *vs.* square root of time for the

CPOP tablets at various coating levels

Keys: ○, 8%; Δ , 12%; □ , 16%.

Table 30. Fitting of drug release data of CPOPs based on mathematical models

Formulations	Model	Parameters used to assess the fit of model			
		r^2	k^*	$SSR \times 10^2$	AIC
BI-20-8%	Zero-order	0.9953	9.664	0.25	46.5
	First-order	0.8424	0.4664	12.75	86.7
	Higuchi	0.9252	30.256	3.92	77.7
BI-20-12%	Zero-order	0.9952	8.675	0.26	50.3
	First-order	0.7893	0.5885	28.22	103.3
	Higuchi	0.8851	27.939	64.59	120.1
BI-20-16%	Zero-order	0.9892	7.625	0.70	71.7
	First-order	0.7118	0.679	95.14	136.3
	Higuchi	0.8644	26.591	179.0	152.9

r^2, goodness of fit; SSR, sum of squared residuals; AIC, Akaike information criterion; and k^*, release rate constant for respective model (k_0 in mg/h, k_1 in h^{-1}, and k_H in %/h$^{1/2}$ for zero-order, first-order and Higuchi rate equations, respectively)

12. *In vivo* evaluation of the developed propranolol osmotic pump tablets

Two formulations of CPOPs, i.e., bilayered tablets with 20 mg of CS-PAA:HPMC at the coating levels of 8 and 12%, which provided *in vitro* release profiles following the criteria of USP 28, were compared to a rapid release dosage form used as a reference formulation (See Figure 49). The *in vivo* test was studied in 9 pigs. A three-way crossover study design with a three-day washout period was employed in the present study. The drug in plasma was assayed by a HPLC method with fluorescence detection. Assay performances was validated and conducted according to the US FDA guideline for biological method validation (129). The method of analysis was validated in detail as follows:

12.1. Validation of HPLC method for determination of propranolol in plasma

12.1.1. Separation and specificity

Figures 50–52 show the typical chromatograms received from HPLC analysis of blank plasma, plasma spiked with benzimidazole (internal standard; IS), and plasma spiked with propranolol and IS, respectively. The retention time of propranolol was approximately 7.6 min, whereas that of the IS was around 4.3 min, with a total run-time of 26 min. Under these conditions, all compounds of interest were completely separated and there was no interference peaks from endogenous substances in plasma that was co-eluted with propranolol as well as the IS.

12.1.2. Calibration of standard curve

Calibration curves over the 1 to 50 ng/mL concentration range of propranolol were constructed in blank plasma. Linearity of the method was demonstrated by multiple analyses of spiked plasma samples containing propranolol and IS. The calibration curves were plotted between peak height ratios of propranolol to the IS against propranolol concentrations as shown in Figure 54; compared with those of pure drug and IS in ultra-purified water as presented in Figure 53. A good linear relationship with the coefficient of determination (r^2) of more than 0.99 was employed for determining of propranolol concentration in plasma.

12.1.3. Recovery

Extraction efficiency was analyzed using the low, medium, and high QC samples, as given in Table 31. The percent recovery was calculated based on a

comparison of the HPLC responses from plasma to those from water samples. The extraction efficiencies demonstrated no concentration dependency, and were similar between each concentration. More than 64% of propranolol can be detected from the plasma samples after the extraction, compared to the amount of propranolol found in the standard solution directly injected to the HPLC system. The extents of recovery of propranolol and of the IS were consistent, precise, and reproducible as demonstrated by good linearity of the calibration curve, and good precision and accuracy of this analytical method.

12.1.4. Precision and accuracy

The assay demonstrated good precision and accuracy over the entire calibration range, both within and between days, as depicted in Table 32. The precisions of the assay procedure were lower than 9.89% at all QC levels with the accuracy ranged from 95.9 to 103.8%.

12.1.5. The lower limit of quantification

The lowest limit of quantification (LLOQ) of propranolol in plasma was found at 1 ng/mL, with the coefficient of variation of 8.43% and the accuracy of 105.8% (Table 32). Determinations of plasma propranolol concentration below the quantification limit was defined as zero ng/mL.

12.2. Stability

Stability studies of the propranolol stock solution are presented in Table 33. These results indicated that the stock solutions kept at 4 °C were stable for at least 3 months; the concentration reduced 2.95% in relation to time zero. Additionally, stability of propranolol in plasma at three QC concentrations of 2, 20, and 40 ng/mL kept frozen at -20 °C for 1, 2, 4, 8 and 12 weeks was also studied. The initial propranolol concentration freshly after sample preparation was assumed to be 100%. The stability results of propranolol in plasma at each concentration are summarized in Table 34. At the concentrations of 2, 20 and 40 ng/mL, the percentage remaining of propranolol in plasma after the storage period of 8 weeks were 92.2, 96.4 and 96.2%, respectively. However, after the storage period of 12 weeks, the propranolol amounts at all concentrations were reduced drastically and showed the percent remaining less than 80%. From these results it can be confirmed that propranolol was stable in plasma stored at -20 °C for at least 8 weeks.
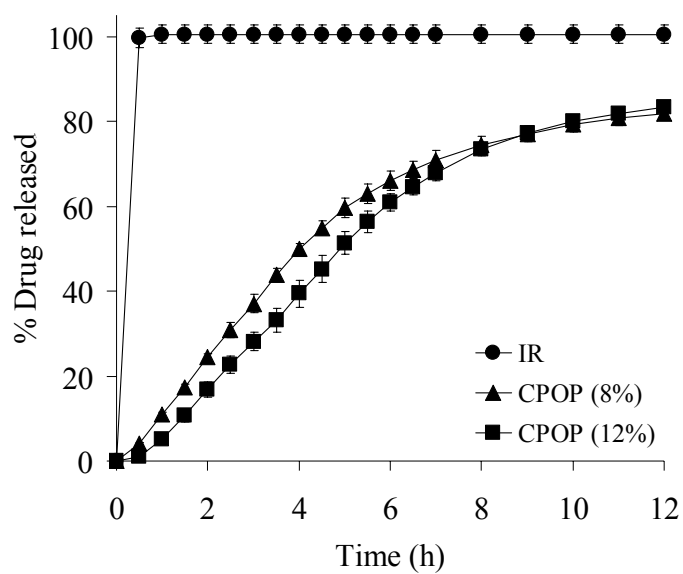
Figure 49. Comparison of dissolution profiles between the reference (IR) and the test
            formulations
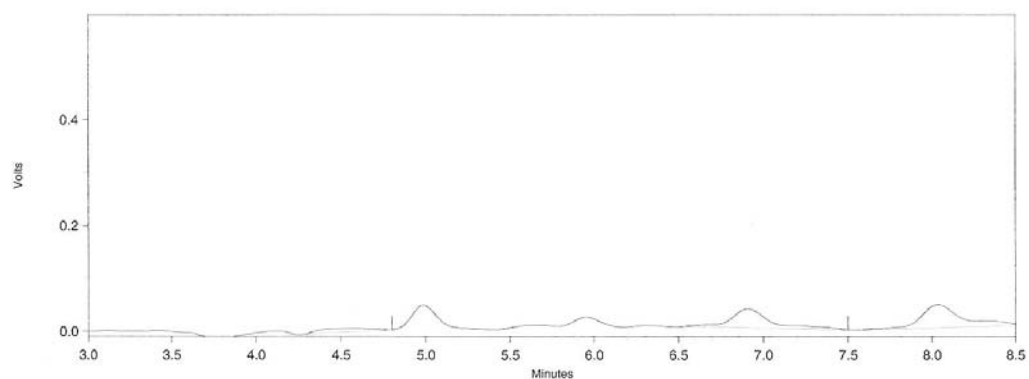
Figure 50. Typical chromatogram of HPLC analysis of blank plasma
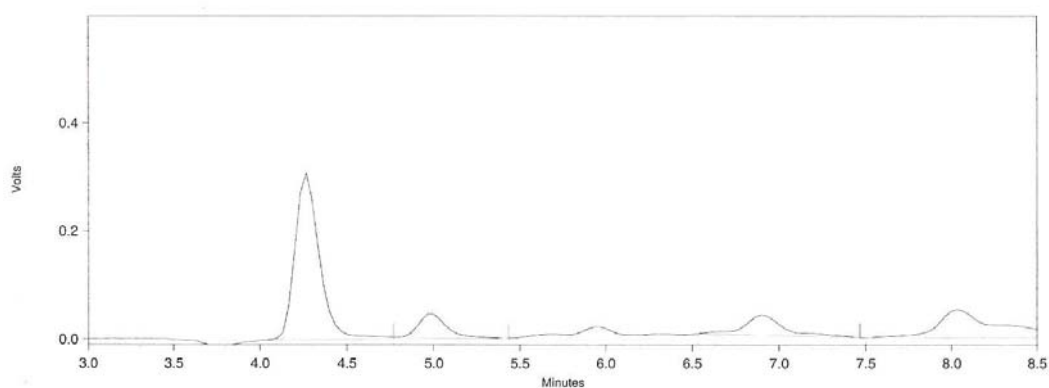
Figure 51. Typical chromatogram of HPLC analysis of spiked benzimidazole (IS) in plasma
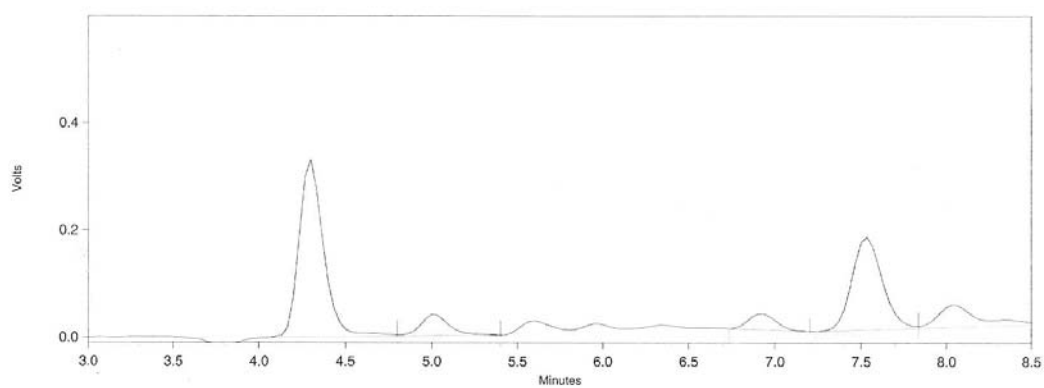
Figure 52. Typical chromatogram of HPLC analysis of propranolol and benzimidazole (IS) in plasma
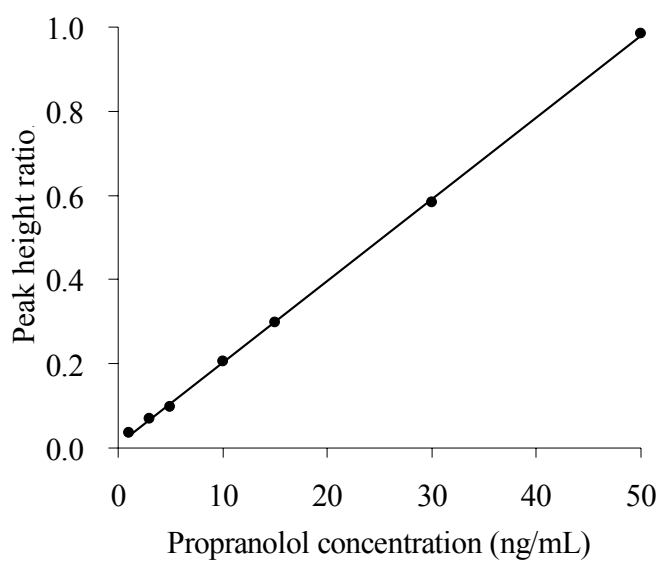
Figure 53. Typical calibration curve of propranolol in water analyzed by HPLC
            ($y = 0.0194x + 0.0084$, $r^2 = 0.9997$)
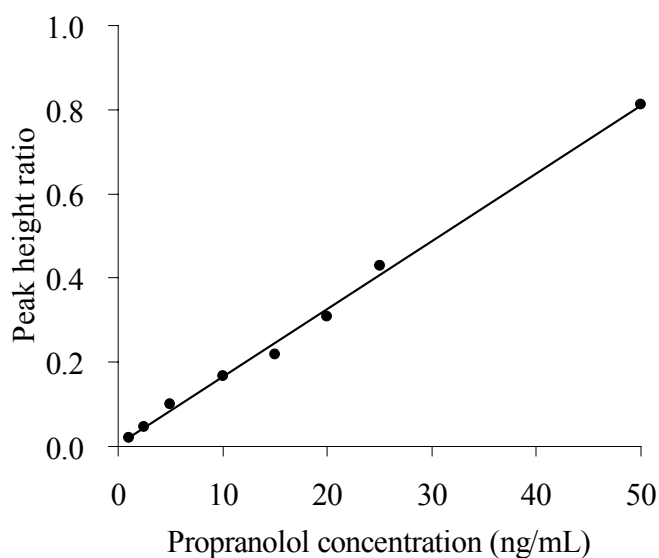
Figure 54. Typical calibration curve of propranolol in plasma analyzed by HPLC
            ($y = 0.0161x + 0.0037$, $r^2 = 0.9962$)

Table 31. Recovery of propranolol in spiked plasma

Spiked concentration of propranolol (ng/mL)	Peak height ratios (mean ± SD), n = 5		% Recovery
	Propranolol in water	Propranolol in plasma	
2	0.0493 ± 0.0066	0.0378 ± 0.0020	76.6
20	0.5191 ± 0.0101	0.3349 ± 0.0279	64.5
40	0.7887 ± 0.0129	0.5941 ± 0.0146	75.3

Table 32. Assay precision and accuracy of the analytical method for propranolol in plasma (n = 7 assays)

Propranolol concentration	Mean Accuracy (%)	Inter-assay Precision (%CV)	Intra-assay Precision (%CV)
LLOQ (1 ng/mL)	105.8	8.43	4.14
Low-QC (2 ng/mL)	103.8	9.89	5.03
Medium-QC (20 ng/mL)	102.2	0.00	7.38
High-QC (40 ng/mL)	95.9	4.90	9.24

Table 33. Stability of propranolol stock solution stored at 4 °C

Storage period (weeks)	Propranolol concentration (mg/mL, mean ± SD, n = 3)	% Propranolol remaining
0	1.0030 ± 0.0015	100.0
4	0.9978 ± 0.0087	99.5
8	0.9920 ± 0.0071	98.9
12	0.9934 ± 0.0025	97.1

Table 34. Stability of propranolol in spiked plasma stored at -20 °C

Spiked propranolol concentration (ng/mL)	Storage period (weeks)	Propranolol concentration (mg/mL) (mean ± SD, n = 3)	% Propranolol remaining
2	0	2.0414 ± 0.1264	100.0
	1	2.1046 ± 0.0708	103.1
	2	2.0369 ± 0.0283	99.8
	4	1.9946 ± 0.0276	97.7
	8	1.8828 ± 0.1877	92.2
	12	1.2145 ± 0.1203	59.5
20	0	20.3819 ± 1.7245	100.0
	1	20.8893 ± 0.4278	102.5
	2	20.8754 ± 0.2635	102.4
	4	19.8217 ± 0.7498	97.3
	8	19.6963 ± 0.2374	96.4
	12	14.6773 ± 0.5398	72.0
40	0	39.3857 ± 0.9035	100.0
	1	40.0486 ± 1.0730	101.7
	2	39.2544 ± 0.7675	99.7
	4	39.1011 ± 0.3135	99.3
	8	37.9028 ± 0.6155	96.2
	12	29.0628 ± 2.0030	73.8

12.3. Pharmaceutical parameters determination

Observations were made in 9 pigs, each received 40 mg propranolol IR tablets, and 80 mg propranolol *in house*-formulated CPOPs at 8 and 12% coating levels on separate occasions with at least 3 days between each treatment. The mean plasma propranolol concentration–time profiles after single oral dose of the IR tablets and the developed CPOPs are demonstrated in Figures 55 and 56–57, respectively. Overlays of the mean plasma profiles of each formulation are shown in Figure 58. Table 35–42 specify individual values of $AUC_{0\text{-last}}$, $AUC_{0\text{-}\infty}$, $AUMC_{0\text{-}\infty}$, F, C_{max}, T_{max}, T_{lag}, and MRT, respectively. Mean values of pharmacokinetic parameters obtained are expressed in Table 43. It is mentioned that the AUC up to the concentration measured at the last time point ($AUC_{0\text{-last}}$) in most formulations were not determined up to the last sampling time, i.e., up to 5 or 6 h for IR tablets and 12 h for CPOPs, even blood samples were taken up to 12 h for IR tablets and 24 h for CPOPs. This is due to the fact that the concentration of propranolol in some pig plasma samples taken after 5 or 6 h for IR, or 12 h for CPOPs was below the LLOQ of the analytical methods employed in this study.

Comparison of propranolol plasma profiles (See Figure 58) shows that both of CPOPs produced lower peak plasma concentrations of propranolol and longer times to peak than that after administration of the IR preparation. The mean peak plasma level of 20.7 ng/mL after IR tablets occurred at 1.33 h; the plasma level then declined exponentially with time with the elimination rate constant of 0.644 h^{-1} and the elimination half-life of 1.08 h. After administrations of propranolol CPOPs, the mean plasma level increased gradually and reached a peak of 9.84 ng/mL at 4.33 h and 6.97 ng/mL at 4.94 h, for 8% and 12% coating CPOPs, respectively. C_{max} for IR tablets was significantly higher than those of for both 8% and 12% coating CPOPs based on one-way ANOVA and Student's *t*-test ($p < 0.05$). The peak levels between 8% and 12% coating formulations were also significantly different ($p < 0.05$). The time to peak level for IR tablets was significantly shorter than those of for the CPOPs ($p < 0.05$). Interestingly, the time to peak propranolol concentration for 8% coating tablets was also significantly faster than that of for 12% coating tablets ($p < 0.05$); however, lag times of both osmotically controlled-release formulations were not statistically different ($p > 0.05$).

The AUC was estimated using the trapezoidal rule. The mean values obtained for the IR tablets, and for 8% and 12% coating CPOPs were 47.7, and 78.3 and 59.6 ng.h/mL, respectively. Due to the dose of propranolol administered to pigs from a reference formulation and from the test formulations were not equivalent; it was 40 mg from a rapid release formulation, and 80 mg from *in house* CPOP tablets (over the range of 40 to 160 mg propranolol there was a linear relationship of AUC with dose (111)). Therefore, for comparison between formulations, the AUCs of propranolol from the conventional product were corrected to a dose of 80 mg by multiplying by two. It was found that the $AUC_{0-\infty}$ of the CPOP with 8% coating was not significantly different from the reference ($p > 0.05$); whereas the 12% coating tablet gave the significantly lower $AUC_{0-\infty}$ compared to the reference ($p < 0.05$). On the contrary, the mean MRT value obtained from both 8% and 12% coating CPOPs were significantly longer than that of the reference ($p < 0.05$). As a consequence, it can be considered from the results that these CPOP formulations in general remained in systemic circulation longer than that of the IR tablets, possibly owing to the fact that they exhibited the slower release profiles. C_{max} levels in the pig were lower than those observed in human (23–28 ng/mL) (169, 170). Moreover, AUCs was much lower than in man (308–311 ng.h/mL) (169, 170) and may due to higher clearance and/or higher metabolism.

The corresponding relative bioavailability (F) values calculated based on the ratio of $AUC_{0-\infty}$ of propranolol CPOPs tablets to that of propranolol IR tablets corrected by the doses administered were averaging as 86.2% (ranged: 45.6–121.7%) for 8% coating CPOPs, and 63.5% (ranged: 34.5–116.3%) for 12% coating CPOPs. In summary, administration of the CPOP with 8% coating level resulted in plasma concentrations maintained at a level of 5–10 ng/mL for 6 h (between 2.5–8.5 h) while the CPOP with 12% coating level could maintain the same range for only 4 h (between 4–8 h).

These are in agreement with the results observed during the dissolution experiments. The same rank order was observed between *in vitro* release rate and *in vivo* rate of absorption, i.e., IR tablets > 8% coating level > 12% coating level. The faster drug release was obtained from 8% coating CPOPs, due to the thinner of the micro/nanoporous semipermeable membrane, with $T_{10\%}$ about 1 h; subsequently,

results from *in vivo* study revealed that T_{lag} were approximately 1.11 min. On the other hand, the slower release profile was attained from 12% coating CPOPs with $T_{10\%}$ around 1.5 h and became to be 1.39 h of T_{lag} in pigs. The higher percent *in vitro* releases from 8% coating CPOPs than that from 12% coating level were corresponding to the higher plasma concentration observed in pigs. Two formulations of CPOP, which gave comparable *in vitro* dissolution profiles (f_2 values = 58.2), could be sustained propranolol plasma concentration *in vivo* by up to 12 h with no significant difference of the $AUC_{0-\infty}$ ($p > 0.05$).

The dosage forms were designed to be the rate-limiting step in the absorption process; therefore it should follow that the rise in the percent of the amount absorbed should mimic the release of drug from formulations. Since the release of propranolol from the CPOPs followed the zero-order mechanism of release (See Figure 46), it should follow that the increase in the cumulative AUC should mimic this release, then be linear with respect to time, and it did as shown in Figure 59. The slope of the *in vivo* data were determined to be about 5.94 and 5.26 for the 8% and 12% coating CPOPs corresponding to the *in vitro* release rate of 9.66 and 8.68 for the corresponding dosage forms. The *in vivo* values were rather lower than those of *in vitro* due to systemic bioavailability of propranolol is restricted, approximately 33%, as a result of hepatic first-pass metabolism (109). These are good indications that the mechanism and rates of release *in vivo* mimic mechanism and rates of release *in vitro* (91).

Graphical plots of pharmacokinetic parameters obtained from propranolol osmotically-controlled release formulations were illustrated in Figures 60–66. When compared the parameters against the IR reference product, the plots of AUC_{0-last} and $AUC_{0-\infty}$ show high variation both in inter-pig and intra-pig variation. Moreover, as shown in the figures, the pharmacokinetic parameters obtained from the 12% coating CPOP were the most variable among the other. When compared between two CPOP formulations, the high variation both in inter-pig and intra-pig were also observed from the T_{max} and T_{lag} plots. In contrast, the plots of C_{max} show differences from pig to pig, while within pig variations are considerably smaller as indicated by the slopes of the lines. Inter-subject variability in propranolol pharmacokinetics following a single oral dose was also observed in human (171).
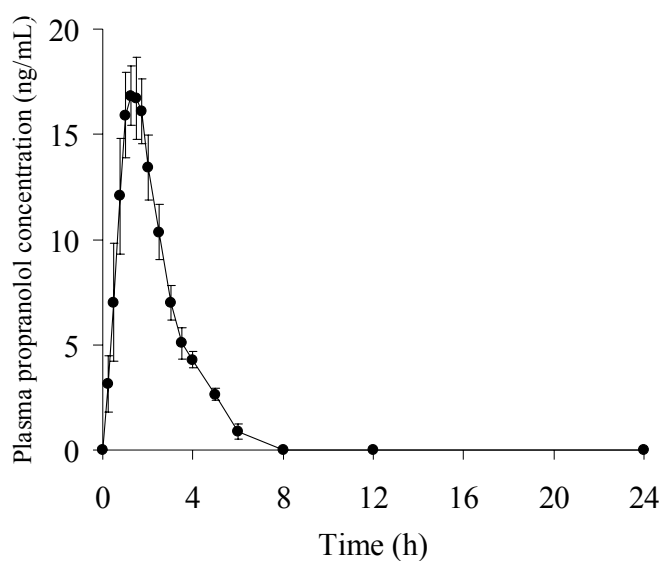
Figure 55. Pig plasma propranolol concentration–time profile after single administration of the immediate release tablets of propranolol (40 mg). Each data point represents mean ± SEM of 9 pigs.
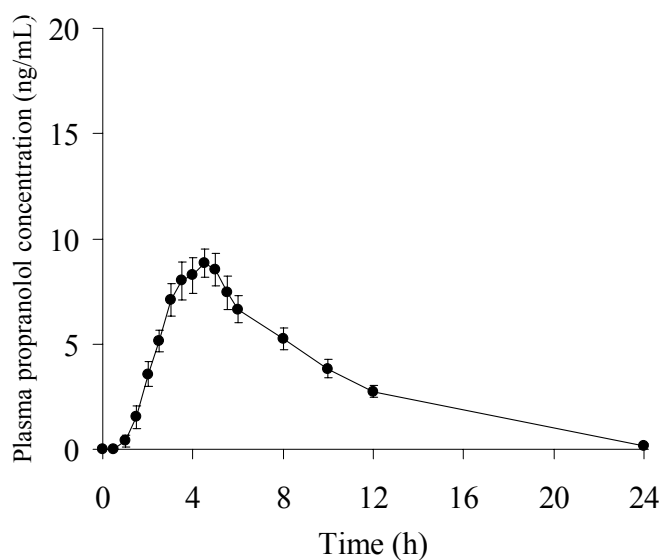
Figure 56. Pig plasma propranolol concentration–time profile after single administration of 80 mg propranolol CPOP tablets with coating level of 8%. Each data point represents mean ± SEM of 9 pigs.
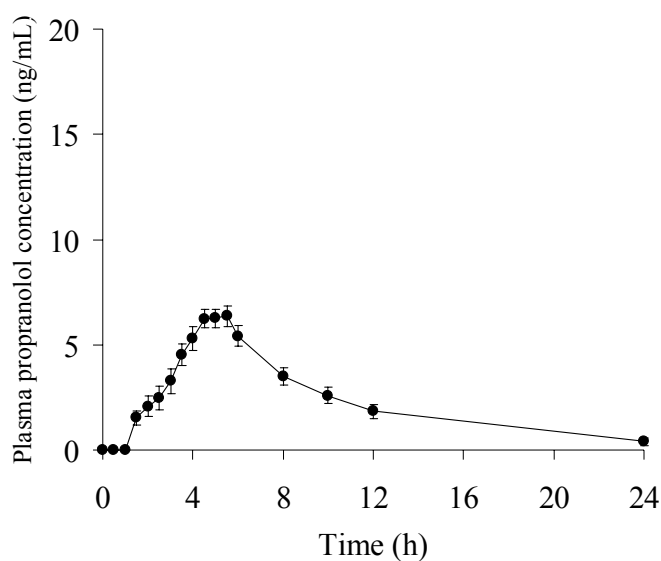
Figure 57. Pig plasma propranolol concentration–time profile after single administration of 80 mg propranolol CPOP tablets with coating level of 12%. Each data point represents mean ± SEM of 9 pigs.
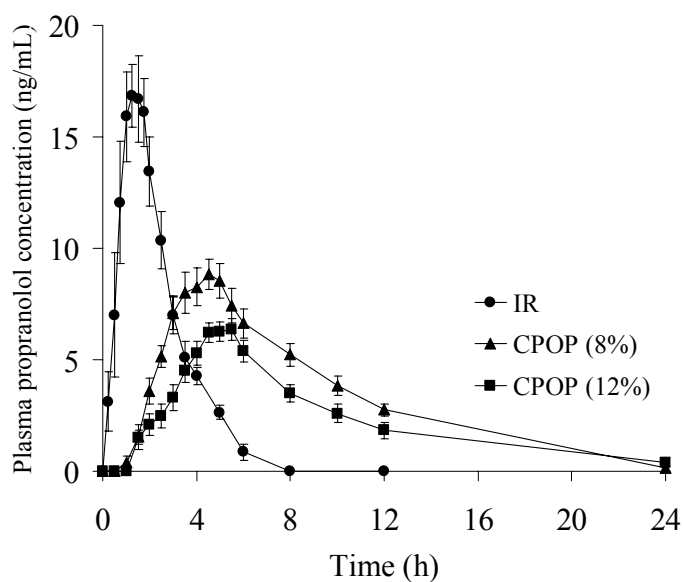
Figure 58. Comparison of plasma propranolol concentration–time profile after single administration of the immediate release (IR) tablets (40 mg propranolol) and the developed CPOP tablets (80 mg propranolol) with various coating levels. Each data point represents mean ± SEM of 9 pigs.

Table 35. Calculated area under the plasma concentration-time curves from time zero to the last determined time point ($AUC_{0\text{-last}}$, ng.h/mL) after single oral administrations of propranolol formulations

Pig	IR tablets	8% coating CPOPs	12% coating CPOPs
	(40 mg propranolol)	(80 mg propranolol)	(80 mg propranolol)
1	41.89	70.19	66.32
2	32.35	54.83	20.66
3	44.93	47.77	31.10
4	60.54	61.82	48.34
5	34.85	81.52	36.63
6	38.41	46.07	36.89
7	56.74	47.66	45.87
8	46.94	80.40	69.55
9	39.56	72.94	86.25
Mean	44.02	62.58	49.07
S.D.	9.49	14.21	21.04
CV (%)	21.55	22.71	42.89

Table 36. Calculated area under the plasma concentration-time curves from time zero
to infinity ($AUC_{0-\infty}$, ng.h/mL) after single oral administrations of
propranolol formulations

Pig	IR tablets	8% coating CPOPs	12% coating CPOPs
	(40 mg propranolol)	(80 mg propranolol)	(80 mg propranolol)
1	44.03	97.03	82.51
2	34.55	70.56	23.86
3	48.81	58.63	40.75
4	66.25	85.83	63.22
5	37.92	92.31	41.72
6	44.22	69.87	40.16
7	62.11	56.61	57.65
8	49.17	86.23	89.58
9	41.82	87.60	97.23
Mean	47.65	78.30	59.63
S.D.	10.51	14.75	25.46
CV (%)	22.05	18.84	42.70

Table 37. Calculated area of the first moment of the plasma concentration-time curves extrapolated to infinity ($AUMC_{0-\infty}$, $ng.h^2/mL$) after single oral administrations of propranolol formulations

Pig	IR tablets	8% coating CPOPs	12% coating CPOPs
	(40 mg propranolol)	(80 mg propranolol)	(80 mg propranolol)
1	88.46	965.77	1245.19
2	95.50	614.20	157.49
3	122.08	471.85	369.42
4	165.66	808.37	545.64
5	103.54	1121.91	288.34
6	147.70	719.45	266.00
7	172.53	422.95	483.19
8	83.04	561.66	1447.51
9	107.40	682.14	1167.27
Mean	120.66	707.59	663.34
S.D.	33.54	228.00	486.64
CV (%)	27.80	32.22	73.36

Table 38. Relative bioavailability (F, %) values after single oral administrations of propranolol CPOP tablets with various coating levels using propranolol immediate release tablets as a reference (corrected by the doses of administration)

Pig	8% coating CPOPs	12% coating CPOPs
1	110.17	93.69
2	102.11	34.53
3	60.06	41.75
4	64.78	47.72
5	121.70	55.00
6	79.00	45.41
7	45.57	46.61
8	87.67	91.08
9	104.75	116.25
Mean	86.20	63.54
S.D.	25.69	28.96
CV (%)	29.80	45.57

Table 39. Maximum observed plasma propranolol concentration (C_{max}, ng/mL) after single oral administrations of propranolol formulations

Pig	IR tablets	8% coating CPOPs	12% coating CPOPs
	(40 mg propranolol)	(80 mg propranolol)	(80 mg propranolol)
1	18.97	10.68	8.93
2	16.18	9.75	4.49
3	18.74	8.74	5.26
4	29.63	10.42	8.89
5	17.30	8.90	7.02
6	20.17	8.18	7.61
7	22.85	7.57	6.31
8	25.99	13.08	6.94
9	16.14	11.38	7.31
Mean	20.66	9.84	6.97
S.D.	4.64	1.72	1.48
CV (%)	22.46	17.52	21.23

Table 40. Observed time to maximum plasma propranolol concentration (T_{max}, h) after single oral administrations of propranolol formulations

Pig	IR tablets	8% coating CPOPs	12% coating CPOPs
	(40 mg propranolol)	(80 mg propranolol)	(80 mg propranolol)
1	0.75	4.50	5.50
2	1.75	4.50	5.00
3	1.25	3.50	4.50
4	1.50	5.50	4.00
5	1.00	5.50	4.50
6	1.75	3.50	5.50
7	1.25	4.50	5.00
8	0.75	3.50	5.00
9	2.00	4.00	5.50
Mean	1.33	4.33	4.94
S.D.	0.45	0.79	0.53
CV (%)	33.80	18.24	10.66

Table 41. Observed lag-time (T_{lag}, h) after single oral administrations of propranolol formulations

Pig	IR tablets	8% coating CPOPs	12% coating CPOPs
	(40 mg propranolol)	(80 mg propranolol)	(80 mg propranolol)
1	0.00	1.50	3.00
2	0.50	1.50	2.50
3	0.00	1.50	1.00
4	0.00	1.00	1.00
5	0.25	1.50	1.00
6	0.25	0.50	1.00
7	0.00	1.00	1.00
8	0.00	1.00	1.00
9	0.00	0.50	1.00
Mean	0.11	1.11	1.39
S.D.	0.18	0.42	0.78
CV (%)	163.46	37.50	56.28

Table 42. Mean residence time (MRT, h) after single oral administrations of propranolol formulations

Pig	IR tablets	8% coating CPOPs	12% coating CPOPs
	(40 mg propranolol)	(80 mg propranolol)	(80 mg propranolol)
1	2.01	9.95	15.09
2	2.76	8.70	6.60
3	2.50	8.05	9.07
4	2.50	9.42	8.63
5	2.73	12.15	6.91
6	3.34	10.30	6.62
7	2.78	7.47	8.38
8	1.69	6.51	16.16
9	2.57	7.79	12.00
Mean	2.54	8.93	9.94
S.D.	0.47	1.72	3.64
CV (%)	18.62	19.26	36.57

Table 43. Mean pharmacokinetic parameters after single oral administrations of propranolol formulations[a]

Parameters	IR tablets	8% coating CPOPs	12% coating CPOPs
	(40 mg)	(80 mg)	(80 mg)
$AUC_{0\text{-last}}$ (ng.h/mL)	44.02 (9.49)	62.68 (14.21)	49.07 (21.04)
$AUC_{0\text{-}\infty}$ (ng.h/mL)	47.65 (10.51)	78.30 (14.75)	59.63 (25.46)
F^{b} (%)	-	86.20 (25.69)	63.54 (28.96)
C_{max} (ng/mL)	20.66 (4.64)	9.84 (1.72)	6.97 (1.48)
T_{max} (h)	1.33 (0.45)	4.33 (0.79)	4.94 (0.53)
T_{lag} (h)	0.11 (0.18)	1.11 (0.42)	1.39 (0.78)
MRT (h)	2.54 (0.47)	8.93 (1.72)	9.94 (3.64)

[a] Data shown as arithmetic mean (standard deviation), n = 9

[b] Relative bioavailability employing the IR tablets as reference
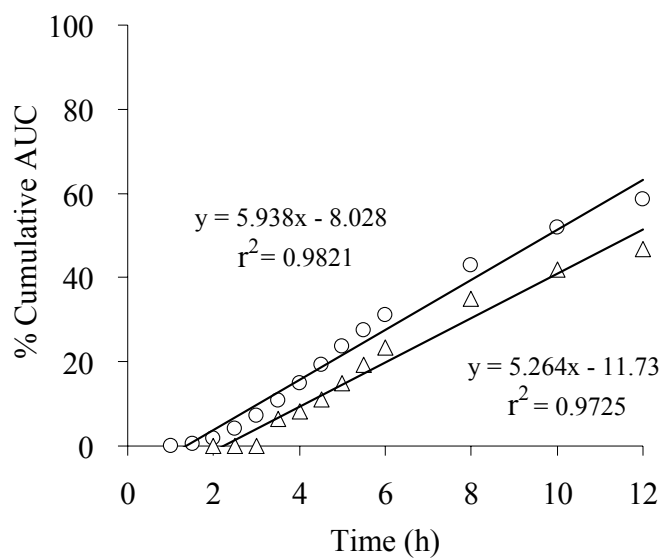
Figure 59. Plots of cumulative AUC *vs*. time after propranolol administrations

Keys: ○, 8% coating CPOPs

△ , 12% coating CPOPs.

(A)
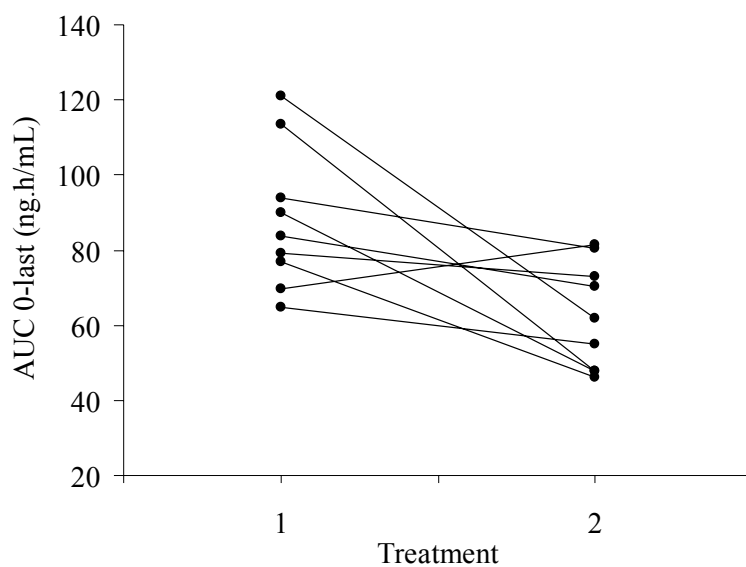
(B)
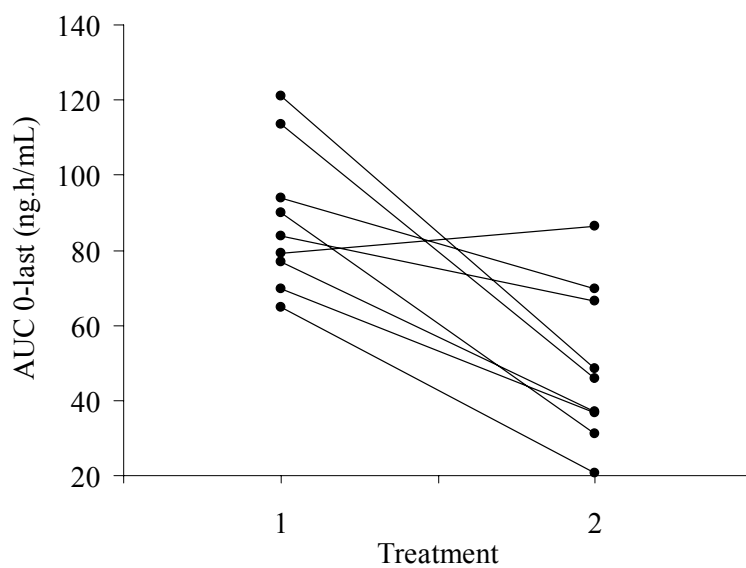
Figure 60. Graphical presentations of AUC_{0-last} value comparison of propranolol CPOP tablet formulations at various coating levels using IR propranolol tablets as reference for each of 9 pigs (corrected by the doses of administration)

Keys: A = IR tablets against CPOPs with coating level of 8%

B = IR tablets against CPOPs with coating level of 12%

(A)
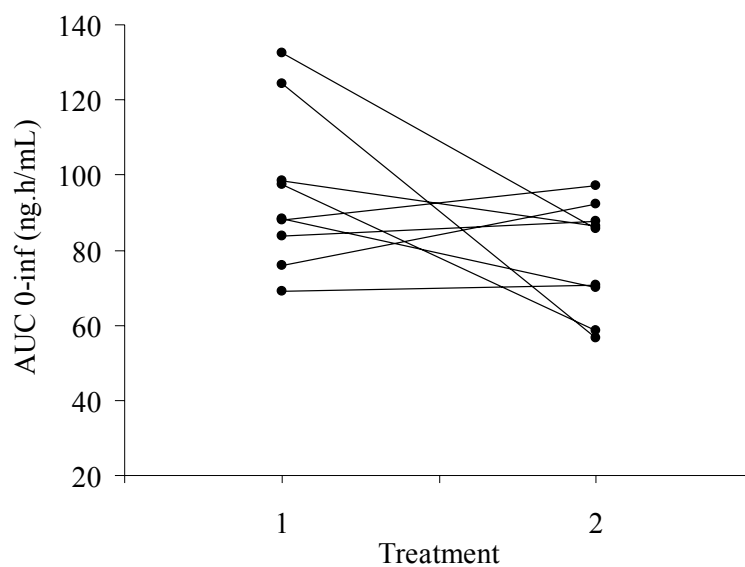
(B)
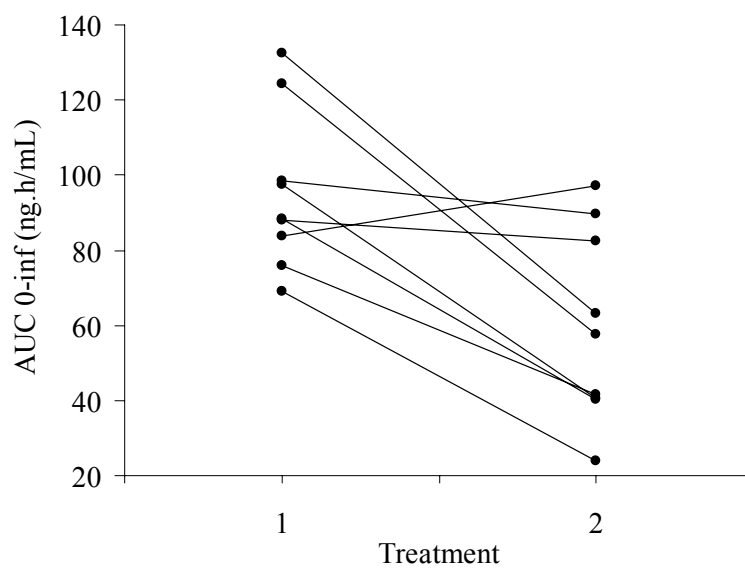
Figure 61. Graphical presentations of $AUC_{0-\infty}$ value comparison of propranolol CPOP tablet formulations at various coating levels using IR propranolol tablets as reference for each of 9 pigs (corrected by the doses of administration)

Keys: A = IR tablets against CPOPs with coating level of 8%

B = IR tablets against CPOPs with coating level of 12%
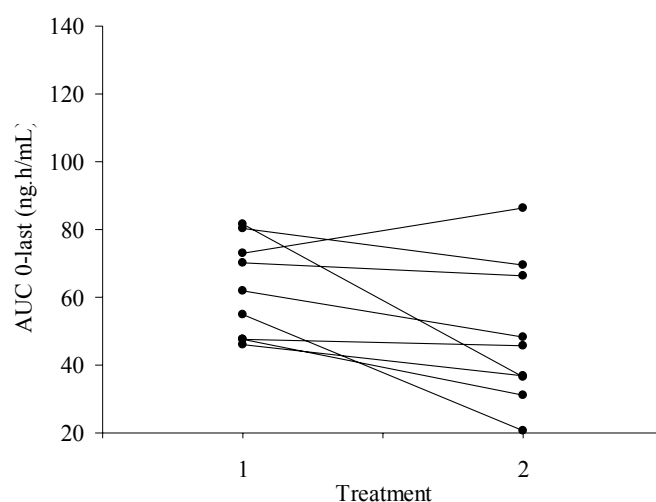
Figure 62. Graphical presentation of AUC_{0-last} value comparison between different
formulations of propranolol CPOP tablets at various coating levels for
each of 9 pigs

Keys: Treatment 1 = CPOPs with coating level of 8%

Treatment 2 = CPOPs with coating level of 12%
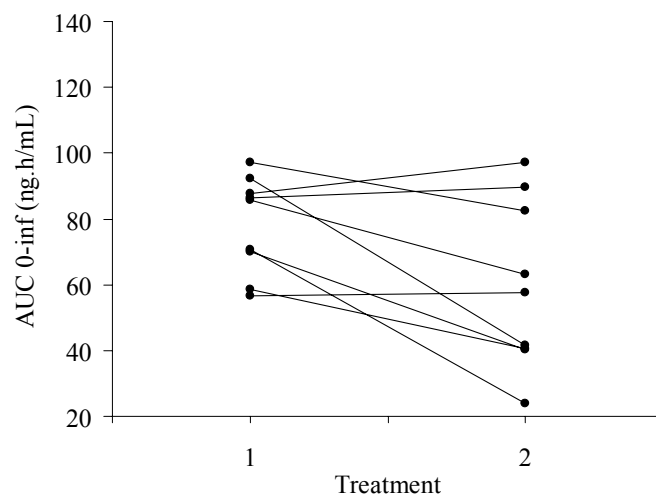
Figure 63. Graphical presentation of $AUC_{0-\infty}$ value comparison between different
formulations of propranolol CPOP tablets at various coating levels for
each of 9 pigs

Keys: Treatment 1 = CPOPs with coating level of 8%

Treatment 2 = CPOPs with coating level of 12%
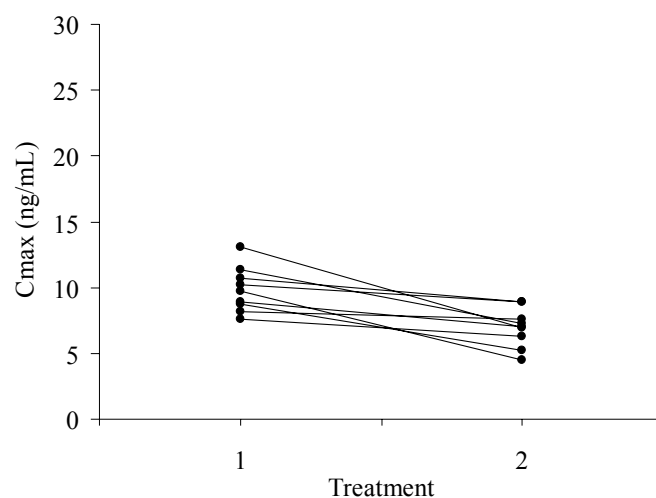
Figure 64. Graphical presentation of C_{max} value comparison between different formulations of propranolol CPOP tablets at various coating levels for each of 9 pigs

Keys: Treatment 1 = CPOPs with coating level of 8%

Treatment 2 = CPOPs with coating level of 12%
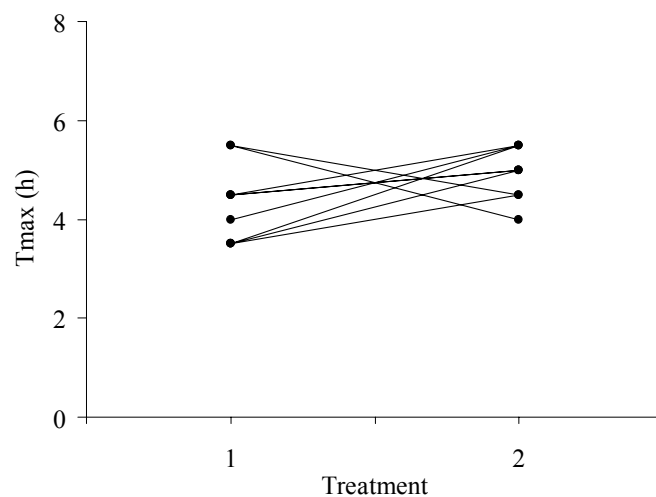
Figure 65. Graphical presentation of T_{max} value comparison between different formulations of propranolol CPOP tablets at various coating levels for each of 9 pigs

Keys: Treatment 1 = CPOPs with coating level of 8%

Treatment 2 = CPOPs with coating level of 12%
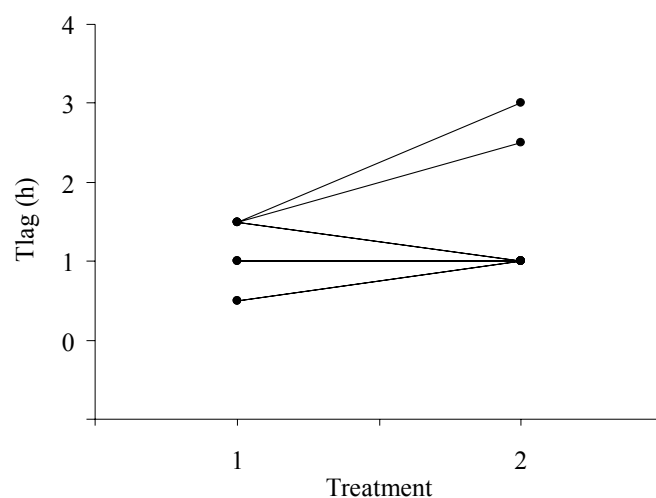
Figure 66. Graphical presentation of T_{lag} value comparison between different formulations of propranolol CPOP tablets at various coating levels for each of 9 pigs

Keys: Treatment 1 = CPOPs with coating level of 8%

Treatment 2 = CPOPs with coating level of 12%

For the purpose of *in vivo* equivalence analysis using ANOVA, no statistically significant difference was observed between both CPOP-formulations in the logarithmically transformed $AUC_{0-\infty}$ ($p > 0.05$). On the other hand, significant difference was observed between both CPOP-formulations in the logarithmically transformed C_{max} ($p < 0.05$). Moreover, the 12% coating formulation was not able to achieve 80% of relative bioavailability compared to the reference formulation.

On the subject of bioequivalence (BE) studies' criteria (172), $AUC_{0-\infty}$ and C_{max} which were respected as the primary variables; a test product is considered bioequivalent to a reference product if the 90% confidence intervals for the geometric mean test/reference ratios of the $AUC_{0-\infty}$ and C_{max} both fall within the predefined BE limits of 80–125%. In this aspect, the test and reference products were the 12% and 8% coating CPOP formulations, respectively. Table 44 shows 90% confidence interval for the ratio of the logarithmically transformed $AUC_{0-\infty}$ values of the test products over those of the reference products lay between 48.6% and 93.1%, while C_{max} values lay between 56.7% and 83.9%. These are outside the acceptable BE limits of 80–125%. Based on the above results, CPOP with 12% coating level was *in vivo* inequivalent to CPOP with 8% in both rate and extent of absorption.

Similarity of dissolution data (between 8% and 12% coating CPOPs; f_2 value = 58.2) indicated by similarity factor (f_2) defined by US FDA (95) was declared as previously discussed; however, their *in vivo* performances were inequivalent. It could be due to a false estimation of similarity between the dissolution profiles. Owing to the f_2 are (i) insensitive to the shape of the dissolution profiles and do not take into account the information of unequal spacing between sampling time points (173); and (ii) too liberal in concluding similarity between release profiles (174). Moreover, the false estimation might be as a consequence of an incorrect definition of the acceptance limit (175) and lack of variability issue in dissolution data (176), especially in case of borderline of f_2 values. Recently, hence, new concepts for improving the assessment of similarity factors was proposed (173, 175, 176).

Table 44. Pharmacokinetic parameters comparison of propranolol CPOP tablets[a]

Parameters	Test product (T)	Reference product (F)	Ratio T/F (%)	90% Confidence Interval
$AUC_{0-\infty}$	54.54 (1.59)	76.99 (1.22)	70.84	48.59–93.08
C_{max}	6.82 (1.25)	9.71 (1.19)	70.32	56.70–83.94

[a] Data shown as geometric mean (SD), n = 9.

Keys: Test product   = 12% coating CPOPs

    Reference product = 8% coating CPOPs

Refinement of lower acceptance value of the f_2 in comparison of dissolution profiles was suggested in the literature (175). In their opinion, the current lower limit of f_2 is very liberal, especially for sustained release formulation, and may inadvertently lead to the declaration of similarity of dissolution profiles which otherwise are quite dissimilar. In the current acceptance criteria, two dissolution profiles are considered "similar" when the absolute percent difference allowed at all time is less than 10 (95, 122). A new concept proposed was suggested that instead of the absolute 10%, 10% of reference deviation should be considered between two dissolution profiles to be similar. Then, a new lower acceptance value of 60 for f_2 was recommended (175). Based on this concept, two dissolution profiles of CPOP formulations were conclude as dissimilar with $f_2 = 58.2$.

Table 45 displays the values of the similarity factor calculated by the conventional method (f_2) (95), and the alternative methodology expressed under Costa's ($f_{2\text{-m1}}$) (173), and Gohel's ($f_{2\text{-m2}}$) approaches (176). The alternative methods determine the value of similarity factor using different values of the optional weight (w) to consider the variability in dissolution data. In all the proposed approaches, if the weight at each time point is equal to one, the f_2 will remain unchanged. Weights higher than one can cause a drop in value of f_2 and weights less than one can cause a rise in f_2 value (176).

Regarding the approach introduced by Costa et al. (173), individual values of dissolution results of reference (R) and test (T) formulations in place of average dissolution data of R and T were compared. The standard deviation of different values of absolute difference between R and T was calculated at each time point. Whenever, within-samples variability and variability between samples will be observed. In this approach, the weight was calculated from the equation (1+SD/maximum allowed SD). The maximum allowed SD was arbitrarily chosen as 10 to allow within-samples as well as variability between samples. Thus, the calculated value of $f_{2\text{-m1}}$ by this proposed method was lower than the f_2 calculated by the classical method (w = 1), equaled to 54.3.

In another approach (176), the weight was calculated by taking the ratio of the absolute difference of the percentage of drug dissolve between R and T to 10% of percentage of drug dissolved from R at each time point to consider the variability

between samples with more specificity. The obtained value of modified similarity factor ($f_{2\text{-m2}}$) for this proposed was 48.4, means dissimilar between R and T. These results reveal that in borderline cases of similarity/dissimilarity (f_2 is around 50); in some cases, the status of similarity changed to dissimilarity when the alternative approaches were adopted.

12.4. In Vitro–In Vivo Correlation (IVIVC)

The pharmacokinetic parameters were used to develop a level A IVIVC. First, propranolol fraction absorbed profiles correlating propranolol input against time, which estimate the rate at which the drug reaches the systemic circulation, were established. The Wagner–Nelson procedure was employed to obtain an *in vivo* cumulative release profile. Individual F_a values from each plasma propranolol concentration–time curve resulted after oral administration of propranolol formulations are listed in Tables 46–47. The average F_a profiles are displayed in Figure 67. The *in vitro* and *in vivo* cumulative release profiles of the propranolol formulations are compared in Figure 68. At last, the percent drug absorbed versus the amount of drug released *in vitro* plots are demonstrated in Figures 69 and 70. A good linear regression relationship between the percent *in vitro* dissolution and the percent absorption after single oral administration of CPOP formulations in pigs was observed ($r^2 = 0.9764$).

Table 45. Similarity factors calculated by different methods

Methods	Similarity factor values
f_2	58.2
$f_{2\text{-m1}}$	54.3
$f_{2\text{-m2}}$	48.4

Keys: $f_2 = 50.\log\left\{\left[1 + \dfrac{1}{n}\sum_{t=1}^{n} w_t \left(R_t - T_t\right)^2\right]^{-0.5} \times 100\right\}$; $w_t = 1$ (95),

$f_{2\text{-m1}} = f_2$; $w_t = 1 + $ (SD/maximum allowed SD) (173),

$f_{2\text{-m2}} = f_2$; $w_t = (R - T)/10\%$ of R (176).

Table 46. Individual fraction propranolol absorbed (F_a) after single oral administration of 80 mg propranolol CPOP at 8% coating level

Pig	Time (h)								
	0.0	0.5	1.0	1.5	2.0	2.5	3.0	3.5	
1	0.0000	0.0000	0.0000	0.0000	0.0984	0.1582	0.1979	0.2561	
2	0.0000	0.0000	0.0000	0.0000	0.0745	0.1831	0.2910	0.3155	
3	0.0000	0.0000	0.0000	0.0000	0.0894	0.1840	0.2456	0.3966	
4	0.0000	0.0000	0.0000	0.0767	0.1117	0.1747	0.1916	0.2456	
5	0.0000	0.0000	0.0000	0.0000	0.0383	0.0759	0.1361	0.1293	
6	0.0000	0.0000	0.0649	0.1300	0.1870	0.1747	0.3171	0.3811	
7	0.0000	0.0000	0.0000	0.0845	0.1354	0.1972	0.2681	0.3798	
8	0.0000	0.0000	0.0000	0.0407	0.0969	0.1879	0.3214	0.4209	
9	0.0000	0.0000	0.0303	0.0769	0.1743	0.2119	0.2939	0.3762	
Mean	0.0000	0.0000	0.0106	0.0454	0.1118	0.1720	0.2514	0.3233	
SEM	0.0000	0.0000	0.0076	0.0162	0.0157	0.0130	0.0213	0.0317	

Table 46. Individual fraction propranolol absorbed (F_a) after single oral administration of 80 mg propranolol CPOP at 8% coating level (cont.)

Pig	Time (h)							
	4.0	4.5	5.0	5.5	6.0	8.0	10.0	12.0
1	0.3066	0.3931	0.4341	0.4701	0.4889	0.5977	0.7206	0.7802
2	0.4245	0.5013	0.5053	0.4551	0.5231	0.6757	0.7681	0.8361
3	0.4351	0.4855	0.5623	0.5772	0.6165	0.7273	0.8079	0.8647
4	0.2631	0.3389	0.4091	0.4921	0.5194	0.6475	0.6906	0.7943
5	0.1740	0.2253	0.3082	0.3604	0.4005	0.5086	0.6082	0.6622
6	0.4315	0.4949	0.4623	0.4971	0.4862	0.5617	0.6349	0.7292
7	0.4452	0.5175	0.5722	0.6249	0.6461	0.7727	0.8305	0.8923
8	0.4862	0.5449	0.6372	0.6346	0.6649	0.8436	0.9413	0.9682
9	0.4544	0.5111	0.5540	0.5822	0.6105	0.7317	0.8332	0.8782
Mean	0.3801	0.4458	0.4939	0.5215	0.5507	0.6741	0.7595	0.8228
SEM	0.0354	0.0352	0.0336	0.0300	0.0294	0.0356	0.0355	0.0308

Table 47. Individual fraction propranolol absorbed (F_a) after single oral administration of 80 mg propranolol CPOP at 12% coating level

Pig	Time (h)							
	0.0	0.5	1.0	1.5	2.0	2.5	3.0	3.5
1	0.0000	0.0000	0.0000	0.0000	0.0000	0.0000	0.0000	0.1456
2	0.0000	0.0000	0.0000	0.0000	0.0000	0.0000	0.1973	0.2335
3	0.0000	0.0000	0.0000	0.0830	0.1117	0.01417	0.2055	0.2461
4	0.0000	0.0000	0.0000	0.0794	0.1325	0.1754	0.2197	0.2811
5	0.0000	0.0000	0.0000	0.1041	0.1512	0.1971	0.3077	0.3953
6	0.0000	0.0000	0.0000	0.1020	0.1315	0.1593	0.1903	0.3180
7	0.0000	0.0000	0.0000	0.0754	0.1454	0.2042	0.2704	0.3301
8	0.0000	0.0000	0.0000	0.0375	0.0465	0.0843	0.1281	0.1982
9	0.0000	0.0000	0.0000	0.0708	0.1047	0.1267	0.1524	0.1860
Mean	0.0000	0.0000	0.0000	0.0614	0.0915	0.1210	0.1857	0.2593
SEM	0.0000	0.0000	0.0000	0.0133	0.0201	0.0259	0.0295	0.0264

Table 47. Individual fraction propranolol absorbed (F_a) after single oral administration of 80 mg propranolol CPOP at 12% coating level (cont.)

Pig	Time (h)							
	4.0	4.5	5.0	5.5	6.0	8.0	10.0	12.0
1	0.1751	0.2676	0.3374	0.4010	0.4231	0.5011	0.5585	0.6081
2	0.3806	0.5405	0.6422	0.6980	0.7652	0.8643	0.9310	n/a
3	0.3371	0.4358	0.4625	0.5508	0.5508	0.6573	0.7562	0.8184
4	0.4241	0.4842	0.5255	0.5306	0.6023	0.6628	0.7476	0.8283
5	0.4650	0.5972	0.6336	0.6871	0.6872	0.8054	0.8734	0.9205
6	0.4235	0.5404	0.5763	0.7372	0.6978	0.8503	0.9186	0.9573
7	0.3727	0.4149	0.4911	0.5385	0.5744	0.7091	0.7865	0.8495
8	0.2183	0.2710	0.3120	0.3507	0.3634	0.7387	0.5124	0.5630
9	0.2156	0.2401	0.2970	0.3425	0.3793	0.4900	0.5918	0.6555
Mean	0.3347	0.4213	0.4753	0.5374	0.5604	0.6643	0.7418	0.7751
SEM	0.0353	0.0445	0.0446	0.0500	0.0485	0.0533	0.0521	0.0491
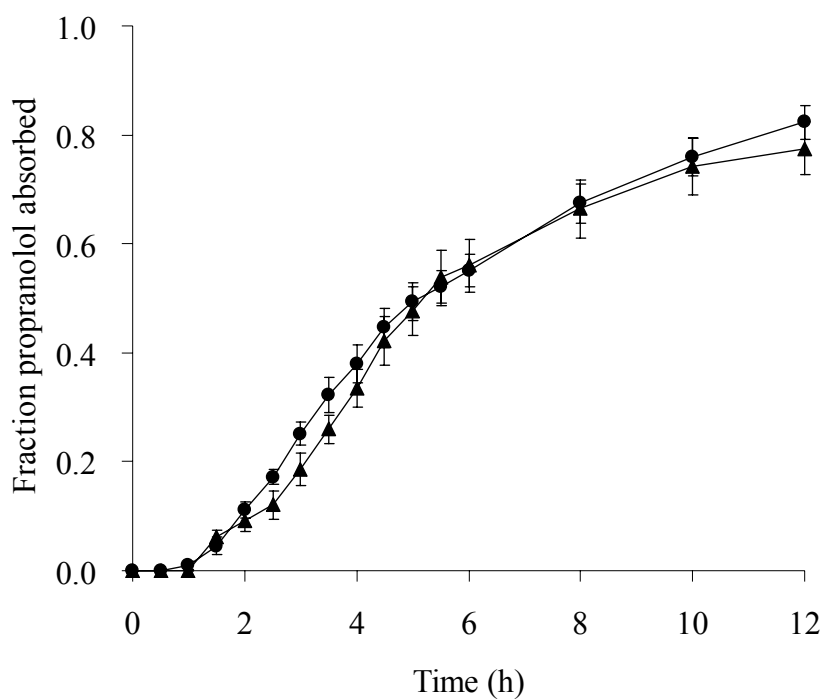
Figure 67. Fraction absorbed obtained by Wagner–Nelson method after propranolol
administrations. Each data point represents mean ± SEM of 9 pigs.

Keys: ●, 8% coating CPOPs

▲, 12% coating CPOPs.

(A)
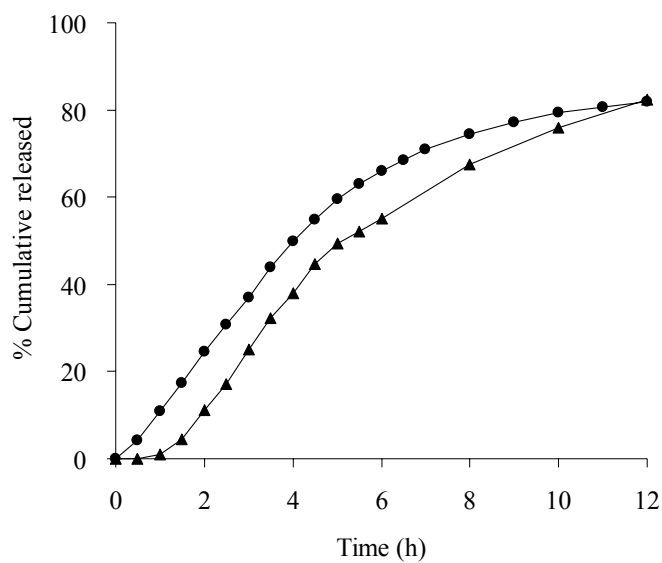
(B)
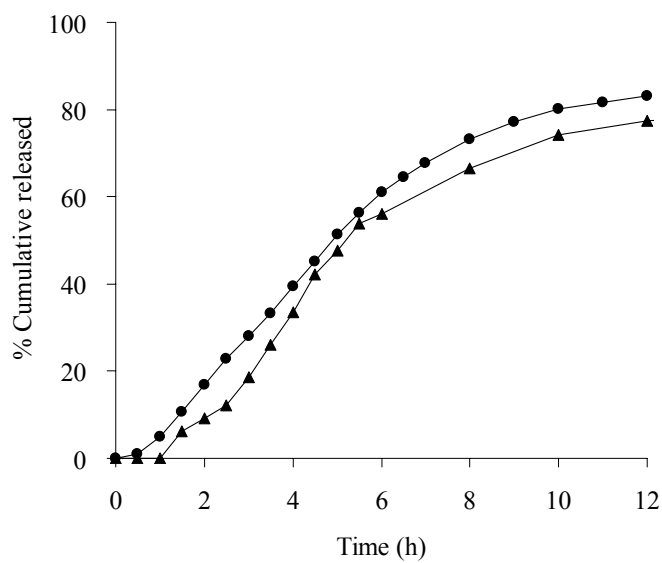
Figure 68. *In vitro* and *in vivo* cumulative releases using Wagner–Nelson method from propranolol CPOP tablets at various coating levels

Keys: (A) 8%; (B) 12%

●, in vitro; ▲, in vivo.

(A)
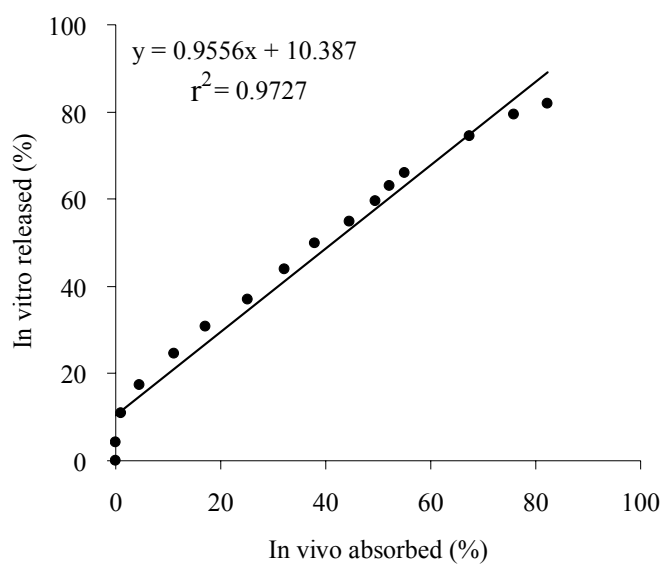
(B)
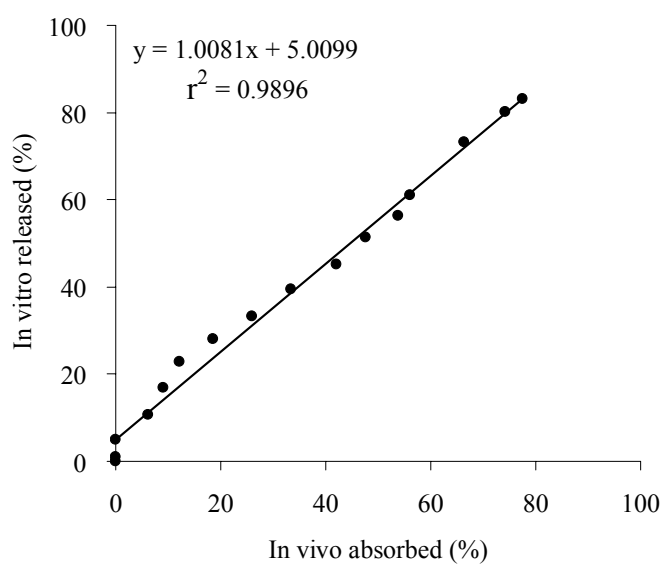
Figure 69. IVIVC model linear regression plots of cumulative absorption *vs*. percent
drug release of propranolol from CPOP tablets at various coating levels
Keys: (A) 8%; (B) 12%
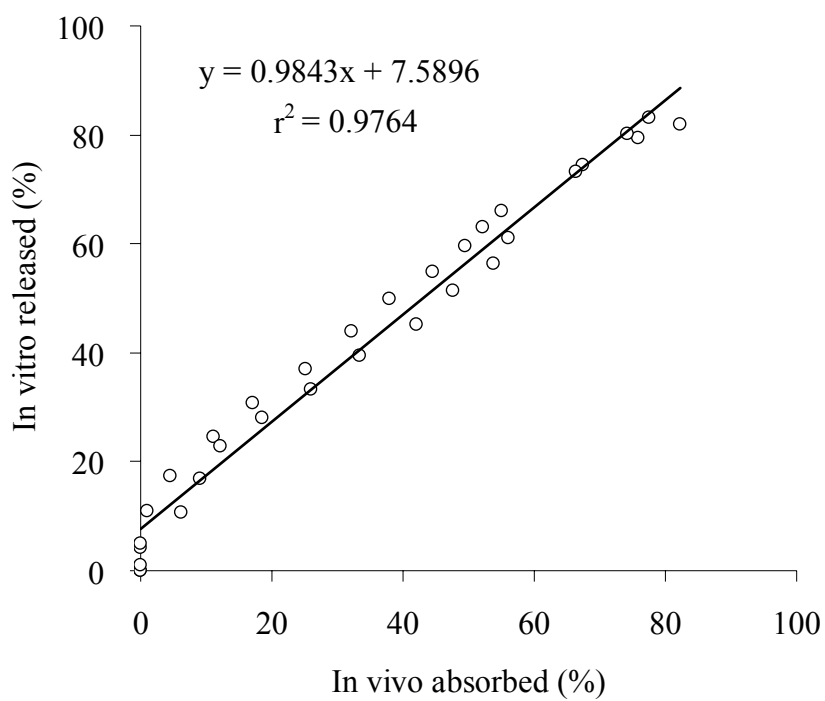
Figure 70. IVIVC model linear regression plots of cumulative absorption *vs*. percent
           drug release of propranolol from CPOP tablets

13. Conclusions

The controlled-porosity osmotic pump (CPOP) tablets used the ternary mixtures of CS-PAA:HPMC as polymeric osmogents were successfully prepared. The method to create the delivery orifice is relatively simple with the elimination of the common laser drilling technique. With the optimization of membrane and formulation variables, the *in vitro* releases in the zero-order release manner can be achieved and the *in vivo* release profiles of propranolol, a model drug, were prolonged. The results of the present study have demonstrated that the bilayered CPOP containing 20 mg of CS-PAA:HPMC at 8% coating level formulations which provided *in vitro* releases more than 10% and 37% at 1 h and 3 h, respectively, can obtain comparable *in vivo* availability of propranolol in pigs when compared with a commercial immediate release formulation.

Formulation and evaluation of CPOP with a coating level less than 8% would be promising to provide an appropriate plasma profile with approximately 100% relative bioavailability. However, robustness of the semipermeable membrane should be considered due to the pressure created inside the systems which might be able to break the membrane.

CHAPTER V
CONCLUSIONS

In this study, a controlled-porosity osmotic pump tablet (CPOP) using alternative hydrogels of chitosan-polyacrylic acid:hydroxypropyl methylcellulose (CS-PAA:HPMC) as an osmogent was developed. Propranolol, a β-adrenergic blocker, was used as a water-soluble model drug. Due to the release of drug from osmotic systems was governed by various formulation factors, including nature of the rate-controlling membrane and osmotic pressure inside the system; by optimizing the formulation and processing factors, it was possible to develop the osmotic systems which deliver drug with a desired release profile.

A central composite design was used to find the optimum membrane composition that achieves the desired propranolol release profiles. The micro/nanoporous osmotic pump tablets fabricated with cellulose acetate (CA) coating containing PVP K30 or K90 as pore forming agents released the drug at almost a constant rate over a prolonged period of time regardless of environmental conditions. Drug release up to 70% from CPOPs fitted well into a zero-order kinetic. The drug release was dependent on molecular weight of PVP, PVP content and membrane weight increase. The surface morphology of the semipermeable membrane was studied by SEM and AFM. At a given PVP content, the higher molecular weight of PVP, the larger pore size of the micro/nanoporous was created and the higher drug release was observed. The formulation that gave the desired release profile for both once and twice daily dosing interval was only CPOP using PVP K30 as a pore former. It was found that the optimized formulation was the CPOP with CA coating containing 35% of PVP K30 at 4.2% membrane weight increase. For the CPOP with CA coating containing PVP K90, the desired release profile for once daily dose was achieved at PVP content of 23% and membrane weight increase of 4.2%.

To evaluate the use of an alternative hydrogel of CS-PAA:HPMC as an osmogent in CPOPs, the different mixtures were prepared by varying ratios of CS-

PAA:HPMC hydrogel and examined for swelling behavior, an important factor for controlling the drug release. Mixtures of CS and PAA were prepared and studied the effects of the molecular weight of CS and the ratio of CS:PAA. The CS-PAA hydrogels rapidly hydrated, swelled, and reached the equilibrium within 10–60 min. FTIR spectra indicated the electrostatic interactions between CS and PAA which became a polyelectrolyte complex during the formation of CS-PAA hydrogels. The swelling force and swelling ratio increased with the increased molecular weight of CS. Therefore, CS with high molecular weight was selected for the preparation of CS:PAA interpolymer complex due to its high swelling force and swelling ratio.

There was a direct correlation between the increased proportion of CS within the complex and the effect on the maximum swelling force and swelling ratio. Increasing CS content showed the greater swelling force and swelling ratio which could be caused by the expansion of the polymer chains due to ionic repulsion of amino groups. The ratio of CS:PAA at 1:1 was selected for further study based on its good swelling characteristics. HPMC was added in order to improve the swelling pattern. With increasing HPMC proportions, the decreasing order of the swelling rates was observed as 1:0 > 0.75:0.25 > 0.5:0.5 > 0.25:0.75 > 0:1. Since the CS-PAA complexes had more swelling property than HPMC, increasing the amount of HPMC decreased the swelling property of the ternary mixtures. For further development of the propranolol osmotically-controlled release system, the proportion of CS-PAA:HPMC at 1:1 was selected.

The CPOP tablets, coated with CA containing 60% PVP K30 as a pore former and 10% PEG 400 as a plasticizer and used the ternary mixtures of CS-PAA:HPMC as polymeric osmogents, were successfully prepared. The formulation variables, i.e., amount of osmogent and tablet characteristics, were evaluated. The results showed that a bilayer system which polymer swelled and directly pushed the drug out was more appropriate than a monolithic system in order to control the drug release conforming to the USP criteria. Furthermore, the pharmacokinetics of propranolol CPOP systems were evaluated in pigs in order to explore the relationship between *in vitro* dissolution and *in vivo* absorption. Two formulations of CPOPs, i.e., bilayered CPOP containing 20 mg of CS-PAA:HPMC at 8% and 12% coating levels, which provided the *in vitro* release profiles following the criteria of USP 28, were evaluated

the *in vivo* absorption by a three-way crossover study design with a 3-day washout period. The drug was assayed in plasma by HPLC, and the results were compared with the commercially available immediate-release propranolol tablets as a reference formulation. Cumulative percent input *in vivo* was compared to the *in vitro* release profiles. Pharmacokinetic parameters were obtained by a noncompartmental method.

With the optimization of the membrane and formulation variables, the *in vitro* drug releases in the zero-order release manner were achieved and the *in vivo* absorption profiles were prolonged. The present study has demonstrated that the formulation of bilayered CPOP containing 20 mg of CS-PAA:HPMC at 8% coating level provided the *in vitro* drug releases more than 10% and 37% at 1 h and 3 h, respectively, and revealed comparable bioavailability of the drug in pigs, comparing with the commercial immediate release formulation. In conclusion, CPOPs used ternary mixtures of CS-PAA:HPMC as osmogents are feasible for controlling the drug release both *in vitro* and *in vivo* conditions. In particular, the results provide useful information for the development of controlled-porosity osmotic pump tablets for industrial purposes.

REFERENCES

1. Theeuwes F. Elementary osmotic pump. J Pharm Sci 1975;64(12):1987-91.

2. Wong PSL, Gupta SK, Stewart BE. Osmotically controlled tablets. In: Rathbone MJ, Hadgraft J, Roberts MS, editors. Modified-release drug delivery technology. New York: Marcel Dekker; 2003. p. 101-14.

3. Zentner GM, McClelland GA, Sutton SC. Controlled porosity solubility- and resin-modulated osmotic drug delivery systems for release of diltiazem hydrochloride. J Control Release 1991;16(1-2):237-44.

4. Zentner GM, Rork GS, Himmelstein KJ. Osmotic flow through controlled porosity films: An approach to delivery of water soluble compounds. J Control Release 1985;2:217-29.

5. Zentner GM, Rork GS, Himmelstein KJ. The controlled porosity osmotic pump. J Control Release 1985;1(4):269-82.

6. McClelland GA, Sutton SC, Engle K, Zentner GM. The solubility-modulated osmotic pump: *in vitro/in vivo* release of diltiazem hydrochloride. Pharm Res 1991;8(Jan):88-92.

7. Santus G, Baker RW. Osmotic drug delivery: review of the patent literature. J Control Release 1995;35:1-21.

8. Verma RK, Mishra B, Garg S. Osmotically controlled oral drug delivery. Drug Dev Ind Pharm 2000;26(7):695-708.

9. Verma RK, Krishna DM, Garg S. Formulation aspects in the development of osmotically controlled oral drug delivery systems. J Control Release 2002;79(1-3):7-27.

10. Appel LE, Clair JM, Zentner GM. Formulation and optimization of a modified microporous cellulose acetate latex coating for osmotic pumps. Pharm Res 1992;9(12):1664-7.

11.   Sinchaipanid N, Pongwai S, Limsuwan P, Mitrevej A. Design of salbutamol EOP tablets from Pharmacokinetics parameters. Pharm Dev Technol 2003;8(2):135-42.

12.   Appel LE, Zentner GM. Use of modified ethylcellulose lattices for microporous coating of osmotic tablets. Pharm Res 1991;8(5):600-4.

13.   Okimoto K, Rajewski RA, Stella VJ. Release of testosterone from an osmotic pump tablet utilizing $(SBE)_{7m}$-β-cyclodextrin as both a solubilizing and an osmotic pump agent. J Control Release 1999;58(1):29-38.

14.   Okimoto K, Miyake M, Ohnishi N, Rajewski RA, Stella VJ, Irie T, Uekama K. Design and evaluation of an osmotic pump tablet (OPT) for prednisolone, a poorly water soluble drug, using $(SBE)_{7m}$-β-CD. Pharm Res 1998;15(19):1562-8.

15.   Okimoto K, Ohike A, Ibuki R, Aoki O, Ohnishi N, Irie T, Uekama K, Rajewski RA, Stella VJ. Design and evaluation of an osmotic pump tablet (OPT) for chlorpromazine using $(SBE)_{7m}$-β-CD. Pharm Res 1999;16(4):549-54.

16.   Okimoto K, Ohike A, Ibuki R, Aoki O, Ohnishi N, Rajewski RA, Stella VJ, Irie T, Uekama K. Factors affecting membrane-controlled drug release for an osmotic pump tablet (OPT) utilizing $(SBE)_{7m}$-β-CD as both a solubilizer and osmotic agent. J Control Release 1999;60(2-3):311-9.

17.   Okimoto K, Tokunaga Y, Ibuki R, Irie T, Uekama K, Rajewski RA, Stella VJ. Applicability of $(SBE)_{7m}$-β-CD in controlled-porosity osmotic pump tablets (OPTs). Int J Pharm 2004;286(1-2):81-8.

18.   Zentner GM, Rork GS, Himmelstein KJ, inventors; Merck & Co., Inc., assignee. Controlled porosity osmotic pump. US patent 4,880,631. November 6, 1990.

19.   Verma RK, Garg S. Development and evaluation of osmotically controlled oral drug delivery system of glipizide. Eur J Pharm Biopharm 2004;57:513-25.

20. Verma RK, Kaushal AM, Garg S. Development and evaluation of extended release formulations of isosorbide mononitrate based on osmotic technology. Int J Pharm 2003;263:9-24.

21. Liu L, Che B. Preparation of monolithic osmotic pump system by coating the indented core tablet. Eur J Pharm Biopharm 2006;64:180-4.

22. Prabakaran D, Singh P, Kanaujia P, Jaganathan KS, Rawat A, Vyas SP. Modified push-pull osmotic system for simultaneous delivery of theophylline and salbutamol: development and in vitro characterization. Int J Pharm 2004;284:95-108.

23. Rose S, Nelson JF. A continuous long-term injector. Aust J Exp Biol Med Sci 1955;33:415-20.

24. Higuchi T, Leeper HM, inventors; Alza Corporation, assignee. Improved osmotic dispenser employing magnesium sulphate and magnesium chloride. US patent 3,760,804. September 25, 1973.

25. Higuchi T, inventor; Alza Corporation, assignee. Osmotic dispenser with collapsible supply container. US patent 3,760,805. September 25, 1973.

26. Higuchi T, Leeper HM, inventors; Alza Corporation, assignee. Osmotic dispenser with means for dispensing active agent responsive to osmotic gradient. US patent 3,995,631. December 7, 1976.

27. Theeuwes F, Higuchi T, inventors; Alza Corporation, assignee. Osmatic dispensing device for releasing beneficial agent. US patent 3,845,770. November 5, 1974.

28. Jerzewski RL, Chien YW. Osmotic drug delivery. In: Kydonieus A, editor. Treatise on controlled drug delivery: fundamentals, optimization, application. New York: Marcel Dekker; 1992. p. 225-53.

29. Swanson DR, Barclay BL, Wong PSL, Theeuwes F. Nifedipine gastrointestinal therapeutic system. Am J Med 1987;83(Suppl 6B):3-9.

30. Theeuwes F, Wong PSL, Burkoth TL, Fox DA. Osmotic systems for colon-targeted drug delivery. In: Bieck PR, editor. Colonic drug absorption and metabolism. New York: Marcel Dekker; 1993. p. 137-58.

31. Liu L, Ku J, Khang G, Lee B, Rhee JM, Lee HB. Nifedipine controlled delivery by sandwiched osmotic tablet system. J Control Release 2000;68(2):145-56.

32. Herbig SM, Cardinal JR, Korsmeyer RW, Smith KL. Asymmetric-membrane tablet coatings for osmotic drug delivery. J Control Release 1995;35(2-3):127-36.

33. Thombre AG, Cardinal JR, DeNoto AR, Herbig SM, Smith KL. Asymmetric membrane capsules for osmotic drug delivery I. Development of a manufacturing process. J Control Release 1999;57:55-64.

34. Thombre AG, Cardinal JR, DeNoto AR, Gibbes DC. Asymmetric membrane capsules for osmotic drug delivery II. In vitro and in vivo drug release performance. J Control Release 1999;57:65-73.

35. Sotthivirat S, Haslam JL, Stella VJ. Evaluation of various properties of alternative salt forms of sufobutylether-(β)-cyclodextrin, $(SBE)_{7m}$-β-CD. Int J Pharm 2007;330:73-81.

36. Gan Y, Pan W, Wei M, Zhang R. Cyclodextrin complex osmotic tablet for glipizide delivery. Drug Dev Ind Pharm 2002;28(8):1015-21.

37. Li X-d, Pan W-s, Nie S-f, Wu L-j. Studies on controlled release effervescent osmotic pump tablets from Traditional Chinese Medicine Compound Recipe. J Control Release 2004;96(3):359-67.

38. Thombre AG, DeNoto AR, Gibbes DC. Delivery of glipizide from asymmetric membrane capsules using encapsulated excipients. J Control Release 1999;60:333-41.

39. Wong PSL, Barclay B, Deters JC, Theeuwes F, inventors; Alza Corporation, assignee. Osmotic device with dual thermodynamic activity. US patent 4,612,008. September 16, 1986.

40. Theeuwes F, Swanson DR, Wong PSL, Bonsen P, Place V, Heimlich K, Kwan KC. Elementary osmotic pump for indomethacin. J Pharm Sci 1983;72(3):253-8.

41. Cortese R, Theeuwes F, inventors; Alza Corporation, assignee. Osmotic device with hydrogel driving member. US patent 4,327,725. May 4, 1982.

42. Liu L, Khang G, Rhee JM, Lee HB. Monolithic osmotic tablet system for nifedipine delivery. J Control Release 2000;67(2-3):309-22.

43. Ozdemir N, Sahin J. Design of a controlled release osmotic pump system of ibuprofen. Int J Pharm 1997;158(1):91-7.

44. Theeuwes F, Saunders RJ, Mefford WS, inventors; Alza Corporation, assignee. Process for forming outlet passageways in pills using a laser. US patent 4,088,864. May 9, 1978.

45. Makhija SN, Vavia PR. Controlled porosity osmotic pump-based controlled release systems of pseudoephedrine: I. Cellulose acetate as a semipermeable membrane. J Control Release 2003;89(1):5-18.

46. Zentner GM, Rork GS, Himmelstein KJ, inventors; Merck & Co., Inc., assignee. Controlle porosity osmotic pump. US patent 4,968,507. November 6, 1990.

47. Kelbert M, Bchard SR. Evaluation of cellulose acetate (CA) latex as coating material for controlled release products. Drug Dev Ind Pharm 1992;18:519-38.

48. Theeuwes F, Ayer AD, inventors; Alza Corporation, assignee. Osmotic devices having composite walls. US patent 4,077,407. March 7, 1978.

49. Guittard GV, Deters JC, Theeuwes F, Cortese R, inventors; Alza Corporation, assignee. Osmotic system with instant drug availability. US patent 4,673,405. June 16, 1987.

50. Jensen JL, Appel LE, Clair JH, Zentner GM. Variables that affect the mechanism of drug release from osmotic pumps coated with acrylate/methacrylate copolymer latexes. J Pharm Sci 1995;84:530-3.

51. Zhang Y, Zhang Z, Wu F. A novel pulsed-release system based on swelling and osmotic pumping mechanism. J Control Release 2003;89(1):47-55.

52. Yuan J, Wu SH. Sustained-release tablets via direct compression: a feasibility study using cellulose acetate and cellulose acetate butyrate. Pharm Tech 2000;24(10):92-106.

53. Guo J. Effects of plasticizers on water permeation and mechnical properties of cellulose acetate: Antiplasticization in slightly plasticized polymer film. Drug Dev Ind Pharm 1993;19:1541-55.

54.   Hejazi R, Amiji M. Chitosan-based gastrointestinal delivery systems. J Control
         Release 2003;89:151-65.

55.   Brine CJ, Sandford PA, Zikakis JP. Advances in chitin and chitosan. Essex:
         Elsevier Applied Sciences; 1992.

56.   Kato Y, Onishi H, Machida Y. Application of chitin and chitosan derivatives in
         the pharmaceutical field. Curr Pharm Biotechnol 1992;4(5):303-9.

57.   Harish Prashanth KV, Tharanathan RN. Chitin/chitosan: modifications and their
         unlimited application potential-an overview. Trends Food Sci Tech
         2007;18:117-31.

58.   Wang H, Li W, Lu Y, Wang Z. Studies on chitosan and poly(acrylic acid)
         interpolymer complex. I. Preparation, structure, pH-sensitivity, and
         salt sensitivity of complex-forming poly(acrylic acid):chitosan semi-
         interpenetrating polymer network. J Appl Polym Sci 1997;65:1445-
         50.

59.   Risbud MV, Hardikar AA, Bhat SV, Bhonde RR. pH-sensitive freeze-dried
         chitosan-polyvinyl pyrrolidone hydrogels as controlled release system
         for antibiotic delivery. J Control Release 2000;68:23-30.

60.   Remunan-Lopez C, Portero A, Vila-Jato JL, Alonso MJ. Design and evaluation
         of chitosan/ethylcellulose mucoadhesive bilayered devices for buccal
         drug delivery. J Control Release 1998;55:143-52.

61.   De la Torre PM, Torrado S, Torrado S. Interpolymer complexes of poly(acrylic
         acid) and chitosan: influence of the ionic hydrogel-forming medium.
         Biomaterials 2003;24:1459-68.

62.   De la Torre PM, Enobakhare Y, Torrado G, Torrado S. Release of amoxicillin
         from polyionic complexes of chitosan and poly(acrylic acid). Study of
         polymer/polymer and polymer/drug interactions within the network
         structure. Biomaterials 2003;24:1499-506.

63.   Torrado S, Prada P, De la Torre PM, Torrado S. Chitosan-poly(acrylic) acid
         polyionic complex: in vivo study to demonstrate prolonged gastric
         retention. Biomaterials 2004;25:917-23.

64. Hu Y, Jiang X, Ding Y, Ge H, Yuan Y, Yang C. Synthesis and characterization of chitosan-poly(acrylic acid) nanoparticles. Biomaterials 2002;23:3193-201.

65. Rossi S, Sandri G, Ferrari F, Bonferoni MC, Caramella C. Buccal delivery of acyclovir from films based on chitosan and polyacrylic acid. Pharm Dev Technol 2003;8(2):199-208.

66. Varshosaz J. The promise of chitosan microspheres in drug delivery systems. Expert Opin Drug Deliv 2007;4(3):263-73.

67. Illum L. Chitosan and its use as a pharmaceutical excipient. Pharm Res 1998;15(9):1326-31.

68. Bae YH, Kim SW. Hydrogel delivery systems based on polymer blends, block co-polymers or interpenetrating networks. Adv Drug Deliver Rev 1993;11:109-35.

69. Lee JW, Kim SY, Kim SS, Lee YM, Lee KH, Kim SJ. Synthesis and characteristics of interpenetrating polymer network hydrogel composed of chitosan and poly(acrylic acid). J Appl Polym Sci 1999;73:113-20.

70. Wang H, Li W, Lu Y, Wang Z, Zhong W. Studies on chitosan and poly(acrylic acid) interpolymer complex. II. Solution behaviors of the mixture of water-soluble chitosan and poly(acrylic acid). J Appl Polym Sci 1996;61:2221-4.

71. Nge TT, Yamaguchi M, Hori N, Takemura A, Ono H. Synthesis and characterization of chitosan/poly(acrylic acid) polyelectrolyte complex. J Appl Polym Sci 2002;83:1025-35.

72. Ahn J-S, Choi H-K, Cho C-S. A novel mucoadhesive polymer prepared by template polymerization of acrylic acid in the presense of chitosan. Biomaterials 2001;22:923-8.

73. Ahn J-S, Choi H-K, Chum M-K, Ryu J-M, Jung J-H, Kim Y-U, Cho C-S. Release of triamcinolone acetonide from mucoadhesive polymer composed of chitosan and poly(acrylic acid) in vitro. Biomaterials 2002;23:1411-6.

74.   De la Torre PM, Torrado G, Torrado S. Poly(acrylic acid) chitosan interpolymer
           complexes for stomach controlled antibiotic delivery. J Biomed Mater
           Res 2004;72B(1):191-7.

75.   Schwartz JB, O'Connor RE, Schnaare RL. Optimization techniques in
           pharmaceutical formulation and processing. In: Banker GS, Rhodes
           CT, editors. Modern pharmaceutics. 4th ed. New York: Marcel
           Dekker; 2002. p. 607-26.

76.   Sastry SV, Reddy IK, Khan MA. Atenolol gastrointestinal therapeutic system:
           optimization of formulation variables using response surface
           methodology. J Control Release 1997;45:121-30.

77.   Huang Y, Tsai Y, Yang W, Chang J, Wu P, Takayama K. One-daily propranolol
           extended-release tablet dosage form: formulation design and *in
           vitro/in vivo* investigation. Eur J Pharm Biopharm 2004;58:607-14.

78.   Kramar A, Turk S, Vrecer F. Statistical optimization of diclofenac sustained
           release pellets coated with polymethacrylic films. Int J Pharm
           2003;256:43-52.

79.   Chang J-S, Huang Y-B, Hou S-S, Wang R-J, Wu P-C, Tsai Y-H. Formulation
           optimization of meloxicam sodium gel using response surface
           methodology. Int J Pharm 2007;338:48-54.

80.   Kim M-S, Kim J-S, You Y-H, Park HJ, Lee S, Park J-S, Woo J-S, Hwang S-J.
           Development and optimization of a novel oral controlled delivery
           system for tamsulosin hydrochloride using response surface
           methodology. Int J Pharm 2007;341:97-104.

81.   Montgomery DC. Design and analysis of experiments. 4th ed. New York: John
           Wiley & Sons; 1997.

82.   Lim CP, Quek SS, Peh KK. Prediction of drug release profiles using an
           intelligent learning system: an experimental study in transdermal
           iontophoresis. J Pharmaceut Biomed 2003;31:159-68.

83.   Pandey PK, Ramaswamy HS, St-Gelais D. Water-holding capacity and gel
           strength of rennet curd as affected by high-pressure treatment of milk.
           Food Res Int 2000;33:655-63.

84.   Ficarra R, Cutroneo P, Aturki Z, Tommasini S, Calabro ML, Phan-Tan-Luu R, Fanali S, Ficarra P. An experimental design methodology applied to the enantioseparation of a non-steroidal anti-inflammatory drug candidate. J Pharmaceut Biomed 2002;29:989-97.

85.   Sastry SV, Khan MA. Aqueous based polymeric dispersion: Plackett-Burman design for screening of formulation variables of atenolol GITS. Pharm Acta Helv 1998;73:105-12.

86.   U.S. Department of Health and Human Service Food and Drug Administration Center for Drug Evaluation and Research (CDER). Guidance for industry: Extended release oral dosage forms: Development, evaluation, and application of *in vitro*/*in vivo* correlations. September 1997 BP 2. http://www.fda.gov/cder/guidance/1306fnl.pdf [Accessed September 5, 2007].

87.   Emami J. *In vitro-in vivo* correlation: from theory to applications. J Pharm Sci 2006;9(2):169-89.

88.   Jorgensen ED, Bhagwat D. Development of dissolution tests for oral extended-release products. Pharm Sci Tech Today 1998;1(3):128-35.

89.   Uppoor VRS. Regulatory perspectives on *in vitro* (dissolution)/*in vivo* (bioavailability) correlations. J Control Release 2001;72:127-32.

90.   Skelly JP, Amidon GL, Barr WH, Benet LZ, carter JE, Robinson JR, Shah VP, Yacobi A. *In vitro* and *in vivo* testing and correlation for oral controlled/modified-release dosage forms. Pharm Res 1990;7(9):975-82.

91.   Takka S, Sakr A, Goldberg A. Development and validation of an in vitro-in vivo correlation for buspirone hydrochloride extended release tablets. J Control Release 2003;88:147-57.

92.   Ghimire M, McInnes FJ, Watson DG, Mullen AB, Stevens H, N. E. *In vitro*/*in vivo* correlation of pulsatile drug release from press-coated tablet formulations: A pharmacoscintigraphic study in the beagle dog. Eur J Pharm Biopharm 2007;67:515-23.

93. Chu D-F, Fu X-Q, Liu W-H, Liu K, Li Y-X. Pharmacokinetics and *in vitro* and *in vivo* correlation of huperzine: A loaded poly(lactic-co-glycolic acid) microspheres in dogs. Int J Pharm 2006;325:116-23.

94. Rossi RC, Dias CL, Donato EM, Martins LA, Bergold AM, Froehlich PE. Development and validation of dissolution test for ritonavir soft gelatin capsules based on *in vivo* data. Int J Pharm 2007;338:119-24.

95. U.S. Department of Health and Human Service Food and Drug Administration Center for Drug Evaluation and Research (CDER). Guidance for industry: Modified release solid oral dosage forms: SUPAC-MR: Chemistry, manufacturing and controls, *in vitro* dissolution testing and *in vivo* bioequivalence documentation. September 1997. http://www.fda.gov/cder/guidance/1214fnl.pdf [Accessed September 5, 2007].

96. Dressman JB, Yamada K. Animal models for oral drug absorption. In: Welling PG, Tse FL, Gighe SV, editors. Pharmaceutical Bioequivalence. New York: Marcel Dekker; 1991. p. 235-66.

97. U.S. Department of Health and Human Service Food and Drug Administration Center for Drug Evaluation and Research (CDER). Guidance for industry: Waiver of in vivo bioavailability and bioequivalence studies for immediate-release solid oral dosage forms based on a biopharmaceutics classification system. August 2000 BP. http://www.fda.gov/cder/guidance/3618fnl.pdf [Accessed September 5, 2007].

98. Kararli TT. Comparison of the gastrointestinal anatomy, physiology and biochemistry of humans and commonly used laboratory animals. Biopharm Drug Dispos 1995;16:351-80.

99. Kabanda L, Lefebvre RA, Van Bree HJ, Remon JP. *In vitro* and *in vivo* evaluation in dogs and pigs of a hydrophilic matrix containing propylthiouracil. Pharm Res 1994;11(11):1663-8.

100. Liaw J, Rubinstein A, Robinson JR. Bioavailability study of Theo-dur tablets in the fasted cannulated dog. Int J Pharm 1990;59:105-14.

101. Krishnan TR, Abraham I, Craig S. Use of the domestic pig as a model for oral bioavailability and pharmacokinetic studies. Biopharm Drug Dispos 1994;15:341-6.

102. Davis SS. Gastrointestinal transit of dosage forms in the pig. J Pharm Pharmacol 2001;53:33-9.

103. Kostewicz E, Sansom L, Fishlock R, Morella A, Kuchel T. Examination of two sustained release nifedipine preparations in humans and in pigs. Eur J Pharm Sci 1996;4:351-7.

104. Barillaro V, Evrard B, Delattre L, Piel G. Oral bioavailability in pigs of a micronazole/hydroxypropyl-gamma-cyclodextrin/L-tartaric acid inclusion complex produced by supercritical carbon dioxide processing. AAPS J 2005;7(1):E149-55.

105. Koritz GD, Bourne DWA, Hunt JP, Prasad VI, Bevill RF, Gautam SR. Pharmacokinetics of theophylline in swine: a potential model for human drug bioavailability studies. J Vet Pharmacol Therap 1981;4:233-9.

106. Larsen F, Jensen BH, Olesen HP, Larsen C. Multiple oral administration of a ketoprofen-dextran ester prodrug in pigs: assessment of gastrointestinal bioavailability by deconvolution. Pharm Res 1992;9(7):915-9.

107. Amidon GL, Lennernas H, Shah VP, Crison JR. A theoretical basis for a biopharmaceutic drug classification: the correlation of *in vitro* drug product dissolution and *in vivo* bioavailability. Pharm Res 1995;12(3):413-20.

108. Dutta H, Sengupta M, Pal DK, De AU, Sengupta C. Effect of propranolol hydrochloride on blood cell lipids in relation to partition coefficient and biological activity. Indian J Biochem Bio 1993;30(2):128-32.

109. Nace GS, Wood AJJ. Pharmacokinetics of long acting propranolol. Implications for therapeutic use. Clin Pharmacokinet 1987;13(1):51-64.

110. Silberstein SD. Preventive treatment of headaches. Curr Opin Neurol 2005;18(3):289-92.

111. Routledge PA, Shand DG. Clinical pharmacokinetics of propranolol. Clin Pharmacokinet 1979;4(2):73-90.

112. Barrett AM, Cullum VA. The biological properties of the optical isomers of propranolol and their effects on cardiac arrythemia. Br J Pharmacol 1968;34:43-55.

113. Sweetman SC. Martindale: the complete drug reference. 35th ed. London: Pharmaceutical Press; 2007.

114. Mehuys E, Vervaet C, Gielen I, Van Bree HJ, Remon JP. In vitro and in vivo evaluation of a matrix-in-cylinder system for sustained drug delivery. J Control Release 2004;96:261-71.

115. Eddington ND, Rekhi GS, Lesko LJ, Augsburger LL. Scale-up effects on dissolution and bioavailability of propranolol hydrochloride and metoprolol tartrate tablet formulations. AAPS PharmSciTech 2000;1(2):article 14.

116. Perez-Marcos B, Ford JL, Armstrong DJ, Elliott PNC, Rostron C, Hogan JE. Influence of pH on the release of propranolol hydrochloride from matrices containing hydrosypropylmethylcellulose K4M and Carbopol 974. J Pharm Sci 1996;85(3):330-4.

117. Gil EC, Colarte AI, Bataille B, Pedraz JL, Rodriquez F, Heinamaki J. Development and optimization of a novel sustained-release dextran tablet formulation for propranolol hydrochloride. Int J Pharm 2006;317:32-9.

118. Mohammadi-Samani S, Adrangui M, Siahi-Shadbad MR, Nokhodchi A. An approach to controlled-release dosage form of propranolol hydrochloride. Drug Dev Ind Pharm 2000;26(1):91-4.

119. The United States Pharmacopeia-National Formulary. USP 28/NF 23. Rockville, MD: The United States Pharmacopeial Convention; 2005.

120. Yuksel N, Kanik AE, Baykara T. Comparison of in vitro dissolution profiles by ANOVA-based, model-dependent and -independent methods. Int J Pharm 2000;209:57-67.

121. Moore JW, Flanner HH. Mathematical comparison of dissolution profiles. Pharm Tech 1996;20:64-74.

122. Shah VP, Tsong Y, Sathe P, Liu J-P. *In vitro* dissolution profile comparison-
      statistics and analysis of the silimarity factor, f_2. Pharm Res
      1998;15(6):889-96.

123. Schultz P, Kleinebudde P. A new multiparticulate delayed release system. Part I:
      Dissolution properties and release mechanism. J Control Release
      1997;47:181-9.

124. Dietz P, Hansma PK, Inacker O, Lehmann H, Herrmann K. Surface pore
      structures of micro- and ultrafiltration membranes imaged with the
      atomic force microscope. J Membrane Sci 1992;65:101-11.

125. Gondaliya D, Pundarikakshudu K. The fabrication and evaluation of the
      formulation variables of a controlled-porosity osmotic drug delivery
      system with diltiazem hydrochloride. Pharm Tech 2003;27(9):58-68.

126. Juhasz AL, Smith E, Weber J, Rees M, Rofe A, Kuchel T, Sansom L, Naidu R.
      In vivo assessment of arsenic bioavailability in rice and its
      significance for human health risk assessment. Environ Health
      Perspect 2006;114:1826-31.

127. Rekhi GS, Jambhekar SS, Souney PF, Williams DA. A fluorimetric liquid
      chromatographic method for the determination of propranolol in
      human serum/plasma. J Pharmaceut Biomed 1995;13:1499-505.

128. Drummer OH, McNeil J, Pritchard E, Louis WJ. Combined high-performance
      liquid chromatographic procedure for measuring 4-
      hydroxypropranolol and propranolol in plasma: pharmacokinetic
      measurements following conventional and slow-release propranolol
      administration. J Pharm Sci 1981;70(9):1030-2.

129. U.S. Department of Health and Human Service Food and Drug Administration
      Center for Drug Evaluation and Research (CDER). Guidance for
      industry: Bioanalytical method validation. May 2001 BP.
      http://www.fda.gov/cder/guidance/4252fnl.pdf [Accessed September
      5, 2007].

130. Foster DJR, Morton EB, Heinkele G, Mürdter TE, Somogyi AA. Stereoselective
      quantification of methadone and a d_6-labeled isotopomer using high
      performance liquid chromatography-atmospheric pressure chemical

ionization mass-spectrometry: application to a pharmacokinetic study in a methadone maintained subject. Ther Drug Monit 2006;28:559-67.

131. R Development Core Team. The R project for statistical computing. http://www.r-project.org/ [Accessed September 5, 2007].

132. Rowland M, Tozer T. Clinical pharmacokinetics: concepts and applications. 3rd ed. Baltimore: Williams & Wilkins; 1995.

133. Gabrielsson J, Weines D. Pharmacokinetic/pharmacodynamic data analysis: concepts and applications. 3rd ed. Stockholm: Swedish Pharmaceutical Press; 2000.

134. Boroujerdi M. Pharmacokinetics: principles and applications. New York: McGraw-Hill; 2002.

135. Wagner JG, Nelson E. Kinetic analysis of blood levels and urinary excretion in the absorptive phase after single doses of drug. J Pharm Sci 1964;53(11):1392-409.

136. Sirisuth N, Eddington ND. The influence of first pass metabolism on the development and validation of an IVIVC for metoprolol extended release tablets. Eur J Pharm Biopharm 2002;53:301-9.

137. Eddington ND, Marroum P, Uppoor R, Hussain A, Augsburger L. Development and internal validation of an *in vitro-in vivo* correlation for a hydrophilic metoprolol tartrate extended release tablet formulation. Pharm Res 1998;15(3):466-73.

138. He F, MacGregor G. How far should salt intake be reduced? Hypertension 2003;42(6):1093-9.

139. He F, MacGregor G. Salt, blood pressure and cardiovascular disease. Curr Opin Cardiol 2007;22(4):298-305.

140. Ramakrishna N, Mishra B. Plasticizer effect and comparative evaluation of cellulose acetate and ethylcellulose-HPMC combination coatings as semipermeable membranes for oral osmotic pumps of naproxen sodium. Drug Dev Ind Pharm 2002;28(4):403-12.

141. Lin S-Y, Lin K-h, Li M-J. Influence of excipients, drugs, and osmotic agent in the inner core on the time-controlled disintegration of compression-coated ethylcellulose tablets. J Pharm Sci 2002;91(9):2040-6.

142. Lundstedt T, Seifert E, Abramo L, Thelin B, Nystrom A, Pettersen J, Bergman
      R. Experimental design and optimization. Chemometr Intell Lab
      1998;42:3-40.

143. Shanghai Sunpower Material. PVP. http://www.chinapvp.com/technoinfo-1.htm
      [Accessed September 5, 2007].

144. Rowe RC, Sheskey PJ, Weller PJ. Handbook of pharmaceutical excipients. 4th
      ed. London: Pharmaceutical Press; 2003.

145. Myer RH, Montgomery DC. Response surface methodology. 2nd ed. New York:
      John Wiley & Sons; 2002.

146. Kim YK, Park HB, Lee YM. Gas separation properties of carbon molecular
      sieve membranes derived from polyimide/polyvinylpyrrolidone
      blends: effect of the molecular weight of polyvinylpyrrolidone. J
      Membrane Sci 2005;251:159-67.

147. De Muth JE. Basic statistics and pharmaceutical statistical applications. 2nd ed.
      New York: Chapman & Hall; 2006.

148. Dietrich P, Bauer-Brandi A, Schubert R. Influence of tableting forces and
      lubricant concentration on the adhesion strength in complex layer
      tablets. Drug Dev Ind Pharm 2000;26:745-54.

149. Rani M, Mishra B. Comparative in vitro and in vivo evaluation of matrix,
      osmotic matrix, and osmotic pump tablets for controlled delivery of
      diclofenac sodium. AAPS PharmSciTech 2004;5(4):article 71.

150. Royce A, Li S, Weaver M, Shah U. *In vivo* and *in vitro* evaluation of three
      controlled release principles of 6-N-cyclohexyl-2'O-methyladenosine.
      J Control Release 2004;97:79-90.

151. Costa P, Lobo JMS. Modeling and comparison of dissolution profiles. Eur J
      Pharm Sci 2001;13:123-33.

152. Fritzsche AK, Arevalo AR, Moore MD, Elings VB, Kjoller K, Wu CM. The
      surface structure and morphology of polyvinylidenefluoride
      microfiltration membranes by atomic force microscopy. J Membrane
      Sci 1992;68:65-78.

153. Palacio L, Prádanos P, Calvo JI, Hernández A. Porosity measurements by a gas penetration method and other techniques applied to membrane characterization. Thin Solid Films 1999;348:22-9.

154. Stamatialis DF, Dias CR, de Pinho MN. Atomic force microscopy of dense and asymmetric cellulose-based membranes. J Membrane Sci 1999;160:235-42.

155. Seitavuopio P, Rantanen J, Yliruusi J. Tablet surface characterization by various imaging techniques. Int J Pharm 2003;254:281-6.

156. Kim JH, Min BR, Park HC, Won J, Kang YS. Phase behavior and morphological studies of polyimide/PVP/solvent/water system by phase inversion. J Appl Polym Sci 2001;81:3481-8.

157. Ochoa NA, Prádanos P, Palacio L, Pagliero C, Marchese J, Hernández A. Pore size distributions based on AFM imaging and retention of multidisperse polymer solutes: characterisation of polyethersulfone UF membranes with dopes containing different PVP. J Membrane Sci 2001;187:227-37.

158. Kim YK, Park HB, Lee YM. Carbon molecular sieve membrane derived from thermally labile polymer containing blend polymers and their gas separation properties. J Membrane Sci 2004;243:9-17.

159. Nakao S-i. Determination of pore size and pore size distribution 3.Filtration membranes. J Membrane Sci 1994;96:131-65.

160. Moharram MA, Balloomal LS, El-Gendy HM. Infrared study of the complexation of poly(acrylic acid) with poly(acrylamide). J Appl Polym Sci 1996;59(6):987-90.

161. Wu Y, Guo J, Yang W, Wang C, Fu S. Preparation and characterization of chitosan-poly(acrylic acid) polymer magnetic microspheres. Polymer 2006;47:5287-94.

162. Shin HS, Kim SY, Lee YM. Indomethacin release behaviors from pH and thermoresponsive poly(vinyl alcohol) and poly(acrylic acid) IPN hydrogels for site-specific drug delivery. J Appl Polym Sci 1997;65:685-93.

163. Siepmann J, Peppas NA. Modeling of drug release from delivery systems based on hydroxypropyl methylcellulose (HPMC). Adv Drug Deliver Rev 2001;48:139-57.

164. Prabakaran D, Singh P, Kanaujia P, Vyas SP. Effect of hydrophilic polymers on the release of diltiazem hydrochloride from elementary osmotic pumps. Int J Pharm 2003;259:173-9.

165. Miranda A, Millán M, Caraballo I. Study of the critical points of HPMC hydrophilic matrices for controlled drug deliver. Int J Pharm 2006;311:75-81.

166. Takka S. Propranolol hydrochloride-anionic polymer binding interaction. Il Farmaco 2003;58:1051-6.

167. Siemoneit U, Schmitt C, Alvarez-Lorenzo C, Luzardo A, Otero-Espinar F, Concheiro A, Blanco-Méndez J. Acrylic/cyclodextrin hydrogels with enhanced drug loading and sustained release capability. Int J Pharm 2006;312:66-74.

168. Ramírez Rigo MV, Allemandi DA, Manzo RH. Swellable drug-polyelectrolyte matrices (SDPM) of alginic acid. Characterization and delivery properties. Int J Pharm 2006;322:36-43.

169. McAinsh J, Baber NS, Smith R, Yong J. Pharmacokinetic and pharmacodynamic studies with long-acting propranolol. Br J Clin Pharmac 1978;6:115-21.

170. Rekhi GS, Jambhekar SS. Bioavailability and in-vitro/in-vivo correlation for propranolol hydrochloride extended-release bead products prepared usin aqueous polymeric dispersions. J Pharm Pharmacol 1996;48:1276-84.

171. Shand DG, Nuckolls EM, Oates JA. Plasma propranolol levels in adults with observations in four children. Clin Pharmacol Ther 1970;11:112-20.

172. U.S. Department of Health and Human Service Food and Drug Administration Center for Drug Evaluation and Research (CDER). Guidance for industry: Bioavailability and bioequivalence studies for orally administered drug products - general considerations. March 2003 BP.

http://www.fda.gov/cder/guidance/5356.pdf [Accessed September 5, 2007].

173. Costa P. An alternative method to the evaluation of similarity factor in dissolution testing. Int J Pharm 2001;220:77-83.

174. Liu J-P, Ma MC, Chow SC. Statistical evaluation of similarity factor f_2 as a criterion for assessment of similarity between dissolution profiles. Drug Inf J 1997;31:1255-71.

175. Gohel MC, Panchal MK. Refinement of lower acceptance value of the similarity factor f_2 in comparison of dissolution profiles. Dissolution Technologies 2002;9(1):1-5.

176. Gohel MC, Sarvaiya KG, Mehta NR, Soni CD, Vyas VU, Dave RK. Assessment of similarity factor using different weighting approaches. Dissolution Technologies 2005;12(4):22-7.

APPENDIX

EXPERIMENTAL DATA

Drug Release Data

Table 48. Release data[a] (% released) of CPOPs with membrane containing various amounts of PVP in preliminary study, *Drug Release Test 2*

Time (h)	No PVP	PVP K 30			PVP K90	
		12.5%	25%	50%	12.5%	25%
0	0.00±0.00	0.00±0.00	0.00±0.00	0.00±0.00	0.00±0.00	0.00±0.00
1	0.00±0.00	0.15±0.38	0.00±0.00	17.36±1.23	2.10±0.80	4.04±1.65
2	0.15±0.37	4.45±0.67	10.15±3.24	45.04±1.45	10.27±2.01	23.41±2.69
3	3.35±1.10	10.28±1.30	25.70±5.64	63.17±1.18	21.04±3.52	42.68±3.21
4	6.02±1.08	16.15±1.91	38.64±7.15	73.80±1.73	30.73±4.40	56.32±3.01
5	8.82±1.33	21.95±2.39	50.21±7.93	79.77±2.26	39.30±5.00	66.68±3.31
6	11.59±1.64	27.51±2.83	58.90±7.65	83.52±2.88	47.13±5.10	72.35±3.25
7	14.38±1.92	32.86±3.24	65.44±6.54	85.54±3.40	54.12±4.92	76.08±3.35
8	17.25±2.23	38.03±3.65	70.02±5.23	86.40±3.62	59.98±4.63	79.30±3.12
9	20.20±2.45	42.89±4.11	73.42±4.03	86.77±3.76	64.62±4.11	81.98±3.05
10	22.96±2.71	47.56±4.43	76.07±3.13	87.04±3.81	68.21±3.61	84.33±2.92
11	25.74±3.01	51.88±4.49	78.19±2.57	87.22±3.78	71.04±3.28	86.49±2.86
12	28.46±3.22	55.58±4.39	79.90±2.18	87.25±3.86	73.22±2.98	86.77±3.74

[a]Mean ± SD, n = 6

Table 49. Release data[a] (% released) of CPOPs with various coating formulations in response surface methodology, *Drug Release Test 1*

Time (h)	Coating formulations				
	No PVP	PVP K30-1	PVP K30-2	PVP K30-3	PVP K30-4
0	0.00±0.00	0.00±0.00	0.00±0.00	0.00±0.00	0.00±0.00
0.5	0.00±0.00	0.48±0.16	9.55±0.74	0.00±0.00	4.22±1.02
1	0.05±0.42	3.09±0.52	21.28±0.76	0.00±0.00	11.19±0.92
1.5	0.87±0.41	5.95±0.51	32.20±0.85	0.05±0.02	18.52±0.85
2	1.43±0.89	7.49±0.84	43.75±1.59	0.50±0.14	24.65±1.90
2.5	2.05±1.14	9.46±0.98	56.64±1.72	2.43±0.50	34.48±1.72
3	3.01±1.32	12.72±1.12	67.15±1.66	4.84±0.49	43.90±1.69
3.5	4.04±1.41	16.19±1.25	73.97±1.69	7.01±0.59	52.36±1.69
4	5.11±1.30	19.63±1.42	78.43±1.69	9.04±0.73	59.73±1.69
4.5	6.14±1.33	22.99±1.79	82.15±1.66	11.22±0.79	65.21±1.70
5	7.22±1.25	26.12±1.69	85.27±1.71	13.31±0.83	69.22±1.73
5.5	8.23±1.04	29.12±2.04	88.13±1.87	15.41±1.00	72.03±1.74
6	9.26±1.22	32.12±2.12	90.48±1.72	17.48±1.12	74.32±1.82
7	11.33±1.56	38.07±2.38	94.31±1.72	21.83±1.32	78.51±2.04
8	13.69±1.80	43.80±2.53	96.44±1.72	26.16±1.58	81.82±2.31
9	15.97±2.00	49.31±2.73	97.49±1.71	30.57±1.90	84.53±2.63
10	18.19±2.13	54.52±2.67	98.06±1.72	35.01±2.09	87.12±3.04
11	20.76±2.56	59.42±2.77	98.46±1.72	39.41±2.18	89.18±3.35
12	22.89±2.92	63.43±2.90	98.72±1.72	43.61±2.20	90.59±3.32
14	26.48±2.80	69.81±2.54	98.99±1.72	51.17±2.58	92.48±2.90
16	30.56±2.84	74.35±2.41	98.87±1.72	56.87±2.87	93.80±2.28
18	35.55±3.22	77.65±2.23	99.06±1.59	61.41±2.89	94.63±1.84
20	39.95±3.55	80.02±2.16	99.09±1.72	64.87±2.80	95.40±1.70
22	44.49±3.45	81.65±2.01	99.39±1.76	67.84±2.75	96.24±1.69
24	47.86±3.70	82.81±1.97	99.56±1.72	70.57±2.61	96.50±1.77

[a]Mean ± SD, n = 6

Table 49. Release data[a] (% released) of CPOPs with various coating formulations in response surface methodology, *Drug Release Test 1*

Time	Coating formulations				
(h)	PVP K30-5	PVP K30-6	PVP K30-7	PVP K30-8	PVP K30-9
0	0.00±0.00	0.00±0.00	0.00±0.00	0.00±0.00	0.00±0.00
0.5	0.48±0.14	9.02±0.81	8.74±0.79	0.32±0.14	1.02±0.70
1	0.49±0.14	20.90±1.65	20.21±0.93	1.16±0.18	8.85±0.79
1.5	0.50±0.15	31.57±2.32	31.07±0.84	4.48±1.09	17.22±0.96
2	1.02±0.11	40.36±2.45	39.82±1.64	6.33±1.43	21.39±1.60
2.5	1.52±0.33	54.85±4.35	55.73±1.68	9.40±1.62	28.64±1.97
3	2.64±1.01	65.08±3.88	68.92±1.63	13.65±1.84	36.52±2.02
3.5	4.03±1.17	71.92±2.51	76.81±1.68	17.95±2.10	43.74±2.02
4	5.20±1.53	76.35±1.93	81.09±1.87	21.93±2.15	53.01±2.11
4.5	6.40±1.63	79.43±1.72	84.02±1.66	25.87±2.14	58.29±2.02
5	7.73±1.63	81.90±1.64	86.05±1.63	29.56±2.01	64.19±2.05
5.5	8.99±1.74	83.94±1.60	87.68±1.67	33.23±2.10	68.87±2.04
6	10.28±1.76	85.66±1.60	88.93±1.64	36.65±2.48	72.55±2.03
7	12.83±1.83	88.81±1.17	91.03±1.72	42.95±2.47	78.13±2.03
8	15.51±1.88	91.29±1.12	92.76±1.70	48.78±2.05	83.12±2.08
9	18.10±2.00	93.18±1.10	94.31±1.75	54.24±1.97	84.70±2.03
10	20.89±2.12	97.70±1.09	95.61±1.64	59.22±1.87	86.89±2.07
11	23.65±2.26	95.72±1.10	96.69±1.69	63.67±1.84	88.85±2.03
12	26.32±2.30	96.17±1.14	97.76±1.63	67.22±1.91	90.40±2.07
14	31.65±2.52	96.66±1.23	99.21±1.65	72.49±1.93	93.18±1.87
16	36.71±2.72	96.72±1.31	100.33±1.63	76.18±1.53	95.21±2.05
18	41.43±2.87	96.74±1.41	101.05±1.65	78.85±1.48	96.93±2.03
20	46.00±3.05	96.68±1.44	101.41±1.62	80.81±1.67	98.35±2.03
22	50.30±3.22	96.75±1.50	101.58±1.62	81.93±1.66	98.90±2.03
24	54.02±3.20	96.78±1.50	101.65±1.64	82.87±1.37	100.10±1.82

[a]Mean ± SD, n = 6

Table 49. Release data[a] (% released) of CPOPs with various coating formulations in response surface methodology, *Drug Release Test 1* (cont.)

Time (h)	Coating formulations				
	PVP K30-10	PVP K30-11	PVP K90-1	PVP K90-2	PVP K90-3
0	0.00±0.00	0.00±0.00	0.00±0.00	0.00±0.00	0.00±0.00
0.5	1.71±0.85	2.11±1.85	0.58±0.12	12.06±1.52	0.00±0.00
1	9.54±1.18	10.32±2.11	3.78±0.21	26.44±2.52	0.03±0.02
1.5	18.07±1.63	19.15±2.87	7.52±0.65	45.41±2.59	0.30±0.29
2	23.86±1.79	24.33±3.06	10.02±0.87	57.69±2.51	1.94±0.89
2.5	31.11±2.06	32.02±2.93	13.07±1.22	69.73±2.39	3.94±1.72
3	39.09±3.01	41.02±3.77	17.50±1.58	76.73±2.31	6.24±1.56
3.5	46.31±2.99	48.13±3.84	21.98±2.15	82.00±2.31	8.34±2.49
4	54.37±2.96	55.76±3.29	26.52±2.65	85.82±2.27	10.57±2.74
4.5	60.86±2.98	62.56±3.53	30.86±3.32	88.53±2.26	12.66±2.95
5	66.76±2.97	68.39±3.44	34.84±3.82	90.26±2.25	14.78±3.48
5.5	71.44±2.97	73.02±3.18	38.61±4.18	91.47±2.24	16.98±3.73
6	75.13±2.98	76.78±2.77	42.21±4.41	92.21±2.24	19.25±3.74
7	80.71±2.98	82.30±3.11	49.10±5.08	92.94±2.24	24.41±4.92
8	84.51±2.31	86.77±3.04	55.39±5.59	93.46±2.25	29.12±5.02
9	87.28±2.25	88.66±2.95	60.60±5.52	93.86±2.23	33.65±5.37
10	89.47±2.26	90.21±2.86	65.00±4.96	94.24±2.23	38.52±5.51
11	91.43±2.27	92.02±2.88	68.64±4.31	94.45±2.23	42.99±5.95
12	92.98±2.28	93.71±2.75	71.70±3.79	94.55±2.23	46.20±6.04
14	95.61±1.99	96.25±2.36	76.04±2.63	94.75±2.23	56.19±5.93
16	97.80±2.00	98.06±2.51	78.59±1.85	94.75±2.23	61.63±5.82
18	99.51±1.97	99.24±2.54	80.62±1.43	94.75±2.23	65.48±5.67
20	100.93±1.98	99.85±2.46	82.21±1.03	94.75±2.23	67.41±5.19
22	101.48±1.95	100.31±2.69	83.36±0.83	94.75±2.23	69.18±4.60
24	101.79±1.97	100.50±2.66	84.35±0.79	94.75±2.23	70.94±4.78

[a]Mean ± SD, n = 6

Table 49.   Release data[a] (% released) of CPOPs with various coating formulations in
response surface methodology, *Drug Release Test 1* (cont.)

Time	Coating formulations				
(h)	PVP K90-4	PVP K90-5	PVP K90-6	PVP K90-7	PVP K90-8
0	0.00±0.00	0.00±0.00	0.00±0.00	0.00±0.00	0.00±0.00
0.5	3.48±1.17	0.00±0.00	8.00±0.32	16.97±1.26	1.76±0.15
1	11.92±1.46	0.39±0.09	26.53±2.22	29.16±1.12	11.56±1.64
1.5	22.42±1.88	2.10±0.05	42.89±2.74	44.56±2.52	22.64±2.53
2	31.01±4.70	2.54±0.10	59.36±3.17	57.13±2.79	32.87±4.24
2.5	45.64±6.83	3.73±0.17	71.01±2.48	70.57±1.48	44.95±5.39
3	55.60±6.53	5.84±0.59	77.38±2.57	76.98±2.36	55.28±4.49
3.5	61.31±7.36	6.67±0.72	82.51±2.48	81.35±2.35	63.29±5.29
4	67.30±6.06	9.36±0.82	86.65±2.36	84.68±2.36	69.41±4.77
4.5	70.23±6.16	10.38±1.12	89.73±2.38	87.28±2.34	73.93±3.70
5	75.33±4.77	12.56±0.45	91.42±1.88	89.17±2.34	77.11±3.55
5.5	78.31±4.34	14.13±1.21	92.58±1.87	90.50±2.17	79.92±3.13
6	81.79±3.73	15.64±1.70	92.23±1.68	91.25±2.04	82.37±2.09
7	85.30±3.76	18.63±1.53	93.87±1.50	92.00±1.95	86.59±1.77
8	87.43±4.03	22.21±1.53	94.31±1.60	92.31±1.94	90.08±1.62
9	90.43±3.31	26.50±1.43	94.55±1.59	92.80±1.92	93.20±1.61
10	91.99±2.99	29.68±1.94	94.67±1.50	93.25±2.09	94.94±1.67
11	92.42±2.93	32.06±1.24	94.86±1.46	93.40±2.12	96.26±1.65
12	92.92±2.92	34.69±1.45	95.13±1.47	93.60±2.12	97.08±1.84
14	93.92±2.97	42.97±1.78	95.52±1.47	93.60±2.12	98.00±1.90
16	94.62±3.02	48.98±2.56	95.99±1.43	93.60±2.12	98.49±1.71
18	95.02±2.87	53.95±2.79	96.46±1.46	93.60±2.12	98.92±1.72
20	95.42±3.31	58.36±2.02	96.93±1.55	93.60±2.12	99.27±1.81
22	95.42±3.31	60.10±1.88	97.04±1.58	93.60±2.12	99.17±1.89
24	95.42±3.31	63.53±2.16	97.08±1.59	93.60±2.12	99.22±1.92

[a]Mean ± SD, n = 6

Table 49. Release data[a] (% released) of CPOPs with various coating formulations in response surface methodology, *Drug Release Test 1* (cont.)

Time	Coating formulations		
(h)	PVP K90-9	PVP K90-10	PVP K90-11
0	0.00±0.00	0.00±0.00	0.00±0.00
0.5	5.02±0.87	5.31±1.00	5.11±1.03
1	14.69±0.81	15.24±1.16	16.05±1.07
1.5	29.21±1.00	31.11±0.88	30.34±1.43
2	41.30±1.75	44.94±1.72	43.36±2.46
2.5	54.31±2.80	56.42±2.04	56.68±3.04
3	62.59±2.66	64.25±2.04	64.55±2.85
3.5	69.01±2.63	69.62±1.98	70.36±3.11
4	73.69±2.54	75.12±1.84	74.99±3.02
4.5	77.47±2.44	78.32±1.80	78.39±3.15
5	80.60±2.30	82.14±1.81	81.62±2.97
5.5	83.49±2.23	84.72±2.16	84.45±3.04
6	85.93±2.04	87.21±2.17	86.82±3.01
7	89.73±1.67	91.76±2.08	90.75±2.70
8	91.72±1.33	93.64±2.14	92.18±2.74
9	92.76±1.64	94.59±2.20	93.48±2.51
10	93.22±1.20	95.10±2.24	94.18±2.48
11	93.42±1.16	95.47±2.18	94.69±2.39
12	93.65±1.17	96.03±2.17	95.02±2.40
14	94.05±1.18	96.73±2.13	95.88±2.40
16	94.36±1.26	97.19±2.04	96.14±2.34
18	94.83±1.26	97.35±2.06	96.28±2.32
20	95.09±1.33	97.49±2.06	96.44±2.28
22	95.09±1.33	97.63±2.06	96.64±2.21
24	95.09±1.33	97.73±2.05	96.93±2.11

[a]Mean ± SD, n = 6

Table 50. Release data[a] (% released) of CPOPs with various coating formulations in response surface methodology, *Drug Release Test 2*

Time (h)	Coating formulations					
	No PVP	PVP K30-1	PVP K30-2	PVP K30-3	PVP K30-4	PVP K30-5
0	0.00±0.00	0.00±0.00	0.00±0.00	0.00±0.00	0.00±0.00	0.00±0.00
0.5	0.00±0.00	0.38±0.07	12.57±3.30	0.00±0.00	4.24±1.49	0.44±0.08
1	0.50±0.41	2.43±0.54	26.81±5.65	0.00±0.00	11.24±3.49	0.45±0.07
1.5	0.93±0.77	7.05±1.88	42.71±6.69	2.14±0.40	20.89±4.59	1.97±0.40
2	1.36±1.18	10.29±1.75	56.40±7.97	3.81±0.52	31.63±5.82	3.32±0.33
2.5	2.04±1.37	13.74±1.94	65.55±8.82	5.52±0.64	41.58±6.32	4.54±0.33
3	2.76±1.32	17.43±2.13	71.40±8.74	7.29±0.78	49.85±6.38	5.87±0.53
3.5	3.77±0.91	20.92±2.19	75.22±7.98	9.19±0.85	56.90±6.11	6.94±0.53
4	4.73±0.79	24.43±2.57	78.05±6.99	11.04±0.98	62.45±5.56	8.17±0.57
4.5	5.64±0.67	27.90±2.80	80.17±6.29	12.91±1.18	66.59±5.00	9.59±0.81
5	6.85±0.44	31.49±2.93	82.01±5.89	14.85±1.29	69.62±4.41	10.72±0.74
5.5	7.86±0.54	34.80±2.96	83.26±5.49	16.84±1.42	72.00±4.11	12.02±0.82
6	8.89±0.70	38.12±3.10	84.18±5.12	18.74±1.58	73.96±4.08	13.32±0.96
7	10.96±1.02	44.67±3.17	85.58±4.44	22.66±1.88	77.17±4.36	15.92±1.32
8	13.32±1.46	50.82±3.41	86.56±3.81	26.68±2.21	79.50±4.69	18.74±1.48
9	15.60±1.97	56.87±3.35	86.89±3.26	30.79±2.53	81.26±4.87	21.17±1.61
10	17.94±2.35	62.16±2.79	87.26±2.84	34.94±2.81	82.66±4.87	23.97±1.89
11	20.38±2.71	66.56±2.41	87.67±2.47	38.91±3.03	83.62±4.62	26.82±2.09
12	22.89±3.07	69.94±2.08	87.86±2.18	42.86±3.26	84.41±4.38	29.63±2.33

[a]Mean ± SD, n = 6.

Table 50. Release data[a] (% released) of CPOPs with various coating formulations in response surface methodology, *Drug Release Test 2* (cont.)

Time (h)	Coating formulations					
	PVP K30-6	PVP K30-7	PVP K30-8	PVP K30-9	PVP K30-10	PVP K30-11
0	0.00±0.00	0.00±0.00	0.00±0.00	0.00±0.00	0.00±0.00	0.00±0.00
0.5	4.61±0.72	10.53±0.95	0.00±0.00	2.60±0.69	1.87±0.45	1.98±0.80
1	12.53±1.41	22.46±2.37	1.87±0.46	8.17±0.83	8.13±0.53	7.80±1.39
1.5	24.21±1.86	36.83±6.71	5.40±0.63	15.09±1.61	15.59±0.71	16.81±2.33
2	34.74±1.89	50.66±6.63	9.25±0.94	23.19±1.54	24.10±1.12	24.63±2.25
2.5	42.82±2.05	61.53±6.38	13.08±1.02	30.90±1.94	32.31±1.48	32.61±2.34
3	49.12±2.32	69.53±5.50	16.92±1.26	37.88±1.66	39.43±1.03	40.14±2.42
3.5	54.39±2.64	74.76±4.41	20.72±1.51	43.99±1.78	45.81±1.79	47.38±3.00
4	59.32±2.90	78.29±3.61	24.41±1.79	49.77±1.63	51.60±1.77	53.65±3.08
4.5	63.44±3.03	80.44±3.08	28.10±2.08	54.88±1.77	56.71±2.01	58.94±4.10
5	66.79±2.94	82.06±2.72	31.84±2.36	59.58±1.67	61.44±2.05	63.94±4.47
5.5	69.37±2.95	83.29±2.50	35.50±2.64	63.63±2.01	65.52±2.14	68.42±4.19
6	71.29±2.90	84.26±2.35	39.00±2.90	67.22±1.81	69.06±2.73	72.15±4.78
7	74.14±2.95	85.75±2.07	45.83±3.31	72.65±1.94	74.32±2.64	77.40±4.57
8	76.08±3.01	86.63±1.87	51.92±3.55	75.95±1.98	77.58±3.16	80.41±4.62
9	77.84±3.01	87.31±1.60	57.46±3.67	78.45±2.42	79.96±3.04	82.71±4.45
10	79.08±3.16	87.83±1.42	61.95±3.43	80.12±2.28	81.78±3.35	84.40±3.86
11	80.26±3.21	88.15±1.26	65.77±2.97	81.52±2.14	83.20±3.06	85.60±3.42
12	81.16±3.28	88.37±1.19	68.84±2.59	82.66±2.01	84.38±3.14	86.71±3.01

[a]Mean ± SD, n = 6.

Table 50. Release data[a] (% released) of CPOPs with various coating formulations in response surface methodology, *Drug Release Test 2* (cont.)

Time (h)	Coating formulations				
	PVP K90-1	PVP K90-2	PVP K90-3	PVP K90-4	PVP K90-5
0	0.00±0.00	0.00±0.00	0.00±0.00	0.00±0.00	0.00±0.00
0.5	1.02±0.98	8.29±0.85	0.04±0.04	1.86±0.17	0.30±0.05
1	4.98±0.82	25.01±1.35	0.07±0.05	9.73±1.27	0.46±0.07
1.5	11.98±1.25	43.39±2.69	1.64±0.54	23.60±2.09	1.07±0.71
2	16.98±1.33	57.80±2.50	3.62±0.40	36.76±2.00	2.83±0.69
2.5	22.24±1.73	68.20±3.29	5.51±0.45	47.63±1.96	4.35±0.59
3	27.41±1.85	74.85±2.97	7.47±0.70	56.75±2.24	5.77±0.65
3.5	31.38±2.06	79.52±2.82	9.41±0.97	63.11±2.52	7.23±0.70
4	35.24±2.08	82.62±2.65	11.40±1.37	67.91±2.65	8.64±0.71
4.5	39.54±2.09	84.94±2.76	13.36±1.63	71.54±2.69	9.99±0.84
5	43.38±2.07	86.36±2.84	15.48±1.91	74.66±2.56	11.59±0.97
5.5	47.19±1.85	87.08±3.01	17.59±2.19	77.66±2.57	12.95±1.03
6	50.78±1.91	87.68±3.11	19.72±2.40	79.84±2.33	14.38±1.25
7	56.19±1.66	88.35±3.27	24.02±2.88	83.02±2.18	17.21±1.39
8	60.62±1.69	88.62±3.31	28.57±3.22	84.36±2.22	20.26±1.67
9	63.66±1.76	88.72±3.36	33.09±3.46	84.82±2.20	23.37±1.76
10	65.97±1.76	88.96±3.37	37.66±3.68	85.30±2.31	26.46±1.92
11	67.85±1.94	89.16±3.35	42.31±3.82	85.59±2.35	29.66±2.13
12	69.07±1.76	89.36±3.35	46.62±3.90	85.90±2.32	32.91±2.34

[a]Mean ± SD, n = 6

Table 50. Release data[a] (% released) of CPOPs with various coating formulations in
response surface methodology, *Drug Release Test 2* (cont.)

Time (h)	Coating formulations					
	PVP K90-6	PVP K90-7	PVP K90-8	PVP K90-9	PVP K90-10	PVP K90-11
0	0.00±0.00	0.00±0.00	0.00±0.00	0.00±0.00	0.00±0.00	0.00±0.00
0.5	7.46±0.88	13.04±2.62	1.47±1.15	4.78±1.24	2.13±0.52	3.10±0.36
1	25.22±1.20	29.00±3.21	10.76±2.61	16.88±2.49	16.02±2.18	12.44±1.97
1.5	44.55±3.85	48.93±4.97	23.51±3.29	33.08±4.33	31.72±3.37	25.93±3.43
2	59.59±6.16	63.78±5.45	36.58±3.55	48.29±5.47	45.80±2.82	40.00±3.65
2.5	69.90±5.85	73.41±4.47	47.92±3.77	59.92±5.09	57.35±3.09	52.13±3.85
3	76.28±4.80	79.12±3.35	57.49±3.87	68.65±4.35	66.14±3.06	61.58±3.36
3.5	80.60±3.90	82.63±2.70	64.90±3.70	74.78±3.39	72.34±2.71	69.08±2.76
4	83.61±2.95	85.02±2.12	70.44±3.32	79.36±2.93	76.65±2.85	74.23±2.23
4.5	85.83±2.19	86.55±1.68	74.19±3.13	82.35±2.76	79.70±2.82	77.68±1.98
5	87.13±1.77	87.61±1.23	77.35±3.03	85.02±2.67	82.29±3.17	80.47±2.03
5.5	88.05±1.67	88.21±1.07	79.70±2.89	87.11±2.63	84.37±2.80	82.87±2.09
6	88.52±1.65	88.54±1.03	81.63±2.94	88.82±2.52	86.15±2.75	84.72±1.94
7	88.95±1.72	88.95±1.06	84.88±2.84	91.06±2.55	88.17±2.69	87.76±1.95
8	89.23±1.77	89.06±1.10	87.53±2.54	92.17±2.77	89.35±2.93	89.14±1.78
9	89.61±1.76	89.11±1.11	89.26±2.22	92.62±2.95	89.88±2.97	90.29±1.72
10	89.93±1.79	89.23±1.12	90.16±2.00	92.86±3.04	90.30±3.00	90.91±1.62
11	90.24±1.81	89.37±1.18	90.64±1.85	93.06±3.04	90.96±3.06	91.40±1.55
12	90.54±1.85	89.37±1.17	90.77±1.81	93.08±3.06	91.18±3.07	91.57±1.44

[a]Mean ± SD, n = 6.

Table 51. Release data[a] (% released) of the optimized CPOPs with different coating formulations at 4.2% membrane weight increase, *Drug Release Test 1*

Time	Coating formulations	
(h)	35%	23%
	PVP K30	PVP K90
0	0.00±0.00	0.00±0.00
0.5	1.83±0.19	0.40±0.19
1	5.90±0.60	1.88±1.11
1.5	10.79±0.85	7.89±1.13
2	15.64±1.46	12.47±2.96
2.5	23.68±2.02	18.52±3.49
3	32.28±2.59	25.59±3.94
3.5	40.87±2.96	32.88±4.22
4	48.26±3.04	39.12±3.98
4.5	54.20±3.09	43.95±3.57
5	59.29±3.18	49.17±3.77
5.5	63.32±3.09	54.07±4.03
6	66.76±2.81	58.13±4.58
7	71.53±2.25	64.94±4.24
8	75.01±1.96	70.64±3.42
9	77.62±1.88	74.31±2.96
10	79.79±1.92	77.26±2.52
11	81.69±1.90	79.93±2.17
12	83.75±1.93	81.70±2.07
14	87.47±1.90	85.17±1.78
16	90.61±1.89	87.95±1.73
18	92.62±1.72	90.61±1.89
20	94.26±1.39	92.51±1.94
22	95.49±1.13	94.15±1.75
24	96.06±0.90	95.37±1.75

[a]Mean ± SD, n = 6

Table 52. Release data[a] (% released) of the optimized CPOPs with membrane containing 35% PVP K30 at 4.2% membrane weight increase, *Drug Release Test 2*

Time (h)	Drug released (%)	Time (h)	Drug released (%)
0	0.00±0.00		
0.5	2.23±0.42	5	57.48±4.68
1	6.76±0.91	5.5	61.31±4.35
1.5	13.91±1.56	6	64.71±3.83
2	22.38±2.59	7	69.79±2.67
2.5	29.86±3.24	8	73.14±2.42
3	36.80±3.78	9	75.78±2.31
3.5	42.75±4.30	10	77.77±2.36
4	48.03±4.71	11	79.77±2.03
4.5	52.92±4.77	12	81.84±1.93

[a]Mean ± SD, n = 6

Table 53. Release data[a] (% released) of propranolol from the optimized CPOPs in different media, *Drug Release Test 1*

Time (h)	PVP K30			PVP K90		
	Release media			Release media		
	pH 1.2/ pH 6.8	pH 6.8	pH 7.5	pH 1.2/ pH 6.8	pH 6.8	pH 7.5
0	0.00±0.00	0.00±0.00	0.00±0.00	0.00±0.00	0.00±0.00	0.00±0.00
0.5	1.83±0.19	0.85±0.45	1.44±0.59	0.40±0.19	0.49±0.14	0.09±0.04
1	5.90±0.60	7.30±3.67	8.16±1.86	1.88±1.11	2.24±0.59	1.32±0.80
1.5	10.79±0.85	15.86±5.24	16.34±3.12	7.89±1.13	3.73±0.75	5.82±1.31
2	15.64±1.46	24.56±6.89	25.11±4.61	12.47±2.96	9.27±1.41	12.61±1.79
2.5	23.68±2.02	32.33±7.36	32.48±4.95	18.52±3.49	15.30±2.08	19.55±2.66
3	32.28±2.59	39.96±7.67	39.69±5.35	25.59±3.94	21.47±2.62	26.30±3.85
3.5	40.87±2.96	46.65±8.06	46.49±5.74	32.88±4.22	26.88±3.29	33.05±4.63
4	48.26±3.04	53.09±8.04	52.84±5.81	39.12±3.98	32.95±4.19	39.24±5.00
4.5	54.20±3.09	58.74±7.68	58.55±5.70	43.95±3.57	38.56±4.87	45.30±5.70
5	59.29±3.18	63.28±7.30	63.55±5.19	49.17±3.77	44.26±5.38	50.65±6.29
5.5	63.32±3.09	67.03±6.62	67.62±4.69	54.07±4.03	49.26±6.19	55.10±6.13
6	66.76±2.81	70.45±5.81	70.85±4.00	58.13±4.58	54.84±6.56	58.89±5.76
7	71.53±2.25	75.28±5.52	76.02±3.35	64.94±4.24	61.81±5.92	65.81±4.35
8	75.01±1.96	78.85±5.58	79.68±2.95	70.64±3.42	67.27±4.99	71.95±3.13
9	77.62±1.88	82.06±5.41	82.68±2.93	74.31±2.96	71.67±4.13	76.60±2.48
10	79.79±1.92	85.04±5.07	85.28±2.74	77.26±2.52	75.02±3.64	80.18±2.48
11	81.69±1.90	87.29±4.81	87.56±2.49	79.93±2.17	77.84±3.36	83.38±2.24
12	83.75±1.93	89.73±4.46	89.43±2.23	81.70±2.07	79.88±3.12	85.45±1.93
14	87.47±1.90	92.29±3.37	92.63±1.43	85.17±1.78	83.73±3.02	89.06±1.38
16	90.61±1.89	94.18±2.19	94.35±1.09	87.95±1.73	86.13±2.82	92.01±1.35
18	92.62±1.72	94.70±1.64	95.89±0.82	90.61±1.89	87.50±2.68	94.29±1.06
20	94.26±1.39	95.26±1.50	97.56±0.69	92.51±1.94	89.42±2.67	96.66±0.76
22	95.49±1.13	95.40±1.14	98.21±0.88	94.15±1.75	90.88±2.75	97.96±0.58
24	96.06±0.90	95.45±1.18	98.54±0.87	95.37±1.75	91.67±2.43	98.77±0.61

[a]Mean ± SD, n = 6

Table 54. Release data[a] (% released) of propranolol from the optimized CPOPs at different agitation intensity, *Drug Release Test 1*

Time (h)	PVP K30			PVP K90		
	Rotational speed			Rotational speed		
	50 rpm	100 rpm	150 rpm	50 rpm	100 rpm	150 rpm
0	0.00±0.00	0.00±0.00	0.00±0.00	0.00±0.00	0.00±0.00	0.00±0.00
0.5	1.16±0.45	1.83±0.19	1.31±0.20	0.44±0.08	0.40±0.19	0.28±0.09
1	3.66±1.51	5.90±0.60	5.36±0.58	1.13±0.34	1.88±1.11	0.55±0.03
1.5	7.19±3.00	10.79±0.85	10.21±0.85	5.91±0.48	7.89±1.13	5.37±0.59
2	10.91±3.41	15.64±1.46	14.33±1.01	10.18±2.23	12.47±2.96	11.74±0.97
2.5	18.83±3.84	23.68±2.02	21.20±1.18	15.88±1.99	18.52±3.49	17.20±1.50
3	27.14±4.02	32.28±2.59	29.95±1.52	22.80±1.72	25.59±3.94	23.48±2.03
3.5	34.99±3.79	40.87±2.96	38.72±1.65	29.80±1.24	32.88±4.22	29.90±2.81
4	42.21±3.63	48.26±3.04	46.48±1.90	35.55±1.15	39.12±3.98	35.90±3.22
4.5	48.15±3.38	54.20±3.09	53.35±1.73	40.98±1.13	43.95±3.57	41.44±3.59
5	53.69±3.03	59.29±3.18	59.10±1.52	45.95±1.04	49.17±3.77	46.43±3.78
5.5	58.62±2.68	63.32±3.09	63.51±1.14	50.66±0.81	54.07±4.03	50.90±3.97
6	62.50±2.25	66.76±2.81	67.10±1.02	54.77±0.59	58.13±4.58	55.08±3.99
7	68.36±1.70	71.53±2.25	72.20±0.87	62.32±0.91	64.94±4.24	62.44±4.13
8	72.20±1.60	75.01±1.96	75.84±0.71	68.46±0.74	70.64±3.42	68.44±3.64
9	75.22±1.45	77.62±1.88	78.69±0.70	72.89±0.58	74.31±2.96	73.31±2.81
10	78.10±1.50	79.79±1.92	81.45±0.53	76.41±0.87	77.26±2.52	77.23±2.18
11	80.30±1.62	81.69±1.90	83.59±0.71	79.13±1.17	79.93±2.17	80.08±1.82
12	82.33±1.59	83.75±1.93	85.73±0.72	81.08±1.13	81.70±2.07	82.40±1.50
14	86.18±1.61	87.47±1.90	89.19±0.99	84.58±1.33	85.17±1.78	86.09±1.24
16	89.25±1.67	90.61±1.89	92.18±0.60	87.38±1.50	87.95±1.73	89.13±1.15
18	92.14±1.74	92.62±1.72	94.19±0.70	90.37±1.36	90.61±1.89	91.53±0.99
20	83.70±1.73	94.26±1.39	95.80±0.89	92.17±1.50	92.51±1.94	93.94±0.96
22	94.95±1.73	95.49±1.13	96.82±0.92	94.12±1.41	94.15±1.75	95.95±0.91
24	95.95±1.74	96.06±0.90	97.05±0.93	95.84±1.28	95.37±1.75	97.27±0.89

[a]Mean ± SD, n = 6

Table 55. Release data[a] (% released) of propranolol from the optimized CPOPs in different osmolarity media, *Drug Release Test 1*

Time (h)	PVP K30			PVP K90		
	Osmolarity			Osmolarity		
	0.5 osm	1 osm	2 osm	0.5 osm	1 osm	2 osm
0	0.00±0.00	0.00±0.00	0.00±0.00	0.00±0.00	0.00±0.00	0.00±0.00
0.5	0.39±0.11	0.00±0.00	0.00±0.00	0.00±0.00	0.00±0.00	0.00±0.00
1	0.83±0.14	0.00±0.00	0.00±0.00	0.03±0.02	0.00±0.00	0.00±0.00
1.5	3.22±0.63	0.52±0.33	0.00±0.00	0.22±0.03	0.15±0.07	0.00±0.00
2	6.70±0.88	2.07±0.56	0.04±0.05	1.72±0.47	1.39±0.82	0.00±0.00
2.5	10.35±1.25	3.72±0.67	0.18±0.12	4.22±0.69	3.11±0.60	0.10±0.10
3	14.22±1.46	5.05±0.72	0.54±0.36	7.43±0.94	4.97±0.62	0.84±0.14
3.5	18.14±1.69	6.59±0.93	1.01±0.52	10.60±0.90	6.33±0.61	1.52±0.22
4	21.97±1.80	8.11±1.07	1.43±0.59	13.66±1.03	7.89±0.63	2.04±0.23
4.5	25.80±2.04	9.67±1.19	1.87±0.62	16.90±1.14	9.31±0.62	2.61±0.23
5	29.67±2.18	11.12±1.39	2.43±0.70	20.27±1.20	10.79±0.62	3.14±0.24
5.5	33.46±2.38	12.75±1.48	2.85±0.72	23.36±1.18	12.23±0.64	3.62±0.28
6	37.24±2.51	14.28±1.70	3.16±0.75	26.93±1.51	13.53±0.66	3.85±0.30
7	44.59±2.73	17.42±1.97	4.05±0.85	33.56±1.87	16.19±0.69	5.08±0.28
8	51.58±2.91	20.41±2.26	4.94±0.92	39.86±2.28	18.59±1.20	5.61±0.35
9	57.39±2.80	23.57±2.57	5.65±1.00	45.67±2.65	21.33±0.78	6.33±0.40
10	62.20±2.58	26.80±2.84	6.43±1.08	51.383.36±	23.55±0.82	7.05±0.37
11	65.87±2.37	29.65±3.13	7.22±1.18	56.04±3.47	25.85±0.91	7.70±0.45
12	69.44±2.64	32.74±3.38	7.93±1.28	60.03±3.25	27.98±0.95	8.21±0.43
14	75.46±2.58	38.53±3.98	9.35±1.39	66.25±2.56	31.88±1.14	9.39±0.48
16	80.80±2.68	44.27±4.51	10.65±1.51	70.83±2.38	35.68±1.31	10.37±0.58
18	84.98±2.67	49.94±4.99	12.00±1.67	74.18±2.19	38.98±1.49	11.46±0.65
20	88.72±2.56	55.64±5.37	13.27±1.84	77.09±2.22	42.21±1.64	12.24±0.67
22	91.35±1.96	60.75±5.91	14.57±2.00	79.67±2.23	44.99±1.81	13.23±0.77
24	93.70±1.56	65.57±6.06	15.77±2.18	82.03±2.25	47.54±1.97	13.93±0.86

[a]Mean ± SD, n = 6

Table 56. Release data[a] (% released) of CPOPs using various amounts of CS-PAA:HPMC as osmogents at 8% coating level, *Drug Release Test 2*

Time (h)	No osmogent	Monolithic		Bilayer	
		MN-10	MN-20	BI-10	BI-20
0	0.00±0.00	0.00±0.00	0.00±0.00	0.00±0.00	0.00±0.00
0.5	1.36±0.37	0.86±0.23	0.88±0.19	1.21±0.53	4.13±0.28
1	3.94±0.45	2.54±0.80	2.41±0.88	4.71±0.54	10.93±0.64
1.5	6.61±0.58	3.85±1.18	3.54±1.11	9.43±0.47	17.26±0.72
2	10.32±1.02	6.48±1.55	5.54±1.15	14.75±0.94	24.49±0.70
2.5	16.00±1.15	9.51±1.68	6.70±1.31	19.90±1.18	30.87±1.84
3	22.00±1.21	13.48±1.86	8.02±1.81	26.94±1.03	37.06±2.10
3.5	27.28±1.41	17.36±1.99	9.31±1.98	33.09±0.93	43.91±1.41
4	32.29±1.46	20.86±2.03	10.61±1.98	37.83±1.40	49.95±1.20
4.5	37.00±1.46	24.33±2.03	12.09±2.03	43.15±1.02	54.88±1.61
5	41.18±1.46	27.40±2.02	13.45±1.97	46.59±1.61	59.61±2.19
5.5	44.83±1.57	29.92±2.03	14.31±2.10	50.98±1.98	62.96±2.38
6	48.40±1.53	32.48±2.02	15.84±2.24	54.53±1.50	65.93±2.28
7	54.46±1.43	37.10±1.95	17.50±2.26	61.68±1.20	70.85±2.24
8	59.77±1.32	40.88±1.87	19.55±2.25	67.26±1.52	74.39±2.03
9	64.29±1.18	44.21±1.83	21.03±2.44	71.57±1.72	77.09±1.89
10	68.04±1.10	47.28±1.68	22.25±2.29	75.44±2.11	79.33±1.93
11	71.17±0.98	49.77±1.58	23.53±2.26	79.11±1.88	80.72±1.78
12	73.81±0.92	52.12±1.64	24.89±2.21	82.16±1.63	81.93±1.76

[a]Mean ± SD, n = 6.

Table 57. Release data[a] (% released) of bilayered CPOPs using 20 mg of CS-PAA:HPMC as osmogents at various coating levels, *Drug Release Test 2*

Time	Coating levels		
(h)	8%	12%	16%
0	0.00±0.00	0.00±0.00	0.00±0.00
0.5	4.13±0.28	1.06±0.45	0.14±0.05
1	10.93±0.64	4.99±1.10	1.75±0.72
1.5	17.26±0.72	10.58±1.46	5.58±0.88
2	24.49±0.70	16.85±1.87	10.72±0.99
2.5	30.87±1.84	22.76±2.05	15.88±1.16
3	37.06±2.10	28.11±2.22	20.65±0.92
3.5	43.91±1.41	33.19±2.83	26.08±1.80
4	49.95±1.20	39.40±3.25	31.05±3.27
4.5	54.88±1.61	45.20±3.17	35.79±4.38
5	59.61±2.19	51.29±2.73	41.53±4.60
5.5	62.96±2.38	56.35±2.50	47.35±4.53
6	65.93±2.28	60.96±2.05	52.68±4.17
7	70.85±2.24	67.80±1.80	61.11±3.18
8	74.39±2.03	73.81±1.51	67.68±2.55
9	77.09±1.89	77.17±1.38	72.56±2.13
10	79.33±1.93	80.05±1.31	76.14±1.94
11	80.72±1.78	81.74±1.16	78.08±1.59
12	81.93±1.76	83.23±0.96	80.10±1.68

[a]Mean ± SD, n = 6.

Swelling Characteristic Data

Table 58. Swelling force[a] (N) of CS-PAA interpolymer complexes at different molecular weight of CS

Time (min)	L-CS			M-CS			H-CS		
	CS:PAA 1:2	CS:PAA 1:1	CS:PAA 2:1	CS:PAA 1:2	CS:PAA 1:1	CS:PAA 2:1	CS:PAA 1:2	CS:PAA 1:1	CS:PAA 2:1
0	0.00±0.00	0.00±0.00	0.00±0.00	0.00±0.00	0.00±0.00	0.00±0.00	0.00±0.00	0.00±0.00	0.00±0.00
15	1.49±0.16	2.20±0.56	2.41±0.13	3.48±0.47	5.43±0.57	4.72±0.57	4.35±0.87	6.37±0.62	5.30±0.32
30	1.95±0.08	2.84±0.55	3.08±0.02	5.05±0.57	7.49±0.87	7.29±0.94	6.03±1.00	8.73±0.88	8.39±0.74
45	2.55±0.05	3.25±0.62	3.80±0.19	6.51±0.56	9.28±0.98	9.77±0.82	7.74±0.74	10.93±1.11	10.90±0.54
60	3.26±0.15	3.55±0.69	4.36±0.20	7.81±0.36	10.66±1.17	12.14±0.61	9.07±0.85	13.23±0.54	13.20±0.93
70	3.68±0.26	3.69±0.64	4.70±0.22	8.54±0.58	11.39±1.33	13.57±0.76	9.89±0.92	13.76±0.51	14.64±1.11
90	4.46±0.32	4.14±0.49	5.25±0.24	9.74±0.87	12.63±1.11	16.15±0.98	11.31±0.94	15.26±0.66	17.25±0.95
100	4.47±0.31	4.32±0.61	5.46±0.26	10.25±1.07	13.10±1.10	17.30±1.08	11.75±0.95	15.84±0.66	18.39±1.12
120	5.32±0.39	4.74±0.76	5.85±0.33	11.00±0.80	13.85±1.25	19.40±1.18	12.31±0.93	16.81±0.93	20.33±1.35
150	6.06±0.47	5.26±0.73	6.32±0.41	12.02±1.00	14.78±1.23	21.92±1.26	13.12±0.80	18.03±1.14	22.51±1.40
180	6.71±0.63	5.75±0.83	6.72±0.33	12.78±1.13	15.39±1.28	23.80±1.25	13.89±0.69	18.82±1.17	24.19±1.29
240	7.63±0.68	6.39±0.88	7.20±0.63	13.81±1.30	16.11±1.20	26.66±1.29	14.65±0.55	19.85±1.22	26.07±1.59
300	8.15±0.49	6.99±1.00	7.63±0.57	14.25±1.06	16.13±0.97	28.17±1.24	15.12±0.61	20.45±1.17	26.93±1.84
360	8.66±0.34	7.55±1.06	8.05±0.58	14.74±0.88	16.34±0.87	28.96±1.21	15.49±0.66	20.79±1.31	27.60±1.43

[a]Mean ± SD, n = 3

Table 59. Swelling ratio[a] of CS-PAA interpolymer complexes at different molecular weight of CS

Time (min)	L-CS			M-CS			H-CS		
	CS:PAA 1:2	CS:PAA 1:1	CS:PAA 2:1	CS:PAA 1:2	CS:PAA 1:1	CS:PAA 2:1	CS:PAA 1:2	CS:PAA 1:1	CS:PAA 2:1
0	0.00±0.00	0.00±0.00	0.00±0.00	0.00±0.00	0.00±0.00	0.00±0.00	0.00±0.00	0.00±0.00	0.00±0.00
15	1.71±0.04	1.53±0.06	1.50±0.08	1.72±0.05	2.09±0.04	1.11±0.02	1.79±0.09	2.10±0.05	1.08±0.04
30	2.80±0.04	1.80±0.12	1.97±0.25	2.98±0.03	3.47±0.09	2.00±0.03	2.99±0.17	3.66±0.07	1.89±0.03
45	4.12±0.13	1.83±0.10	2.13±0.03	3.96±0.06	4.26±0.15	2.75±0.04	3.63±0.31	5.32±0.14	2.63±0.07
60	4.98±0.57	1.93±0.07	2.68±0.59	5.36±0.07	5.36±0.32	3.70±0.30	4.70±0.17	6.44±0.24	3.39±0.14
75	5.42±0.33	2.01±0.04	2.66±0.06	4.96±0.08	5.90±0.55	4.35±0.01	4.70±0.13	7.05±0.15	4.20±0.15
90	5.65±0.11	1.82±0.23	2.62±0.10	4.39±0.18	6.21±0.16	5.24±0.03	4.26±0.05	7.61±0.17	4.99±0.17
105	5.60±0.49	0.85±0.42	1.77±0.36	3.14±0.21	6.07±0.17	6.29±0.04	3.28±0.29	8.06±0.08	5.94±0.15
120	4.56±0.87	0.01±0.02	0.66±0.33	2.34±0.36	5.59±0.50	7.46±0.06	2.36±0.03	8.89±0.55	7.09±0.20
150	1.33±0.43	n/a	n/a	0.02±0.04	3.36±0.81	9.97±0.25	0.44±0.45	7.23±0.45	9.17±0.25
180	n/a	n/a	n/a	n/a	n/a	12.46±0.76	n/a	3.86±0.33	11.46±0.31
240	n/a	n/a	n/a	n/a	n/a	17.35±0.47	n/a	n/a	15.28±0.27
300	n/a	n/a	n/a	n/a	n/a	19.11±1.04	n/a	n/a	18.55±0.20
360	n/a	n/a	n/a	n/a	n/a	15.95±0.47	n/a	n/a	17.65±0.31

[a]Mean ± SD, n = 3

Table 60. Swelling force[a] (N) of CS-PAA:HPMC ternary mixtures at various compositions

Time (min)	CS-PAA:HPMC				
	1:0	0.75:0.25	0.5:0.5	0.25:0.75	0:1
0	0.00±0.00	0.00±0.00	0.00±0.00	0.00±0.00	0.00±0.00
15	6.37±0.64	4.76±0.45	4.41±0.27	4.24±0.55	2.90±0.10
30	8.73±0.68	6.49±0.61	5.93±0.07	5.60±0.58	2.60±0.02
45	10.93±0.73	7.75±0.81	7.10±0.16	6.49±0.54	2.45±0.10
60	13.23±0.75	8.72±0.99	8.05±0.30	7.16±0.47	2.32±0.21
70	13.76±0.93	9.21±1.07	8.54±0.30	7.53±0.39	2.31±0.28
90	15.26±0.96	9.89±0.90	9.21±0.21	8.12±0.32	2.70±0.61
100	15.84±0.98	10.14±0.79	9.50±0.21	8.35±0.27	2.88±0.80
120	16.81±0.97	10.63±0.68	9.98±0.20	8.71±0.21	2.98±0.81
150	18.03±0.99	10.98±0.72	10.56±0.27	9.05±0.10	3.03±0.76
180	18.82±1.05	11.15±0.61	11.07±0.19	9.35±0.13	2.95±0.66
240	19.85±0.79	11.53±0.65	11.58±0.12	9.79±0.24	2.78±0.53
300	20.45±0.74	11.73±0.94	11.84±0.25	10.09±0.22	2.46±0.49
360	20.79±0.73	11.98±1.13	12.11±0.18	10.15±0.15	1.99±0.28

[a]Mean ± SD, n = 3

Table 61. Swelling ratio[a] of CS-PAA:HPMC ternary mixtures at various compositions

Time	CS-PAA:HPMC				
(min)	1:0	0.75:0.25	0.5:0.5	0.25:0.75	0:1
0	0.00±0.00	0.00±0.00	0.00±0.00	0.00±0.00	0.00±0.00
15	2.14±0.02	1.99±0.03	1.72±0.10	1.42±0.10	0.46±0.03
30	3.74±0.03	2.80±0.07	2.56±0.80	2.06±0.03	0.53±0.02
45	5.38±0.34	3.42±0.08	3.14±0.13	2.72±0.01	0.60±0.05
60	6.71±0.09	3.82±0.12	3.67±0.04	3.22±0.08	0.53±0.02
75	7.19±0.10	3.87±0.08	4.20±0.07	3.51±0.03	0.52±0.01
90	7.65±0.14	4.02±0.04	4.25±0.23	3.73±0.14	0.50±0.04
105	7.99±0.03	4.33±0.24	4.53±0.46	3.76±0.08	0.44±0.03
120	8.26±0.08	4.01±0.41	4.48±0.14	3.97±0.04	0.40±0.00
150	6.67±0.11	2.94±0.43	3.31±0.24	3.52±0.09	0.30±0.02
180	3.65±0.16	2.15±0.59	2.54±0.33	3.01±0.17	0.21±0.05
210	n/a	0.57±0.48	1.17±0.17	1.62±0.09	0.16±0.06
240	n/a	n/a	n/a	n/a	n/a
300	n/a	n/a	n/a	n/a	n/a
360	n/a	n/a	n/a	n/a	n/a

[a]Mean ± SD, n = 3

Propranolol Plasma Concentration Data

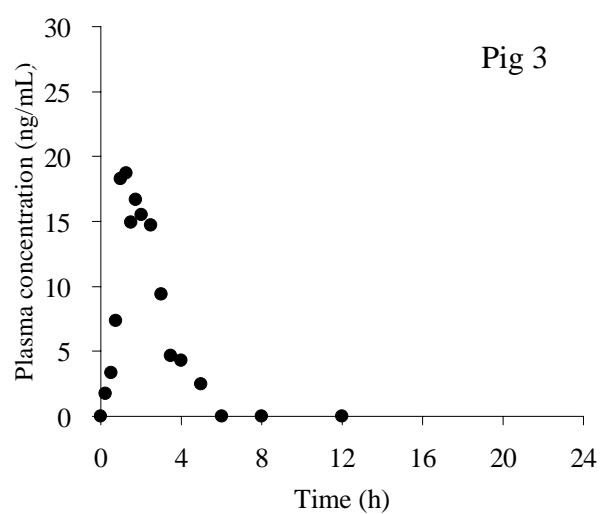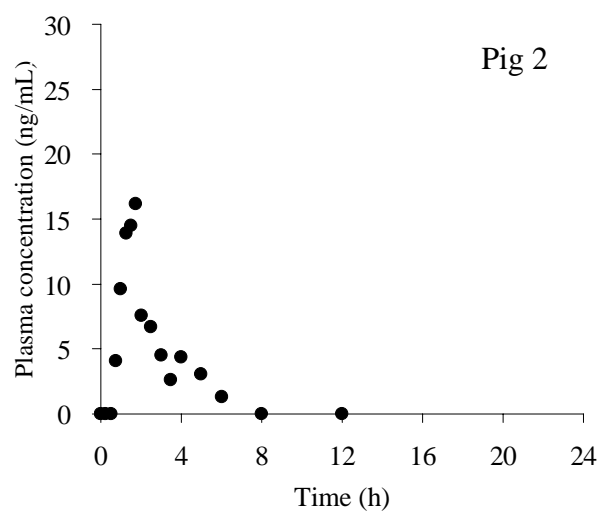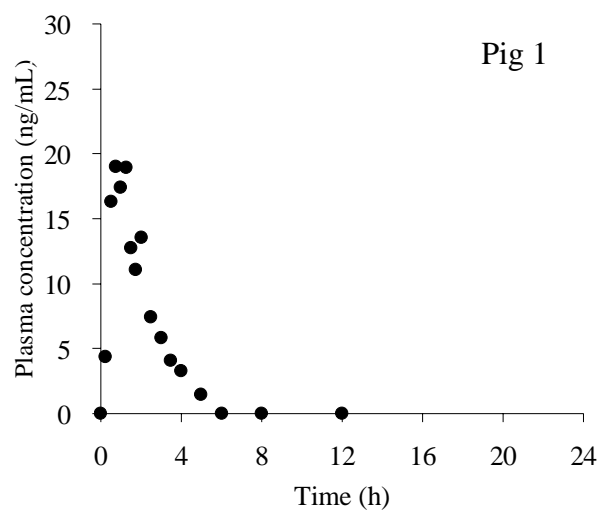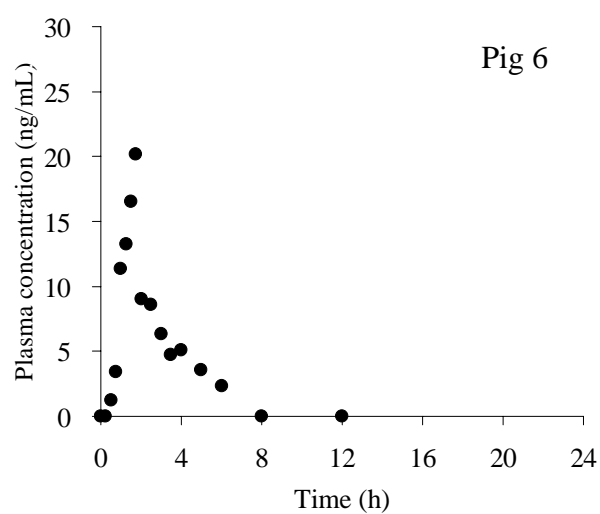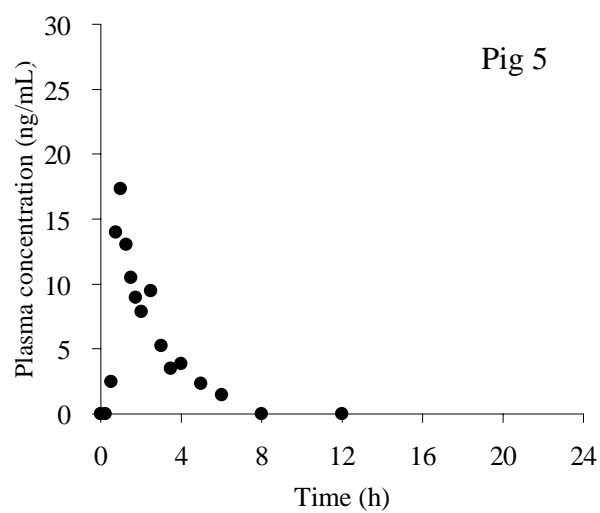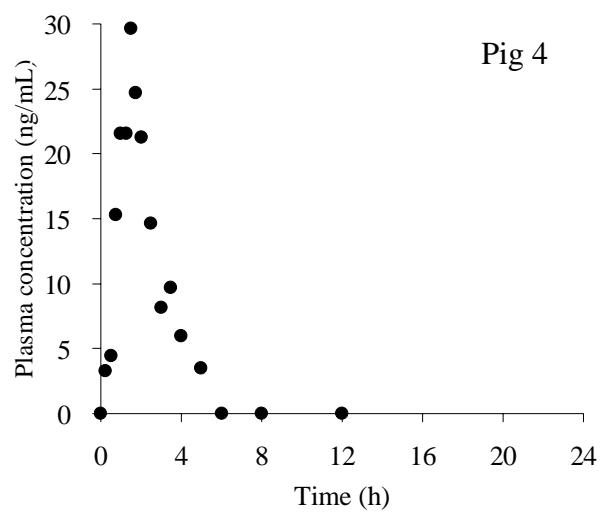Table 62. Propranolol plasma concentration (ng/mL) after a single oral dose of 40 mg propranolol immediate release tablets

Time (h)	Pig 1	Pig 2	Pig 3	Pig 4	Pig 5	Pig 6	Pig 7	Pig 8	Pig 9
0.00	0.00	0.00	0.00	0.00	0.00	0.00	0.00	0.00	0.00
0.25	4.38	0.00	1.73	3.26	0.00	0.00	1.45	12.62	4.61
0.50	16.32	0.00	3.36	4.46	2.44	1.27	7.29	25.36	2.58
0.75	18.97	4.06	7.33	15.28	13.95	3.43	17.34	25.99	2.21
1.00	17.43	9.60	18.26	21.57	17.30	11.33	19.92	23.06	4.73
1.25	18.96	13.87	18.74	21.52	13.04	13.23	22.85	18.42	10.81
1.50	12.73	14.47	14.96	29.63	10.46	16.56	21.39	17.70	12.42
1.75	11.04	16.18	16.66	24.66	8.97	20.17	16.55	14.85	15.81
2.00	13.56	7.59	15.52	21.55	7.83	9.01	17.33	12.60	16.14
2.50	7.46	6.73	14.69	14.65	9.50	8.60	13.16	4.34	14.11
3.00	5.82	4.55	9.42	8.17	5.24	6.35	9.12	3.45	10.85
3.50	4.11	2.65	4.67	9.67	3.47	4.72	6.87	3.10	6.50
4.00	3.25	4.38	4.29	5.99	3.83	5.11	5.04	1.91	4.70
5.00	1.42	3.03	2.48	3.47	2.36	3.55	3.90	1.67	1.92
6.00	0.00	1.32	0.00	0.00	1.47	2.31	2.57	0.00	0.00
8.00	0.00	0.00	0.00	0.00	0.00	0.00	0.00	0.00	0.00
12.00	0.00	0.00	0.00	0.00	0.00	0.00	0.00	0.00	0.00

Table 63. Propranolol plasma concentration (ng/mL) after a single oral dose of 80 mg propranolol CPOPs at 8% coating level

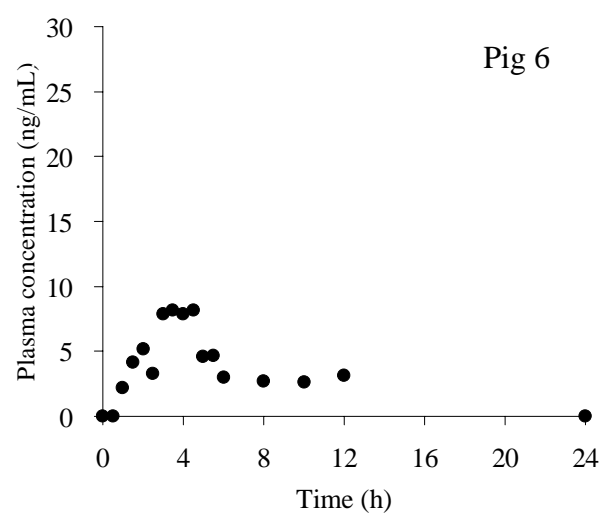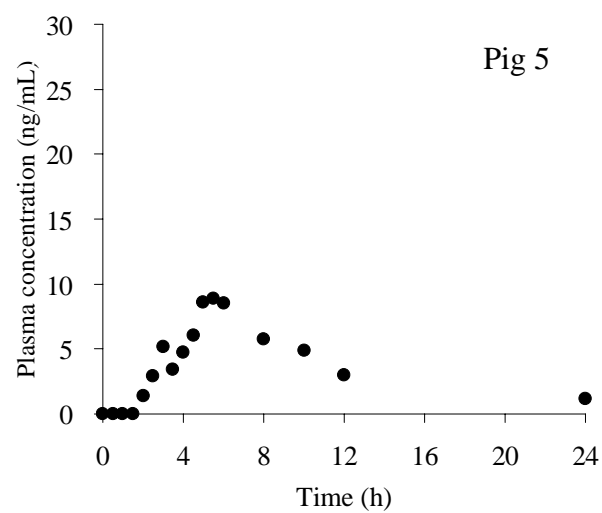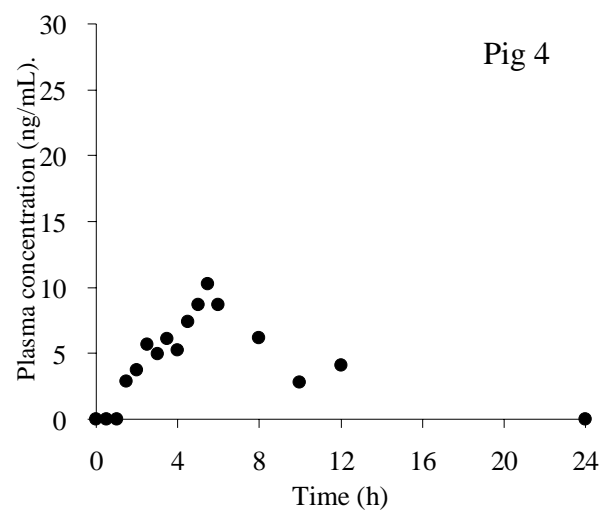| Time (h)	Pig 1	Pig 2	Pig 3	Pig 4	Pig 5	Pig 6	Pig 7	Pig 8	Pig 9
0.00	0.00	0.00	0.00	0.00	0.00	0.00	0.00	0.00	0.00
0.50	0.00	0.00	0.00	0.00	0.00	0.00	0.00	0.00	0.00
1.00	0.00	0.00	0.00	0.00	0.00	2.21	0.00	0.00	1.29
1.50	0.00	0.00	0.00	2.86	0.00	4.12	2.08	1.52	3.20
2.00	3.74	2.06	2.05	3.73	1.39	5.19	3.10	3.79	7.05
2.50	5.92	5.74	4.56	5.70	2.93	3.27	4.18	7.09	6.92
3.00	6.42	8.37	5.30	4.92	5.20	7.88	5.25	11.51	8.98
3.50	7.77	7.01	8.74	6.13	3.41	8.18	7.30	13.08	10.49
4.00	8.33	9.33	7.57	5.26	4.75	7.86	7.33	12.57	11.38
4.50	10.68	9.75	7.11	7.41	6.06	8.14	7.57	11.89	10.98
5.00	9.92	7.20	7.64	8.70	8.62	4.62	7.19	13.01	10.02
5.50	9.11	3.24	6.00	10.24	8.90	4.68	6.85	9.28	8.61
6.00	7.60	5.00	5.61	8.70	8.49	2.97	5.61	8.15	7.60
8.00	5.78	5.30	3.76	6.19	5.75	2.71	4.02	7.80	5.80
10.00	5.92	3.70	2.66	2.79	4.84	2.59	2.15	4.99	4.74
12.00	3.55	2.68	1.88	4.09	3.00	3.14	1.84	1.99	2.57
24.00	0.00	0.00	0.00	0.00	1.18	0.00	0.00	0.00	0.00

Table 64. Propranolol plasma concentration (ng/mL) after a single oral dose of 80 mg propranolol CPOPs at 12% coating level

Time (h)	Pig 1	Pig 2	Pig 3	Pig 4	Pig 5	Pig 6	Pig 7	Pig 8	Pig 9
0.00	0.00	0.00	0.00	0.00	0.00	0.00	0.00	0.00	0.00
0.50	0.00	0.00	0.00	0.00	0.00	0.00	0.00	0.00	0.00
1.00	0.00	0.00	0.00	0.00	0.00	0.00	0.00	0.00	0.00
1.50	0.00	0.00	1.47	2.18	1.89	1.78	1.89	1.46	2.99
2.00	0.00	0.00	1.71	3.44	2.45	1.94	3.60	1.50	3.99
2.50	0.00	0.00	1.91	3.99	2.83	2.02	4.48	2.96	4.07
3.00	0.00	1.54	2.83	4.44	4.61	2.15	5.36	4.32	4.32
3.50	3.64	1.59	2.96	5.36	5.36	4.40	5.78	6.60	4.94
4.00	3.98	3.10	4.20	8.89	5.48	5.53	5.54	5.77	5.17
4.50	7.12	4.36	5.26	8.53	7.02	6.60	5.35	6.79	5.06
5.00	8.33	4.49	4.41	7.61	5.92	5.57	6.31	6.94	6.72
5.50	8.93	3.99	5.18	5.68	5.51	7.61	6.07	6.94	7.31
6.00	7.46	3.77	3.74	6.62	3.99	4.62	5.53	5.65	7.27
8.00	4.14	1.74	2.51	2.93	2.80	3.40	4.24	3.86	5.79
10.00	2.75	1.00	2.12	2.73	1.72	1.81	2.67	3.42	5.13
12.00	2.20	0.00	1.45	2.59	1.14	1.00	2.00	2.52	3.54
24.00	1.06	0.00	0.00	0.00	0.00	0.00	0.00	1.32	1.13

Figure 71. Propranolol plasma concentrations after a single oral dose of 40 mg propranolol immediate release tablets, pigs 1–9
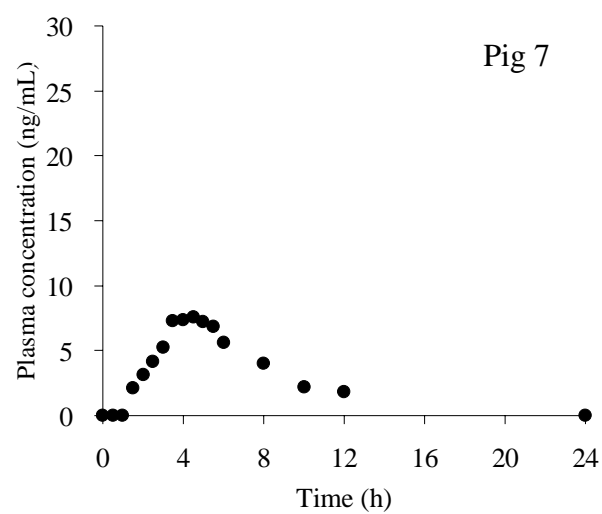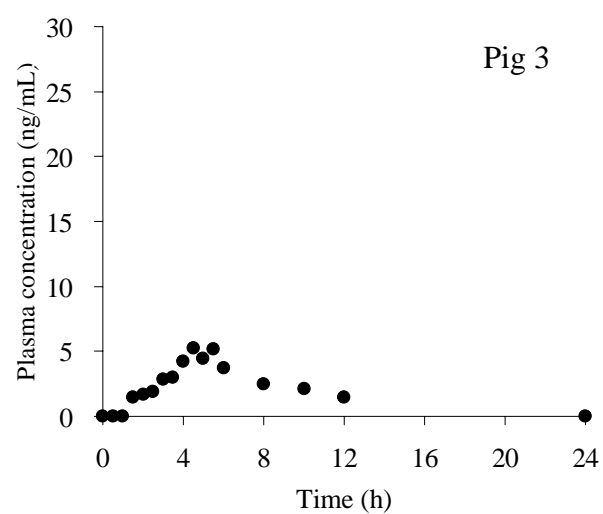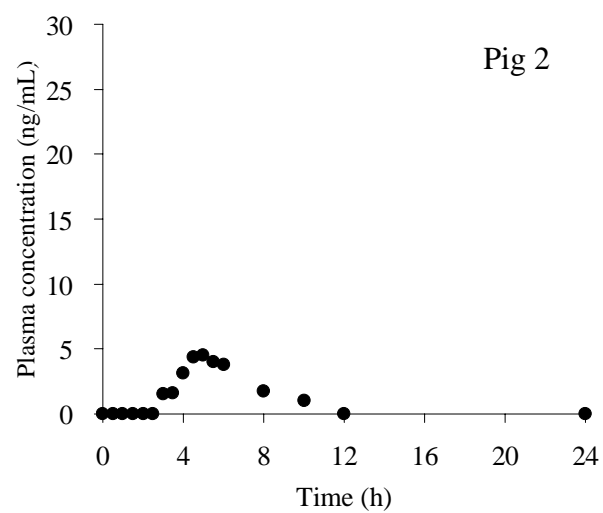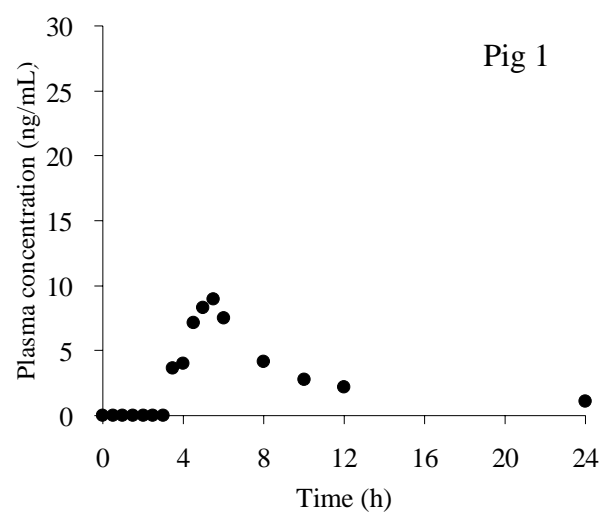
Figure 71. Propranolol plasma concentrations after a single oral dose of 40 mg propranolol immediate release tablets, pigs 1–9 (cont.)
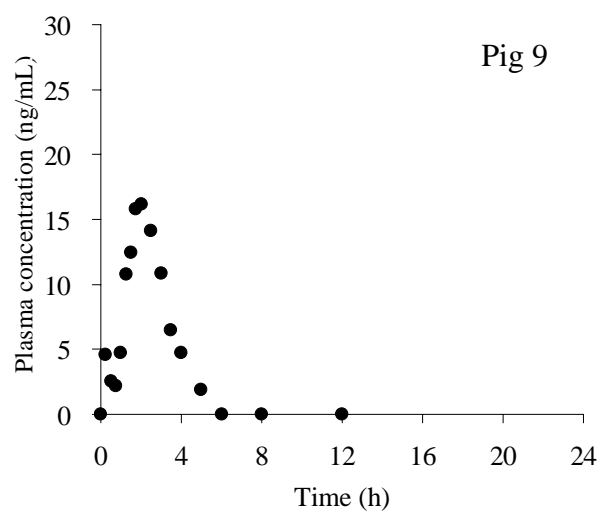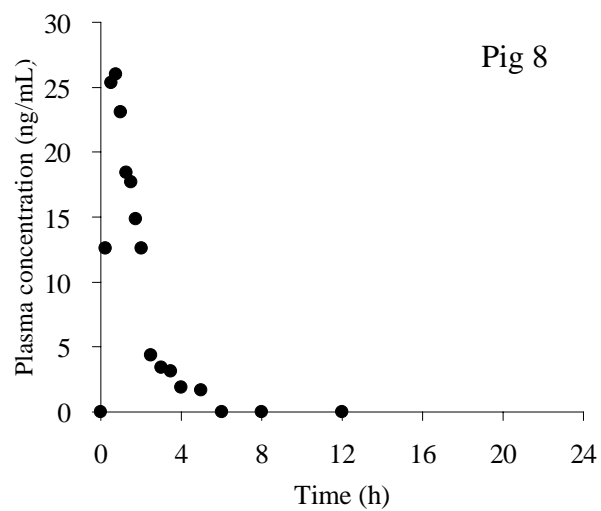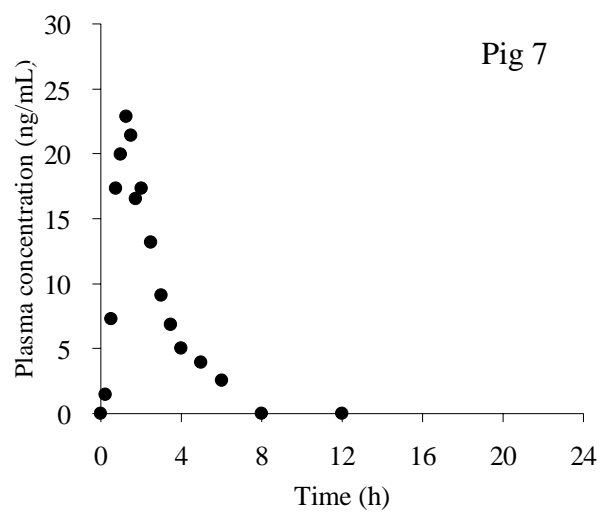
Figure 71. Propranolol plasma concentrations after a single oral dose of 40 mg propranolol immediate release tablets, pigs 1–9 (cont.)
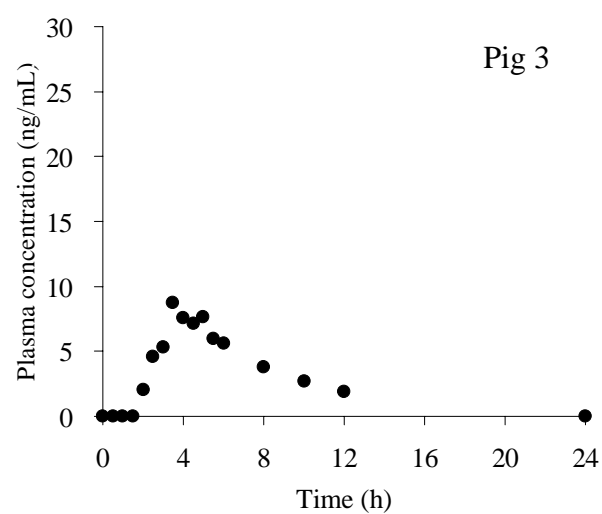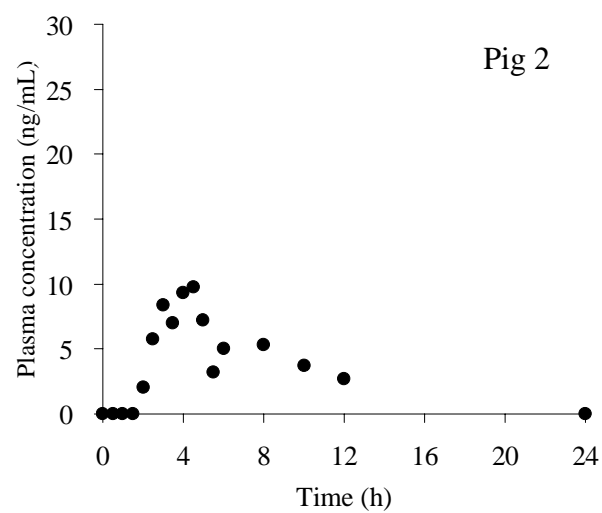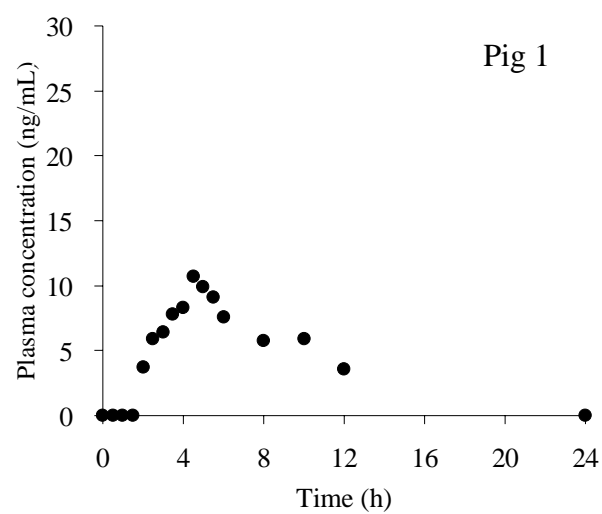
Figure 72. Propranolol plasma concentrations after a single oral dose of 80 mg propranolol CPOPs at 8% coating level, pigs 1–9
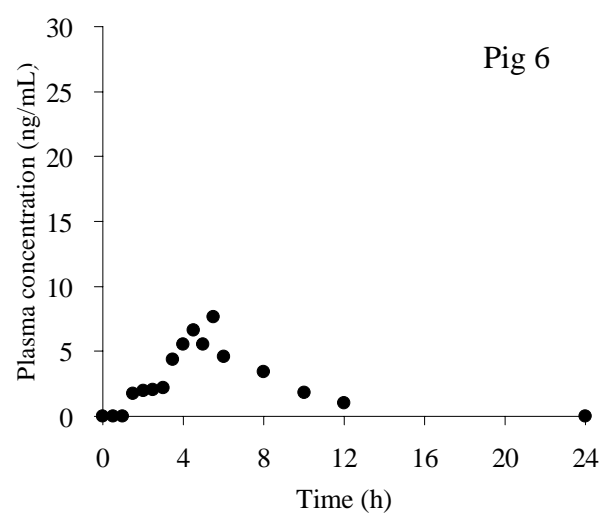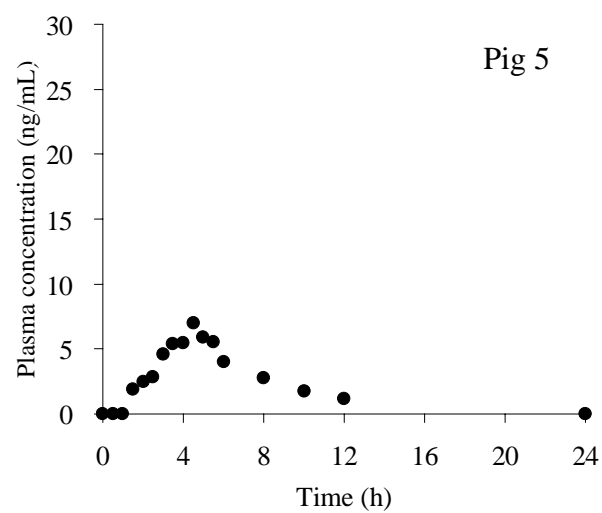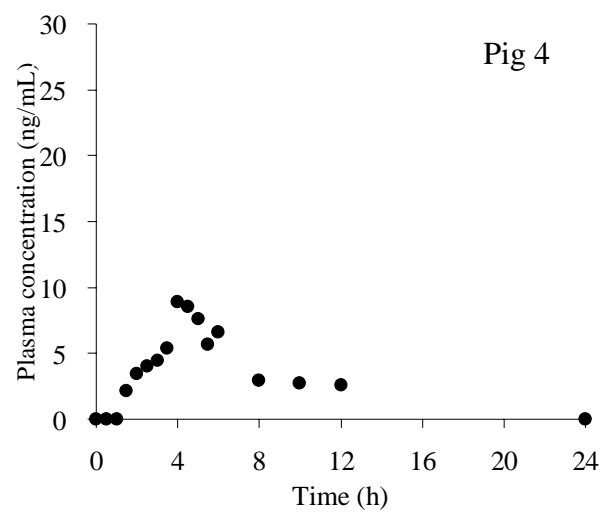
Figure 72. Propranolol plasma concentrations after a single oral dose of 80 mg propranolol CPOPs at 8% coating level, pigs 1–9 (cont.)
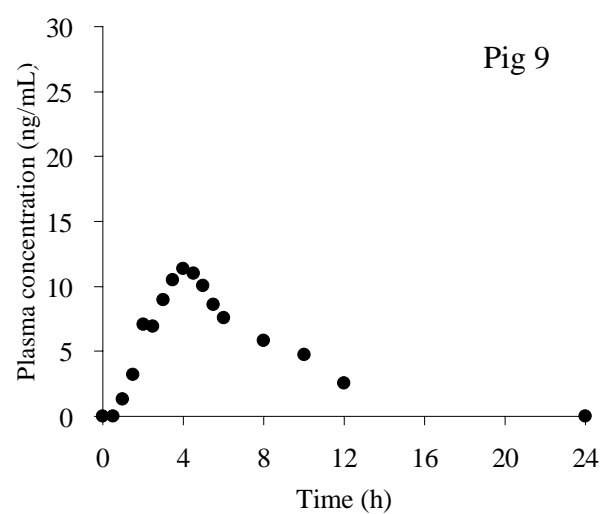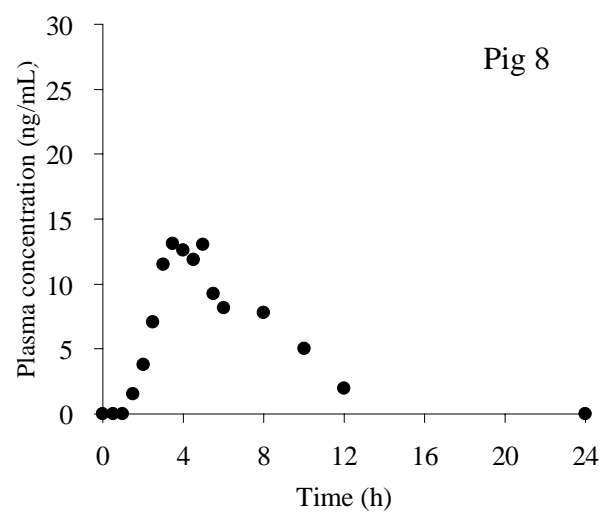
Figure 72. Propranolol plasma concentrations after a single oral dose of 80 mg propranolol CPOPs at 8% coating level, pigs 1–9 (cont.)

Figure 73. Propranolol plasma concentrations after a single oral dose of 80 mg propranolol CPOPs at 12% coating level, pigs 1–9

Figure 73. Propranolol plasma concentrations after a single oral dose of 80 mg
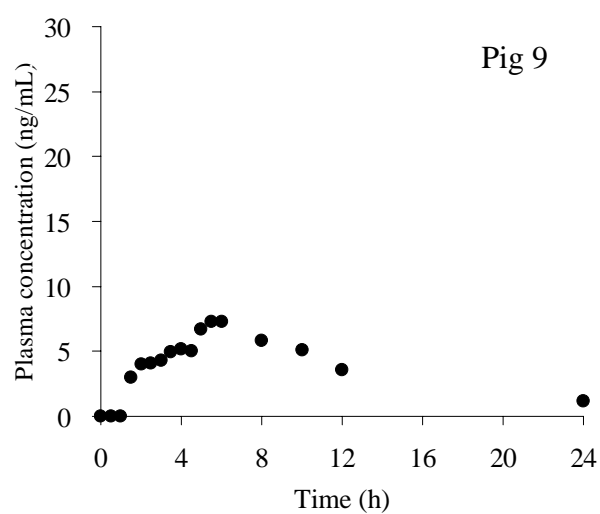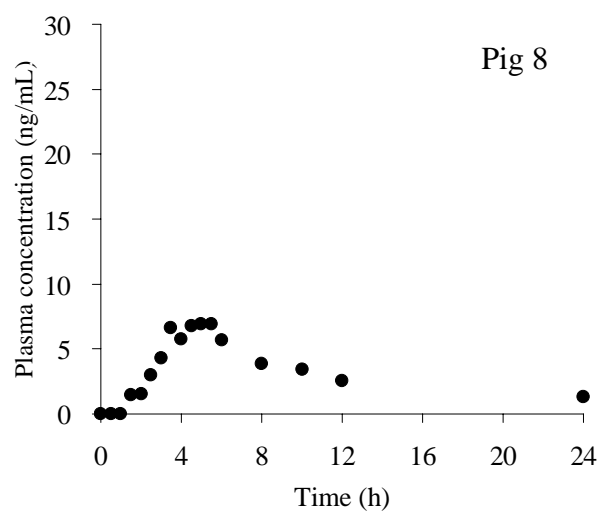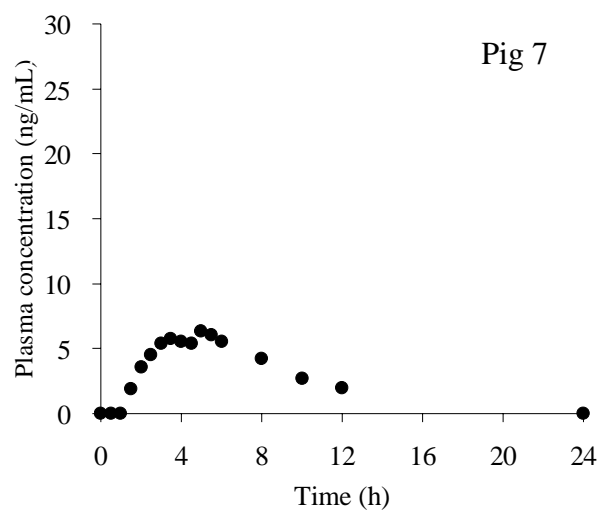propranolol CPOPs at 12% coating level, pigs 1–9 (cont.)

Figure 73. Propranolol plasma concentrations after a single oral dose of 80 mg propranolol CPOPs at 12% coating level, pigs 1–9 (cont.)

BIOGRAPHY

NAME   Ms. Siracha Tuntikulwattana

DATE OF BIRTH   October 4, 1975

PLACE OF BIRTH   Bangkok, Thailand

INSTITUTION ATTENED   Mahidol University, 1993–1998:

        Bachelor of Science in Pharmacy

        (Second class honors)

        Mahidol University, 2000–2007:

        Doctor of Philosophy

        (Pharmaceutics)

GRADUATION GRANT   Thailand Research Fund through the

        Royal Golden Jubilee Ph.D. Program

        (Grant No. PHD/0095/2544)

POSITION & OFFICE   Ramathibodi Hospital, 1998–2000:

        Hospital pharmacist

        National Healthcare Systems Co., Ltd.,

        2004–2005:

        In charge of Inventory product section,

        Central Procurement Center

ADDRESS   79/296 Sammakorn Village, Samwa Road,

        Bangchan, Klongsamwa,

        Bangkok 10510 Thailand

        E-mail: sirachaa@yahoo.com